

Evaluation of Techniques to Remove Defective Grout from Post-Tensioning Tendons

Final Report

February 2020

Principal investigator:

H. R. Hamilton

Research assistants:

Satyajeet R. Patil

Eduardo Torres

Department of Civil and Coastal Engineering
University of Florida
P.O. Box 116580
Gainesville, Florida 32611

Sponsor:

Florida Department of Transportation (FDOT)

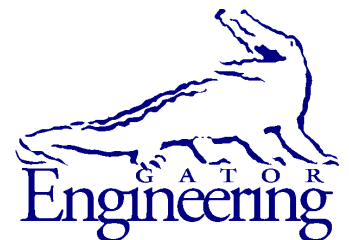
Project Manager:

William Potter

Contract:

UF Project No. 00127093 & 00127094

FDOT Contract No. BDV31-977-58



University of Florida

Engineering School of Sustainable Infrastructure and Environment
Department of Civil and Coastal Engineering
University of Florida
P.O. Box 116580
Gainesville, Florida 32611

Disclaimer

The opinions, findings, and conclusions expressed in this publication are those of the authors and not necessarily those of the State of Florida Department of Transportation

Unit of Measurement Conversions

SI* (MODERN METRIC) CONVERSION FACTORS

APPROXIMATE CONVERSIONS TO SI UNITS

SYMBOL	WHEN YOU KNOW	MULTIPLY BY	TO FIND	SYMBOL
LENGTH				
in	inches	25.4	millimeters	mm
ft	feet	0.305	meters	m
yd	yards	0.914	meters	m
mi	miles	1.61	kilometers	km
AREA				
in²	square inches	645.2	square millimeters	mm ²
ft²	square feet	0.093	square meters	m ²
yd²	square yard	0.836	square meters	m ²
ac	acres	0.405	hectares	ha
mi²	square miles	2.59	square kilometers	km ²
VOLUME				
fl oz	fluid ounces	29.57	milliliters	mL
gal	gallons	3.785	liters	L
ft³	cubic feet	0.028	cubic meters	m ³
yd³	cubic yards	0.765	cubic meters	m ³
NOTE: volumes greater than 1000 L shall be shown in m ³				
MASS				
oz	ounces	28.35	grams	g
lb	pounds	0.454	kilograms	kg
T	short tons (2000 lb)	0.907	megagrams	Mg (or "t")
TEMPERATURE (exact degrees)				
°F	Fahrenheit	5(F-32)/9 or (F-32)/1.8	Celsius	°C
ILLUMINATION				
fc	foot-candles	10.76	lux	lx
fl	foot-Lamberts	3.426	candela/m ²	cd/m ²
FORCE and PRESSURE or STRESS				
kip	1000 pound force	4.45	kilonewtons	kN
lbf	pound force	4.45	newtons	N
lbf/in²	pound force per square inch	6.89	kilopascals	kPa

*SI is the symbol for the International System of Units. Appropriate rounding should be made to comply with Section 4 of ASTM E380.

SI* (MODERN METRIC) CONVERSION FACTORS
APPROXIMATE CONVERSIONS FROM SI UNITS

SYMBOL	WHEN YOU KNOW	MULTIPLY BY	TO FIND	SYMBOL
LENGTH				
mm	millimeters	0.039	inches	in
m	meters	3.28	feet	ft
m	meters	1.09	yards	yd
km	kilometers	0.621	miles	mi
AREA				
mm²	square millimeters	0.0016	square inches	in ²
m²	square meters	10.764	square feet	ft ²
m²	square meters	1.195	square yards	yd ²
ha	hectares	2.47	acres	ac
km²	square kilometers	0.386	square miles	mi ²
VOLUME				
mL	milliliters	0.034	fluid ounces	fl oz
L	liters	0.264	gallons	gal
m³	cubic meters	35.314	cubic feet	ft ³
m³	cubic meters	1.307	cubic yards	yd ³
MASS				
g	grams	0.035	ounces	oz
kg	kilograms	2.202	pounds	lb
Mg (or "t")	megagrams (or "metric ton")	1.103	short tons (2000 lb)	T
TEMPERATURE (exact degrees)				
°C	Celsius	1.8C+32	Fahrenheit	°F
ILLUMINATION				
lx	lux	0.0929	foot-candles	fc
cd/m²	candela/m ²	0.2919	foot-Lamberts	fl
FORCE and PRESSURE or STRESS				
kN	kilonewtons	0.225	1000 pound force	kip
N	newtons	0.225	pound force	lbf
kPa	kilopascals	0.145	pound force per square inch	lbf/in ²

*SI is the symbol for the International System of Units. Appropriate rounding should be made to comply with Section 4 of ASTM E380.

Technical Report Documentation Page

1. Report No.		2. Government Accession No.		3. Recipient's Catalog No.	
4. Title and Subtitle Evaluation of Techniques to Remove Defective Grout from Post-Tensioning Tendons				5. Report Date February 2020	
				6. Performing Organization Code	
7. Author(s) Patil, S. R., Torres, E. and Hamilton, H. R.				8. Performing Organization Report No.	
9. Performing Organization Name and Address University of Florida Department of Civil & Coastal Engineering P.O. Box 116580 Gainesville, FL 32611-6580				10. Work Unit No. (TRAVIS)	
				11. Contract or Grant No. BDV31-977-58	
12. Sponsoring Agency Name and Address Florida Department of Transportation 605 Suwannee Street, MS 30 Tallahassee, FL 32399				13. Type of Report and Period Covered Final Report May 2016 – Feb 2020	
				14. Sponsoring Agency Code	
15. Supplementary Notes					
16. Abstract <p>Bridge girders in the U.S. are commonly constructed using multistrand post-tensioned (PT) tendons. Defective grout has been found in some of recently constructed bridges in the form of soft grout, which consists of segregated and unhardened grout with free moisture and is often the cause of corrosion of prestressing strands. To address this problem, two techniques of remediation were tested and evaluated: hydrodemolition removal of the defective grout and drying of the defective grout. Hydrodemolition involved use of a high-pressure water jet to break up and remove soft grout from inside the PT duct, but it did not completely remove grout from any one section of the mockup and was deemed unsuitable for use in the removal of grout.</p> <p>To evaluate drying as a means to remediate soft grout, two types of PT tendon mockup specimens were fabricated and filled with multiple layers of grout with varying quality. Grout was dried in place by passing dehumidified air through the tendon to remove moisture. Mockup specimens containing normal grout required 167 days to dry and the specimen containing only soft grout dried in 117 days. Moisture content measurements on dried layers of soft grout were consistently below 1%, which indicated that drying had effectively removed moisture from the soft grout. Dried specimens, however, exhibited strand corrosion in several locations, which did not occur in the control specimens.</p> <p>To better understand the corrosion behavior discovered in the mockup testing, a series of small-scale corrosion tests were conducted using specimens consisting of a 1.5-in. diameter PVC pipe and a single prestressing strand. Forty-eight of the seventy-two specimens were fabricated and dried. Drying was terminated when the difference in RH between the inlet and outlet was indistinguishable. During and after drying, corrosion potential was measured in specimens containing two strands, macrocell current was measured between strand pairs after drying. After monitoring corrosion for a designated time, corrosion specimens were dissected to evaluate grout moisture content and strand corrosion. Moderate corrosion was found on the prestressing strands when the specimens were dissected, with the majority of the corrosion occurring in chloride-contaminated specimens.</p> <p>Given the unknowns in the field application of this method and the fact that corrosion occurred during drying in laboratory conditions, it is advisable to combine the grout drying with the use of a corrosion inhibitor injected into the tendon immediately following drying. For PT tendons with chloride-contaminated grout, it is advisable to use an inert gas for drying followed by injection with a corrosion inhibitor effective in high-chloride environments.</p>					
17. Key Words post-tensioning tendons, defective grout, drying, hydrodemolition, tendon corrosion, soft grout.			18. Distribution Statement No restrictions		
19. Security Classif. (of this report) Unclassified		20. Security Classif. (of this page) Unclassified		21. No. of Pages 222	22. Price

Acknowledgments

The authors would like to gratefully acknowledge and thank the Florida Department of Transportation (FDOT) for the financial support of this research project. The project was managed by William Potter, and the authors thank him for his technical input and support throughout the project. The authors would like to thank Christina Freeman, Justin Robertson, Paul Tighe and the strong floor personnel from the FDOT Structures Research Center in Tallahassee, and Ivan Lasa, Ronald Simmons, Charlotte Kasper, and David Hudson of the FDOT State Materials Office in Gainesville for their assistance with experimental testing. The authors would like to thank the University of Florida, in particular Dr. Taylor Rawlinson (structures lab manager), Steve Schein, and Shelby Brothers. The authors would also like to thank the assistants (Dylan DiCarlo, Jacob Montgomery, Ming Li, Miguel Morales and Taylor Humbarger) who helped the authors during the project.

Executive Summary

Corrosion problems discovered in grouted multi-strand, post-tensioned (PT) tendons used in bridge construction have led to the discovery of defective grout in a number of PT concrete bridge structures in the U.S. and abroad. Remediation of such tendons is particularly difficult and expensive if significant corrosion is expected to occur. To address this problem, two techniques of remediation were tested and evaluated: hydrodemolition removal of the defective grout and drying of the defective grout.

Hydrodemolition involved use of a high-pressure water jet to break up and remove soft grout from inside the PT duct. A mockup specimen was constructed using 4-in. diameter electrical metal tubing (EMT) conduit with nineteen 0.6-in. dia., 7-wire low-relaxation strands to simulate a tendon located in the negative bending moment region of a bridge girder. Grout was placed in layers, with the stronger grout at lower elevation and weaker grout at higher elevation. Hydrodemolition was performed in four trials, each starting at a different section to evaluate the level of difficulty while performing hydrodemolition in different types of grout. Hydrodemolition did not completely remove grout from any one section of the mockup and was deemed unsuitable for use in the removal of grout.

Drying of grout was evaluated as an alternative to rehabilitate tendons filled with soft grout. Two types of PT tendon mockup specimens were fabricated and filled with multiple layers of grout with varying quality. One specimen had alternating soft grout layers with varying volumes of portland cement. This specimen was designed to evaluate drying of tendons containing isolated soft grout. The other specimen had alternating soft and normal grout layers and was used to study the effectiveness in drying of soft grout trapped between normal grout layers. Grout was dried in place by passing dehumidified air through the tendon to remove moisture. This approach required drilling a single hole at one end of the specimen for the dry air inlet and a second hole at the opposite end to discharge moist air. In practice, this method would require fewer penetrations into the duct and result in less damage than hydrodemolition. The change in relative humidity of the dry air as it passed through the specimen was used to determine if the moisture content of the grout had decreased enough to be considered dry. Mockup specimens containing normal grout required 167 days to dry while the specimen containing only soft grout dried in 117 days. Moisture content measurements on dried layers of soft grout were consistently below 1%, which indicated that drying had effectively removed moisture from the soft grout. Dried specimens, however, exhibited strand corrosion in several locations, which did not occur in the control specimens. Although grout pH was not measured, the corrosion was thought to be caused by the availability of oxygen to supply the corrosion reaction and carbon dioxide to carbonate the grout, thus reducing its ability to protect the prestressing steel.

To better understand the corrosion behavior discovered in the mockup testing, a series of small-scale corrosion tests were conducted. Seventy-two corrosion specimens consisting of a 1.5-in. diameter PVC pipe fitted with PVC tees and bushings were fabricated. Each specimen had an inlet and outlet for the passage of dry air through the tendon to dry the grout. Variables included the use of one or two layers of grout, use of one or two sections of prestressing strand, variation in the grout consistency, and addition of chlorides. In specimens with two grout layers, each grout layer contained a prestressing strand and a reference electrode (RE) with electrical wiring to allow measurement of corrosion potential and resistance.

Forty-eight of the seventy-two specimens were dried using a drying system producing air of RH about 0.2%. Relative humidity (RH) of air was measured at both the inlet and outlet of

each specimen. Drying was terminated when the difference in RH between the inlet and outlet was indistinguishable. During and after drying, corrosion potential was measured between the strands and their RE. After drying, in specimens containing two strands, macrocell current was measured between strand pairs using a modified version of the corrosion specimens described in ASTM G109. After monitoring corrosion for a designated time, corrosion specimens were dissected to evaluate grout moisture content and strand corrosion.

Similar to the mockup specimen tests, drying of small-scale specimens was found to cause corrosion on the prestressing strands. Results of the small-scale testing, however, show that during the drying process there was a period of increased probability of corrosion compared to the probability of corrosion after the grout has been dried. Once the grout dried, corrosion potential became more positive. In general, as corrosion potential became more positive and approached zero, the probability of corrosion decreased.

The average pH of dried soft grout (5 PC and 15 PC), conditioned defective prepackaged grout (PT), and normal grout (100 PC) was 8.7, 8.7, and 9.5, respectively. Average pH of soft grout, defective PT grout, and normal grout in control specimens was 11.8, 11, and 12.3, respectively, which indicates that the drying resulted in a reduction in pH, likely due to carbonation.

Drying using atmospheric air was found to cause corrosion, which was most probably due to the supply of oxygen and carbonation of grout. As an alternative, use of an inert gas such as nitrogen, would help reduce the availability of oxygen to drive the corrosion process, if moisture happens to be available. Nitrogen gas has been successfully used for drying unbonded strands (Vander Velde, 2002). Soft grout was found to be friable and porous after drying and could allow oxygen and moisture to reach strands, resulting in corrosion, particularly if recharging with moisture is possible.

Given the unknowns of field application of this method and the fact that corrosion occurred during drying, it is advisable to combine the grout drying with the use of a corrosion inhibitor injected into the tendon immediately following drying. For PT tendons with chloride-contaminated grout, it is advisable to use an inert gas for drying followed by injection with a corrosion inhibitor effective in high-chloride environments.

Table of Contents

Disclaimer	ii
Unit of Measurement Conversions	iii
Technical Report Documentation Page	v
Acknowledgments.....	vi
Executive Summary	vii
Table of Contents.....	ix
List of Figures	xi
List of Tables	xvi
Part One—Introduction and Initial Investigations.....	1
1 Introduction.....	2
1.1 Report organization.....	2
2 Background.....	4
3 Research approach	5
4 Soft grout mixture design.....	7
5 Hydrodemolition remediation tests.....	10
Part Two—Mockup Drying Tests.....	12
6 Drying	13
6.1 Specimen design	13
6.2 Specimen fabrication	15
7 Drying system and procedures.....	17
8 Results and discussion	20
8.1 Dissection.....	20
8.1.1 ISG observations.....	22
8.1.2 TSG observations.....	24
8.1.3 Corrosion observations	24
8.2 Moisture content	28
8.2.1 ISG results.....	28
8.2.2 TSG results.....	32
8.3 Relative humidity analysis.....	35
8.3.1 ΔRH_d measurement.....	35
8.3.2 RH_g analysis.....	39
9 Mockup drying test findings	41
Part Three—Drying Corrosion Tests	42
10 Background and approach.....	43
11 Corrosion specimen design.....	44
12 Specimen fabrication	50
12.1 Materials	50
12.2 Strands and reference electrodes.....	50
12.3 Electrical connections	50
12.4 Specimen assembly.....	52
12.5 Mixing and placing grout.....	53
13 Drying system	55
14 Drying test procedures	59
15 Corrosion test procedures	61
15.1 During drying.....	61

15.2	Post-drying.....	61
16	Dissection procedures.....	64
17	Physical corrosion evaluation procedure.....	68
18	Drying results and discussion.....	72
19	Dissection results and discussion.....	77
19.1	Grout moisture content.....	77
19.2	Grout pH.....	77
19.3	Prestressing strand corrosion rating.....	80
19.4	Prestressing strand section loss and pitting.....	83
20	Corrosion results and discussion.....	87
20.1	During drying.....	87
20.2	Post-drying.....	90
21	Comparison of section loss and post-drying corrosion potential measurements.....	95
22	Summary and conclusions.....	99
23	Implementation and future work.....	104
24	References.....	105
APPENDIX A— Hydrodemolition.....		107
A.1	Detailed drawings.....	107
A.2	Hydrodemolition test design.....	115
A.3	Inclined hydrodemolition tests.....	117
A.4	Mockup hydrodemolition tests.....	129
APPENDIX B— Grout drying.....		137
B.1	Detailed drawings.....	137
B.2	Procedure for RH measurements.....	141
B.3	Probe response time.....	142
B.4	Effect of probe port depth on RH _g readings.....	144
B.5	Dryness evaluation using corrosion potential charts.....	144
B.6	Delta T analysis.....	159
APPENDIX C— Corrosion specimens.....		162
C.1	Schematic drawings of corrosion specimens.....	162
C.2	Corrosion readings during drying.....	165
C.3	Corrosion readings after drying.....	188

List of Figures

Figure 2-1. Deficient grout in PT (post-tensioned) tendon in Sicily, Italy (Anania et al., 2018)..	4
Figure 3-1. Drying test setup	5
Figure 4-1. Mini-inclined testing	8
Figure 4-2. Length of soft grout versus percentage of portland cement in soft grout mixture	9
Figure 4-3. Dissection of tube for mini-inclined testing.....	9
Figure 5-1. Hydrodemolition specimen: (a) EMT before installation of 2x8; (b) schematic figure with location of 2x8	10
Figure 5-2. Grout layers used in hydrodemolition specimen.....	11
Figure 5-3. East elevation of mockup section identification	11
Figure 6-1. Fully assembled specimens with downward angle of PVC tee.....	14
Figure 6-2. HDPE connection at PVC tee of inlet	14
Figure 6-3. Soft grout removed at PVC tee inlet and outlet	14
Figure 6-4. Mockup specimens for drying with RH measurement locations shown.....	15
Figure 6-5. Preparation of grout mixture	15
Figure 6-6. Grout mixture placed into specimen through funnel and PVC tee	16
Figure 6-7. PVC tee through which grout was introduced	16
Figure 7-1. Layout of drying equipment.....	17
Figure 7-2. RH _g measurement.....	18
Figure 7-3. Location of readings.....	18
Figure 7-4. Vaisala DM70 hand-held dewpoint meter	19
Figure 8-1. Three divisions of 1-ft-long exposed section. Samples were collected from the inner 4-in. section.....	20
Figure 8-2. Dissection schematic.....	21
Figure 8-3. Removal of PVC with circular saw.....	21
Figure 8-4. Sampling of soft grout: (a) Hacksaw, hammer, and chisel used to remove soft grout; (b) Section after removing soft grout.....	22
Figure 8-5. Sampling of normal grout: (a) Cracks in 100 PC grout layer at approximately 4-in. spacing; (b) Section after removing normal grout	22
Figure 8-6. Soft grout crumbled with hand.....	23
Figure 8-7. Soft grout as wet clayey sand.....	23
Figure 8-8. Pores on grout surface	23
Figure 8-9. End caps and outlet port on specimens	24
Figure 8-10. Shrinkage cracks: (a) Normal grout; (b) Soft grout	24
Figure 8-11. In situ corroded strands near port C dried TSG specimen	25
Figure 8-12. Location of corroded strands in the dried specimens.....	25
Figure 8-13. Macrocell formation on peripheral strands of tendon	26
Figure 8-14. Corroded strands near port C dried ISG specimen.....	26
Figure 8-15. Corroded strands near port C dried TSG specimen	27
Figure 8-16. Corroded strands near port C control ISG specimen	27
Figure 8-17. Non-corroded strands near port C control TSG specimen	27
Figure 8-18. In situ corroded strands at: (a) port E; (b) port F dried ISG specimen.....	28
Figure 8-19. Oven drying of grout samples	28
Figure 8-20. Comparison of moisture content for dried and control ISG.....	29
Figure 8-21. Variation of moisture content along the length of control specimen ISG.....	30

Figure 8-22	Variation of moisture content along the length of the dried specimen ISG.....	31
Figure 8-23.	Shrinkage in grout due to drying: (a) Void present at the top; (b) Schematic of air flow through void (not to scale).....	31
Figure 8-24.	Comparison of moisture content for dried and control TSG specimens.....	33
Figure. 8-25	Variation of moisture content along the length of control specimen TSG	34
Figure 8-26.	Variation of moisture content along the length of dried specimen ISG.....	35
Figure 8-27.	ΔRH_d vs. time.....	36
Figure 8-28.	Dryness checks for dried specimen ISG	37
Figure 8-29.	Dryness checks for dried specimen TSG	37
Figure 8-30.	Depiction of drying behavior early in the process. Variation in RH following suspension of drying (a) immediately after drying restart and (b) two hours after drying restart.....	38
Figure 8-31.	Depiction of drying behavior later in the process. Variation in RH following suspension of drying (a) immediately after drying restart and (b) two hours after restart ...	38
Figure 8-32.	Location of ports for RH_g measurements.....	39
Figure 8-33.	RH_g readings vs. time (ISG specimen)	40
Figure 8-34.	RH_g readings vs. time (TSG specimen)	40
Figure 10-1.	Mockup specimens.....	43
Figure 11-1.	Corrosion specimen.....	44
Figure 11-2.	Idealized strand pattern	44
Figure 11-3.	Ratio of duct to strand area for different size tendons	45
Figure 11-4.	Specimen design: (a) Mockup specimen ISG with 15 PC and 5 PC interface highlighted; (b) Replicate corrosion specimen	46
Figure 11-5.	Corrosion specimen: (a) specimen photo; (b) schematic drawing for two-strand specimen; and (c) one-strand specimen	46
Figure 11-6.	Pair of strand and titanium mixed-metal oxide electrode	47
Figure 11-7.	Corrosion specimen placed at 60° inclination.....	47
Figure 11-8.	Grout interface in trial specimens cast at varying slopes	47
Figure 12-1.	Zip ties and marks in preparation for strand cutting	50
Figure 12-2.	RE clamped in horizontal saw.....	50
Figure 12-3.	Separated stranded wire	51
Figure 12-4.	Wire soldered to end of 7-wire prestressing strand.....	51
Figure 12-5.	Crimping of RE.....	51
Figure 12-6.	Finished reference electrode electrical.....	52
Figure 12-7.	Finished strand	52
Figure 12-8.	Specimens prepped for placement of first grout layer	53
Figure 12-9.	Instrumentation wiring in PVC specimen	53
Figure 12-10.	Grout mixing	54
Figure 13-1.	Drying system setup.....	56
Figure 13-2.	RH of drying air	56
Figure 13-3.	Dry air distribution system schematic.....	57
Figure 13-4.	Schematic of specimen setup for drying on one shelving rack.....	58
Figure 14-1.	RH_{d0} measured at specimen outlet using Vaisala dewpoint meter.....	59
Figure 15-1.	Corrosion potential measurement during drying.....	61
Figure 15-2.	Schematic circuit diagram for monitoring after drying.....	62
Figure 15-3.	User interface of DAQ software	62

Figure 15-4. Typical corrosion specimen connection to DAQ	62
Figure 15-5. Resistor between anode and cathode.....	63
Figure 16-1. Longitudinal axis of corrosion specimens.....	65
Figure 16-2. Dissection of specimen: (a) Use of concrete saw; (b) Specimen after cut in PVC. 66	
Figure 16-3. pH testing: (a) Location of grout; (b) pH measurement using spray-on chemical indicator	66
Figure 16-4. Sampling during dissection: (a) Grout; (b) Strand.....	67
Figure 17-1. Photographs documenting strand corrosion and associated ratings 1 to 4 (Sason, 1992)	69
Figure 17-2. Photographs documenting strand corrosion and associated ratings 5 to 8 (Sason, 1992)	70
Figure 17-3. Cleaning of corrosion products on strands following ASTM G1-03	71
Figure 17-4. Corrosion evaluation of strands measurement (a) Loss in section (b) Pit depth.....	71
Figure 18-1. ΔRH_d (%) vs. time (weeks) for dried corrosion specimens	74
Figure 19-1. Corrosion rating = 6 for strand in 5 PC grout of 15 PC/5 PC D1C specimen: (a) Before cleaning; (b) After cleaning	80
Figure 20-1. Corrosion readings for specimen 5/100D1 (a) Corrosion potential (b) Resistance	87
Figure 20-2. Corrosion readings for specimen 5/100D2 (a) Corrosion potential (b) Resistance	88
Figure 20-3. Corrosion readings for specimen 5/100C1 (a) Corrosion potential (b) Resistance	88
Figure 20-4. Relative humidity readings vs. time for specimen type 1 with no chlorides	89
Figure 20-5. Corrosion readings for specimen 5 PC/100 PC D2C: (a) Corrosion potential; (b) Resistance.....	89
Figure 20-6. Relative humidity readings vs. time for specimen 5 PC/100 PC D2C	90
Figure 20-7. Post-drying corrosion measurements for 5/100D1: (a) Corrosion potential; (b) Macrocell current	90
Figure 20-8. Post-drying corrosion measurements for 100/5D2C: (a) Corrosion potential; (b) Macrocell current	91
Figure 20-9. Post-drying corrosion measurements for 5/100C1: (a) Corrosion potential; (b) Macrocell current	91
Figure 20-10. Post-drying measurements for 100/5C1C: (a) Corrosion potential; (b) Macrocell current	92
Figure 20-11. Percentage of specimens with respect to minimum corrosion potentials during drying	93
Figure 20-12. Percentage of specimens with respect to minimum corrosion potentials after drying	93
Figure A.1-1. Hydrodemolition mockup fabrication and grout installation	108
Figure A.1-2. Hydrodemolition mockup: Mixture proportions and injection procedure	109
Figure A.1-3. Hydrodemolition mockup frame design (sheet 1/5).....	110
Figure A.1-4. Hydrodemolition mockup frame design (sheet 2/5).....	111
Figure A.1-5. Hydrodemolition mockup frame design (sheet 3/5).....	112
Figure A.1-6. Hydrodemolition mockup frame design (sheet 4/5).....	113
Figure A.1-7. Hydrodemolition mockup frame design (sheet 5/5).....	114
Figure A.2-1. Inclined hydrodemolition specimen design.....	115
Figure A.2-2. Hydrodemolition specimen: schematic figure with location of 2x8	115
Figure A.2-3. Hydrodemolition specimen: EMT before installation of 2x8	116
Figure A.2-4. Shrink wrap and coupler connecting two EMT sections.....	116

Figure A.2-5. Simulation of concrete surrounding a tendon using wood.....	116
Figure A.2-6 Anchor details	117
Figure A.2-7. Grout layers used in hydrodemolition specimen.....	117
Figure A.3-1 Grout mixture material: (a) ground limestone; (b) portland cement.....	118
Figure A.3-2. Inclined specimens using: (a) PVC pipe and; (b) electrical metal tubing.....	118
Figure A.3-3. Grout Plant	119
Figure A.3-4. Injection point	119
Figure A.3-5. EMT conduit: (a) coupling and; (b) shrink-wrap sleeves used to seal couplings	120
Figure A.3-6. Grout preparation for EMT specimens with buckets, paddle mixer, and power drill	121
Figure A.3-7. Pouring grout into EMT specimen with funnel and tube	121
Figure A.3-8. Partial removal of PVC for inspection	122
Figure A.3-9. Verification of soft grout.....	123
Figure A.3-10. Trial clean-out conducted on PVC specimens: (a) 2-ft spacing of holes; (b) Conducting clean out; (c) 1-ft spacing of holes; (d) Debris at specimen end after clean out	124
Figure A.3-11 Cleaning equipment.....	125
Figure A.3-12. Demonstration of preparing hydrodemolition specimen: (a) coring hole; (b) opening in duct.....	125
Figure A.3-13. Demonstration of cleaning of opening: (a) lance used to clear grout away from opening; (b) grout cleared from opening	125
Figure A.3-14. Demonstration of performing hydrodemolition: (a) flexible tube and nozzle; (b) inserting nozzle and tube into the specimen	126
Figure A.3-15. EMT1 and EMT2 after hydrodemolition	126
Figure A.3-16. EMT3 after hydrodemolition	127
Figure A.3-17. Visual Inspection of 19S20PC-10 PC after grout removal	127
Figure A.3-18. Distribution of grout per section: (a) EMT1; (b) EMT2	128
Figure A.3-19. Percent of remaining grout per section: (a) EMT1; (b) EMT2	128
Figure A.4-1. East elevation of mockup section identification.	129
Figure A.4-2. Sections covered by each trial to remove grout: (a) Trial 1; (b) Trial 2; (c) Trial 3; and (d) Trial 4	130
Figure A.4-3. Hole drilled for Trial 1: prestressing strand prevented insertion of blasting nozzle.	131
Figure A.4-4. Insertion of nozzle into the hole opening prior to hydrodemolition in trial 2.....	132
Figure A.4-5. Fitting for hydrodemolition used in trial 3.....	132
Figure A.4-6. Execution of trial 4.....	133
Figure A.4-7. Summary of residual grout after hydrodemolition.....	134
Figure A.4-8. Visual inspection of section 2 after water-blasting	135
Figure A.4-9. Visual inspection of section 3 after water-blasting	135
Figure A.4-10. Visual inspection of section 7 after water-blasting	135
Figure A.4-11. Visual inspection of section 6 after water-blasting	136
Figure A.4-12. Visual inspection of section 7 after water-blasting	136
Figure A.4-13. Consistency of remaining grout below strands	136
Figure B.1-1. Drying of PVC specimens: grout layer distribution	138
Figure B.1-2. Drying of PVC specimens: grout mixture design.....	139
Figure B.1-3. Drying of PVC specimens: details of key cross-section	140

Figure B.3-1. Test results for probe response time for each of the four tests: (a) Test 1 (Specimen ISG); (b) Test 2 (Specimen ISG); (c) Test 3 (Specimen TSG); (d) Test 4 (Specimen TSG).....	143
Figure B.5-1. Corrosion potential evaluation (CPE) chart	145
Figure B.5-2. Calibration of CPE by Post-Tech (Vander Velde, 2002) dry air rating	146
Figure B.5-3. Drying air relative humidity readings over drying period.....	147
Figure B.5-4. RH probe readings at port A (15 PC grout layer).....	148
Figure B.5-5. RH probe readings at port B (15 PC grout layer).....	149
Figure B.5-6. RH probe readings at port C (5 PC grout layer).....	150
Figure B.5-7. RH probe readings at port D (5 PC grout layer).....	151
Figure B.5-8. RH probe readings at port E (15 PC grout layer)	152
Figure B.5-9. RH probe readings at port F (15 PC grout layer)	153
Figure B.5-10. RH probe readings at port A (100 PC grout layer).....	154
Figure B.5-11. RH probe readings at port B (100 PC grout layer).....	155
Figure B.5-12. RH probe readings at port C (5 PC and 100 PC overlap grout layer)	156
Figure B.5-13. RH probe readings at port D (5 PC grout layer).....	157
Figure B.5-14. RH probe readings at port E (100 PC grout layer)	158
Figure B.5-15. RH probe readings at port F (100 PC grout layer)	159
Figure B.6-1. Delta t vs. time for dried specimen ISG	160
Figure B.6-2. Delta t vs. time for dried specimen TSG	161
Figure C.1-1. Schematic drawings of corrosion specimens.....	164

List of Tables

Table 4-1. Soft grout formulation	8
Table 8-1. Sample locations over height of cross-section	21
Table 11-1. Specimen matrix	49
Table 12-1. Color code for wires	52
Table 12-2. Grout mixture details per cubic feet	54
Table 12-3. NaCl quantity per pound	54
Table 16-1. Specimen matrix	65
Table 18-1. Drying timeline.....	75
Table 19-1. pH of grout in corrosion specimens.....	78
Table 19-2. Strand corrosion rating	80
Table 19-3. Number of specimens with unacceptable strand rating	83
Table 19-4. Scale “C” for pitting evaluation	83
Table 19-5. Loss in section and corrosion pit depths.....	84
Table 19-6. Number of specimens with corrosion based on section loss	86
Table 19-7. Comparison of average section loss for specimens with and without admixed chlorides.....	86
Table 21-1. Summary of results from dissection and corrosion measurements	96
Table A.3-1. Mixture proportion for PVC inclined testing	118
Table A.3-2. Mixture proportion for EMT inclined testing.....	120
Table A.3-3. EMT specimen matrix	120
Table A.3-4. Results of soft grout PVC specimens	122
Table A.4-1. Details of hydrodemolition trials.....	129
Table B.2-1. Comparison of ASTM F2170 procedures and adapted procedures	141
Table B.3-1. Tests to determine variation in RH with time.....	142
Table B.5-1. Corrosion Potential Evaluation Grading System	145

Part One—Introduction and Initial Investigations

1 Introduction

Bonded post-tensioned prestressing members typically use bundled prestressing strands that are passed through hollow ducts to apply the prestressing force; this assembly is a post-tensioning tendon. After the tendon is stressed, the ducts are filled with cementitious grout, which is a mixture of portland cement, admixtures, and water. Grout used in post-tensioning tendons, called PT (post-tensioning) grout, provides a bond between prestressing strands and surrounding concrete, which reduces the reliance on stress transfer through anchorages at the ends of girders. The grout also provides corrosion protection for the prestressing strands. Current practice in the U.S. is to use a proprietary prepackaged dry mixture that is delivered in bags in which the dry ingredients are preblended. This avoids the necessity of proportioning the materials on site. Only water dosage must be controlled.

Mid-Bay Bridge in Okaloosa County, Florida, was one of several bridges in Florida detected with corrosion in external post-tensioned tendons (Corven Engineer Inc, 2001; Vigneshwaran & Lau, 2016). Excess water in the grout mixture sealed in ducts and the presence of oxygen was the primary cause of corrosion in Mid-Bay Bridge. These external tendons were replaced to rehabilitate the Mid-Bay Bridge. In 2001, the estimated cost to replace 11 tendons was \$999,680, and the associated engineering cost was \$657,340. Replacing the tendons involved destructive operations on the tendons, such as cutting of strands. This method of rehabilitation was expensive and dangerous to both the bridge and the workers. In addition, this type of rehabilitation cannot be performed on internal tendons with soft grout because that would involve removal of concrete and grout along the entire length of tendon, which is impractical and cost prohibitive.

The discovery of soft grout in a spliced girder bridge with internal tendons prompted the Florida Department of Transportation (FDOT) to investigate possible remediation techniques for the repair of this bridge. Research by the University of Florida in collaboration with FDOT evaluated two possible remediation techniques: hydrodemolition removal of grout and drying of grout. Hydrodemolition was attempted on several mockup tendons, but the technique did not completely remove soft grout and investigation of this technique was terminated. The second technique was to pass air through the tendon to dry the grout. This report covers the testing conducted using both of these techniques to determine their effectiveness at remediating tendons that contain soft grout.

1.1 Report organization

This report is divided into three parts. Part One contains an introduction and background along with the overall scope of work and other topics relevant to the following parts. In addition, Part One contains a summary of the hydrodemolition work and findings. The full details of the work are included in the appendix, but were not included in the main body of the report because the technique was deemed unsuitable for the purpose of grout removal.

Part Two covers the mockup drying tests that were conducted on full-scale tendon mockups fabricated with soft grout. These specimens were subjected to drying to determine if the free moisture from the soft grout could be removed, thus inhibiting the corrosion process that might occur on strands in soft grout. Chapter 6 covers design and fabrication of the mockup specimens. Chapter 7 covers the details regarding the drying system and procedure for monitoring drying progress. The results and findings from the testing of mockup drying tests are covered in Chapters 8 and 9.

Part Three covers the corrosion testing performed on the small-scale corrosion specimens beginning with a brief background discussion in Chapter 10. Chapters 11 and 12 cover details regarding design and construction of the corrosion specimens. Chapters 13, 14, 15, 16 and 17 discuss the details of drying system and procedures of tests performed for the corrosion specimens. Chapters 18, 19, 20 and 21 cover results and findings from the corrosion specimen testing. The final Chapters 22 and 23 provide a summary for both parts of the report along with suggestions for implementation. Full coverage of the hydrodemolition work is included in Appendix A. Appendix B provides details regarding mockup drying tests including RH measurement procedures and instrumentation. Finally, Appendix C provides details regarding drying corrosion tests including detailed drawings and plots of measurements for all specimens performed in part two of this report.

2 Background

Corrosion has been found during inspection of several grouted post-tensioned bridges in Florida (Azizinamini & Gull, 2012). Corrosion was also found in PT (post-tensioned) concrete bridges outside of Florida (Sprinkel & Balakumaran, 2017), (Anania, Badalà, & D'Agata, 2018). Generally, corrosion occurs when the PT grout is, in some manner, deficient. One such deficiency is when all or a portion of the injected grout does not harden (Figure 2-1). Soft grout can form due to several reasons including prehydration of prepackaged grout and addition of excess water on site to increase grout flowability. Prehydration of prepackaged grout occurs due to improper storage of grout bags and premature hydration of cementitious material when in contact with moisture from the surroundings. Segregation and bleed of prehydrated cement or filler following injection can result in layers of unhydrated solids with high moisture content along the length of the tendon. Moisture content has been found to be in the range of 35 to 50% in soft grout (Randell et al. (2015) and (Sprinkel & Balakumaran, 2017)).



Figure 2-1. Deficient grout in PT (post-tensioned) tendon in Sicily, Italy (Anania et al., 2018)

Moisture must be present to support the chemical reaction that results in corrosion. Therefore, high moisture content without the protection of high alkaline hydrated cement matrix can result in corrosion of the prestressing steel. Even with negligible chloride content, high moisture levels can result in a reduction in steel tensile capacity by 11.4% over a twelve-month period due to corrosion (Trejo, Pillai, Hueste, Reinschmidt, & Gardoni, 2009). Trejo et al. also found that if high levels of both chlorides and moisture are present, then steel tendons could lose as much as 27% of their tensile capacity over a twelve-month period. In a bridge in West Point, West Virginia corrosion was found in a concrete bulb-tee girder at locations with soft grout (Sprinkel & Balakumaran, 2017). During inspection of the Mid-bay Bridge in Florida, corrosion was found along with bleed water and soft grout (Corven Engineer Inc, 2001). Soft grout also has low compressive strength due to high moisture content, which can prevent the transfer of load from internal tendons to adjacent concrete. Therefore, soft grout with its characteristic high moisture content is a major concern.

3 Research approach

Corrosion problems discovered in grouted multi-strand, post-tensioning tendons used in bridge construction have led to the discovery of defective grout in a number of PT concrete bridge structures in the U.S. and abroad. Remediation of such tendons is particularly difficult and expensive if significant corrosion is expected to occur. In this research, two techniques, namely, hydrodemolition and drying were evaluated for remediation of soft grout. First hydrodemolition was performed on a 38.25-ft-long mockup tendon specimen made from 4 in. diameter electrical metal tubing (EMT). This specimen was shaped to simulate the negative bending region of an internal PT tendon. Further, to simulate grout segregation observed in tendons with soft grout, the high elevation region of the specimen was filled with soft grout and lower elevation ends were filled with normal grout. Soft grout mixtures were prepared based on previous studies (Randell, Aguirre, & Hamilton, 2015) using cement and filler material (ground dolomite limestone). Personnel from a company specializing in hydroblasting conducted the hydrodemolition. Hydrodemolition involved high-pressure injection of a water jet inside the duct to loosen and remove both normal and soft grout. A discharge hole was drilled into the EMT to facilitate removal of the debris. After performing several planned trials of hydrodemolition, the specimen was dissected to determine the effectiveness of hydrodemolition in removing the various formulations of grout.

To evaluate the effectiveness of drying, four 31-ft-long, 4-in.-diameter tubular specimens were constructed (Figure 3-1). These specimens were filled with soft grout mixtures prepared using cement and filler material (ground dolomite limestone). A drying system consisting of a compressor and a desiccant dryer was set up to produce dehumidified air. Each specimen had an inlet and outlet to maintain flow of dehumidified air. Relative humidity (RH) of air discharged at the outlet was measured at regular intervals to monitor the drying process. Once the RH of the outlet air was reduced to that of the inlet air, drying was terminated, and specimens were dissected. For comparison, non-dried control specimens, which were replicates of the dried specimens, were also constructed and dissected at the same time as the dried specimens. Moisture content of grout samples collected from control and dried specimens was used to determine the effectiveness of the drying technique. RH readings collected during drying were further analyzed to determine the criteria for termination of drying.

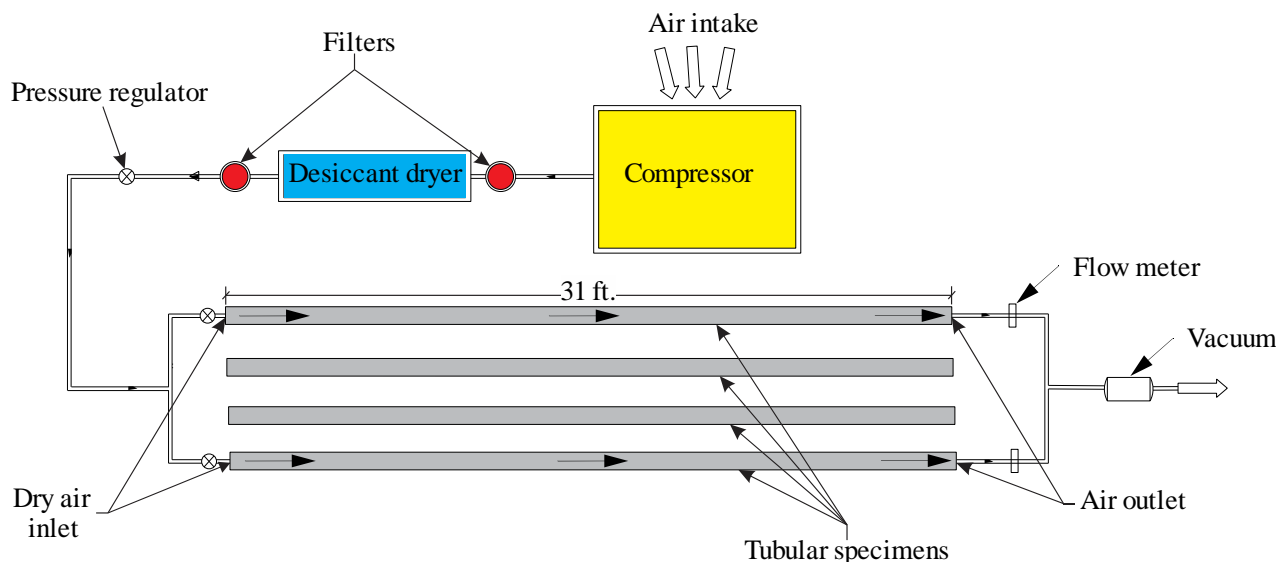


Figure 3-1. Drying test setup

During dissection of dried mockup specimens, corrosion was found on strands. Therefore, additional testing was performed to investigate if drying resulted in corrosion and if dried grout prevents propagation of corrosion. For this, one-foot long corrosion specimens filled with varying grout mixtures were fabricated and dried. Corrosion activity was monitored during and after drying using corrosion potential measurements to detect corrosion due to drying. Additionally, macrocell current was monitored in specimens after drying to determine if the corrosion process stopped after grout was dried. The corrosion specimens were finally dissected in two rounds after drying to quantify and evaluate the strand corrosion.

4 Soft grout mixture design

Prior to testing, it was necessary to develop materials and procedures that were to be used to produce grout with fresh and hardened characteristics consistent with soft grout observed in the field. Soft grout physical characteristics consisted of high moisture content (35% to 50%), segregation, and bleed. The grout mixture formulations were based on results from a previous study (Randell et al., 2015). Randell et al. (2015) found that mixes with more than 45% replacement of portland cement with ground limestone and water-solids ratio (w/s) more than 0.45 resulted in grout with physical characteristics consistent with soft grout. The grout mixtures for this research were formulated using portland cement, non-reactive filler (ground dolomite limestone), and water with w/s of 0.46. Additional testing that evaluated the change in cube compressive strength of each grout mixture was also conducted.

Trial mixtures of portland cement (PC) and ground limestone were developed for use in producing combined layers of normal grout (100 PC) and various soft grouts (40 PC, 30 PC, etc.) in the specimens. The nomenclature for identity (ID) of each grout mixture was based on the percentage of portland cement (PC) present in each mixture. For example, the 5 PC mixture consisted of 5% portland cement and 95% ground limestone. Seven trial specimens with varying mixture proportions (Table 4-1) were tested at the University of Florida to determine the characteristics of the soft grout relative to the proportion of portland cement used. The specimens were three-foot-long and were positioned at an angle of approximately 30° from horizontal (Figure 4-1). The mixtures shown in the Table 4-1 were prepared in a five-gallon bucket using a hand drill and paddle mixer. These mixtures were developed with the hypothesis that reducing the relative proportion of portland cement, while simultaneously increasing ground limestone, would produce grout that exhibited very low compressive strength and had the physical consistency and moisture content of that found in the field.

The mixtures were prepared by measuring water into the bucket followed by portland cement and finally ground limestone. The mixture was mixed for at least one minute and then immediately poured into the open end of the tube at the top of the incline. The end was then covered to prevent evaporation. At 24 hours, the cover was removed and a ¼-in. threaded rod was pushed into the grout from the open end of the tube to determine the total length of the grout column that had not hardened. This measurement was recorded and used as a direct measure of the volume of soft grout produced (Figure 4-2). The maximum possible length of grout was approximately 20 in. The plot shows that a small and constant amount (~3") of grout formed over a wide range of portland cement content (10 to 40% by mass). Only when the relatively quantity of PC fell below 10% did the volume of unhardened grout increase significantly. After using the rod to measure the length of unhardened grout, selected specimens were cut open to examine the physical characteristics of the grout (Figure 4-3). The resulting grout was found to have high moisture content and a putty-like feel when handled.

Table 4-1 shows that compressive strength decreased as the cement percentage decreased indicating that reduced hydration and more bleeding occurred as the limestone filler percentage increased. 5 PC had the second least cement percentage, which led the formation of grout with the most moisture content, while 100 PC had least moisture content. 40 PC, 30 PC, 15 PC and 5 PC grout were used to construct hydrodemolition specimens to produce grout with varying strength along the length which was expected to be found in bridge tendons. On the other hand, only 100 PC, 15 PC, and 5 PC were selected for use in the drying test specimens to evaluate the efficiency of drying on 5 PC grout with most moisture content in presence of denser 15 PC and 100 PC grout in the vicinity.

Table 4-1. Soft grout formulation

ID	Portland Cement (lb/ft ³)	Ground Limestone Filler (lb/ft ³)	Water (lb/ft ³)	Compressive Strength (psi)	Moisture Content (%)
100 PC	78.3	0.0	36.4	8,789.3	16.4
40 PC	30.9	47.2	36.5	1,464.9	-
30 PC	23.5	54.6	36.5	1,406.9	-
15 PC	12.0	66.6	36.6	275.6	21.0
10 PC	8.1	70.5	36.6	116.0	27.3
5 PC	3.9	74.2	36.7	29.0	27.6
2.5 PC	2.0	76.6	36.7	-	



Figure 4-1. Mini-inclined testing

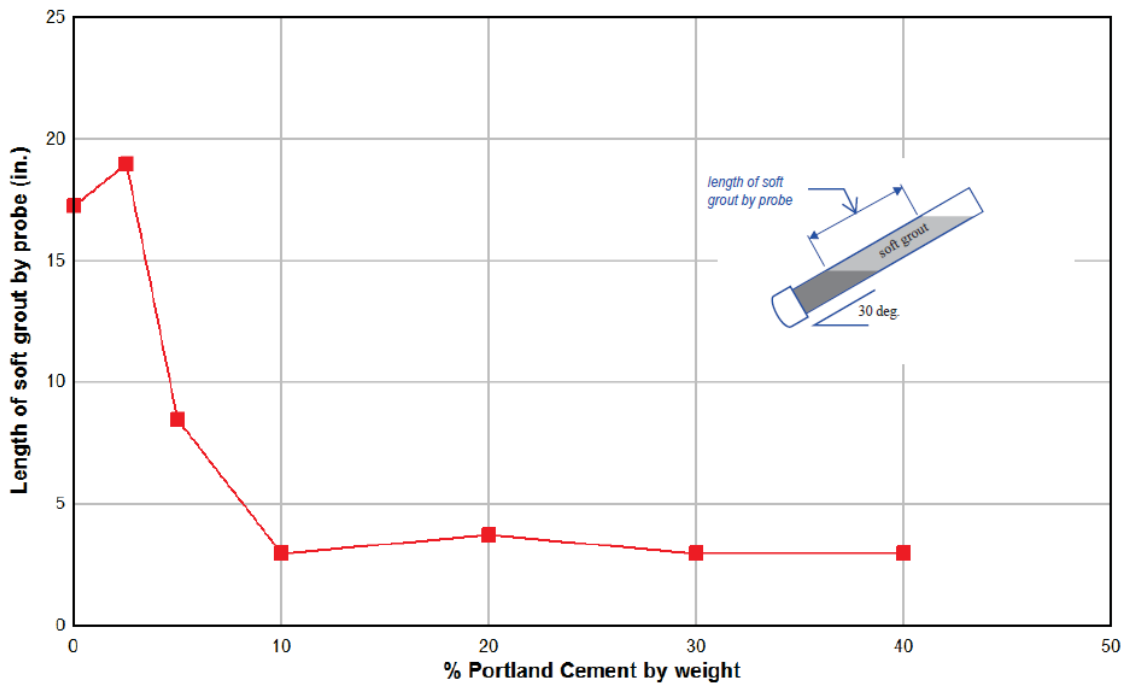


Figure 4-2. Length of soft grout versus percentage of portland cement in soft grout mixture



Figure 4-3. Dissection of tube for mini-inclined testing

5 Hydrodemolition remediation tests

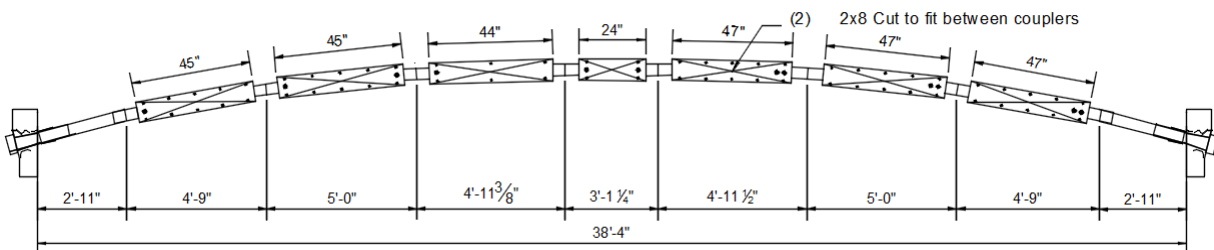
This section of the report provides a summary of the hydrodemolition tests along with the results of the testing. Because the testing showed that the technique did not remove the grout in a satisfactory manner, only a brief description of the testing and results is included in this section. Further information including detailed procedures and results are given in Appendix A.

Hydrodemolition involved blasting and removal of soft grout from a PT tendon by directing a high-pressure water jet into the interior of the PT tendon duct. To evaluate hydrodemolition, a specimen was designed to simulate a tendon in the negative moment region (over a support) of a post-tensioned continuous beam (Figure 5-1). The specimen was constructed using electrical metal tubing (EMT), which was intended to simulate a metal post-tensioning duct. The tubing had a nominal outside diameter of 4 in. and nominal wall thickness of 0.08 in. Nineteen 0.6-in. seven-wire low-relaxation strands were bundled and placed in the EMT. Each strand was prestressed to a force of approximately one kip. To simulate the restricted access that would be caused by the girder concrete surrounding the tendon in field conditions, two pieces of 2x8 timber were attached to the sides of the EMT. To start hydrodemolition, holes were drilled through the wood to access the EMT. The specimen was assembled on the steel frame located at the FDOT Structures Laboratory and had a total length of 38.3 ft with 8 supports between the anchors. The frame was designed to accommodate the EMT with an angle of 14° at each end of the frame.

Multiple grout layers were placed in this specimen as shown in Figure 5-2. Denser grout layers such as 30 PC and 40 PC with higher cement content were poured near the ends of the specimen, while less dense grout was poured in the elevated middle region of the specimen. The intent of such placement was to simulate the layered effect of grout segregation observed in bridge tendons.



(a)



(b)

Figure 5-1. Hydrodemolition specimen: (a) EMT before installation of 2x8; (b) schematic figure with location of 2x8

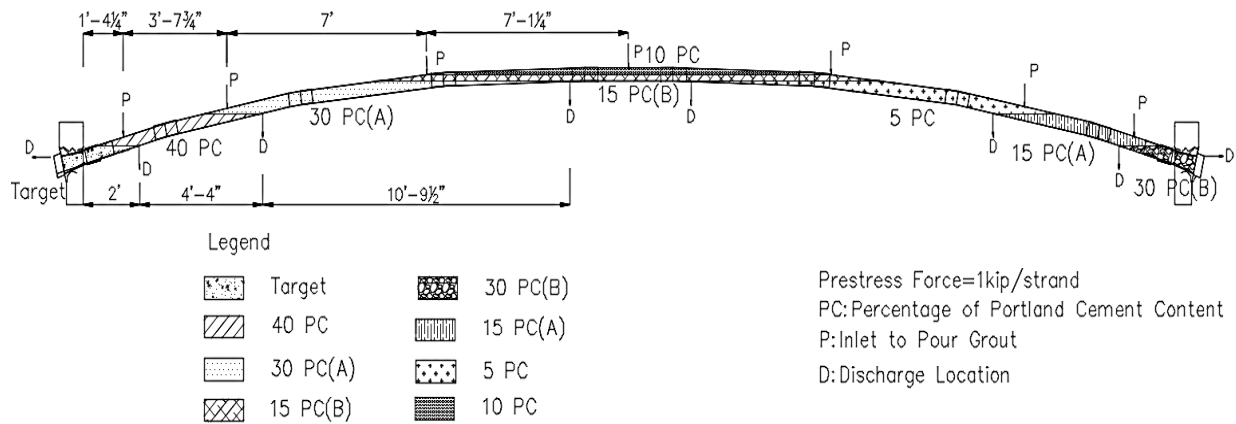


Figure 5-2. Grout layers used in hydrodemolition specimen

Hydrodemolition was performed using three different procedures with varying configurations of water injection and debris discharge hole locations. The conduit length was divided into sections to isolate each method (Figure 5-3). The first method consisted of drilling a water injection hole at one end of a section to inject the pressurized water with a discharge hole placed at the other end of the section; the holes were 40 in. apart. The second method was similar to the first method but had the water injection hole and discharge hole on opposite sides of the conduit. The third method consisted of drilling injection and discharge holes 3 in. apart, allowing debris to flow back out of a hole that was placed in close proximity to the injection hole. This was thought to provide a more practical approach in the field since both operations could occur on the same side of the girder web. A specially fabricated nozzle was used for the hydrodemolition procedure.

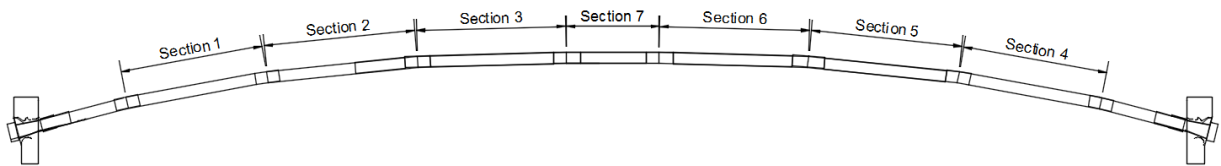


Figure 5-3. East elevation of mockup section identification

During hydrodemolition, determining the correct location to drill the inlet hole was difficult due to the distribution of the strands inside the conduit. Nozzles used for hydrodemolition became lodged between the strands, and between strands and duct. On dissection of the mockup specimen, it was noted that some grout was not completely removed. In some cases, large quantities of grout were left in the duct due to the inability to navigate the water jet around the prestressing strand bundle and into positions in which the grout could be blasted. In sections where grout was removed from above the strand bundle, residual grout was found trapped between strands, and also between strands and the conduit wall. The residual grout after hydrodemolition was visually observed to be moist. Based in these results, the hydrodemolition technique used to remove the grout was found to be ineffective and testing was terminated.

Part Two—Mockup Drying Tests

6 Drying

This portion of the report describes the implementation of drying to remediate the defective grout. Dry air has been shown to remove chemically unbound moisture from unbonded single-strand tendons in parking garages (Vander Velde, 2002). Removal of moisture is thought to reduce the rate of corrosion and increase grout resistivity (López & González, 1993). For unbonded tendons, the technique involves passing dry nitrogen gas through greased and sheathed unbonded, single-strand tendons, and measuring relative humidity and temperature of gas at the outlet of the cable to determine corrosion potential of the tendons. In the case of grouted internal tendons, drying involved pumping air through tendons filled with soft grout to remove unbound moisture and dry the soft grout.

6.1 Specimen design

To test the use of drying on grouted PT tendons, four 4-in. diameter PVC pipe specimens were constructed and injected with multiple layers of grout to evaluate the effectiveness of drying (Figure 6-1). Each specimen was approximately 31 ft long and was constructed by assembling three 8-ft-long PVC sections. Fifteen 0.6-in. 7-wire low-relaxation strands were placed, unstressed, in the specimens. The specimens were designed to represent a typical tendon profile at support sections of bridge girders where soft grout was typically found in affected bridges. The specimens were positioned at a slope of 5 deg. to simulate the slope of a draped PT tendon. Detailed drawings for specimens are provided in Appendix B (Figure B.1-1 through Figure B.1-3).

A 4-in.-dia. tee with HDPE tubing was installed at each end to act as air inlet and outlet (Figure 6-2). A PVC tee fitting was placed at each end to facilitate connection of air fittings and ensure the continuous passage of air through the specimen during drying (Figure 6-3).

Two grout configurations were tested (Figure 6-4). The first configuration had alternating 5 PC and 15 PC soft grout layers and was designed to evaluate drying of tendons containing isolated soft grout (labeled “Isolated Soft Grout” ISG in Figure 6-4). The second configuration had alternating 5 PC and 100 PC layers and was used to study the effectiveness in drying of soft grout trapped between normal grout layers (labeled “Trapped Soft Grout” TSG in Figure 6-4). Normal grout has lower porosity than soft grout and was anticipated to obstruct air flow and slow moisture removal. Two identical specimens were constructed for each configuration for a total of four specimens. One specimen of each configuration was dried, and one was held as a control. To monitor the drying of each grout layer, two ports were drilled through the PVC and into each grout layer for measurement of relative humidity using humidity probes and a concrete moisture meter (see “RH” in Figure 6-4).



Figure 6-1. Fully assembled specimens with downward angle of PVC tee



Figure 6-2. HDPE connection at PVC tee of inlet



Figure 6-3. Soft grout removed at PVC tee inlet and outlet

RH - Location of holes drilled in specimens

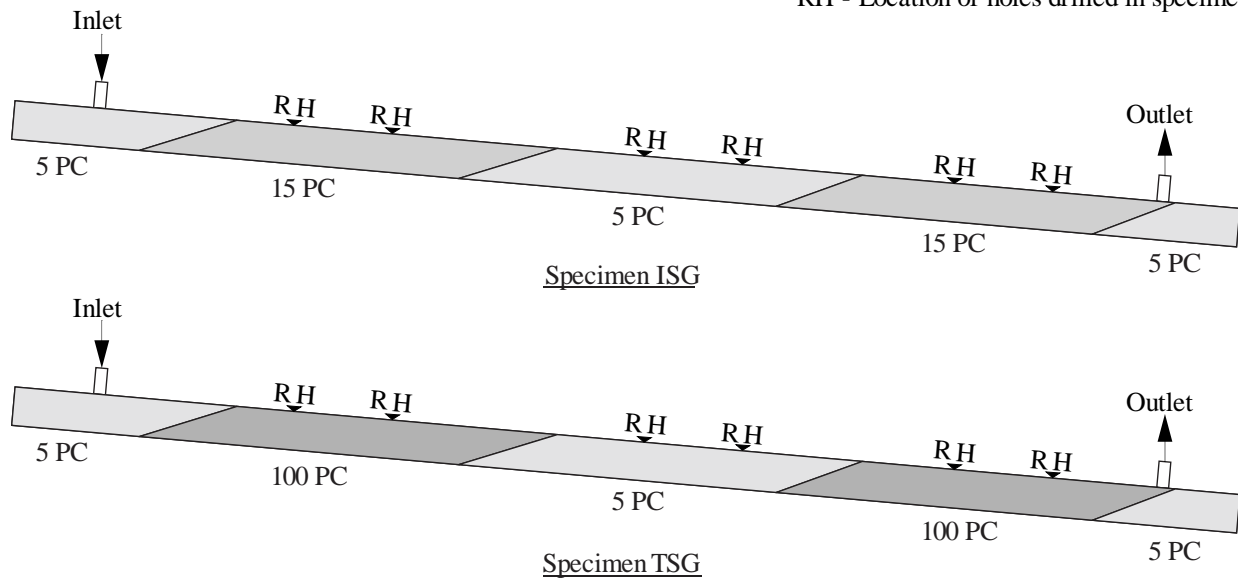


Figure 6-4. Mockup specimens for drying with RH measurement locations shown

6.2 Specimen fabrication

Grout mixtures were prepared using portland cement, ground limestone filler, and water. These components were added to a plastic container and mixed using a paint mixture and power drill (Figure 6-5). Grout was poured into the specimen through a PVC tee installed at the elevated end of each layer (Figure 6-5). Placement was terminated when the PVC layer was filled (Figure 6-6 and Figure 6-7). Grout was allowed to cure for 21 days before drying was commenced.



Figure 6-5. Preparation of grout mixture



Figure 6-6. Grout mixture placed into specimen through funnel and PVC tee



Figure 6-7. PVC tee through which grout was introduced

7 Drying system and procedures

The drying system injected dried, pressurized air into the upslope end of the specimens; this air flowed through the specimen and was discharged at the opposite end (Figure 7-1). The drying system was designed to generate dry air with relative humidity (RH) less than 10% and was composed of a compressor, desiccant dryer, and filters. A pressure regulator was used to reduce the inlet air pressure to about 20 psi to prevent leaks through joints in specimens.

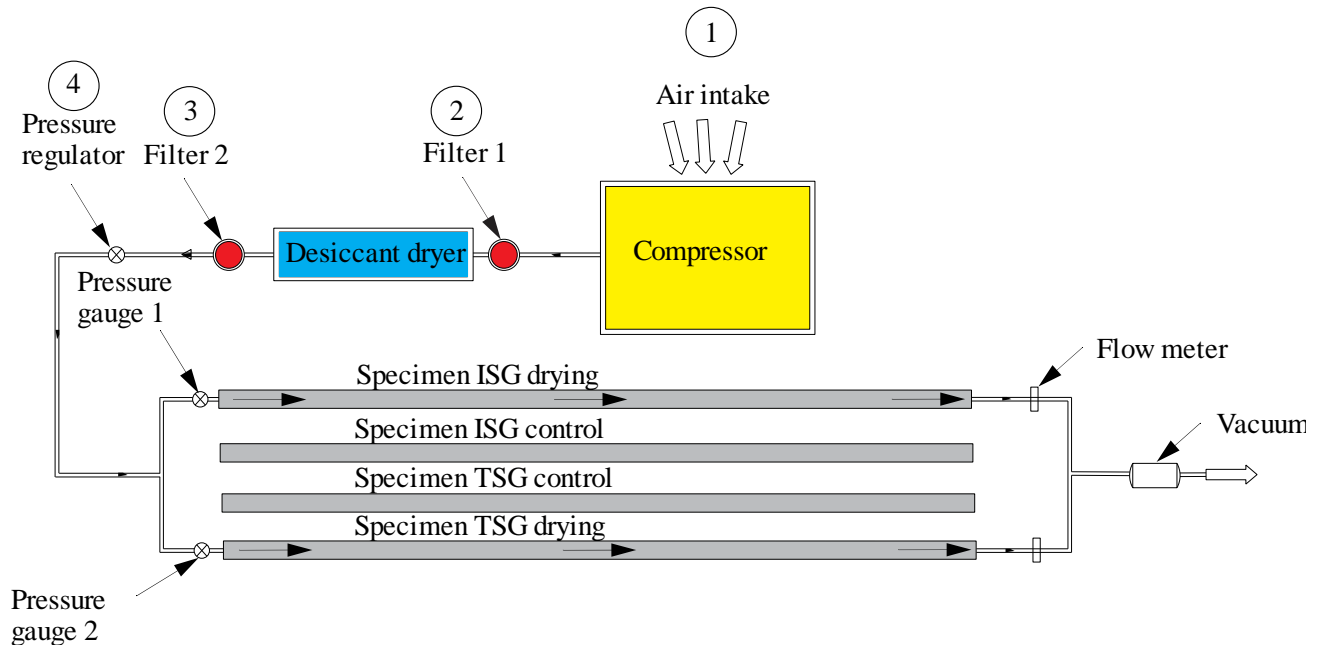


Figure 7-1. Layout of drying equipment

Drying was initiated near the end of November 2016 and was continued until late May 2017. Total drying time, including downtime, was approximately 177 (~26 weeks) days for specimen ISG and 182 (~27 weeks) days for specimen TSG. Initially, there was negligible flow of air at the exit of the specimens. Therefore, after three weeks of drying, a vacuum pump was connected to the exit on specimens to increase air flow. To improve the performance of the desiccant dryer, the pressure regulator was moved from inlet to outlet of the dryer after 8 weeks of drying. Drying equipment was regularly monitored and maintained during the entire drying period. At the same time, probes used for measuring RH of grout were calibrated as per manufacturer's guidelines. Relative humidity (RH) measurements early in the drying process were generally above 90%, which eventually resulted in damage to some the probes; they were replaced after approximately 15 weeks of drying.

RH of the inlet and outlet air was used to monitor the drying progress of specimens. In addition, RH was measured inside the grout through ports drilled in the PVC at selected locations along the specimen length. The change in measured RH of drying air from inlet to outlet of specimens was defined as change in drying air RH (ΔRH_d). RH of grout measured inside ports drilled into the specimens was defined as grout RH (RH_g) (Figure 7-2). Figure 7-3 shows measurement locations of ΔRH_d and RH_g readings. ΔRH_d was measured at least once each month and RH_g was measured at least twice each week. A Vaisala DM70 hand-held dewpoint meter was used to measure ΔRH_d (Figure 7-4) and a Tramex CMEXpert was used to measure RH_g . Appendix B provides detailed procedures for both RH measurements.

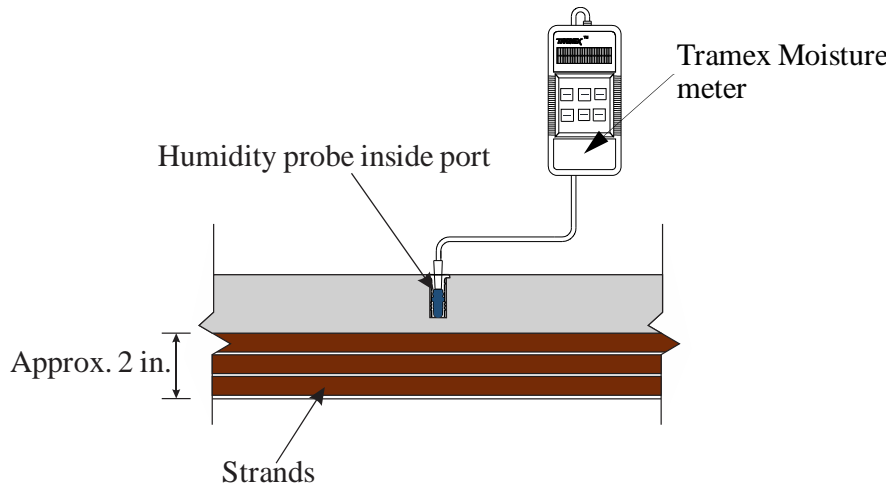


Figure 7-2. RH_g measurement

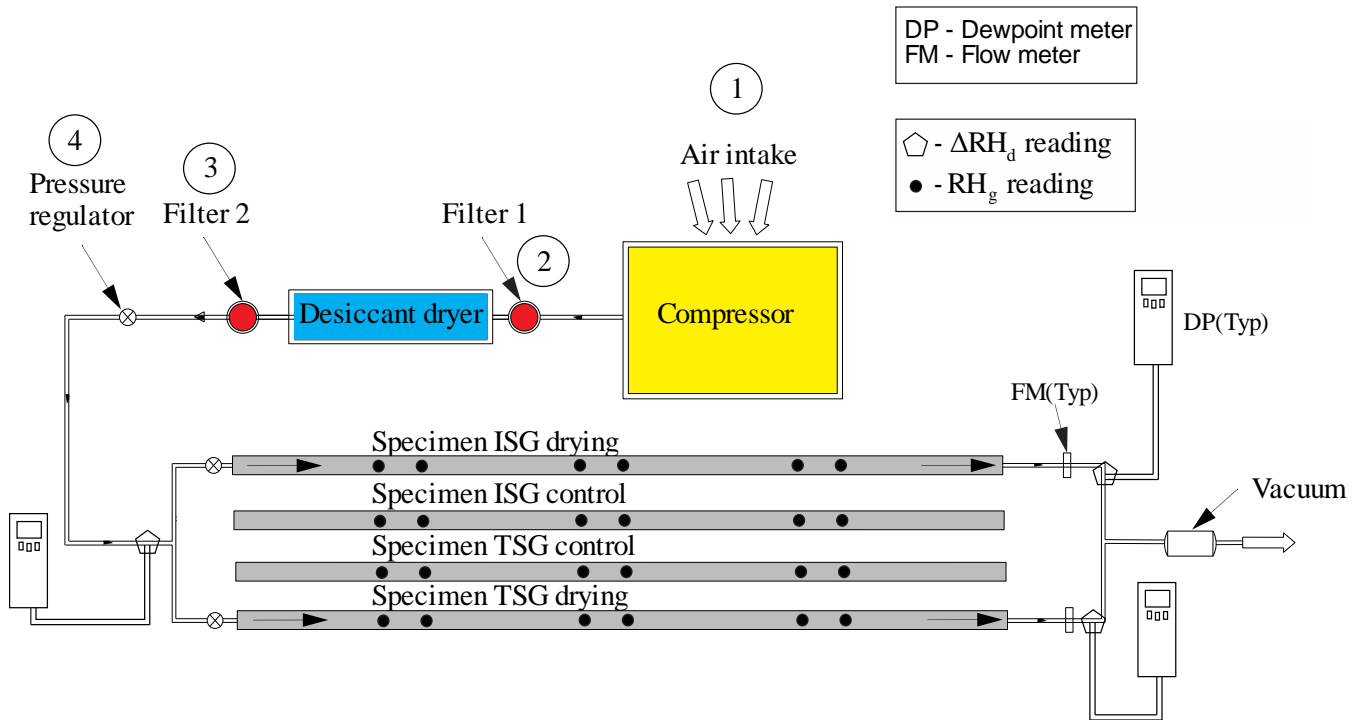


Figure 7-3. Location of readings

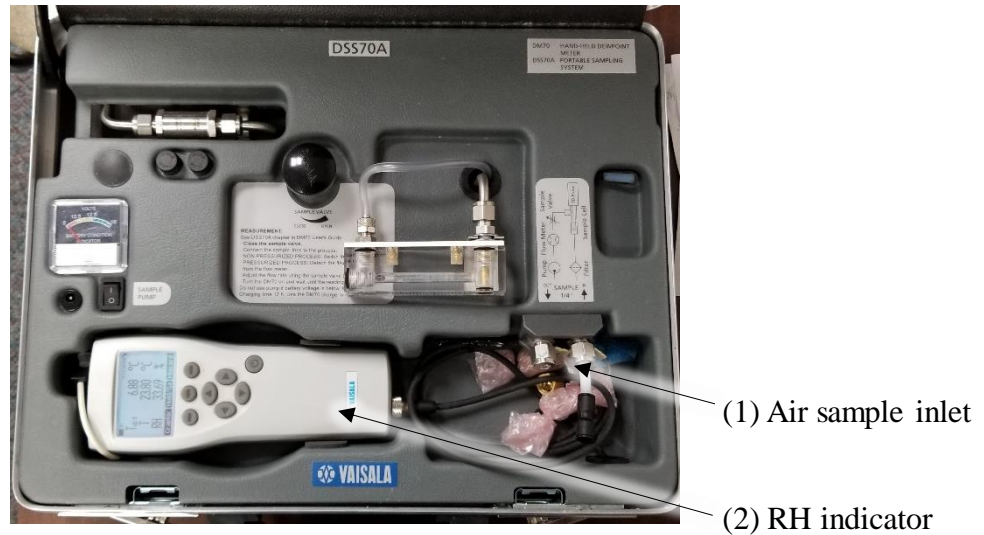


Figure 7-4. Vaisala DM70 hand-held dewpoint meter

Along with monitoring drying progress, ΔRH_d readings were taken to determine if significant free moisture remained in the specimen. The following procedure was used for this dryness check:

1. Turn off drying equipment.
2. After resting for at least 12 hours, restart the drying equipment.
3. Measure ΔRH_d immediately when equipment is restarted and note the reading as ΔRH_{di} .
4. Measure ΔRH_d two hours after restarting the equipment and continuous drying. Note this reading as ΔRH_{df} . If ΔRH_{df} is not measured at exactly two hours after restarting of drying, it is calculated based on interpolation of RH readings measured before and after the second hour of drying.

The specimens were deemed to be dry when ΔRH_{df} was equal to ΔRH_{di} with a tolerance of +5% due to possible leaks in specimens.

8 Results and discussion

8.1 Dissection

After drying was terminated, specimens were dissected for evaluation. Dissection of dried specimens was directed toward measuring moisture content for comparison and possible calibration with the ΔRH_d and RH_g . During dissection, however, localized corrosion of prestressing strand was discovered. The procedures and findings are documented in this chapter.

Both control and dried specimens were dissected after drying. Dissection occurred 176 days and 179 days after drying started for ISG and TSG specimens, respectively.

To determine the most appropriate techniques when cutting and sampling, trial specimens were dissected using a circular saw, chisel, and hammer. Trial dissection showed that heat generated due to use of circular saw caused loss of moisture in soft grout (5 PC and 15 PC) samples, resulting in reduced measured moisture content. Based on this finding, grout samples were planned to be collected at least 4 in. away from saw cuts. Trial dissection also showed that moisture content of grout varied over the height of the specimen cross-section. Therefore, samples were collected at varying locations over the height of the cross-section. Results obtained from the trial dissection guided the development of the following procedures for the dissection of specimens:

1. Mark 1-ft sections on PVC pipe of specimens for cut.
2. Cut the top half semi-circular portion of PVC pipe at the specified locations with saw blade or rotozip as needed.
3. Remove PVC to access grout.
4. Figure 8-1 shows the 1-ft long segment cut from the specimen. Grout from the inner 4-in. length of this piece was sampled at the hatched locations shown in Table 8-1. For 100 PC grout, use a circular saw and chisel to gather samples. For 15 PC and 5 PC, collect samples using a hack saw and chisel.
5. Immediately place the grout sample in an aluminum foil container and measure mass.
6. Place the grout sample in oven until mass has stabilized. Follow ASTM C566 – 13 and ASTM D2216 – 10 to measure MC of grout samples.
7. Compute moisture content based on the change in mass after oven-drying.

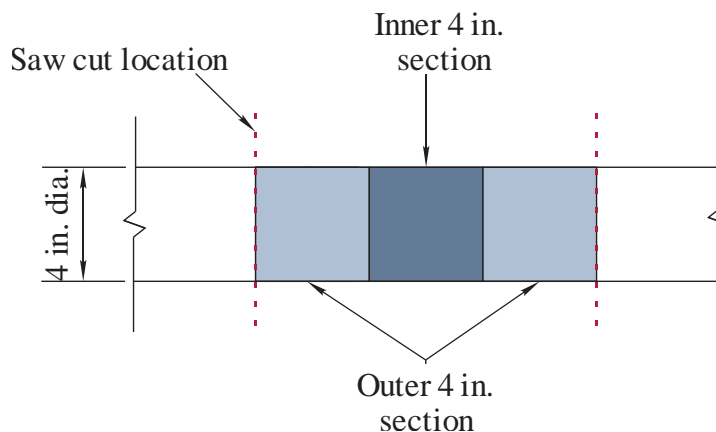


Figure 8-1. Three divisions of 1-ft-long exposed section. Samples were collected from the inner 4-in. section.

Table 8-1. Sample locations over height of cross-section

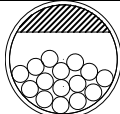
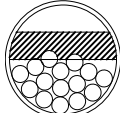
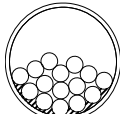
Grout section	Section label
	Top
	Bottom
	Below the strands

Figure 8-2 shows the sampling locations for grout in specimens ISG and TSG relative to the RH port where RH_g was measured. Grout samples were collected during dissection, and immediately weighed prior to placing them in the oven to determine their moisture content.

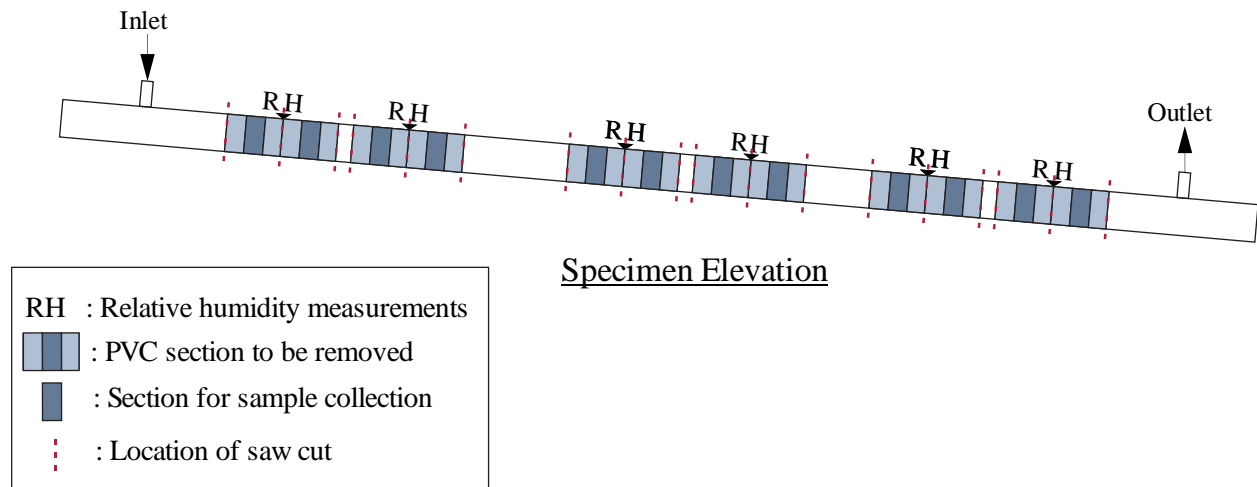


Figure 8-2. Dissection schematic

As shown in Figure 8-3, all specimens were dissected by cutting through the top half of the PVC pipe using a circular saw. The PVC was cut for a length of one foot on each side of the RH ports. After removing the PVC from the top, soft grout samples were collected from the central 4-in. section of the exposed area using a hack saw, chisel, and hammer (Figure 8-4). In addition to these tools, a circular saw was used to remove normal 100 PC grout (Figure 8-5).

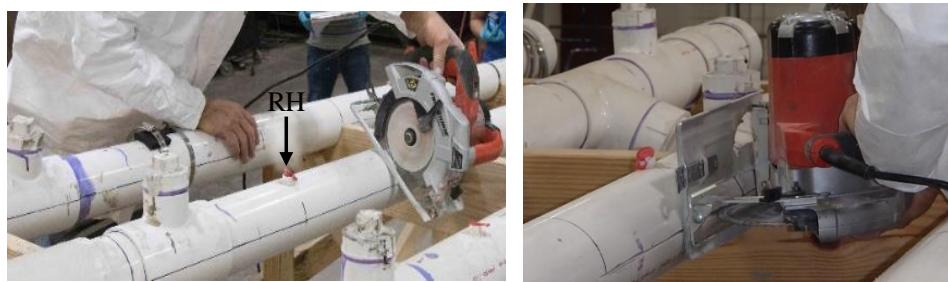


Figure 8-3. Removal of PVC with circular saw

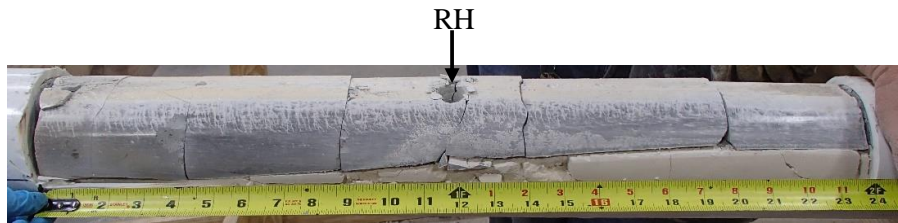


(a)



(b)

Figure 8-4. Sampling of soft grout: (a) Hacksaw, hammer, and chisel used to remove soft grout; (b) Section after removing soft grout



(a)



(b)

Figure 8-5. Sampling of normal grout: (a) Cracks in 100 PC grout layer at approximately 4-in. spacing; (b) Section after removing normal grout

8.1.1 ISG observations

As mentioned previously, drying and control ISG specimens were fabricated with layers of 5 PC and 15 PC grout (Figure 6-4a). By means of visual inspection after dissection, the grout in the dried specimen was deemed dried, while the grout in the control specimen was considered wet. In this context, soft grout is considered dry when it can easily crumble into individual particles or dust (Figure 8-6) and moisture is not obviously present. Wet grout was moldable like wet clayey sand (Figure 8-7) and left a moisture residue on fingers after handling.



Figure 8-6. Soft grout crumbled with hand



Figure 8-7. Soft grout as wet clayey sand

Upon removal of the top portion of the PVC pipe, it was noted that the top surface of the grout had pores, probably due to bleeding of water for both control and drying ISG specimens (Figure 8-8). In the dried specimen, shrinkage cracks were present on the surface, but the control specimen had no visual indication of shrinkage cracks.



Figure 8-8. Pores on grout surface

The 5 PC grout layer in the short length between the end caps and the air inlet or outlet ports (Figure 8-9) appeared to be dry similar to the remaining 5 PC layer in the specimen. From this observation, it can be concluded that the drying method was able to remove some moisture from the grout for a length of approximately 1 ft upstream from the air inlet and downstream from the air outlet even though air was not directed through it. Moisture content (MC) measurements of grout in these areas, however, indicated that the moisture had not been removed as effectively as the grout between the inlet and outlet points.



Figure 8-9. End caps and outlet port on specimens

8.1.2 TSG observations

Specimen TSG consisted of soft grout (5 PC) sandwiched between two layers of normal grout (100 PC) (Figure 6-4b) and was visually determined to be dry. Additionally, soft and normal grout in the dried specimens had shrinkage cracks indicating removal of moisture (Figure 8-10).

Similar to the ISG specimen, soft grout (5 PC) in the area between the end caps and the air inlet and outlet were visually noted as dry. Indicating that some of the moisture was removed from the grout for a length of approximately 1 ft upstream from the air inlet and downstream from the air outlet even though air was not directed towards it. Moisture content (MC) measurements of grout in these areas, however, indicated that the moisture had not been removed as effectively as the grout between the inlet and outlet points.

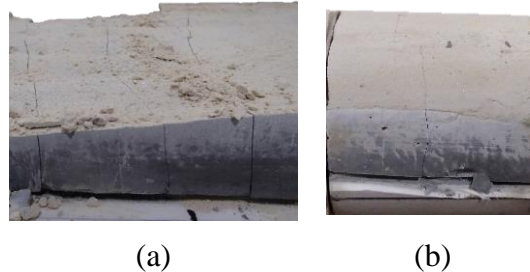


Figure 8-10. Shrinkage cracks: (a) Normal grout; (b) Soft grout

8.1.3 Corrosion observations

During dissection, sampling, and inspection of specimens, the prestressing strands were uncovered and systematically evaluated visually for the presence of corrosion. During visual evaluation, corroded strands were found predominantly in specimens subjected to drying (Figure 8-11). Corrosion was found in larger quantities on the peripheral strands of the tendon. The location of corrosion found on the tendon is shown in Figure 8-12.



Figure 8-11. In situ corroded strands near port C dried TSG specimen

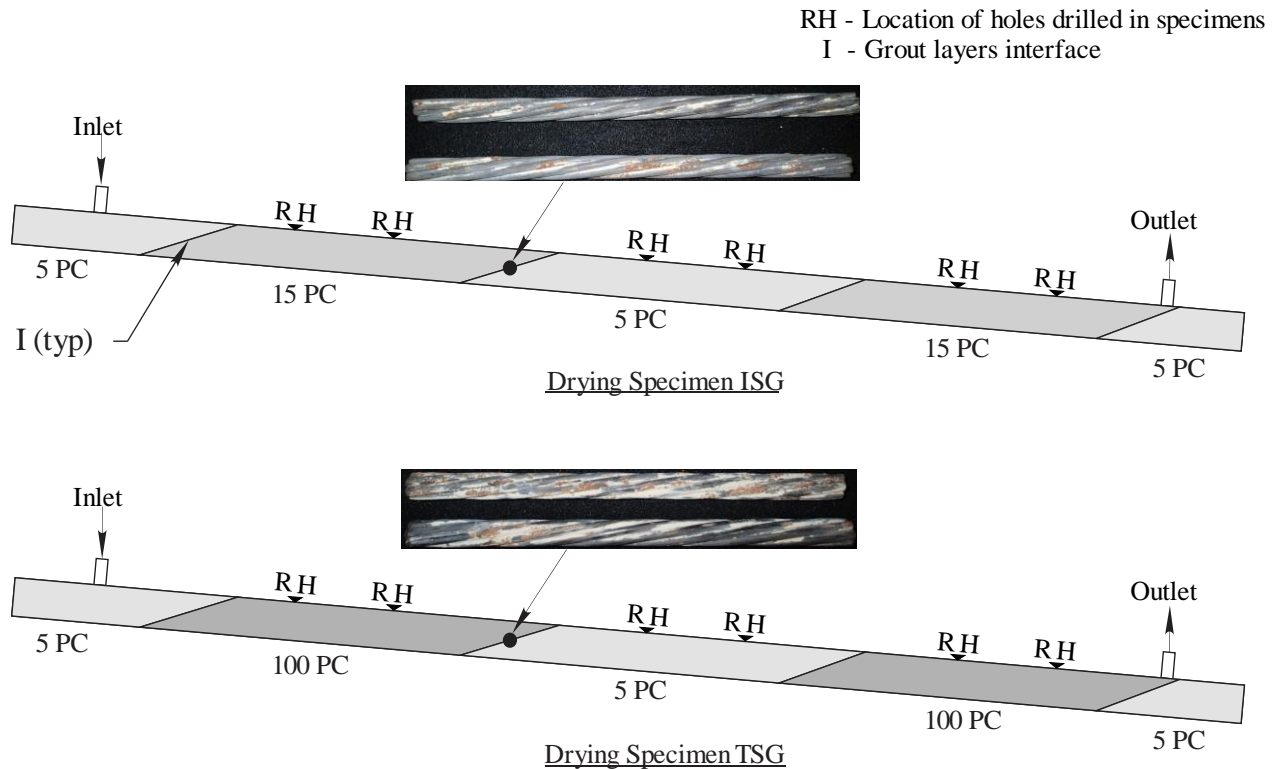


Figure 8-12. Location of corroded strands in the dried specimens

Corrosion was thought to occur due to the formation of a macrocell which was driven by the difference in physical and chemical properties between the two grouts at the interface. Each grout type was different due to different proportions of cement and filler (dolomite limestone) in their mixture designs. On reaction with water, cement forms portlandite ($\text{Ca}(\text{OH})_2$) and keeps the pH of grout over 11. Limestone, however, does not react with water to help increase pH of the grout. Therefore, the 5 PC grout, which had the lowest cement percentage content and highest percentage of limestone, was assumed to have a lower pH compared to its companion grout type in each specimen.

The corrosion process was likely promoted by carbonation of grout through exposure to drying air. Carbonation is a chemical reaction between portlandite ($\text{Ca}(\text{OH})_2$) in the cement matrix with carbon dioxide (CO_2), resulting in formation of calcite (CaCO_3) and depletion of hydroxyl ions (OH^-) (Zhou, Gencturk, Willam, & Attar, 2014). The depletion of hydroxyl ions lowers the pore water pH from above 12.5 to below 9.0. At pH below 11.0, the passive layer on

steel becomes unstable, and corrosion occurs if sufficient water and oxygen are present (Heiyantuduwa, Alexander, & Mackechnie, 2006). In the drying process, both carbon dioxide and oxygen were supplied by the drying air. This, along with the excess moisture available in soft grout, resulted in corrosion.

Although unconfirmed experimentally, it is hypothesized that a macrocell formed in the dried specimens at the locations where the corrosion was most severe (Figure 8-13). The top layer in this region was less porous than the underlying 5 PC grout layer, resulting in slower drying rates in the top layer than the bottom 5 PC layer. Differential drying may have resulted in a moisture gradient between the two grout layers, which caused 5 PC grout to draw moisture from the top layer. At the same time, the dried pores in 5 PC allowed oxygen from air to reach the strands. Thus, corrosion-driving forces, including oxygen and moisture, were available in the corrosion macrocell along with carbonated grout resulting in the local corrosion found in the dried specimens (Figure 8-13 and Figure 8-14). TSG (Figure 8-15) exhibited more corrosion than ISG (Figure 8-14 and Figure 8-15). TSG had a more severe environment than ISG during drying due to the greater moisture gradient between 100 PC and 5 PC grout layers than between 15 PC and 5 PC layers.

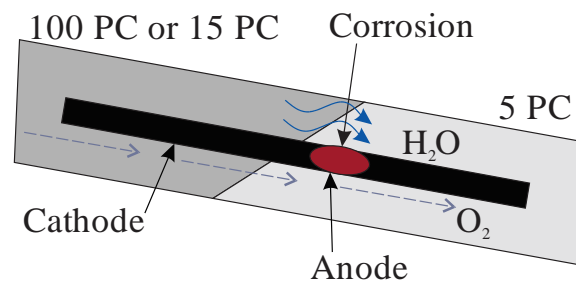


Figure 8-13. Macrocell formation on peripheral strands of tendon



Figure 8-14. Corroded strands near port C dried ISG specimen



Figure 8-15. Corroded strands near port C dried TSG specimen

Control specimens, on the other hand, had less corrosion than the dried specimens or no corrosion at all. The cause of corrosion in control specimens was thought to be due to the presence of bleed water, dissolved oxygen, and varying physical (porosity) and chemical (pH) properties of grout along the length of specimens. However, no drying air was present to carbonate the grout and saturated conditions likely reduced the diffusion of oxygen resulting in slower corrosion rates in control specimens than in the dried specimens. Thus, little or no corrosion was found during dissection of control specimens (Figure 8-16 and Figure 8-17).



Figure 8-16. Corroded strands near port C control ISG specimen



Figure 8-17. Non-corroded strands near port C control TSG specimen

Corrosion was also present in the lower 15 PC layer in the dried specimen ISG which could have been due to dry air pushing moisture towards downstream end of specimen, meaning that moisture was available for longer time at this end. However, this corrosion was less severe than corrosion in 5 PC grout layer and was predominantly present in lower strands on the outer surface (Figure 8-18).



Figure 8-18. In situ corroded strands at: (a) port E; (b) port F dried ISG specimen

8.2 Moisture content

As mentioned previously, the drying process involved removal of excess free moisture from soft grout by using dry air. Therefore, to evaluate the effectiveness of drying, grout samples were collected during dissection to determine grout moisture content. This chapter discusses details of this moisture content (MC) testing. ASTM C566 (2013) and ASTM D2216 (2010) were followed to measure MC of grout samples. Samples of grout, weighing in the range of 30 to 550g, were collected during dissection and oven-dried overnight at 110°C (Figure 8-19). Preliminary tests indicated that sample weight equilibrated in less than 24 hours. Weight lost due to oven drying was used to compute grout MC at different locations along the specimen.



Figure 8-19. Oven drying of grout samples

8.2.1 ISG results

Figure 8-20 shows the variation of the moisture content (MC) measurements along the length of the ISG for both the control (solid markers) and dried specimens (hollow markers). Moisture content in the dried specimen was negligible (<1% by mass) compared to that measured in the control specimen, apart from the measurement taken at the lower end of the slope beyond the air outlet. Thus, it can be concluded that drying was effective in removing almost all moisture from soft grout present in the dried specimen between the air inlet and outlet. Details of variation of moisture content along the length of specimens is explained in detail in Appendix C.

Figure 8-20 shows that MC of 5 PC grout, present upstream of inlet in the dried specimen, was negligible (< 1%) however MC measurement at the low end of the slope was close to 10% indicating that grout beyond outlet was dried but its MC was not as low as grout

along rest of the specimen length. This likely occurred because the section of the specimen beyond the outlet was unable to completely drain water during drying.

Moisture content of grout samples collected during dissection was found to vary along the length and across the cross-section of both control and dried specimens. Table 8-1 shows labels and figures for all levels in the cross-section. In the control specimens, moisture content was higher at the top of the section than below the strands (Figure 8-21), probably due to segregation and bleeding. In the dried specimen, however, moisture content was less at the top than below the strands (Figure 8-22). It is thought that this was due to air flowing freely over the top surface through the void (Figure 8-23) formed by the bleed channel at the top of the section.

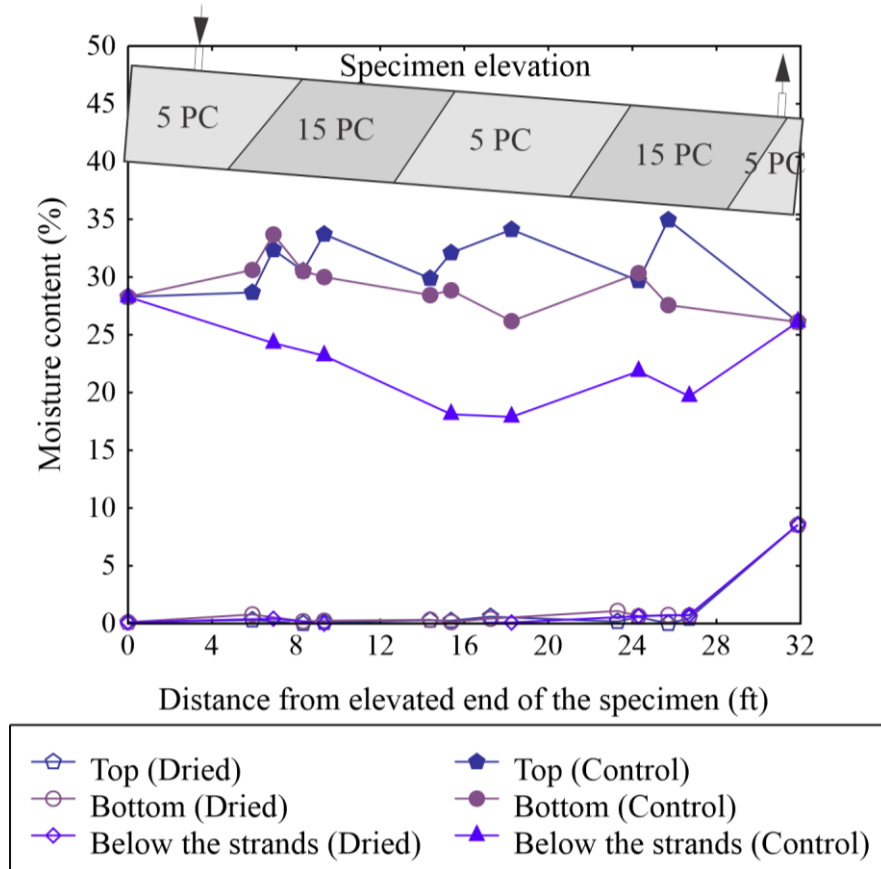


Figure 8-20. Comparison of moisture content for dried and control ISG

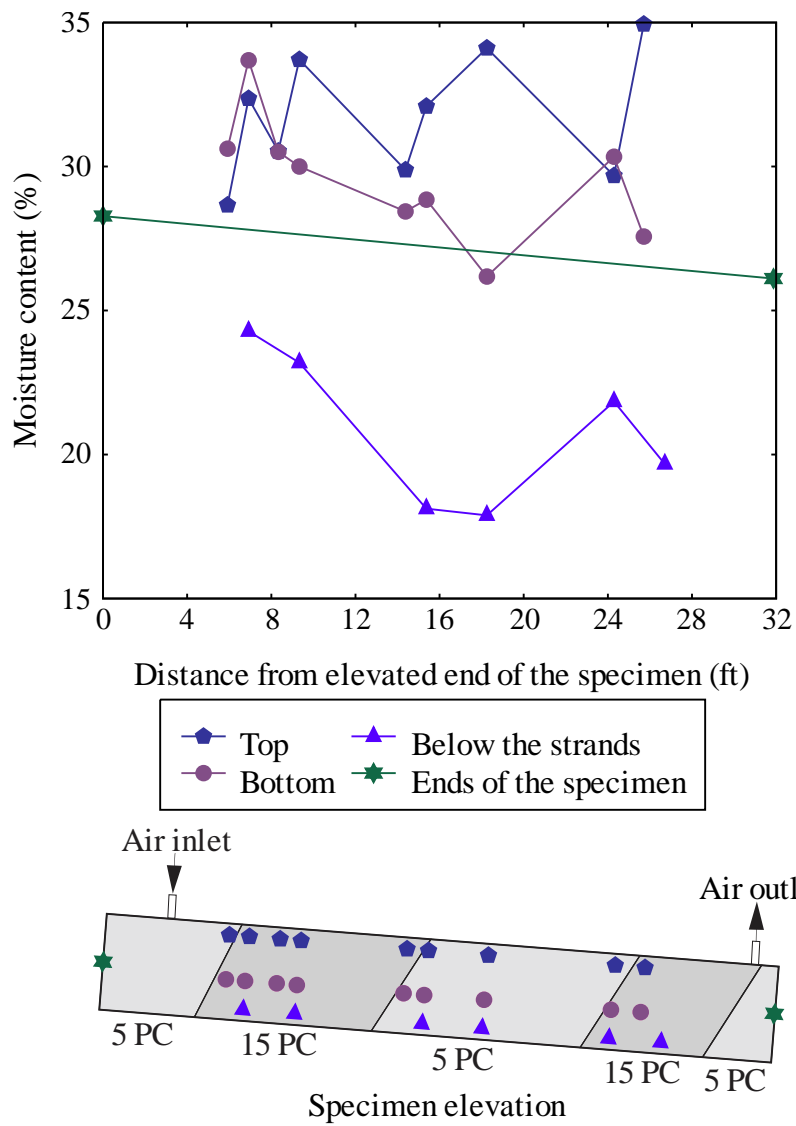


Figure 8-21. Variation of moisture content along the length of control specimen ISG

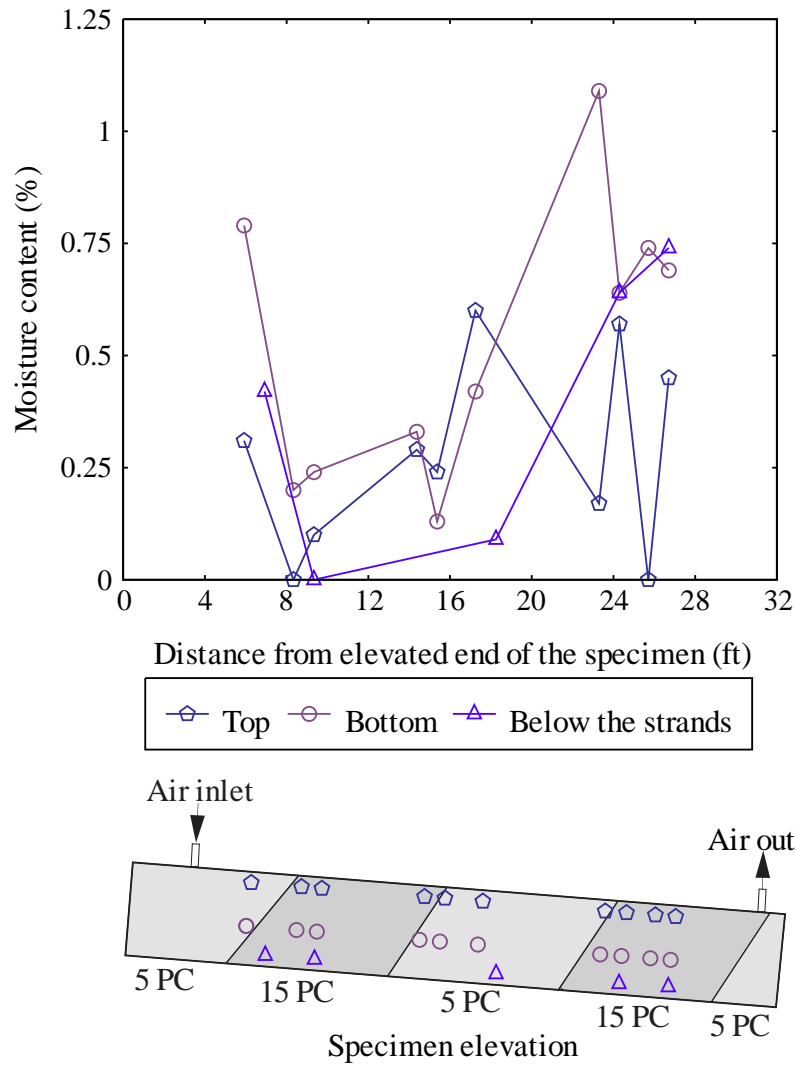


Figure 8-22 Variation of moisture content along the length of the dried specimen ISG

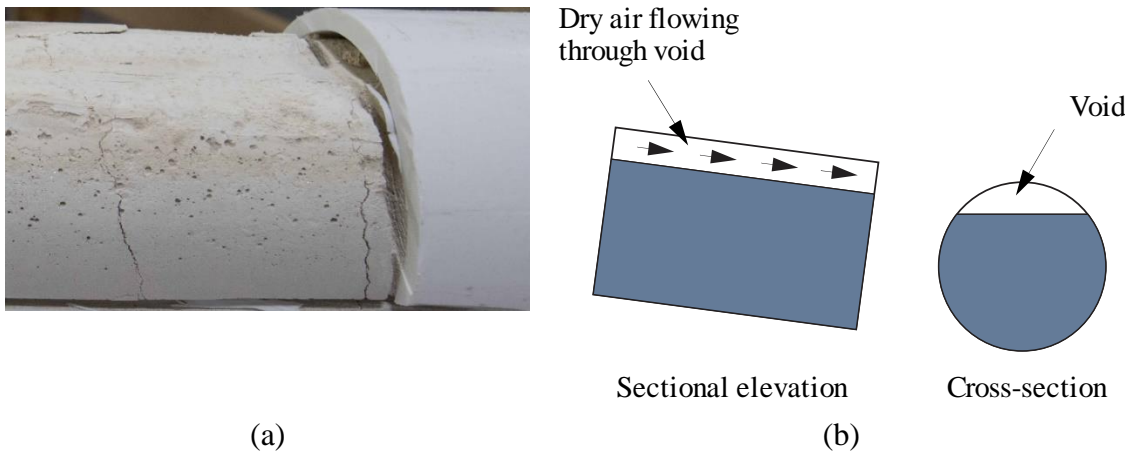


Figure 8-23. Shrinkage in grout due to drying: (a) Void present at the top; (b) Schematic of air flow through void (not to scale)

8.2.2 TSG results

Figure 8-24 shows moisture content measurements plotted as a function of their location in specimen TSG for control (hollow markers) and dried specimens (solid markers). Figure 8-24 shows that in the control specimen, 100 PC normal grout layer had lower moisture content than the adjacent 5 PC soft grout layer even though the water to solids ratio was the same. This was because normal grout had more cement content, resulting in higher degree of hydration and higher consumption of water than soft grout. On the other hand, in dried specimen, dried normal grout layer had higher moisture content than dried soft grout. This was probably due to the less porous nature of the 100 PC, which restricted the removal of moisture compared to the relatively porous soft grout.

In general, moisture content of both 5 PC and 100 PC decreased considerably after drying. Moisture content in the central 5 PC layer of the dried specimen was negligible ($<1\%$) compared to control specimen. These results in specimen TSG were similar to that of specimen ISG, indicating that the air flow through the hardened normal grout layers was sufficient to dry the trapped layer of 5 PC grout. The final “dried” moisture content of the 100 PC grout layers, however, was between 5% and 10% and was unlikely to decrease notably with further drying. Past studies (Randell et al., 2015) have shown that hardened grout has moisture content values varying from 16% to 22%; thus, the presence of 5% to 10% moisture in dried 100 PC was not unexpected.

Soft grout present upstream of the air inlet had negligible moisture content ($<1\%$) but soft grout downstream of the air outlet had around 8% moisture content. This indicated that soft grout beyond the air outlet was not able to completely drain bleed water during drying and did not completely dry.

In conclusion, specimen TSG was considered dry since soft grout between inlet and outlet had negligible moisture content and the moisture content in 100 PC was within expected values for dry normal grout. Note that even though 100 PC grout has less porosity than 5 PC grout, it did not obstruct drying of trapped 5 PC grout.

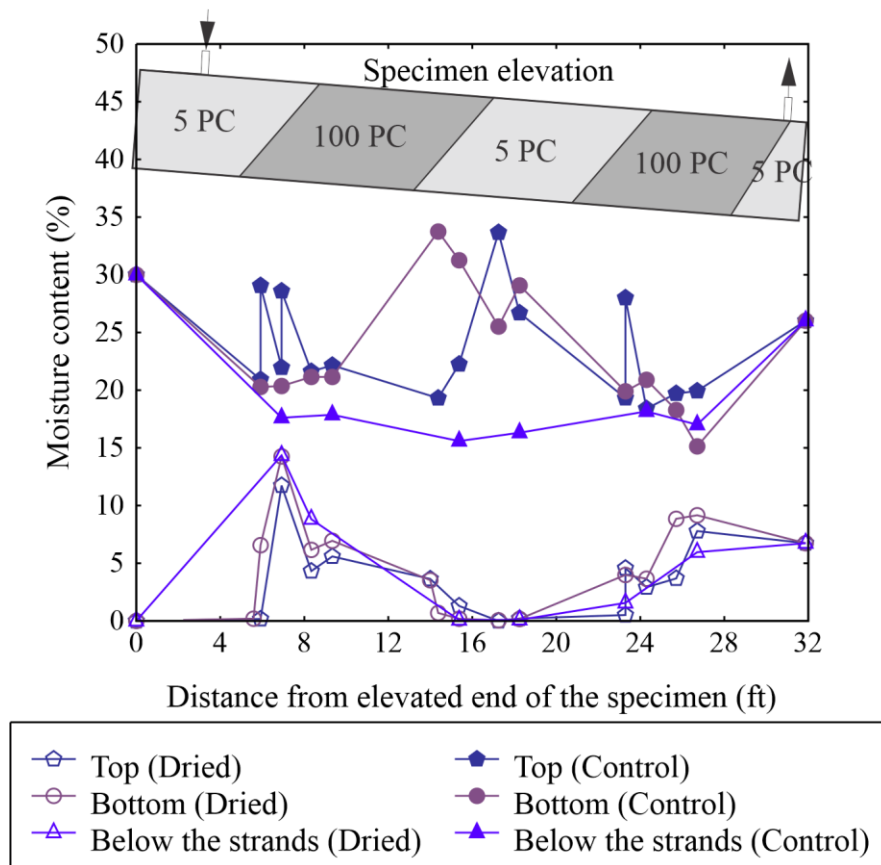


Figure 8-24. Comparison of moisture content for dried and control TSG specimens

Figure 8-25 shows the variation of grout moisture content along the length of the TSG. In general, normal grout had less moisture content than soft grout in the control specimen because of the higher cement content. Conversely, Figure 8-26 shows that normal grout had more moisture content than soft grout in dried specimen TSG due to binding ability of the portland cement in the normal grout. Along the length of the dried specimen, normal grout at the elevated end had higher moisture content than normal grout at lower end. This was attributed to normal grout absorbing moisture released by soft grout present at the elevated end. Across the cross-section in control specimen TSG, moisture content was higher for grout at the top level than for grout at the bottom level and below the strands, which was due to bleeding and segregation. Conversely, dried specimen TSG contained a bleed channel at the top of the section, which allowed dry air to pass easily through the specimen. This resulted in slightly lower moisture content in the grout at the top of the section compared to that at the bottom. But moisture content variation across the cross-section was generally the result of one type of grout filling the space above the layer of a previously placed grout of another type. For example, for the control specimen at a distance of 12 ft to 16 ft (Figure 8-25), moisture content for grout was less at the top than at the bottom because normal grout flowed into the space above the soft grout. Similarly, in Figure 8-26, between 12 ft to 16 ft, normal grout flowed into the space above the soft grout resulting in higher moisture content at the top than the bottom.

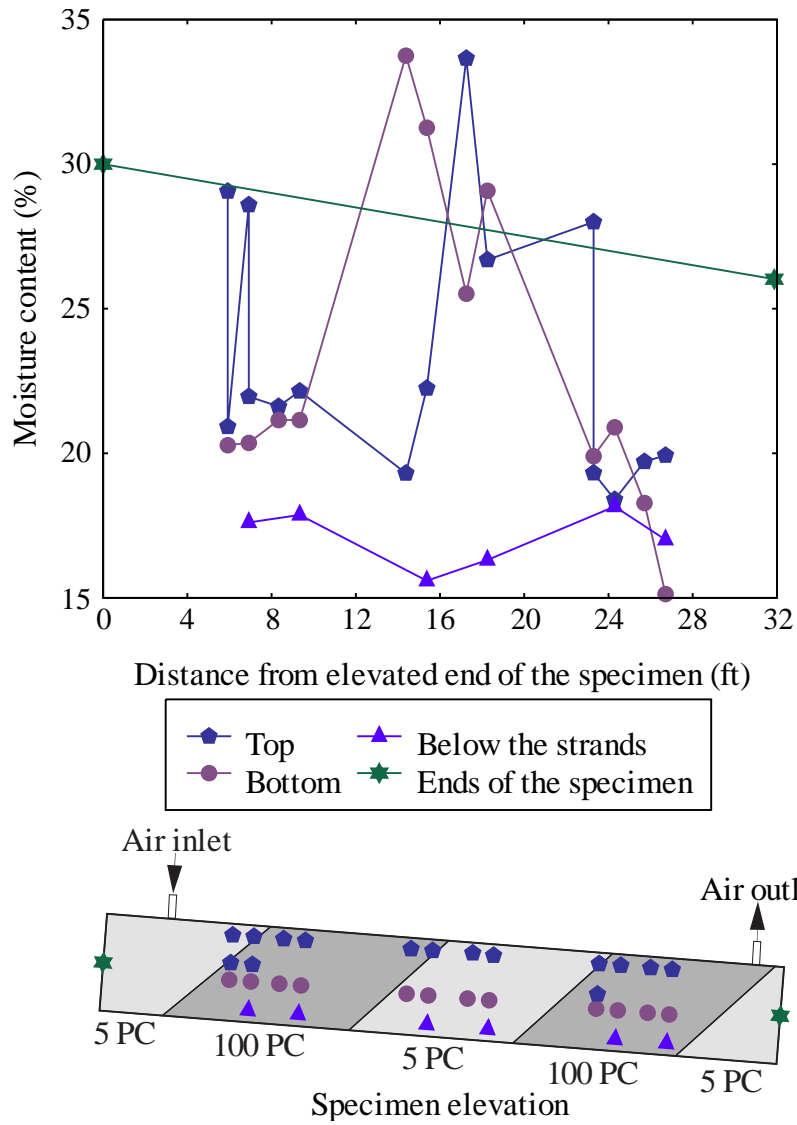


Figure. 8-25 Variation of moisture content along the length of control specimen TSG

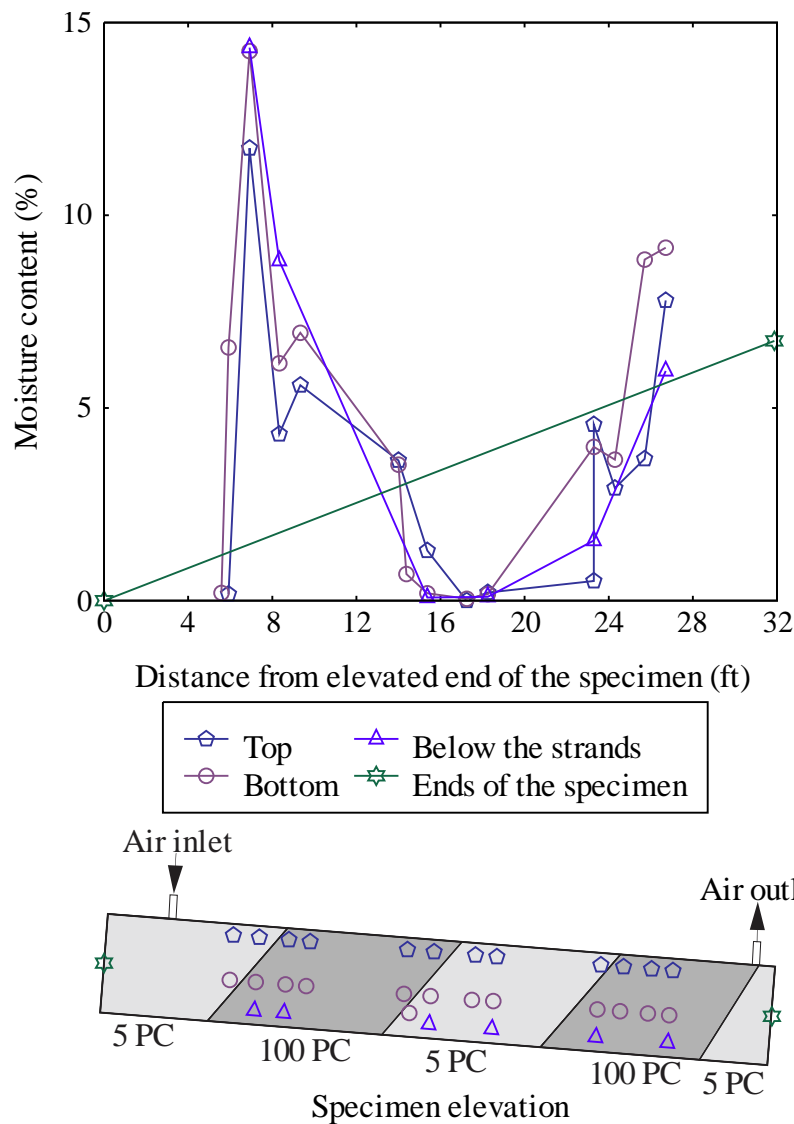


Figure 8-26. Variation of moisture content along the length of dried specimen ISG

8.3 Relative humidity analysis

RH measurements of drying air (ΔRH_d) and grout (RH_g) were recorded while drying was performed. These readings were analyzed to monitor the progress of drying and to determine if the grout moisture content could be calibrated to RH readings. Detailed analysis of the RH readings is presented in the following sections.

8.3.1 ΔRH_d measurement

Figure 8-27 shows the difference between RH of drying air measured at the inlet and outlet (ΔRH_d) over the entire drying period for both specimens. Note that negative ΔRH_d data are not shown in the graph. Positive ΔRH_d designates an increase in RH of drying air, which indicated that the grout was continuing to dry. Conversely, negative ΔRH_d indicated that drying air deposited moisture in the grout. These brief periods of negative ΔRH were due to equipment malfunctioning, which allowed drying air with up to 20% RH to be pumped through the

specimen. Ideally, grout should be considered dry when there is no more free moisture that can be removed from grout and ΔRH_d approaches zero.

In general, ΔRH_d decreased with time, which represented gradual drying of grout. After approximately 50 days, ΔRH_d decreased notably faster for ISG specimen than for TSG specimen. This is thought to be due to the presence of low porosity normal grout (100 PC) which provided more obstruction to the air flow in TSG specimen than in ISG specimen.

Based on criterion of $\Delta RH_d \approx 0\%$, ISG specimen was considered dried in approximately 110 to 120 days (grey shaded area in Figure 8-27). During this period, ΔRH_d was within a range of 0% to 5%. Similarly, TSG specimen was considered dried in approximately 140 to 150 days (blue shaded area in Figure 8-27), and ΔRH_d was within a range of 0% to 20%. For both specimens, ΔRH_d increased over the period between 130 to 160 days. This is thought to be due to equipment malfunctioning and drying system shut down, which allowed dried grout to absorb moisture through leaks in the specimens.

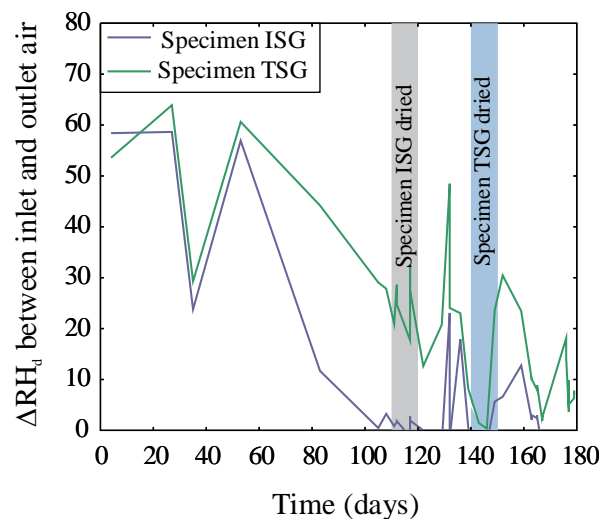


Figure 8-27. ΔRH_d vs. time

To better understand the behavior of the mockup specimens during drying, ΔRH_d measurements were made in the period following suspension of drying. Figure 8-32 and Figure 8-33 show the results of the dryness checks performed on ISG and TSG specimens on days 89, 117 and 167. On day 89, ΔRH_d of ISG was relatively high immediately after restarting the drying system, but decreased significantly after a short period. At the same point, ΔRH_d of TSG was also relatively high immediately after restarting the drying system, but remained high for nearly 2 hours before decreasing. This behavior indicated a ready availability of moisture to be removed as proposed by the behavior illustrated in Figure 8-30a. Drying behavior at this point might have initially removed moisture released by grout in the gap between the grout and the PVC pipe as well as the moisture in the interstitial space between prestressing strands and wires. Shrinkage cracks in the grout (both normal and soft) form more passages for air to flow and moisture to be released.

On day 117, however, both ISG and TSG started with a lower ΔRH_d , that increased over the next hour followed by a decrease as the drying continued. This behavior indicated that moisture was still present in the grout, but that a longer time was required for the moisture to move into spaces where the air was flowing (Figure 8-30b). Of further note is that the first reading for ISG indicated negative ΔRH_d , which means that the inlet air had a slightly higher

measured relative humidity than that of the outlet air. This may be explained partly by the difficulty and variability in measuring low humidity levels as the completion of drying is approached.

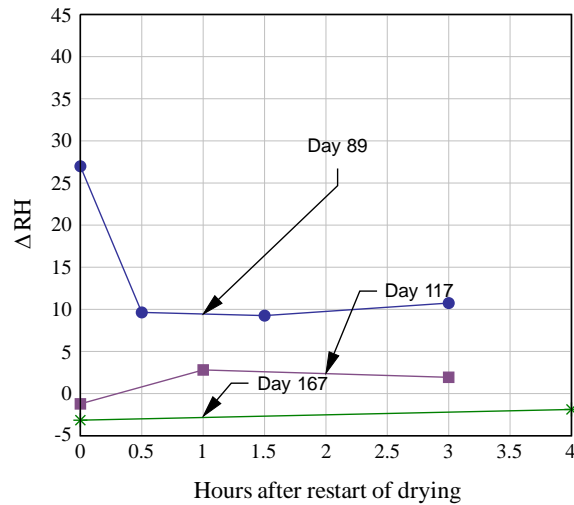


Figure 8-28. Dryness checks for dried specimen ISG

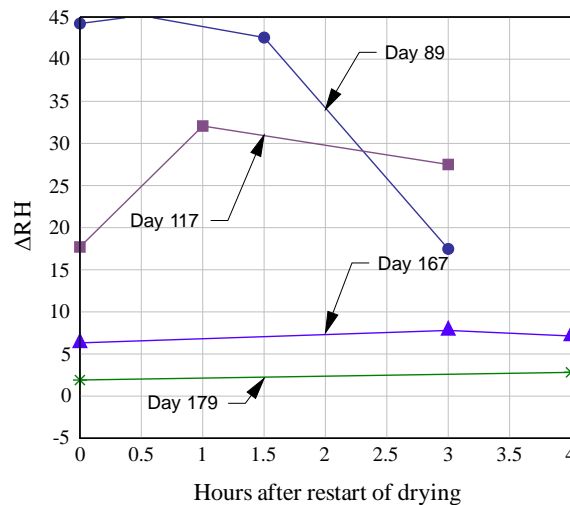
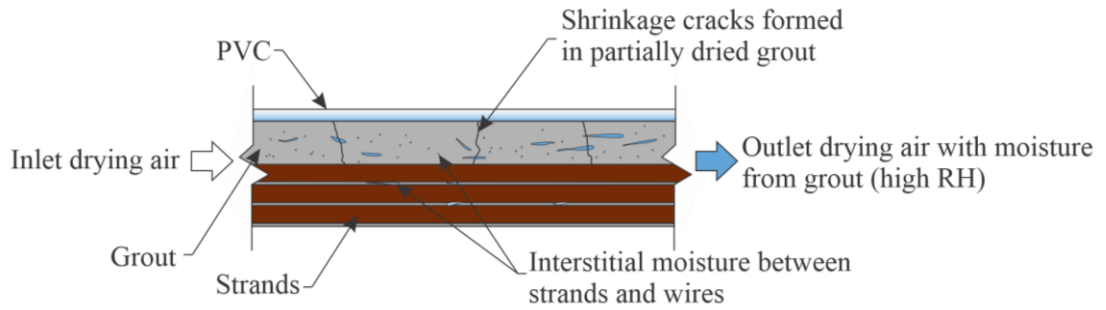


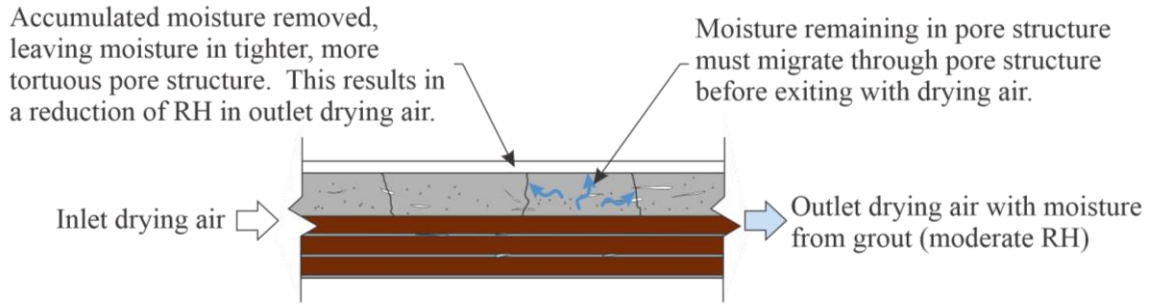
Figure 8-29. Dryness checks for dried specimen TSG

On days 167 and 179, ΔRH_d began at a low value ($< 5\%$) and did not change over the following few hours, which indicated that the grout was dry since little change in RH was detected after drying was initiated. After dissection, soft grout in both specimens ISG and TSG was found to be dry ($< 1\%$ moisture content by mass).

Based on these results, the dryness check can be formalized by comparing the inlet and outlet RH readings. After suspension of drying, ΔRH_d should be measured immediately following restart of drying (defined as ΔRH_{di}) and at 2 hours following restart of drying (defined as ΔRH_{df}). If the absolute value of these readings is less than or equal to 5%, then the grout can be considered dry. This allows for the variability of low RH measurements and other unforeseen field conditions.

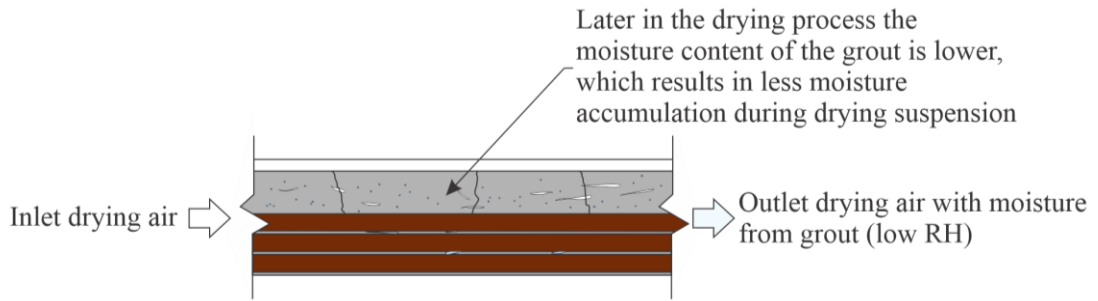


(a)

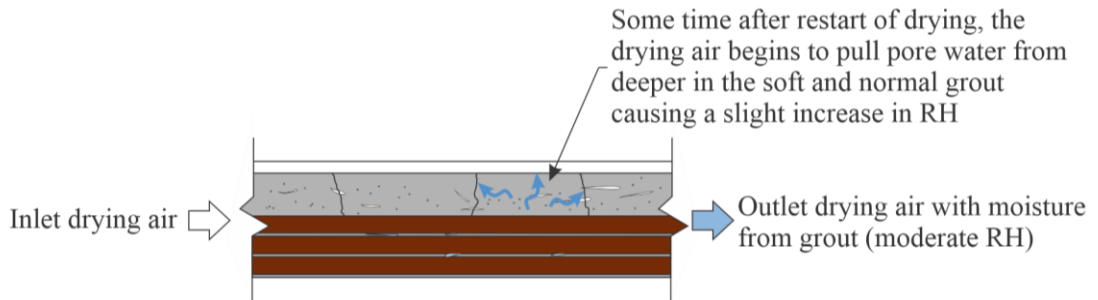


(b)

Figure 8-30. Depiction of drying behavior early in the process. Variation in RH following suspension of drying (a) immediately after drying restart and (b) two hours after drying restart



(a)



(b)

Figure 8-31. Depiction of drying behavior later in the process. Variation in RH following suspension of drying (a) immediately after drying restart and (b) two hours after restart

8.3.2 RH_g analysis

Measurement of ΔRH_d provided a viable method for determining dryness of grout in the field. For comparison purposes in this research, however, companion measurements of grout RH in probe ports drilled into specimens (RH_g) were made during the drying process. RH_g was basically RH of air measured with probes placed inside ports drilled into the grout. The air in these ports was influenced by the moisture content of the surrounding grout. As previously mentioned, each specimen had six ports with two ports drilled in each grout layer (Figure 8-32). Figure 8-33 and Figure 8-34 show RH_g readings variation measured inside ports over the drying period. Similar to ΔRH_d between inlet and outlet air readings, the RH_g values decreased with time, representing drying of grout. However, TSG specimen ports were observed to have higher RH_g than ISG specimen ports near the end of the drying period. This was thought to be due to the presence of normal grout in the TSG specimen, which did not dry as much as soft grout and influenced RH_g of air in all ports. RH_g readings for dried soft grout (5 PC and 15 PC) ranged from 15% to 40% RH for temperatures between 15°C and 35°C. On the other hand, RH_g readings for dried normal grout (100 PC) varied over a wider range of 30% to 70% for the same temperature range.

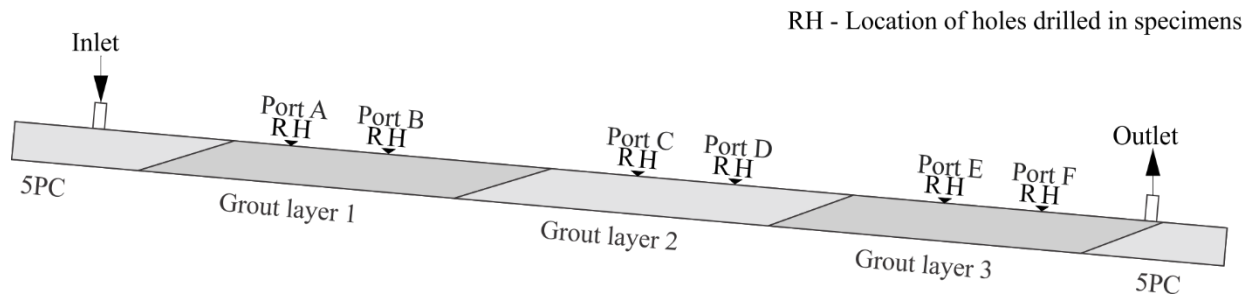


Figure 8-32. Location of ports for RH_g measurements

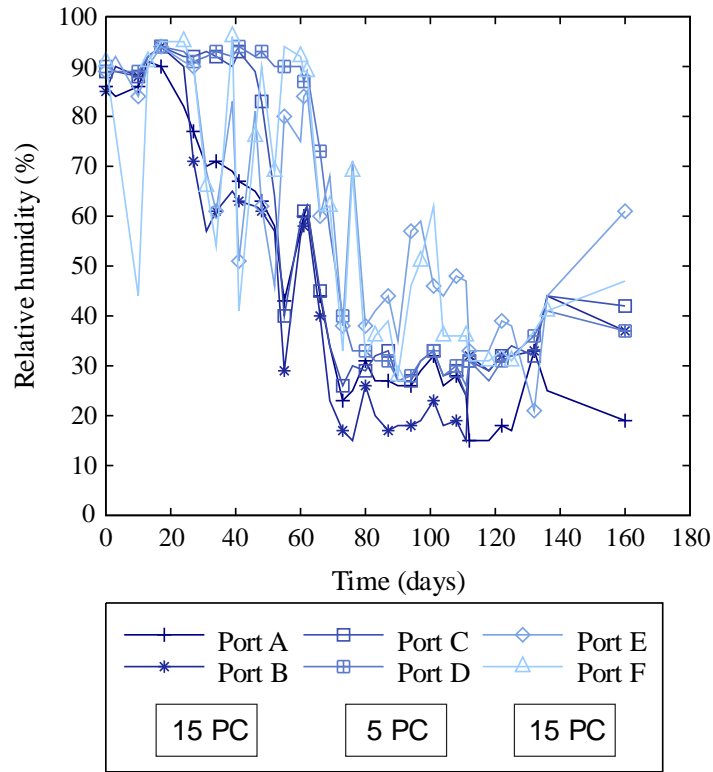


Figure 8-33. RH_g readings vs. time (ISG specimen)

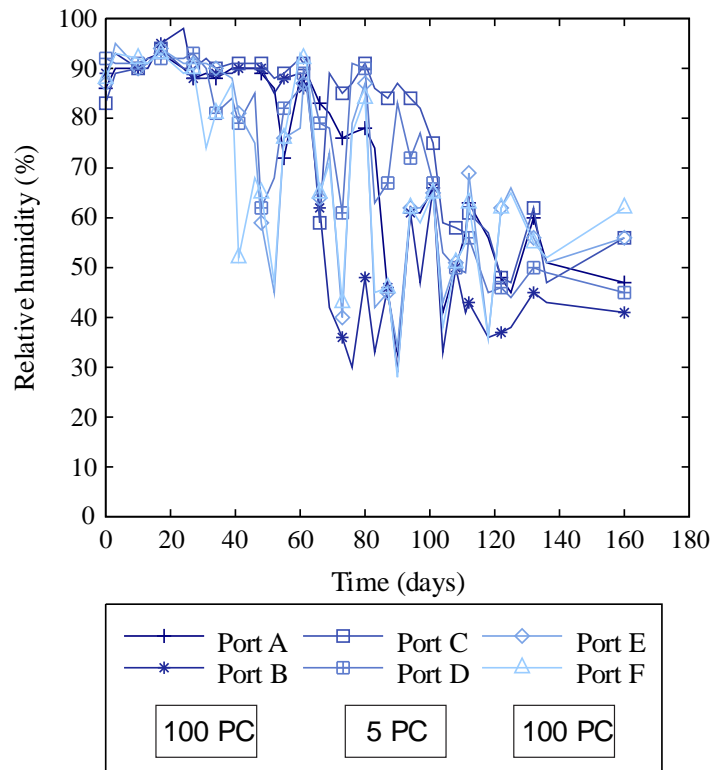


Figure 8-34. RH_g readings vs. time (TSG specimen)

9 Mockup drying test findings

After drying was completed, mockup specimens were dissected and grout samples were collected to measure their moisture content. Based on results from dissection and analysis of RH readings performed during drying, the following findings were made:

- Moisture content measurements on dried layers of 5 PC and 15 PC grout were consistently below 1%, which indicated that drying had effectively removed moisture from the soft grout. This was also true for the dried 5 PC layers trapped between 100 PC hardened grout.
- Based on dryness check readings (ΔRH_{di} and ΔRH_{df}), the ISG specimen was found dried on day 117 and the TSG specimen was found dried on day 167.
- RH_g readings for dried soft grout (5 PC and 15 PC) ranged from 15% to 40% RH for temperatures between 15°C and 35°C. On the other hand, RH_g readings for dried normal grout (100 PC) varied over a wider range of 30% to 70% for the same temperature range.
- Dried specimens exhibited strand corrosion in several locations, which did not occur in the control specimens.
- The porosity of dry grout combined with the constant supply of air provided the strands a direct access to a steady oxygen supply.
- Carbon dioxide in drying air was thought to carbonate the grout, which probably reduced pH below 11 and the passive layer of strands became unstable.
- Sufficient moisture from bleed water of grout, along with lower pH and oxygen, was probably responsible for corrosion.

Part Three—Drying Corrosion Tests

10 Background and approach

The corrosion testing proposed in Part 2 of this report was an extension of the grout drying research reported in Part 1 (Figure 10-1). The work performed in Part One involved the fabrication of 15-strand tendon mockup specimens, which were fabricated with defective grout formulated to have the physical characteristics of soft grout found in the field when using prepackaged post-tensioning grout. The defective grout mixtures were formulated with ground limestone, portland cement, and water, in varying proportions to attain the desired physical characteristics. The mixture designations shown in the Figure 10-1 indicated the relative proportion of portland cement used in formulating the mixture. For instance, 15 PC indicates 15% portland cement and 85% ground limestone by mass. Dry air was pumped through the specimens for about 5 months to dry the defective grout. During the dissection of these specimens following drying, corrosion was found at the interface between grouts of different consistencies.

The corrosion test proposed in part 2 of this report was intended as a follow-up to this finding and to explore the effect of drying on corrosion protection provided by grout. The corrosion specimens consisted of a 1.5-in. diameter PVC pipe with PVC tees and bushings fit on each end. Each specimen had an inlet and outlet for low humidity air to flow through the specimens. Overall, seventy-two specimens were designed and constructed. Corrosion specimens had either one or two grout layers. Each grout layer contained a paired strand and reference electrode (RE). Forty-eight of the seventy-two specimens were dried using a drying system producing air of RH about 0.17%. RH readings of air at inlet and outlet of each specimens were measured. Drying was terminated as the difference in RH between inlet and outlet reduced to zero percent. During and after drying, corrosion potential was measured between the strands and its RE, whereas after drying, macrocell current was measured between two strands if present in a specimen using a modified G109 corrosion monitoring system. After monitoring corrosion for certain time, corrosion specimens were dissected to evaluate grout moisture content and strand corrosion.

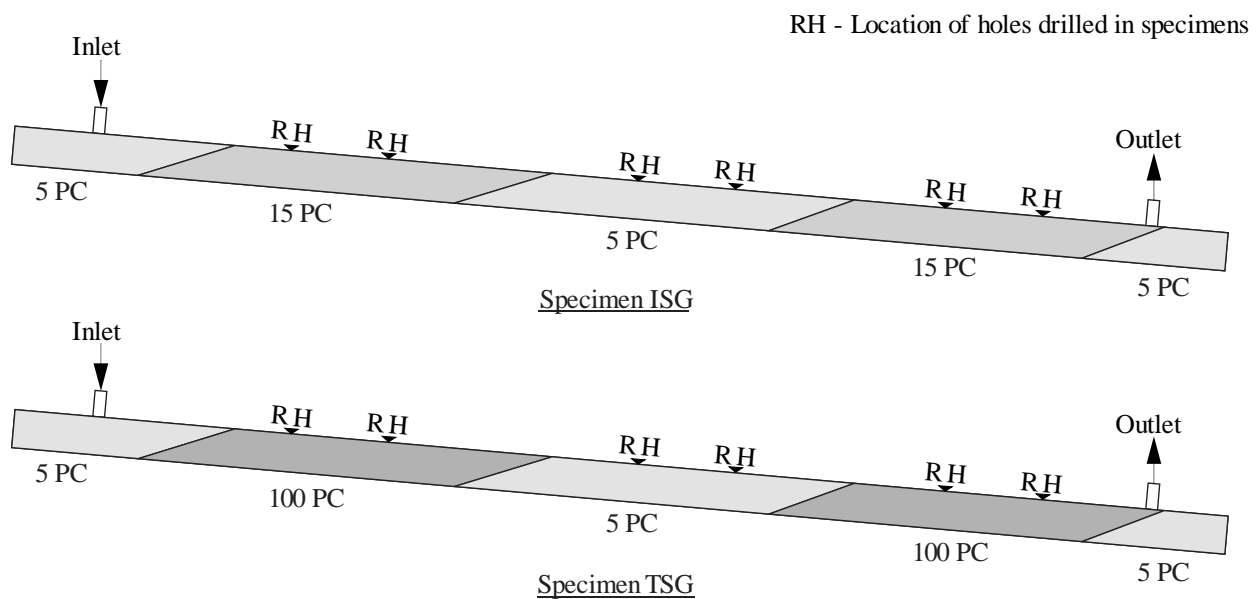


Figure 10-1. Mockup specimens

11 Corrosion specimen design

The corrosion specimens consisted of a 1.5-in. diameter PVC pipe with PVC tees and two bushings fit on each end (Figure 11-1). Each specimen had an inlet and outlet for low humidity air to flow through the specimens through one of the bushings at each end. Wires from inside the specimen were pulled out from the opposing bushing at each PVC tee. These wires were used for electrochemical measurements (for e.g. corrosion potential). The holes through which the wires were passed were sealed with epoxy before pouring grout.

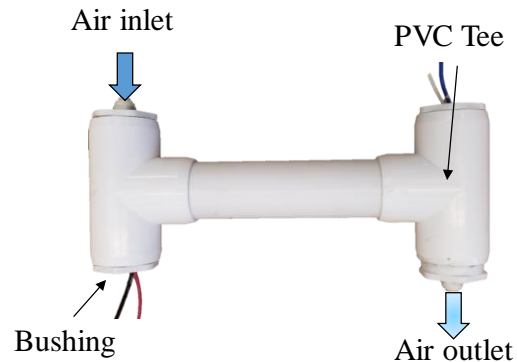


Figure 11-1. Corrosion specimen

The PVC pipe diameter of 1.5-in was determined based on AASHTO and FDOT provisions. According to AASHTO LRFD 2014 Bridge design specifications (5.4.6.2), for multiple strand tendons, the inside cross-sectional area of the duct should be at least 2.5 times the net area of prestressing steel. Further, Structural Design Guidelines by FDOT provides maximum duct dimension for common tendon sizes (SDG Table 1.11.1-1). The diameter of the PVC pipe for the corrosion specimen was intended to maintain a similar ratio of strand-grout contact area to grout volume as that of actual tendons with an idealized strand pattern (Figure 11-2), so that the scaling does not adversely affect the corrosion behavior. To achieve this, S/V was defined as the ratio of surface area of strand-grout contact in a tendon (S) to the volume of grout (V) surrounding the strands. Maximum and minimum S/V was calculated based on minimum and maximum permissible duct sizes and plotted in Figure 11-3. On comparison, the S/V ratio of the 1.5-in diameter corrosion specimens was found to be between S/V of common tendon sizes. Thus, 1.5-in. diameter pipe was selected. Note that the mockup specimen (Figure 6-4) had similar S/V as 15 strands tendon in Figure 11-3.

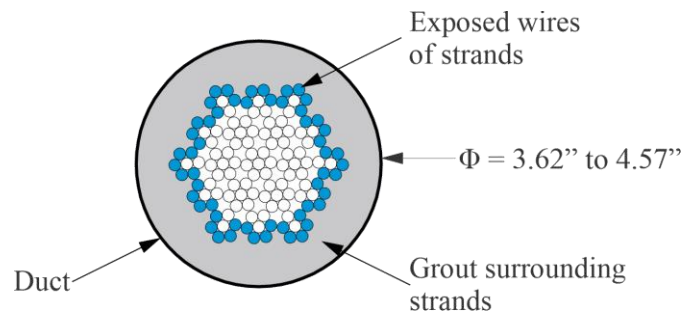


Figure 11-2. Idealized strand pattern

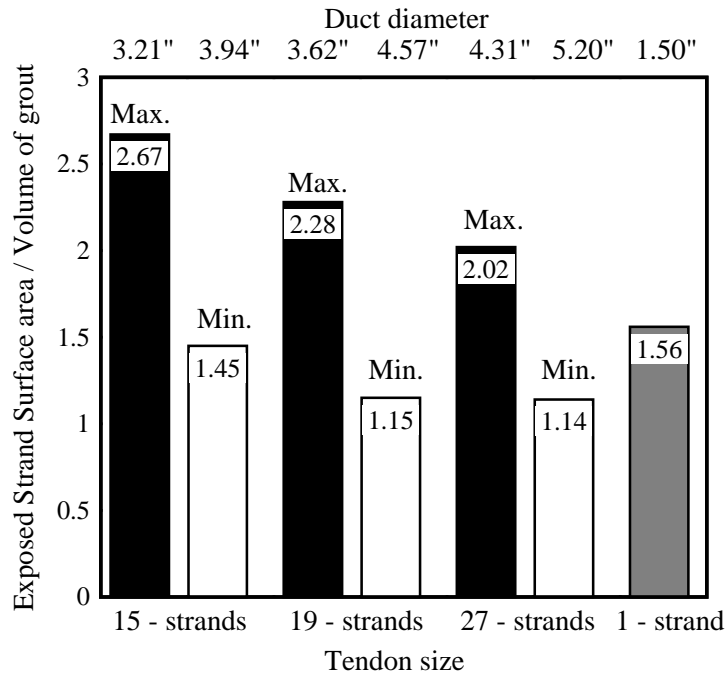


Figure 11-3. Ratio of duct to strand area for different size tendons

The corrosion specimens were designed to replicate similar conditions present in the mockup specimens by using the same grout mixtures, including 5 PC, 15 PC, and 100 PC. Various grout mixtures were layered to replicate the interface between the different grout mixtures. For example, the section of specimen ISG with 15 PC alongside 5 PC (Figure 11-4a) was replicated by a corrosion specimen containing 15 PC and 5 PC grout layers, shown in Figure 11-4b. Similarly, other grout layer combinations were investigated as well. Along with these experimentally developed soft grout mixtures, a commercially available prepackaged post-tensioning (PT) grout, was also used in one of the mixtures. This PT grout was subjected to relative humidity of greater than 90% for over a week in an attempt to prehydrate the powder so that it would produce soft grout. In addition, grout in selected specimens was dosed with a chloride solution (containing 1.5% chloride ions by weight of cement) to determine its effect on corrosion. Lee and Zielske (2014) found a threshold chloride content of 0.8% in PT tendons with defective grout to cause corrosion.

After dissection of mockup dried specimens, macrocell formation was suspected as a cause of corrosion. To test this, strands and grout mixtures were arranged in three basic configurations to facilitate macrocell formation. The first contained two strands with two layers of grout with different mixture proportions (Figure 11-5a). For this specimen type, each strand was entirely embedded in their respective grout layer with nothing crossing the grout interface. The second also contained two strands, but with the designated anode strand crossing the grout layer interface (Figure 11-5b). The third contained a single strand with a single layer of grout (Figure 11-5c). Each strand was paired with a 2-in. long titanium mixed-metal oxide (MMO) reference electrode for electrical measurements (Figure 11-6). Strands and titanium MMO reference electrodes were positioned in PVC pipe using plastic clips that held the strands in position.

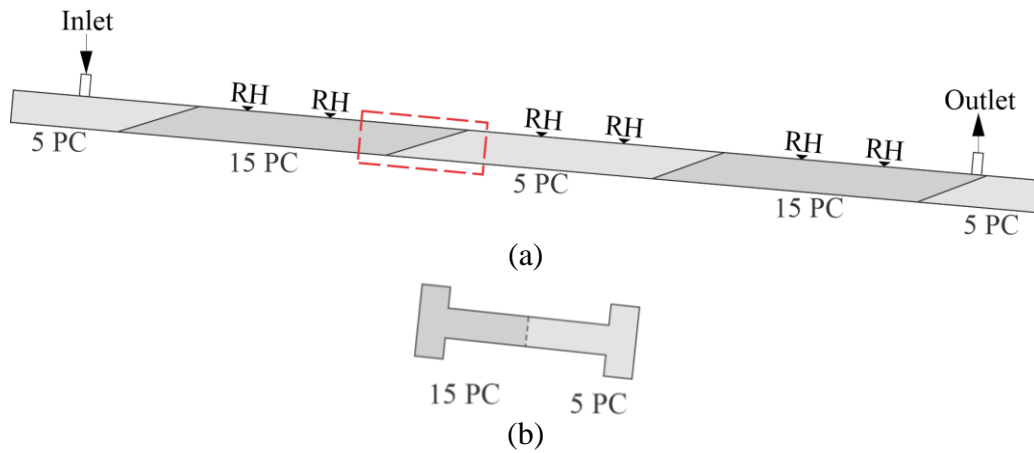


Figure 11-4. Specimen design: (a) Mockup specimen ISG with 15 PC and 5 PC interface highlighted; (b) Replicate corrosion specimen

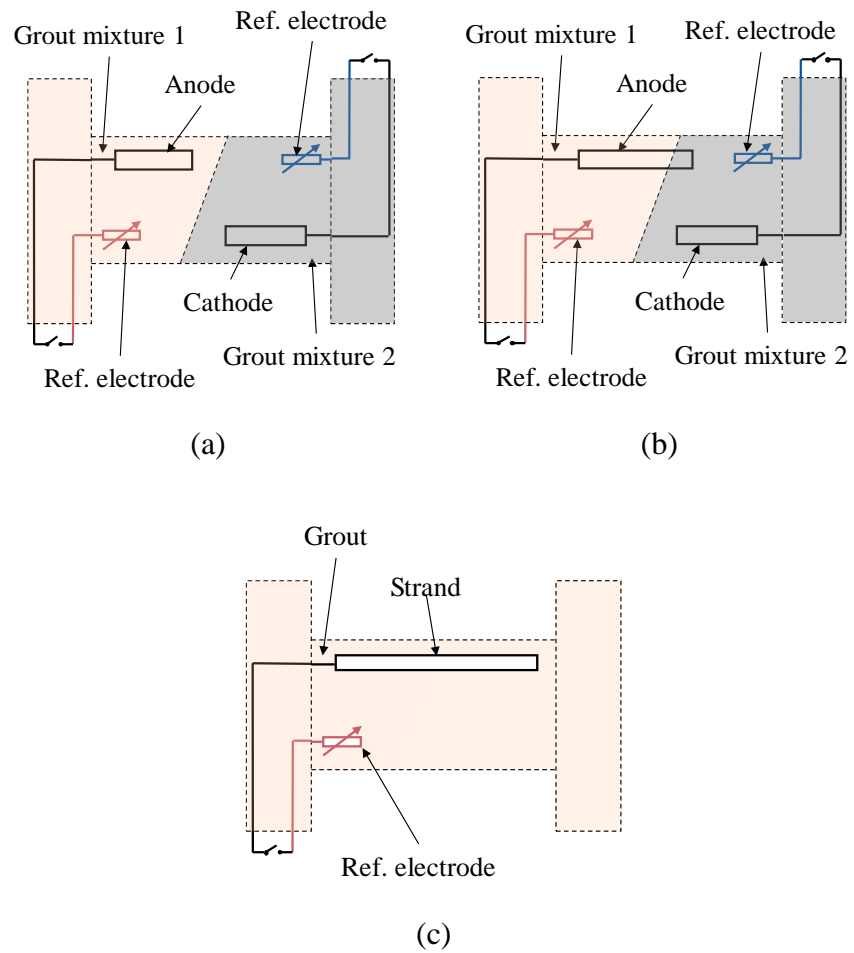


Figure 11-5. Corrosion specimen: (a) specimen photo; (b) schematic drawing for two-strand specimen; and (c) one-strand specimen

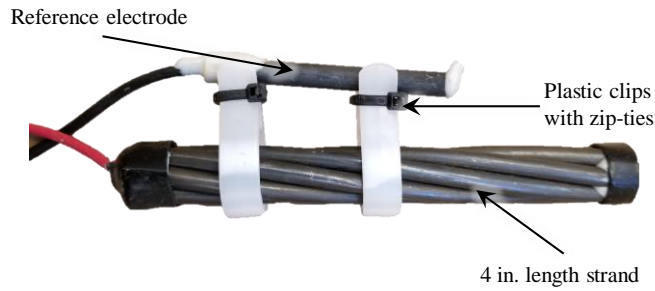


Figure 11-6. Pair of strand and titanium mixed-metal oxide electrode

Similar to the work reported in Part 1, grout mixtures were classified based on the mass of portland cement as a percentage of solids. For example, a 5 PC grout consisted of 5% cement and 95% ground dolomite limestone. The strand placed in the grout layer with the lower cement content was expected to form the anode and was designated as the anode in the specimen. Conversely, the strand in the mixture with higher cement content was expected to form the cathode and was designated as the cathode. Specimens were designed to be resting at a slope of 60° from horizontal to represent the slope of a tendon in the negative bending moment region (Figure 11-7). During trial tests, slopes less than 60° sometimes resulted in strands inadvertently crossing the grout interface, which was not the intent (Figure 11-8).



Figure 11-7. Corrosion specimen placed at 60° inclination

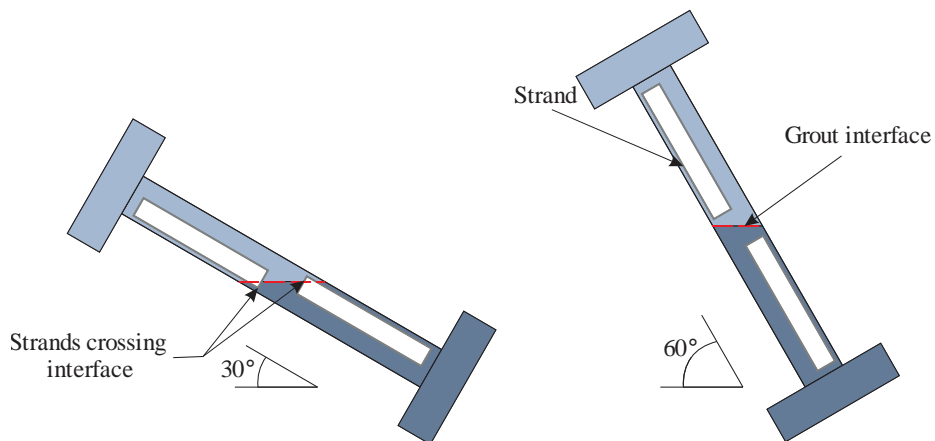


Figure 11-8. Grout interface in trial specimens cast at varying slopes

Seventy-two specimens were designed and organized into the twelve categories in Table 11-1 based on the number of strands, specimen configuration, and grout mixtures used. Each configuration of specimens had three replicates, two of which were subjected to drying and one which was left as control with no drying. The corrosion specimen naming convention was created based on the grout mixture, presence of chlorides in the grout mixture, and positioning of strands. Specimens subjected to drying were assigned a name in the form T/BD# where “T” indicates the top half grout mixture designation, “B” indicates the bottom half grout mixture designation, “D” indicates dried specimen and “#” indicates the replicate specimen number. Control specimens were assigned a name in the form T/BC#, where “C” indicates control specimen and “T”, “B” and “#” carry the same designations as the dried specimen name. Further, if the grout mixture in a specimen contained admixed chlorides, “C” was appended to the label. Similarly, if the designated anode crossed the interface between the grout layers, then “E” was appended to the label. For example, dried specimens that contained a 5 PC top layer and a 100 PC bottom layer with chlorides added in the grout mixture and the anode crossing the grout interface was labeled 5/100D1CE and 5/100D2CE, while the control specimen for the same configuration was labeled 5/100C1CE.

Table 11-1. Specimen matrix

Grout mixture		Number of strands	Strand crosses grout interface (E)	Presence of chlorides (C)	Number of specimens		
Top half	Bottom half				Control (C1)	Dried (D1 and D2)	Total
5 PC	100 PC	1			1	2	3
				x	1	2	3
5 PC	100 PC	1	x		1	2	3
			x	x	1	2	3
100 PC	5 PC	1			1	2	3
				x	1	2	3
100 PC	5 PC	1	x		1	2	3
			x	x	1	2	3
5 PC	15 PC	1			1	2	3
				x	1	2	3
5 PC	15 PC	1	x		1	2	3
			x	x	1	2	3
15 PC	5 PC	1			1	2	3
				x	1	2	3
15 PC	5 PC	1	x		1	2	3
			x	x	1	2	3
PT grout	100 PC	1			1	2	3
				x	1	2	3
100 PC	PT grout	1			1	2	3
				x	1	2	3
5 PC	5 PC	2			1	2	3
				x	1	2	3
100 PC	100 PC	2			1	2	3
				x	1	2	3
							72

12 Specimen fabrication

Seventy-two corrosion specimens and wooden supports for each of them in the UF materials and structures laboratory and at the State Materials Office of FDOT. The construction process was divided into several tasks, which are discussed as follows.

12.1 Materials

Materials required for construction of corrosion specimens were purchased. The materials included cement, ground limestone, prepackaged grout, PVC pipes, fittings and other miscellaneous materials. The prepackaged grout was placed in an environmental chamber at 90% humidity for one week to ensure soft grout formation on mixing.

12.2 Strands and reference electrodes

Seven-wire 0.6-in diameter strands were cut to required lengths using a chop saw fitted with an abrasive blade (Figure 12-1). Titanium reference electrodes (RE) were created by cutting the titanium MMO rod into 2-in. lengths. While cutting, care was taken to prevent damage to the oxide layer on the surface by using a solid plastic grip while clamping the rod in a horizontal saw (Figure 12-2). The blade speed on the horizontal saw was set to 80 SFPM (surface-feet per minute) and a bi-metal blade with a high-speed steel cutting edge welded to a fatigue-resistant alloy steel backing was used to cut the RE.



Figure 12-1. Zip ties and marks in preparation for strand cutting



Figure 12-2. RE clamped in horizontal saw

After cutting strands and RE, the cut surfaces were cleaned and the ends ground flat. Using a lathe, a 1/8 in. diameter by 1 in. deep hole was drilled at the center of one end of RE to allow electrical wire lead connection.

12.3 Electrical connections

Wires were connected to strands and RE to facilitate measurement of corrosion readings such as corrosion potential during and after drying. Wires were connected to strands by soldering and to RE by crimping into the drilled hole. Soldering was done on one end of each

strand. Stranded wires were used for soldering to strands. To perform soldering, strand surface was cleaned to remove any oxide layers. Then the stranded wire was separated into seven parts (Figure 12-3). Finally, each of the seven parts was soldered to one wire of a 7-wire strand (Figure 12-4). On each RE a 14-AWG wire was stripped and inserted in the hole and crimped as shown in Figure 12-5.



Figure 12-3. Separated stranded wire



Figure 12-4. Wire soldered to end of 7-wire prestressing strand.



Figure 12-5. Crimping of RE

Table 12-1 shows the color of the wires used for connection to each of the various electrodes used in the corrosion testing. The strand placed in the grout layer with the lower cement content was designated as the anode and the strand placed in higher cement content grout was designated as cathode. The RE paired with an anode had black wire and RE paired with a cathode had white wire. Specimens with single type of grout had an uncategorized strand and RE with green wire.

Table 12-1. Color code for wires

Category #	Category	Wire color
1	Anodes	Red
2	RE paired with anode	Black
3	Cathodes	Blue
4	RE paired with cathode	White
5	Uncategorized strand	Yellow
6	RE paired with uncategorized strand	Green

12.4 Specimen assembly

Prior to specimen assembly, the strands and RE were cleaned using n-hexane anhydrous, which removed impurities present such as oil from handling, coolant from band saw, and ink from markings on strands. After cleaning, crimped ends of the RE were coated with 3M Scotchkote followed by coating of epoxy at each end (Figure 12-6). After the epoxy was set, heat shrink tube was applied to the crimped end to protect the connection. More epoxy was then applied to completely seal the edges of the shrink wrap. Prestressing strand ends were also coated with epoxy and then fitted with caps (Figure 12-7). These coatings provided protection against moisture intrusion near the electrical connection and against breaking of electrical connection during assembly of specimens. Gloves were used while handling strands and RE.



Figure 12-6. Finished reference electrode electrical



Figure 12-7. Finished strand

After prepping the electrodes (strands and RE), 1.5-in. dia. PVC pipes were cut into 8-in. long segments onto which one PVC tee was glued (Figure 12-8); this was done to facilitate placement of the grout. The inside of the bushing containing wires was sealed with epoxy and a synthetic rubber cap to prevent grout leakage (Figure 12-9).

After placing the first layer of grout, the second tee was glued onto the specimen. One bushing in this tee was left uninstalled to allow for the placement of the second lift of grout. After placement of the second lift, the remaining bushing and fittings were glued.



Figure 12-8. Specimens prepped for placement of first grout layer

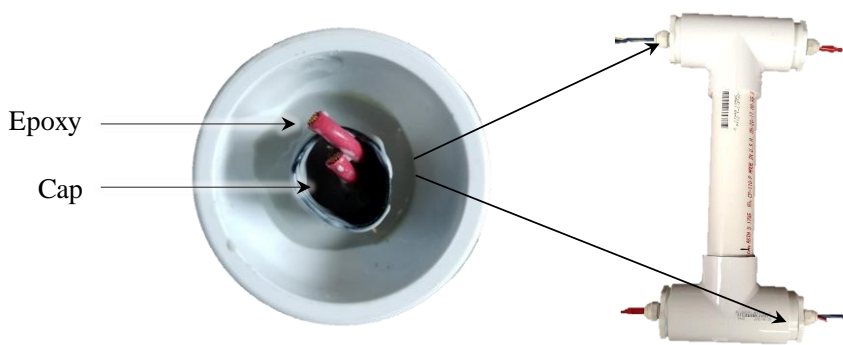


Figure 12-9. Instrumentation wiring in PVC specimen

12.5 Mixing and placing grout

Grout was mixed in 5-gal buckets using a paint mixer and an electric drill (Figure 12-10). The bucket was initially filled with the full proportion of water followed by the intermittent addition of portland cement and mixing. After the portland cement was thoroughly mixed into the water, ground limestone, if required by the mixture design, was added and mixed. The mixing was done continuously for at least two minutes or until the mixture color was uniform.

Table 12-2 gives details of mixture proportions for a one ft³ volume of different grout mixes. The water-to-solids ratio was 0.47 for 5 PC, 15 PC and 100 PC. For prepackaged grout, a water-to-solids ratio of 1.0 was used to create a thick layer of soft grout. Specimens requiring admixed chloride used the proportions shown in Table 12-3

Specimens were placed on supports and filled in two lifts, one lift per day. To account for shrinkage caused by the high-water content, a slight surplus of grout was placed during the first lift. After placing the first lift, bleed water was drained, and the level of grout was checked. If the top of the first lift was not in the desired location, grout was added as needed. This process was repeated for the second lift. Note that grout was not refilled in specimens containing prepackaged grout if strand was not covered completely by grout after second lift. This was intended to simulate exposed strands found in ducts with air pockets in bridges. After inspection, the final bushing was glued, and the specimens were cured for 14 days in laboratory conditions.



Figure 12-10. Grout mixing

Table 12-2. Grout mixture details per cubic feet

Grout type	W/S ratio	Cement (lb.)	Limestone (lb.)	Water (lb.)
5 PC	0.47	3.84	72.87	36.05
15 PC	0.47	11.55	65.42	36.17
100 PC	0.47	79.24	0	37.24
Prepackaged grout	1	26.42	0	26.42

Table 12-3. NaCl quantity per pound

Weight of solids	1.00	lb.
Required percentage of chloride by weight	1.50	%
Required weight of chloride	0.015	lb.
Chloride % in NaCl	60.70	%
Required weight of NaCl	0.02	lb.

13 Drying system

Prior to performing corrosion testing, selected specimens were subjected to drying in a system similar to that used on the mockup dried specimens in Part 1. The drying system was sized for these smaller specimens based on the equipment requirements of the drying system used previously.

The basic design objective of the drying system was to produce dry air (no more than 10% RH) and deliver it to the specimens at a relatively constant pressure of no more than 20 psi. The drying system is shown in Figure 13-1. Air was drawn into the compressor where moisture was partially removed from the air. Air was then passed through a desiccant dryer. This removed any remaining moisture and impurities in the air. A pressure regulator then reduced and controlled the pressure to a range of 20-25psi. After passing through the regulator, air was distributed to each group of specimens using a manifold system. Figure 13-2 shows RH of drying air plotted versus time, which was measured at the outlet of the drying system to monitor its performance. Figure 13-2 indicated that the system was able to successfully produce dry air with RH of less than 1 percent consistently, except for four weeks during which the compressor was subjected to maintenance repair, which appear as outliers in the plot.

Figure 13-3 and Figure 13-4 show the air distribution system. In this system, four dried specimens of same type with the same number of strands, specimen configuration, and grout mixtures were arranged in parallel to form a group. All specimens of the same type in a group were assumed to dry at a similar rate and to provide equal resistance to air flow through each specimen throughout the drying time. This was intended to prevent the air from flowing primarily through the specimen with the lowest resistance of the group. One HDPE tube was branched with the help of a manifold and supplied dry air to each specimen in that group. This ensured consistency of the RH of air entering each specimen. The outlets of specimens in each group were connected to another manifold to converge into a single outlet. Twelve such groups were assembled using groups of similar type specimens.

Pressure at the inlet of a group of specimens was controlled using a second pressure regulator. Air flow, however, depended on the resistance to air flow by the grout in each of the specimens. This resistance depended on the grout formulation and changed with time as the grout dried. To control the air flow through each group and to ensure that a sufficient backpressure was maintained on the manifold system upstream from the specimens, needle valves were installed at the outlet of each group. During drying, air flow and pressure were monitored and the valves were adjusted as needed to ensure consistent air flow.

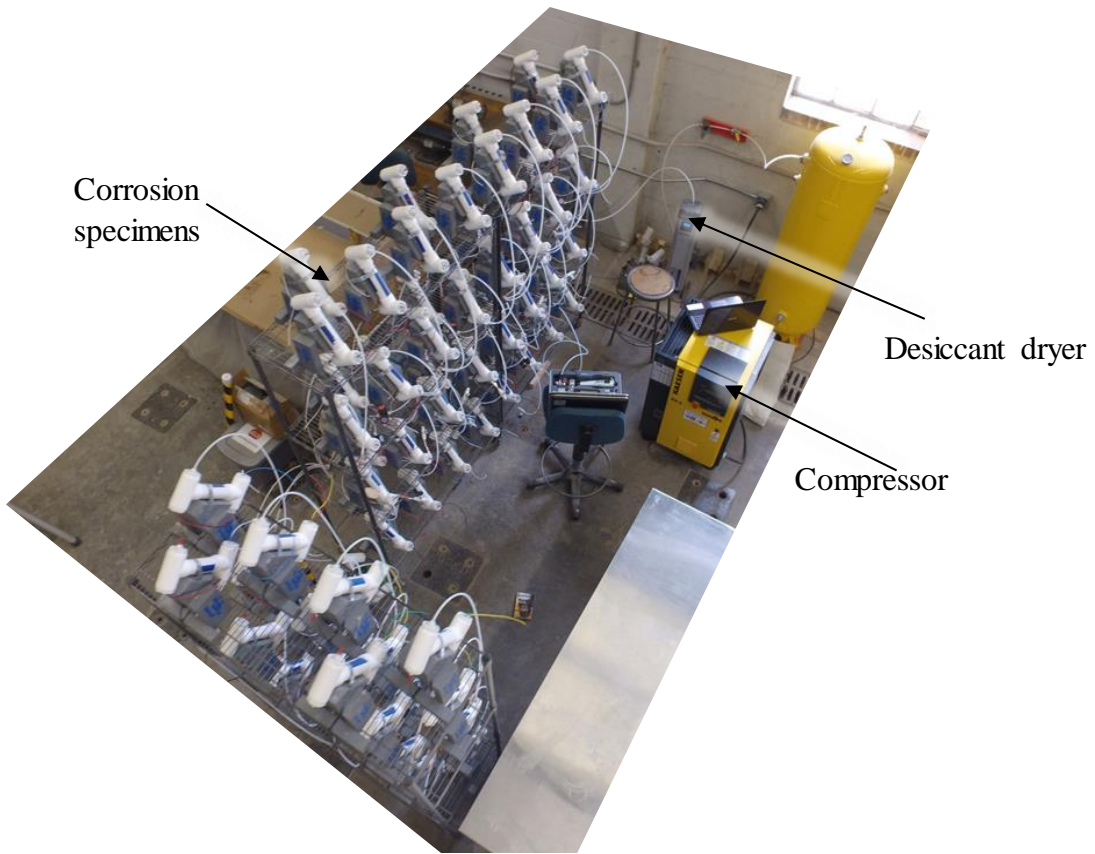


Figure 13-1. Drying system setup

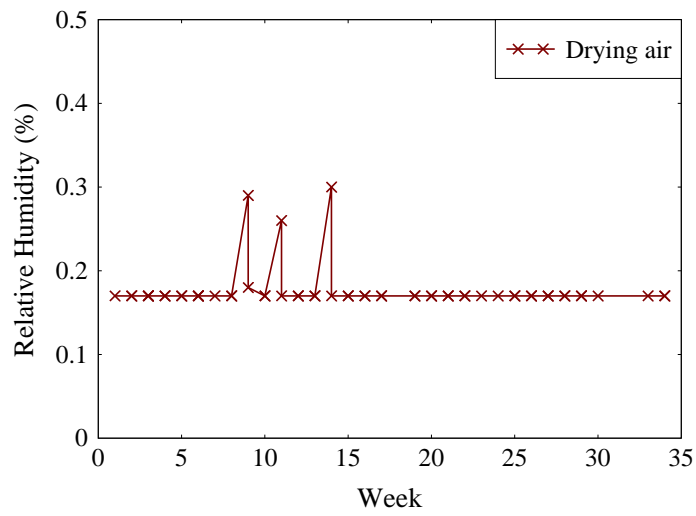


Figure 13-2. RH of drying air

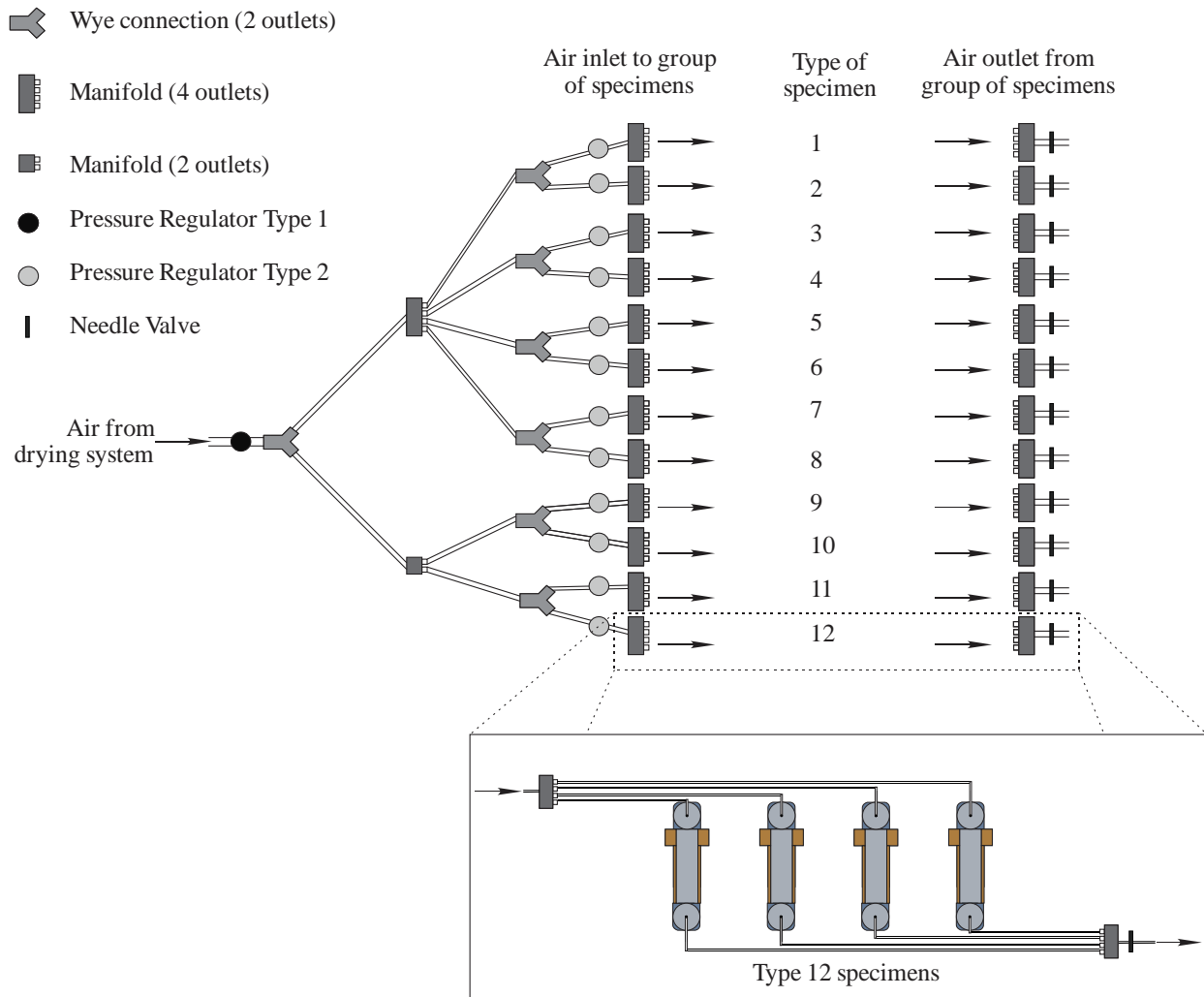
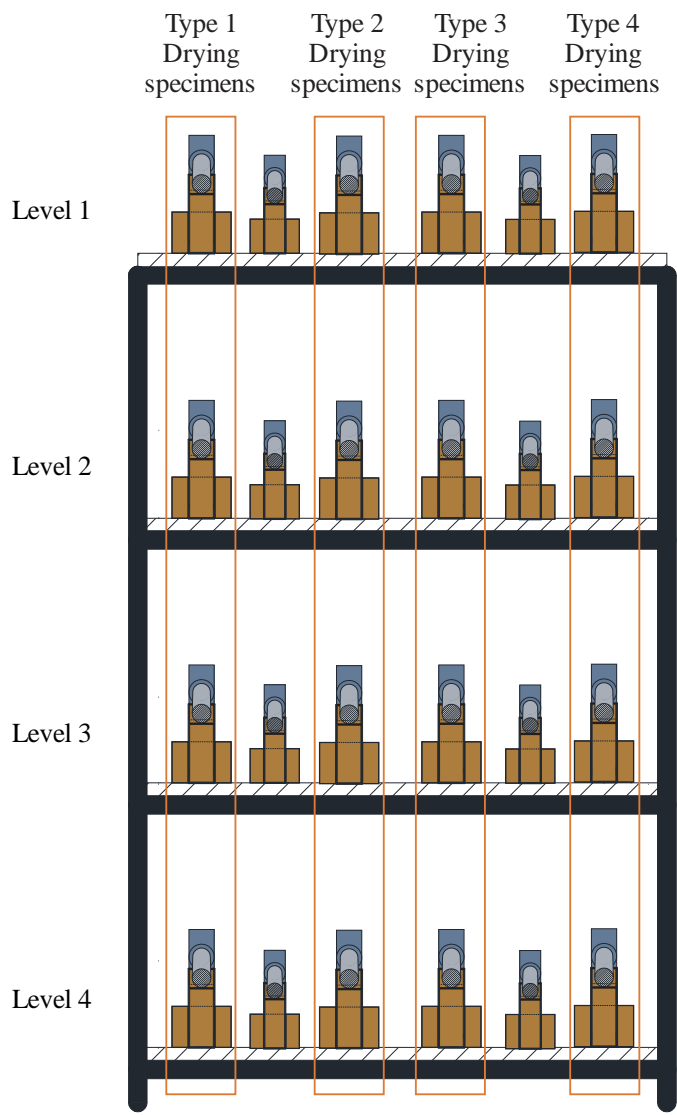


Figure 13-3. Dry air distribution system schematic



Front elevation

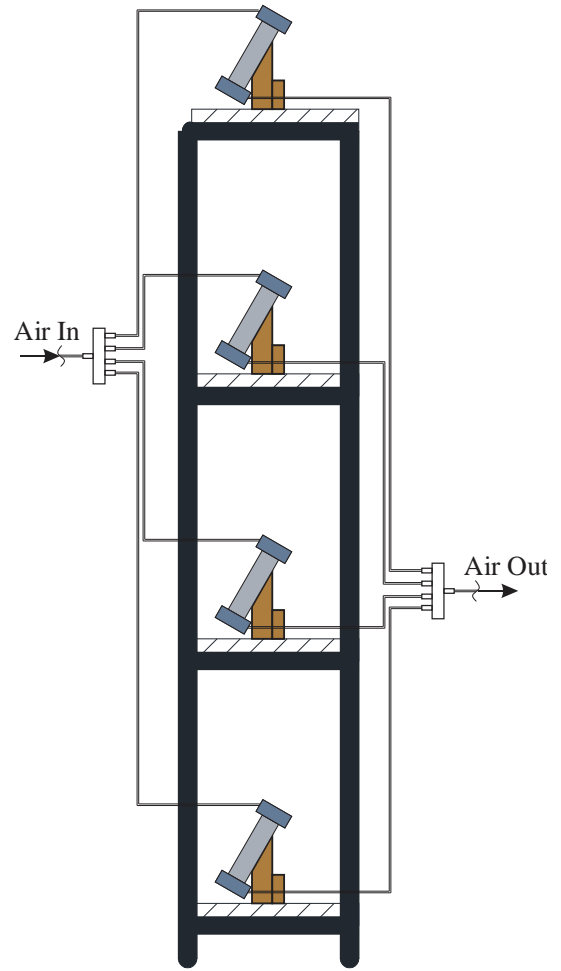


Figure 13-4. Schematic of specimen setup for drying on one shelving rack

14 Drying test procedures

Drying corrosion specimens were connected to the drying system to remove chemically unbound moisture from grout. Change in relative humidity (ΔRH_d) of drying air flowing through these specimens was measured to monitor their drying progress. To measure this change in humidity, RH of drying air at inlet (RH_{dI}) and RH of drying air at outlet (RH_{dO}) was measured for each specimen. If RH_{dO} was equal to RH_{dI} (i.e., $\Delta RH_d = RH_{dO} - RH_{dI} = 0$), the specimen was considered to be dry.

ΔRH_d readings were measured for all dried specimens every week on Mondays and Thursdays during the entire drying period using a Vaisala dewpoint meter. Figure 14-1 shows the dewpoint meter measurement system used to measure relative humidity of air at specimen outlet (RH_{dO}).

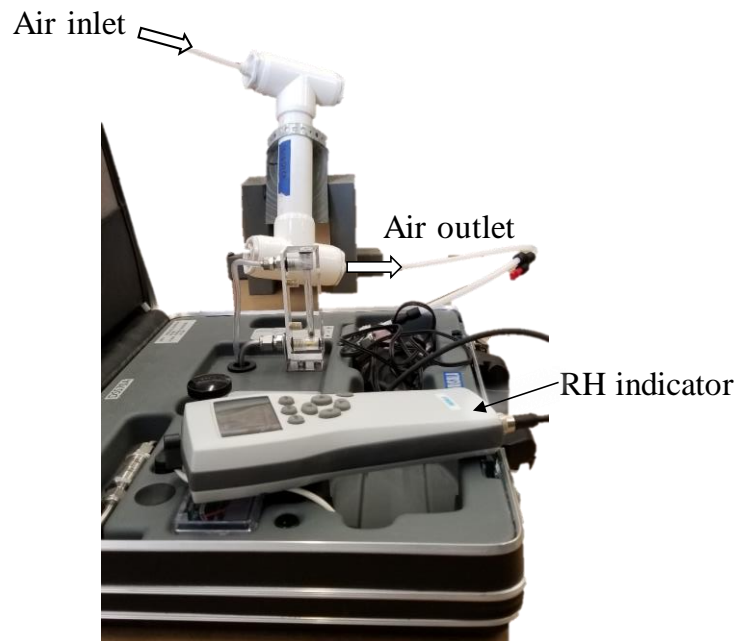


Figure 14-1. RH_{dO} measured at specimen outlet using Vaisala dewpoint meter

The steps for ΔRH_d measurements were as follows:

1. Measure RH_d of air at outlet of drying system and note the performance of drying system.
2. Measure RH_{dI} and RH_{dO} for each specimen. Readings were considered valid when they varied no more than 1% RH over 5 minutes as per ASTM F2170 – 16b (Standard Test Method for Determining Relative Humidity in Concrete Floor Slabs Using in situ Probes).
3. Calculate ΔRH_d using the following formula: $\Delta RH_d = RH_{dO} - RH_{dI}$

If ΔRH_d for a specimen was equal to zero, a dryness check was performed for that specimen using the following procedure:

1. Disconnect drying air inlet for the specimen with $\Delta RH_d = 0$ from the drying system. The specimen was disconnected on Thursday of the week when ΔRH_d was zero.
2. Allow humidity in the specimen to stabilize over the course of four days (Thursday to Sunday).
3. Reconnect the specimen inlet to the drying system on Monday.

4. Measure RH_{dO} and RH_{dI} twice: once on Monday within 5 minutes after reconnecting and a second time on Thursday. If ΔRH_d calculated on both Monday and Thursday was equal to zero again (+1% tolerance for leakages), the specimen was considered dried and disconnected from the drying system permanently. On the other hand, if ΔRH_d was greater than zero (+1% tolerance) on either day, grout in the specimen was assumed to contain free moisture, some of which was released during the four-day stabilization period. In this case, drying was continued for the specimen.

15 Corrosion test procedures

15.1 During drying

During drying, the potential difference between each strand and its paired reference electrode (RE) was measured in both drying and control specimens and recorded as corrosion potential of the respective strand. A fluke digital multimeter (87-5/E2KIT Industrial True-RMS Multimeter) was used to measure the corrosion potential (CP) and resistance (Figure 15-1). For this multimeter, the maximum specified resistance was 50 M Ω and the maximum specified voltage was 1000V. When measuring CP, the meter acted approximately like a 10 M Ω impedance in parallel with the circuit. To measure CP of a strand, the positive terminal was connected to the strand and the negative terminal to its RE. In addition, resistance was measured between anode and cathode, anode and its RE, cathode and its RE, and the two RE. These measurements were performed twice each week. Additionally, ambient temperature was recorded on the day of measurement.



Figure 15-1. Corrosion potential measurement during drying

15.2 Post-drying

After the specimens were dried, both dried and control specimens were connected to the automated data acquisition (DAQ) system. The instrumentation and data acquisition system consisted of embedded electrodes, measurement hardware, and computer software to control data acquisition. Figure 15-2 shows the typical specimen wiring for connection to the DAQ. A LabVIEW virtual instrument was developed to acquire the three voltage readings for each specimen (Figure 15-3). The specimens, along with DAQ hardware and software, were located in a temperature-controlled laboratory environment for continued monitoring after drying. The DAQ was connected to each specimen using three two-wire channels, which were used to measure corrosion potential (CP) and macrocell current for each specimen. The first two pairs were used to measure CP (V_1 and V_2) and the third pair was used to measure the macrocell current (V_3/R) (Figure 15-4). A resistor (R) of 10 ohms was connected across the third two-wire pair (Figure 15-5). Each measurement was recorded and logged automatically every 30 minutes for each specimen.

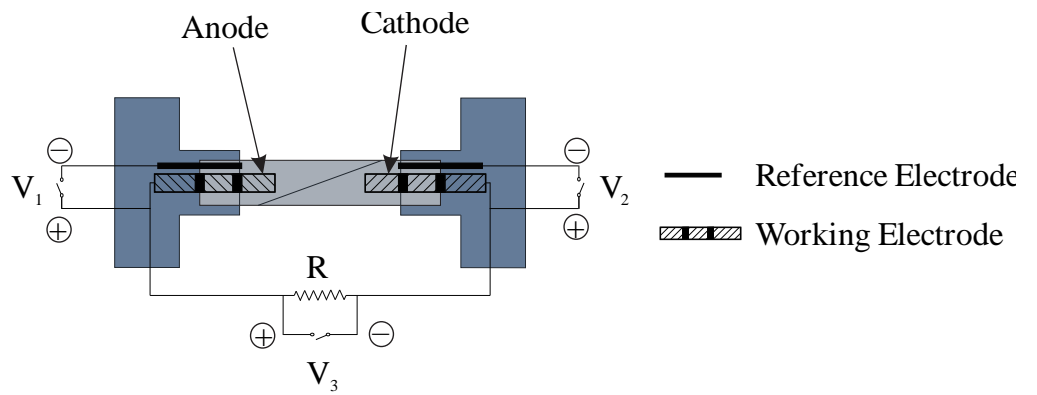


Figure 15-2. Schematic circuit diagram for monitoring after drying

Sample ID	V1 [V]	V2 [V]	I [mA]	
1	S1_5_100D1	-0.002	-0.002	-0.000
2	S2_5_100D2	-0.002	-0.002	-0.000
3	S3_5_100C1	-0.003	-0.128	-0.000
4	S4_5_100D1C	-0.002	-0.003	-0.000
5	S5_5_100D2C	-0.417	-0.491	-0.051
6	S6_5_100C1C	-0.506	-0.507	-0.009
7	S7_5_100D1E	-0.002	-0.002	-0.000
8	S8_5_100D2E	-0.002	-0.002	-0.000
9	S9_5_100C2E	-0.121	-0.128	-0.000
10	S10_5_100D1CE	-0.002	-0.002	-0.000
11	S11_5_100D2CE	-0.000	-0.002	-0.000
12	S12_5_100C1CE	-0.265	-0.453	-0.040
13	S13_100_SD1	-0.002	-0.002	-0.000
14	S14_100_SD2	-0.002	-0.002	-0.000

Figure 15-3. User interface of DAQ software

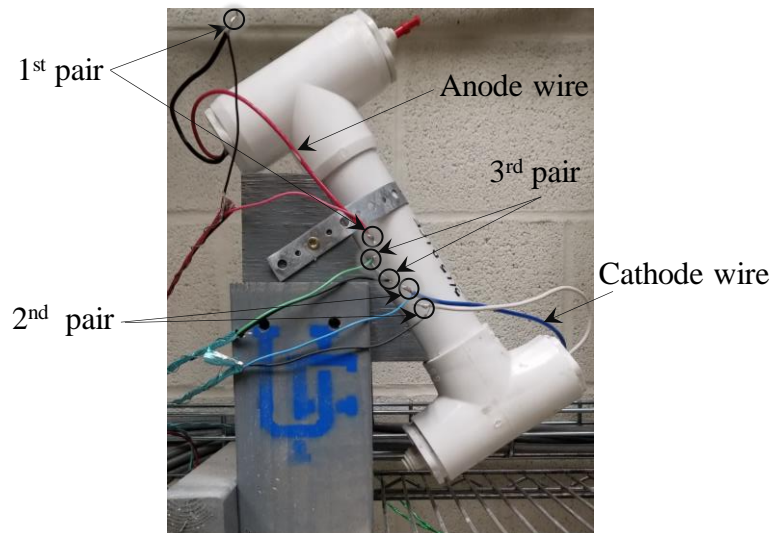


Figure 15-4. Typical corrosion specimen connection to DAQ

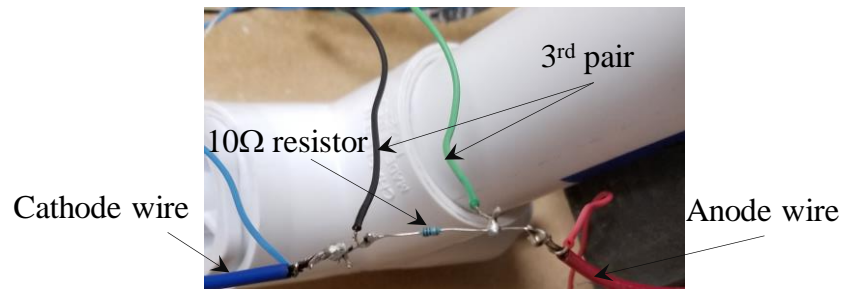


Figure 15-5. Resistor between anode and cathode

16 Dissection procedures

After drying, D1, D2, and C1 specimens were monitored for macrocell current and corrosion potential. D1 specimens were monitored for at least one month and D2 and C1 specimens were monitored for at least four months after specimens were dried. These specimens were monitored using the automated data acquisition system, which was a modified version of the ASTM G109 macrocell corrosion rate monitoring procedures. The number of days the specimens were monitored under modified G109 corrosion monitoring using this approach are shown in Table 16-1. The objective of monitoring dried D2 specimens was to detect any macrocell corrosion formation in specimens with dried grout. However, after four months of monitoring, only 1 out of 24 dried grout D2 specimens was detected with macrocell current. As only one of these dried specimens (D2) indicated macrocell formation after four months, all dried and control specimens were decided to be dissected after four months to evaluate properties of grout and corrosion on strands in the specimens.

The objectives of dissection were to measure moisture content and pH of the grout and to extract prestressing strands for evaluating corrosion. To extract strand and grout samples, the PVC pipe and fittings were cut along the longitudinal axis of specimen (Figure 16-1). A concrete saw was used to cut through the PVC with the depth of cut slightly larger than the PVC wall thickness (Figure 16-2). To track the inlet and outlet locations during disassembly, letters “T” and “B” were marked on PVC at the specimen ends. Letter “T” indicated air inlet end and “B” indicated air outlet end of a specimen (Figure 16-2b).

After cutting through the PVC, the PVC shell was removed to expose grout as shown in Figure 16-3a. To evaluate pH of grout, a spray-on chemical pH indicator was used to estimate the pH of the grout (manufacturer: Germann Instruments). This indicator was sprayed at the two ends and grout interface region of the specimen in order to understand change in pH of grout along the direction of air flow (Figure 16-3b). After measuring the pH, samples of each grout type were collected to measure grout moisture content in both dried and control specimens (Figure 16-4a). Finally, strands were extracted and stored in airtight bags for further corrosion evaluation (Figure 16-4b).

Table 16-1. Specimen matrix

Grout mixture		Number of strands	Strand crosses grout interface (E)	Presence of chlorides (C)	Age when grout dried (days)		Modified G109 corrosion monitoring (days)	
Top half	Bottom half				D1	D2	D1*	D2**
5 PC	100 PC	1			238	238	70	210
				x	238	238	70	210
5 PC	100 PC	1	x		238	238	70	210
			x	x	238	238	65	205
100 PC	5 PC	1			175	161	65	205
				x	154	140	65	350
100 PC	5 PC	1	x		238	196	65	205
			x	x	189	189	65	250
5 PC	15 PC	1			112	105	240	375
				x	140	175	90	320
5 PC	15 PC	1	x		112	105	240	375
			x	x	140	175	200	250
15 PC	5 PC	1			112	112	240	375
				x	112	238	240	225
15 PC	5 PC	1	x		112	105	240	375
			x	x	175	140	200	350
PT grout	100 PC	1			238	238	30	180
				x	238	238	30	180
100 PC	PT grout	1			238	238	42	180
				x	238	238	42	180
5 PC	5 PC	2			49	49	240	375
				x	49	49	240	375
100 PC	100 PC	2			238	238	70	210
				x	238	238	70	210

* Age of dried specimen D1 from casting to dissection was ~308 days

** Age of dried specimen D2 from casting to dissection was ~448 days

*** Age of control specimen C1 from casting to dissection was ~448 days

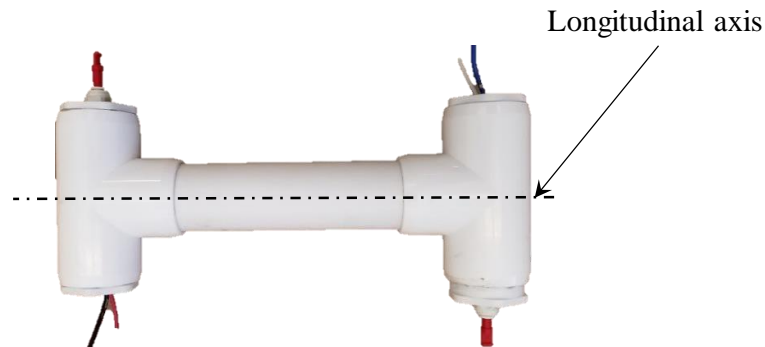


Figure 16-1. Longitudinal axis of corrosion specimens

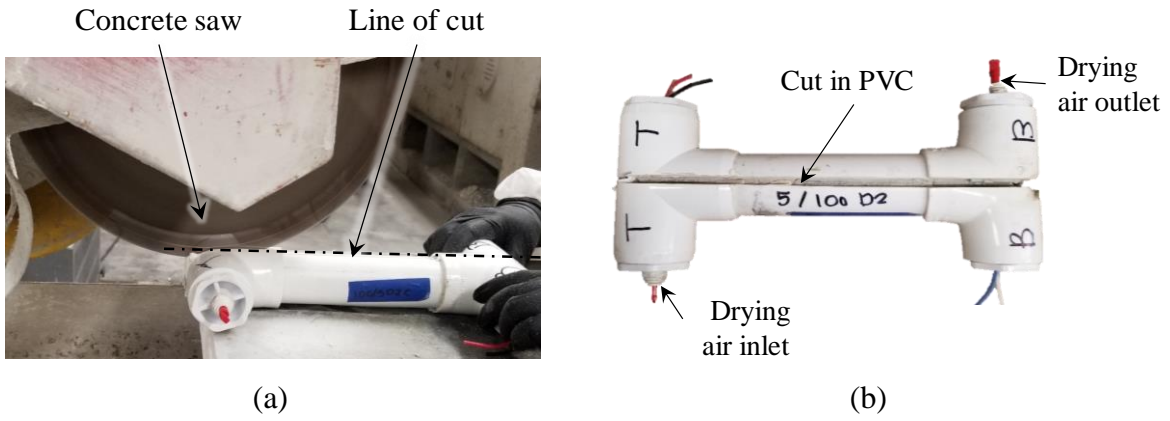


Figure 16-2. Dissection of specimen: (a) Use of concrete saw; (b) Specimen after cut in PVC

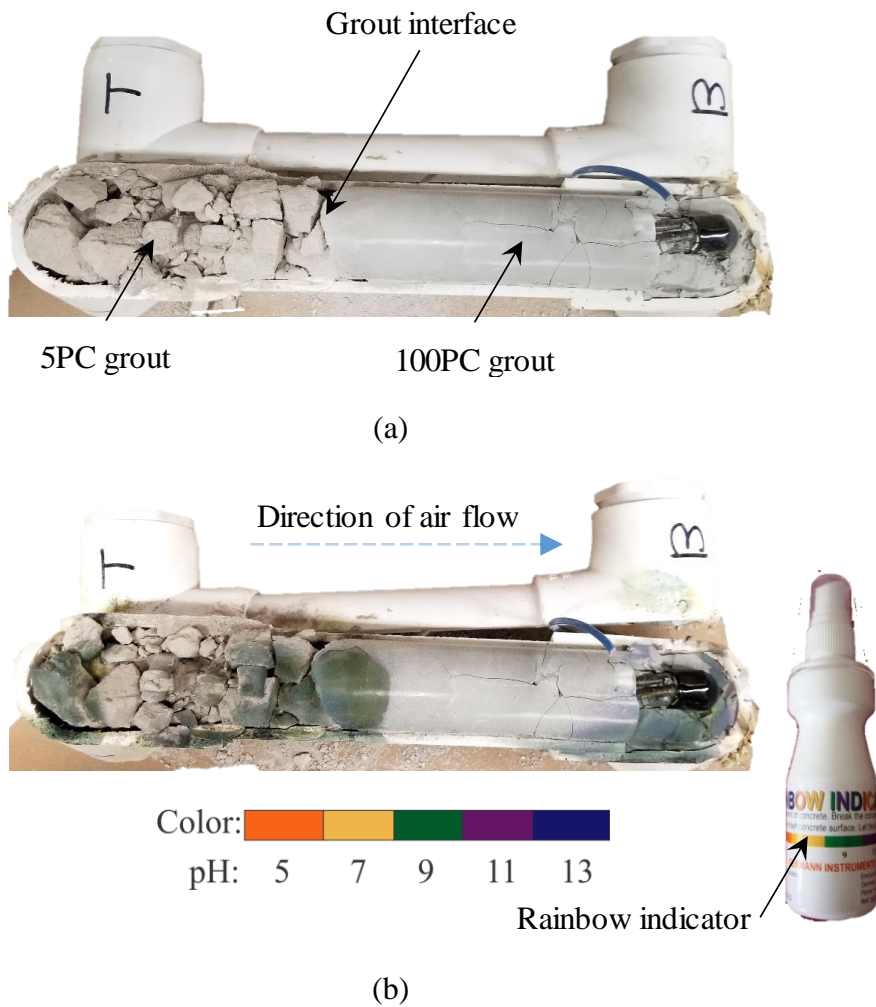


Figure 16-3. pH testing: (a) Location of grout; (b) pH measurement using spray-on chemical indicator



(a)



(b)

Figure 16-4. Sampling during dissection: (a) Grout; (b) Strand

17 Physical corrosion evaluation procedure

Strands in dried and control specimens were extracted during dissection to visually evaluate corrosion, if present. In the first step of evaluation, strands were rated based on work performed by Sason in which the superficial corrosion products were cleaned using a Scotch Brite cleaning pad no. 96 (Sason, 1992). The cleaned strands were visually examined for pits. Because pits can reduce fatigue and ultimate strength of prestressing strand, those pits visible to the unaided eye were classified as objectionable. Based on the extent of pitting observed, prestressing strand corrosion was given a rating based on a rating scale of 1 through 8. According to Sason (1992), strands with ratings of less than or equal to three are considered acceptable for use. Similarly, *PTI M50 Acceptance Standards for Post-Tensioning Systems* also considers strands with corrosion ratings less than or equal to three to be acceptable. Figure 17-1 and Figure 17-2 show photos illustrating the amount of corrosion associated with a corrosion rating of 1 through 8 in which a corrosion rating of 1 indicates a strand that is free of corrosion. The corrosion rating increases as the intensity and coverage of the corrosion increases.

After evaluating corrosion visually, corrosion products were removed chemically using cleaning procedure described in section C.3.5 of ASTM G1-2017 *Preparing, Cleaning, and Evaluating Corrosion Test Specimens*. In this procedure, strands were separated into individual wires and placed in a solution of 500 mL hydrochloric acid and 3.5 g hexamethylene tetramine for at least 10 minutes at 20 to 25°C (Figure 17-3). The cleaning was stopped when corrosion products were completely removed. After cleaning, loss of section in individual wires was measured following the procedure outlined in ACI 364.14T-17 *Section Loss Determination of Damaged or Corroded Reinforcing Steel Bars* (Figure 17-4a). Accordingly, average of section loss in all wires of a strand was measured to determine percentage of area lost due to corrosion. Furthermore, if corrosion pits were visible to naked eyes, pit depths were measured following ASTM G46-94 *Standard Guide for Examination and Evaluation of Pitting Corrosion* (Figure 17-4b) and an average of all pit depths measured on wires of a strand was reported for each strand.

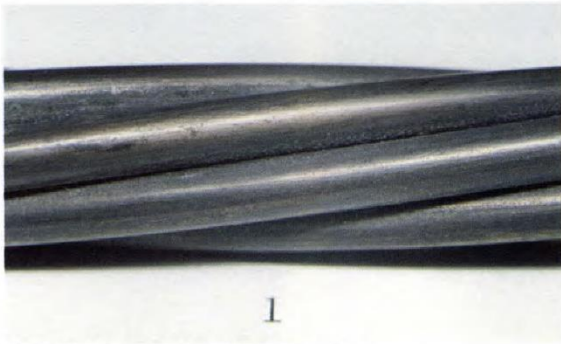


Photo 1. Strand surface before cleaning.

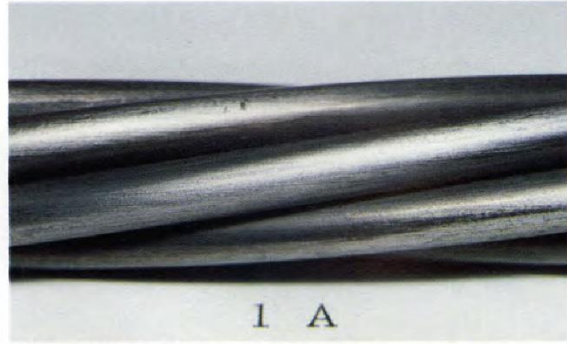


Photo 1A. Strand surface after cleaning.



Photo 2. Strand surface before cleaning.

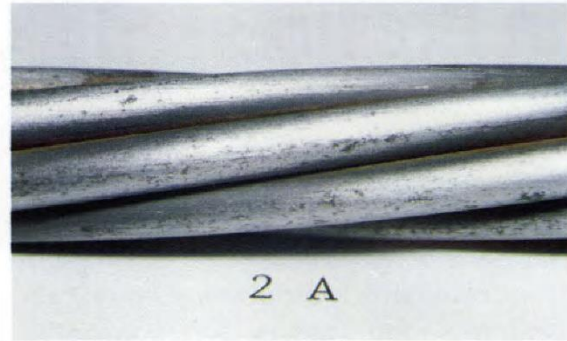


Photo 2A. Strand surface after cleaning.



Photo 3. Strand surface before cleaning.

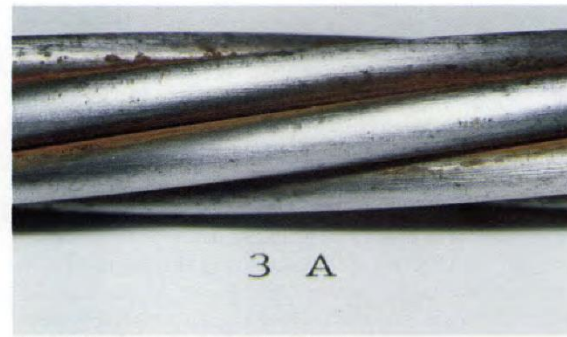


Photo 3A. Strand surface after cleaning.



Photo 4. Strand surface before cleaning.

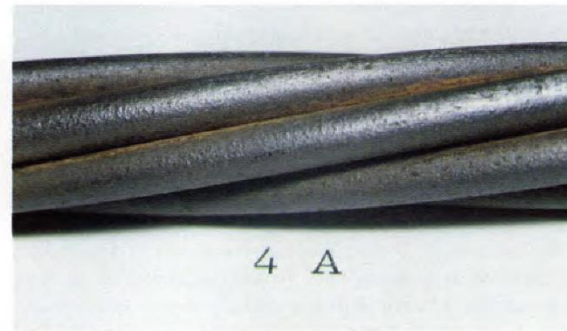


Photo 4A. Strand surface after cleaning.

Figure 17-1. Photographs documenting strand corrosion and associated ratings 1 to 4 (Sason, 1992)



Photo 5. Strand surface before cleaning.

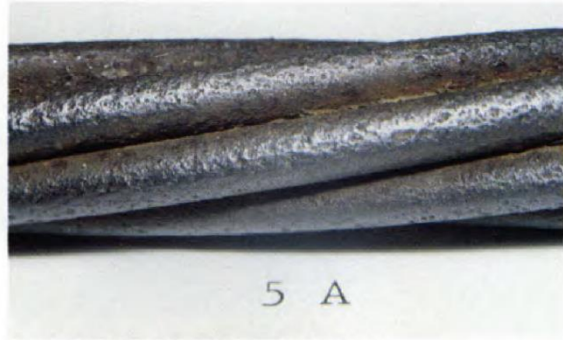


Photo 5A. Strand surface after cleaning.



Photo 6. Strand surface before cleaning.



Photo 6A. Strand surface after cleaning.



Photo 7. Strand surface before cleaning.



Photo 7A. Strand surface after cleaning.



Photo 8. Strand surface before cleaning.



Photo 8A. Strand surface after cleaning.

Figure 17-2. Photographs documenting strand corrosion and associated ratings 5 to 8 (Sason, 1992)

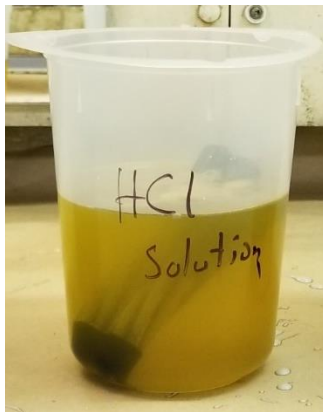


Figure 17-3. Cleaning of corrosion products on strands following ASTM G1-03

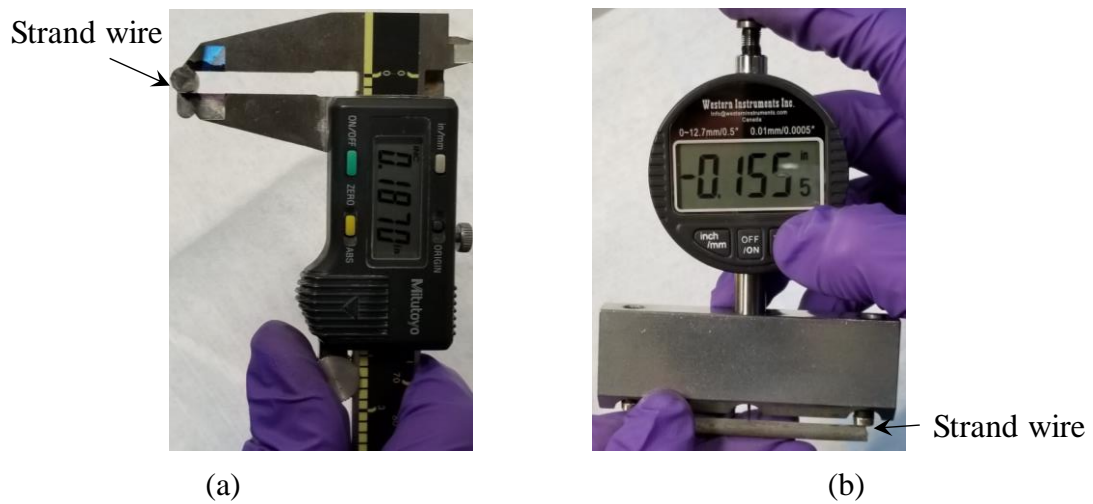


Figure 17-4. Corrosion evaluation of strands measurement (a) Loss in section (b) Pit depth

18 Drying results and discussion

Drying of corrosion specimens was initiated on January 11, 2018. Drying progress of each specimen was monitored using ΔRH_d readings measured every week. Specimens were disconnected from the drying system after they passed the dryness check previously described. Accordingly, the last dried specimens were disconnected on October 8, 2018. However, specimen 5 PC/100 PC D2C was also disconnected on October 8, 2018 even though dryness check indicated it was not dried. This specimen was considered unable to be dried because its ΔRH_d reading was 30.34% even after eight months of drying while ΔRH_d of its replicate, 5 PC/100 PC D1C, was 0%. Table 18-1 provides more details regarding the week during which each specimen passed the dryness check. Table 18-1 also shows the final ΔRH_d readings for each specimen.

Figure 18-1 (a) through (l) show the variation of ΔRH_d readings for dried corrosion specimens over time. Each plot indicated ΔRH_d measurements for dried specimens containing grout with and without addition of chlorides. In these plots, curves dried 1 and dried 2 indicate readings for specimens D1 and D2, respectively. To determine a drying time for each specimen, a dry grout criterion of $\Delta RH_d = 1\%$ was established as discussed in Section 14 of this report. Note that in specimens with E as suffix in their labels, the strand embedded in 5 PC grout extended to cross the interface between two grouts in the specimens. In the remaining specimens, strands did not cross the grout interface.

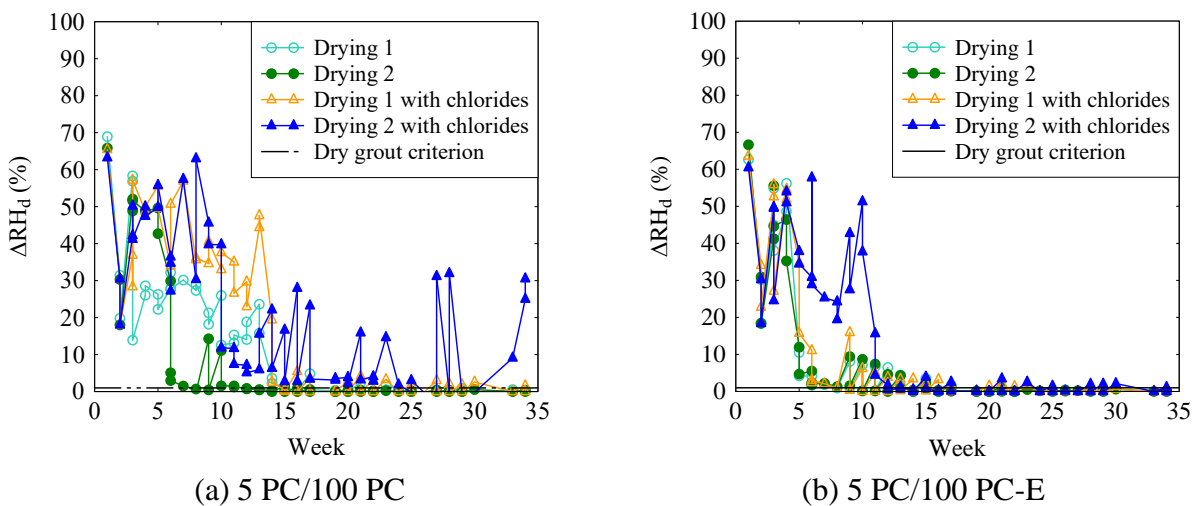
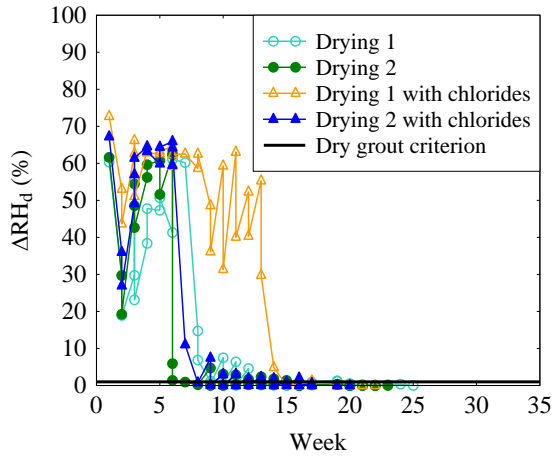
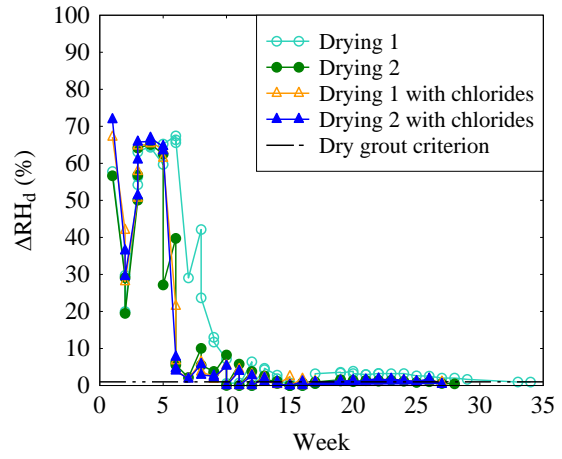


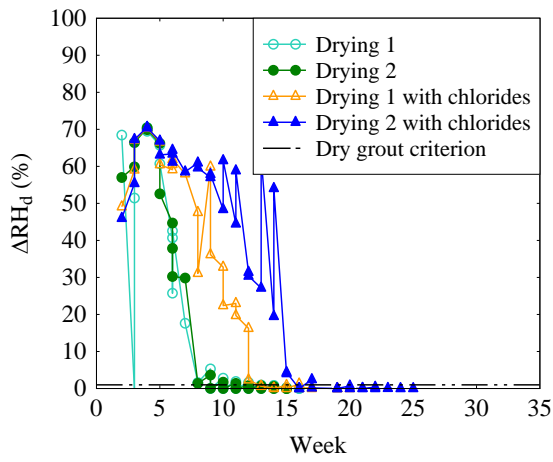
Figure 18-1. ΔRH_d (%) vs. time (weeks) for dried corrosion specimens



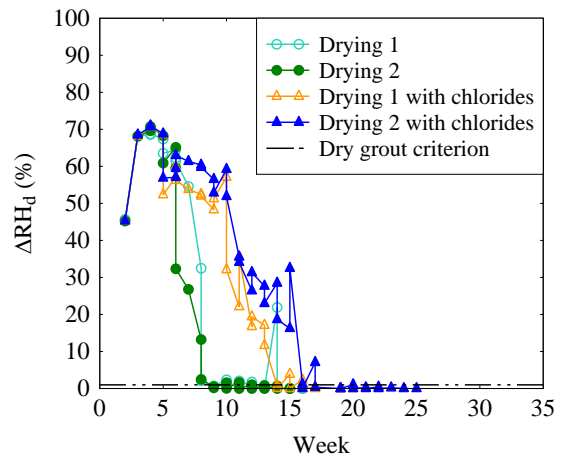
(c) 100 PC/5 PC grout



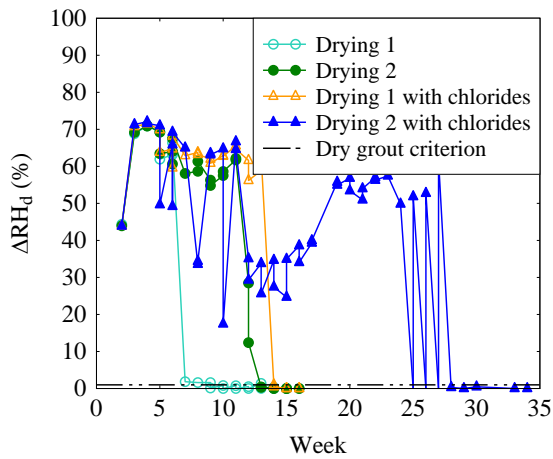
(d) 100 PC/5 PC-E



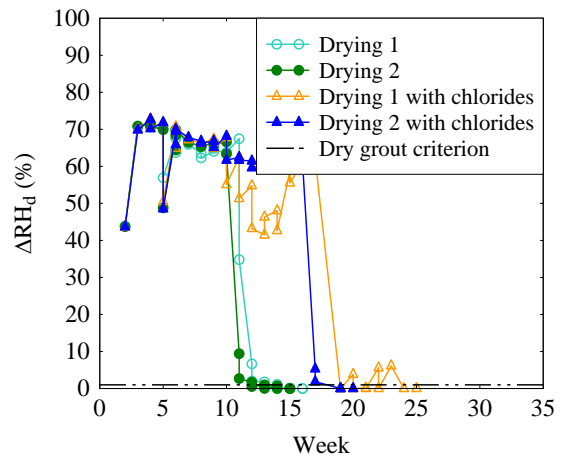
(e) Type 5 (5 PC/15 PC grout) specimen



(f) 5 PC/15 PC-E



(g) 15 PC/5 PC



(h) 15 PC/5 PC-E

Figure 18-1. ΔRH_d (%) vs. time (weeks) for dried corrosion specimens

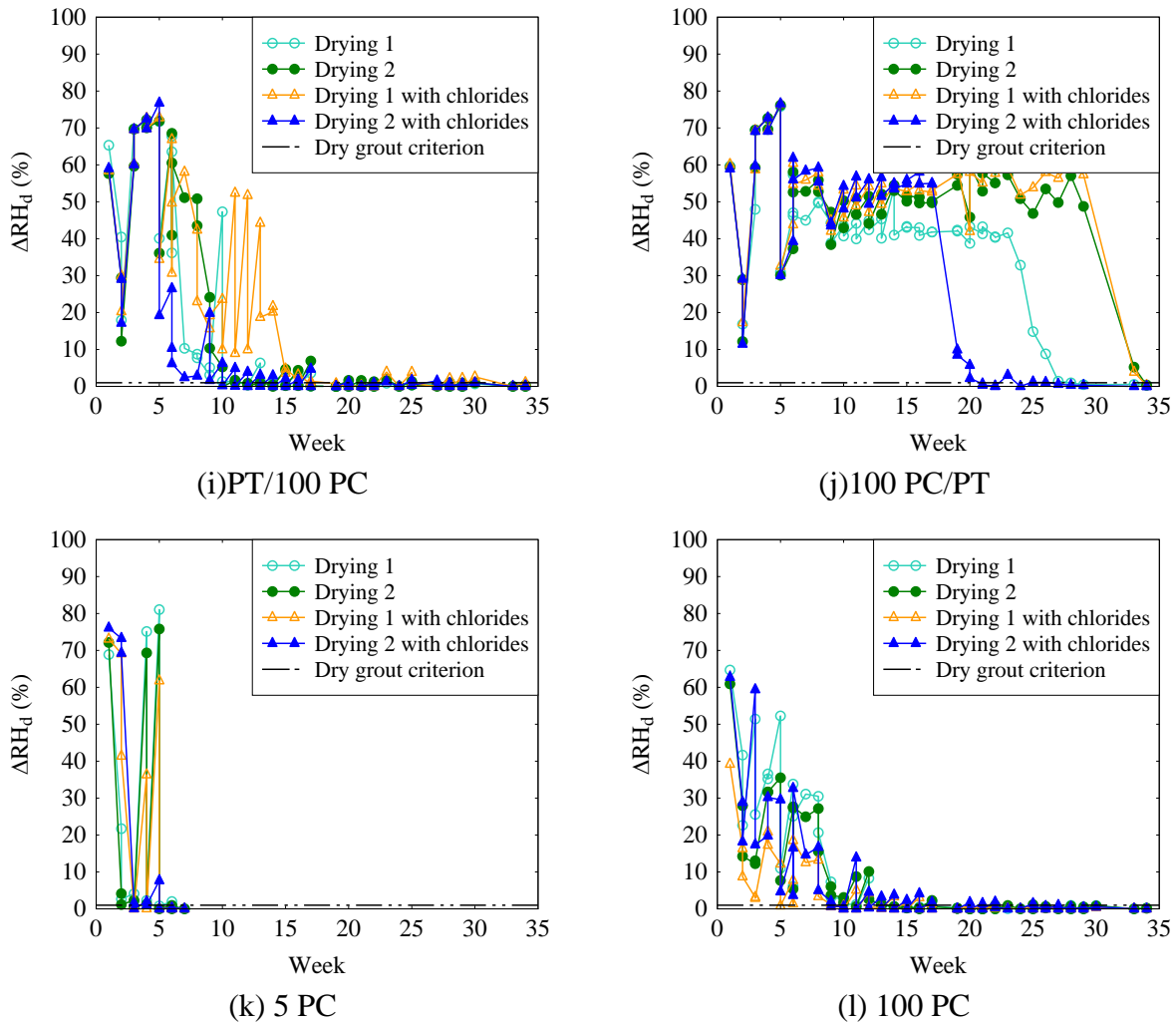


Figure 18-1. ΔRH_d (%) vs. time (weeks) for dried corrosion specimens

Based on these plots, Table 18-1 summarizes the week when each specimen was deemed to be dried. In general, specimens with at least one grout layer of normal grout dried slower than specimen with no normal grout layers because normal grout had greater impermeability compared to soft grout, and delayed air and moisture flow through and out of the specimens. Specimens with no normal grout dried within 24 weeks, while specimens with at least one normal grout layer dried in approximately 34 weeks with the exception of specimens where a soft grout layer was closer to the outlet. This was thought to expedite drying by reducing the distance required for the moisture to travel out of the specimen. Specimens with the lowest cement content (5 PC) dried in 7 weeks, which was the fastest of all of the specimens in 7 weeks. These specimens consisted of one continuous strand along the length which was thought to improve air flow and moisture removal through crevices in the strand inside grout. The criterion of $\Delta RH_d < 1\%$, which was used to predict if grout was dried, was validated after dissection because the moisture content of dried soft grout was found to be less than 1% by weight of the grout.

Table 18-1. Drying timeline

Type no.	Type of specimen		Designation	Week of drying																																				
	Top half grout	Bottom half grout		Final Δ RH	1	2	3	4	5	6	7	8	9	10	11	12	13	14	15	16	17	18	19	20	21	22	23	24	25	26	27	28	29	30	31	32	33	34		
1	5 PC / 100 PC		D1	0.16																																			x	
			D2	0																																				x
			D1 C	0																																				x
			D2 C	30.34																																				x
2	5 PC / 100 PC		D1 E	0																																				
			D2 E	0																																				x
			D1 C E	0																																				x
			D2 C E	0																																				x
3	100 PC / 5 PC		D1	0																																				
			D2	0																																				
			D1 C	0																																				
			D2 C	0																																				
4	100 PC / 5 PC		D1 E	0.88																																			x	
			D2 E	0.28																																			x	
			D1 C E	0.27																																				x
			D2 C E	0.45																																				x
5	5 PC / 15 PC		D1	0																																				
			D2	0																																				
			D1 C	0																																				
			D2 C	0																																				
6	5 PC / 15 PC		D1 E	0																																				
			D2 E	0																																				
			D1 C E	0																																				
			D2 C E	0																																				

19 Dissection results and discussion

19.1 Grout moisture content

Comparison of moisture content (MC) of grout in dried and control specimens was used to verify the effectiveness of drying the corrosion specimens. During drying, grout was considered to be dried, and drying of specimen was discontinued if the difference between the relative humidity of drying air at the inlet and outlet (ΔRH_d) of a specimen was less than 1% for at least two successive weeks. After dissection, the measured average moisture content (MC) of soft grout (5 PC and 15 PC) in dried specimens was 0.7% and in control specimens was 36%. Similarly, measured average MC of expired and prehydrated defective prepackaged grout in dried specimens was 4.5% and in control specimens was 51%. Therefore, drying was successful in removing most of the free moisture in soft and defective grouts and the criterion of $\Delta RH_d < 1\%$ successfully predicted that soft grout was dry in the corrosion specimens. Alternatively, in the case of dried specimen 5 PC/100 PC D2C, ΔRH_d did not decrease below 1% for over two successive weeks, which indicated that the grout was not dry. This indication was confirmed by the high measured MC of more than 23% in the soft grout in this specimen. It was thought that normal grout in this specimen did not develop enough shrinkage cracks to allow enough flow of air and moisture out of the specimen, therefore resulting in high MC. Furthermore, the average MC of normal grout in dried specimens was 3.8% and in control specimens was 27%, which indicated that drying could also remove most of the free moisture from normal grout.

19.2 Grout pH

During dissection, pH of grout in the control and dried specimens was measured using a spray-on chemical indicator to study the effect of drying on the grout pH. Table 19-1 shows the pH of different grout layers in dried specimens (D1 and D2) and control specimens (C1); table cells containing pH less than 11 are shaded. Under pH of 11, the iron-oxide protective layer on steel becomes unstable and allows progression of corrosion. In general, Table 19-1 shows that for any particular type of grout, pH of dried grout was lower than pH of grout in control specimens. The lower pH in dried grout than in undried grout was attributed to carbonation of grout during the drying process due to introduction of carbon dioxide by the air injected into the dried specimens.

The average pH of dried soft grout (5 PC and 15 PC), conditioned defective prepackaged grout (PT), and normal grout (100 PC) was 8.7, 8.7 and 9.5, respectively. Whereas the average pH of soft grout, defective PT grout, and normal grout in the control specimens was 11.8, 11.0 and 12.3 respectively. Therefore, the pH of soft and defective PT grout was less than the pH of normal grout in both dried and control specimens. No trend was observed in the variation of pH along the direction of air flow from inlet end to outlet end. For example, the pH of 5 PC grout along the direction of air flow increased in specimen 5 PC/100 PC D1 but decreased in specimen 5 PC/100 PC D2. No significant difference was observed for pH between dried specimen replicates D1 and D2.

Table 19-1. pH of grout in corrosion specimens

Designation	Strand across grout interface	Presence of chlorides	Type of grout		pH			
					Top grout		Bottom grout	
			Top	Bottom	Inlet end	Grout interface region	Grout interface region	Outlet end
D1			5 PC	100 PC	5	7	10	11
D2					9	8	8	10
C1					10	10	13	13
D1 C		x			5	9	9	11
D2 C		x			9	11	11	11
C1 C		x			10	10	11	11
D1 E	x				9	9	9	9
D2 E	x				9	7	9	10
C1 E	x				10	10	11	13
D1 C E	x	x			9	9	9	9
D2 C E	x	x			8	9	10	11
C1 C E	x	x			10	10	11	11
D1			100 PC	5 PC	9	9	7	7
D2					8	9	10	10
C1					13	13	12	12
D1 C		x			11	9	9	7
D2 C		x			11	11	9	8
C1 C		x			11	11	10	10
D1 E	x				9	9	7	5
D2 E	x				8	9	7	7
C1 E	x				13	13	10	10
D1 C E	x	x			11	9	7	7
D2 C E	x	x			10	8	9	8
C1 C E	x	x			13	12	10	10
D1			5 PC	15 PC	9	9	9	9
D2					9	9	10	10
C1					12	12	12	12
D1 C		x			5	9	9	9
D2 C		x			5	5	7	11
C1 C		x			13	13	12	12
D1 E	x				9	9	9	9
D2 E	x				9	9	10	9
C1 E	x				12	13	13	13
D1 C E	x	x			5	9	11	9
D2 C E	x	x			7	7	7	9
C1 C E	x	x			11	12	12	13

Table 19-1, continued

Designation	Strand across grout interface	Presence of chlorides	Type of grout		pH			
			Top	Bottom	Top grout		Bottom grout	
					Inlet end	Grout interface region	Grout interface region	Outlet end
D1			15 PC	5 PC	9	7	7	9
D2					10	8	8	8
C1					13	13	10	10
D1 C		x			9	11	9	7
D2 C		x			11	9	9	8
C1 C		x			13	13	10	13
D1 E	x				9	9	9	7
D2 E	x				9	7	7	7
C1 E	x				11	13	13	13
D1 C E	x	x			10	10	9	9
D2 C E	x	x			10	9	9	9
C1 C E	x	x			13	13	13	12
D1			PT	100 PC	9	9	9	9
D2					7	9	9	11
C1					13	13	13	13
D1 C		x			5	9	9	11
D2 C		x			9	11	11	11
C1 C		x			9	9	13	13
D1			100 PC	PT	9	9	9	7
D2					11	9	9	8
C1					13	13	13	9
D1 C		x			9	11	11	9
D2 C		x			11	10	10	9
C1 C		x			13	13	13	9
D1			5 PC	5 PC	9	9	9	9
D2					9	9	9	9
C1					11	11	11	11
D1 C		x			9	9	9	9
D2 C		x			9	9	11	10
C1 C		x			10	10	10	12
D1			100 PC	100 PC	9	9	9	9
D2					9	9	9	9
C1					11	12	12	12
D1 C		x			9	9	9	9
D2 C		x			9	9	9	9
C1 C		x			13	13	13	13

19.3 Prestressing strand corrosion rating

The procedure for cleaning and rating corrosion on strands was based on work of Sason (1992) and was performed to visually determine the extent of corrosion in dried and control specimens. Note that strands were cleaned prior to fabrication of specimens and had a corrosion rating of 1. Figure 19-1 shows an example of corrosion rating for strand placed in 5 PC grout of 15 PC/5 PC D1C specimen. Table 19-2 shows the rating of strand corrosion in all the specimens. As per Sason (1992) and PTI M50 criterion for acceptable corrosion rating of strands, strands with corrosion rating of 4 or more were considered as unacceptable. Therefore, in Table 19-2, the table cells containing a corrosion rating of 4 or over are shaded.



Figure 19-1. Corrosion rating = 6 for strand in 5 PC grout of 15 PC/5 PC D1C specimen:
(a) Before cleaning; (b) After cleaning

Table 19-2. Strand corrosion rating

Designation	Strand across grout interface	Presence of chlorides	Type of grout		Corrosion rating	
					Top grout strand	Bottom grout strand
			Top	Bottom		
D1			5 PC	100 PC	1	1
D2					1	1
C1					1	1
D1 C		x			6	4
D2 C		x			7	4
C1 C		x			2	4
D1 E	x				1	1
D2 E	x				1	1
C1 E	x				1	1
D1 C E	x	x			5	3
D2 C E	x	x			6	4
C1 C E	x	x			4	2
D1					100 PC	5 PC
D2			1	1		
C1			1	1		
D1 C		x	3	5		
D2 C		x	5	5		
C1 C		x	3	7		

Table 19-2, continued

Designation	Strand across grout interface	Presence of chlorides	Type of gout		Corrosion rating	
			Top	Bottom	Top grout strand	Bottom grout strand
D1 E	x		100 PC	5 PC	1	2
D2 E	x				1	1
C1 E	x				1	1
D1 C E	x	x			1	7
D2 C E	x	x			3	4
C1 C E	x	x			3	5
D1			5 PC	15 PC	1	1
D2					1	1
C1					1	1
D1 C		x			7	6
D2 C		x			5	5
C1 C		x			6	4
D1 E	x				2	1
D2 E	x				2	1
C1 E	x				2	1
D1 C E	x	x			7	7
D2 C E	x	x			6	4
C1 C E	x	x			4	2
D1			15 PC	5 PC	1	1
D2					1	1
C1					1	1
D1 C		x			4	6
D2 C		x			6	6
C1 C		x			2	3
D1 E	x				5	3
D2 E	x				1	2
C1 E	x				1	1
D1 C E	x	x			6	7
D2 C E	x	x			6	5
C1 C E	x	x			1	5
D1			PT	100 PC	1	2
D2					1	1
C1					2	1
D1 C		x			6	4
D2 C		x			4	3
C1 C		x			4	4

Table 19-2, continued

Designation	Strand across grout interface	Presence of chlorides	Type of grout		Corrosion rating	
			Top	Bottom	Top grout strand	Bottom grout strand
D1			100 PC	PT	1	6
D2					1	4
C1					1	3
D1 C		x			4	7
D2 C		x			4	3
C1 C		x			4	6
D1			5 PC	5 PC	1	
D2					1	
C1					1	
D1 C		x			4	
D2 C		x			5	
C1 C		x			4	
D1			100 PC	100 PC	1	
D2					1	
C1					1	
D1 C		x			2	
D2 C		x			4	
C1 C		x			3	

Table 19-3 summarizes the number of specimens with corrosion based on strand rating. The Table indicates that almost all the specimens with admixed chlorides (CI) had strands with corrosion. Further, the average corrosion rating in CI specimens was also greater than specimens with no admixed chlorides, indicating admixed chlorides probably increased corrosion intensity in specimens. The average corrosion rating of the strands in nonchloride-contaminated grout was less than 3, indicating a general acceptability of the corrosion intensity.

In the case of dried specimens with unacceptable corrosion rating of strands, the average ratings for strands placed in soft grout, defective PT grout, and normal grout were 5.6, 5.4, and 4.2 respectively. Whereas in the case of control specimens with unacceptable corrosion rating of strands, the average ratings for strands in soft grout, defective PT grout, and normal grout were 4.9, 5, and 4, respectively. Therefore, the strand corrosion was more severe on strands in the dried specimens compared to strands in control specimens. Further examination showed that the strand corrosion rating was greater for strands placed in soft and defective PT grout strands than for strands placed in normal grout, which could be due to higher moisture content in soft grout compared to normal grout and formation of macrocell between strands in soft and normal grout. The average corrosion rating of strands in all dried specimens D1 (3.3) was similar to that in dried specimens D2 (3).

Table 19-3. Number of specimens with unacceptable strand rating

Type of specimens	No. of specimens with corrosion (average rating)		Total No. of specimens	
	With Cl	Without Cl	With Cl	Without Cl
All	33 (4.6)	3 (3)	36	36
Dried (D1 and D2)	23 (4.9)	3 (3.3)	24	24
Control (C1)	10 (3.4)	0 (-)	12	12

19.4 Prestressing strand section loss and pitting

Measurements of loss in section and corrosion pit depths were used to further quantify corrosion observed in the dried and control specimens. According to ASTM G46, pitting could be evaluated using three different scales, namely, “A” based on pit density, “B” based on pit area and “C” based on pit depths. In this report, pits were evaluated using scale “C”. Based on scale “C”, pitting on a strand could be classified from level C-1 to C-5 based on the maximum pit depth on the strand as per Table 19-4.

Table 19-4. Scale “C” for pitting evaluation

Classification	Maximum pit depth (in.)
C-1	0.02
C-2	0.03
C-3	0.06
C-4	0.13
C-5	0.25

Table 19-5 shows results of evaluating loss in section and pit depth for dried and control specimens; table cells containing detectable section loss are shaded. Note that for each strand, the reported results are average of loss in section and pit depths found in all the seven wires of the strand. The loss in section was measured using Equation 19-1.

$$\text{percentage area lost } (\%A_t) = \left[\frac{\text{area lost}}{\text{original area}} \right] \times 100 \quad \text{Equation 19-1}$$

Table 19-6 and Table 19-7 summarize the measurements for corrosion based on loss in section, which indicated that loss in section was predominantly present in specimens with admixed chlorides. Further, the average loss in section in specimens with admixed Cl was also greater than specimens with no admixed Cl, indicating admixed chlorides probably increased corrosion intensity in specimens. Note that in the case of dried normal grout with no admixed chlorides, the section loss of 14.1% was observed in only 1 out of 12 normal grout specimens and was considered as an outlier.

Table 19-5. Loss in section and corrosion pit depths

Designation	Strand across grout interface	Presence of chlorides	Type of grout		Pitting depth class (ASTM G46)		Loss in section (%)			
			Top	Bottom	Top	Bottom	Top	Bottom		
D1			5 PC	100 PC			0.0	0.0		
D2								0.0	0.0	
C1								0.0	0.0	
D1 C		x					C2	C1	6.4	3.0
D2 C		x							5.8	0.1
C1 C		x							0.0	0.0
D1 E	x								0.0	0.0
D2 E	x						0.0	0.0		
C1 E	x		5 PC	100 PC			12.9	0.0		
D1 C E	x	x						C2	3.2	0.0
D2 C E	x	x							13.1	0.0
C1 C E	x	x							11.2	0.0
D1			100 PC	5 PC		C3	0.0	3.9		
D2									0.0	0.0
C1									0.0	0.0
D1 C		x					C1		0.5	0.0
D2 C		x							0.9	1.8
C1 C		x							14.0	2.0
D1 E	x								0.0	0.0
D2 E	x								0.0	0.2
C1 E	x								0.0	0.7
D1 C E	x	x						C1	0.2	2.8
D2 C E	x	x							0.0	0.0
C1 C E	x	x					C1	C1	16.8	1.6
D1			5 PC	15 PC			0.0	0.0		
D2									0.0	0.0
C1								C1	0.0	0.0
D1 C		x					C2	C2	3.5	3.2
D2 C		x						C1	16.5	3.4
C1 C		x							14.7	0.0
D1 E	x								0.4	0.2
D2 E	x								0.0	0.0
C1 E	x								0.0	0.0
D1 C E	x	x					C1		7.0	1.6
D2 C E	x	x							13.2	0.1
C1 C E	x	x							13.7	0.0

Table 19-5, continued

Designation	Strand across grout interface	Presence of chlorides	Type of grout		Pitting depth class (ASTM G46)		Loss in section (%)		
			Top	Bottom	Top	Bottom	Top	Bottom	
D1			15 PC	5 PC			0.0	0.0	
D2							0.0	0.0	
C1							0.0	0.0	
D1 C		x				C1	1.9	4.4	
D2 C		x				C1	18.2	13.4	
C1 C		x					0.0	0.0	
D1 E	x						0.0	0.0	
D2 E	x						0.0	0.0	
C1 E	x		15 PC	5 PC			0.0	0.0	
D1 CE	x	x				C2	C3	1.8	9.9
D2 CE	x	x						17.1	3.3
C1 CE	x	x						0.0	0.0
D1			PT	100 PC			0.0	0.0	
D2							0.0	0.0	
C1							0.0	0.0	
D1 C		x				C2	C1	1.9	1.5
D2 C		x						12.3	0.0
C1 C		x						0.0	0.5
D1			100 PC	PT			0.0	0.0	
D2							0.0	0.0	
C1							0.0	0.0	
D1 C		x				C2	C2	2.1	6.2
D2 C		x						13.9	0.0
C1 C		x						11.8	0.0
D1			5 PC	5 PC			0.0	0.0	
D2							0.0	0.0	
C1							9.8	0.0	
D1 C		x					0.8	0.0	
D2 C		x					0.0	0.0	
C1 C		x					12.6	0.0	
D1			100 PC	100 PC			0.0	0.0	
D2							14.1	0.0	
C1							0.0	0.0	
D1 C		x				C2		0.0	0.0
D2 C		x						18.1	0.0
C1 C		x						12.4	0.0

Comparing loss in section of strand wires between dried and control specimens from Table 19-7, loss in section was less in dried specimens than in control specimens probably due to removal of moisture, which is necessary for corrosion, from the grout on drying. When comparing loss of section in either dried or control specimens, strand wires in soft and normal grout had similar loss in section. The average loss in section in dried specimens D1 was 2.5% and in dried specimens D2 was 7.5%. Therefore, specimens D2 had greater average section loss than specimens D1 probably due to the additional three months of monitoring for D2, which provided additional time for section loss to occur. Note that dried specimens D1 and D2 had similar corrosion rating (section 19.3), which indicated that different loss in section values could correspond to similar strand ratings.

Table 19-6. Number of specimens with corrosion based on section loss

Type of specimens	# of specimens with corrosion (section loss %)		Total # of specimens	
	With Cl	Without Cl	With Cl	Without Cl
All	30 (6.6)	7 (5.2)	36	36
Dried (D1 and D2)	21 (6)	4 (6)	24	24
Control (C1)	9 (10.1)	3 (7.8)	12	12

Table 19-7. Comparison of average section loss for specimens with and without admixed chlorides

Grout type	Average section loss (%)					
	With admixed chlorides		With no admixed chlorides		All specimens	
	Dried	Control	Dried	Control	Dried	Control
Soft grout	6.6	10.8	1.2	9.5	5.8	10
Defective PT	6.8	0	0	0	6.8	0
Normal	4.5	11.1	14.1	0	5.4	11.1

Measurable pitting corrosion was observed in 14 out of 48 dried specimens, and 2 out of 24 control specimens. Out of the total 16 specimens with pitting corrosion, only one dried and one control specimen had no admixed chloride. This supports the previously stated finding that corrosion was prominently present in specimens with admixed chlorides in their grout formulations. Note that pitting depth measurements were subjective due to inconsistency in placement and adjustment of depth gauge meter flat on each strand wire because of their small diameter and helical shape. Nevertheless, these readings were indicative of qualitative presence of corrosion on strands.

20 Corrosion results and discussion

20.1 During drying

During drying, the potential difference between each strand and RE pair was measured in both drying and control specimens and recorded as corrosion potential (CP) of the respective strand. At the same time, resistance was measured between the cathode and RE, anode and RE, between the two RE, and between cathode and anode. Typical results are shown in Figure 20-1, Figure 20-2, and Figure 20-3, which show measurements for a specimen with no admixed chlorides. Rafols et al. (2013) found that when the open circuit corrosion potential of one strand was more negative than other strand, then there was corrosion current present, which in turn would cause corrosion in the strand with the more negative potential. Figure 20-1a and Figure 20-2a show that the difference in strand CP was greater in the early stages of drying for 5/100D1 and 5/100D2 indicating an increased risk of corrosion. As the specimen dried, however, the difference declined and eventually reached zero. It is interesting to note that the anode CP reached zero prior to that of the cathode. This is likely due to the 5 PC grout reaching the dried state prior to the 100 PC grout. The loss of free moisture in both grout layers removes the electrolyte necessary to support the reaction at the surface of the mixed-metal oxide (MMO), which is reflected in the lack of a potential difference with the strand (Pawlick, Stoner, & Clemena, 1998). Control specimen 5/100C1, however, exhibited relatively constant difference in corrosion potentials between anode and cathode strands indicating continued risk of corrosion (Figure 20-3). Furthermore, the anode showed much more negative values than that of the cathode, indicating the elevated risk of corrosion in the soft grout compared to that of the normal grout. The CP of both strands also did not reduce to zero which indicated the presence of free moisture in each grout layer to support reactions at MMO reference electrodes.

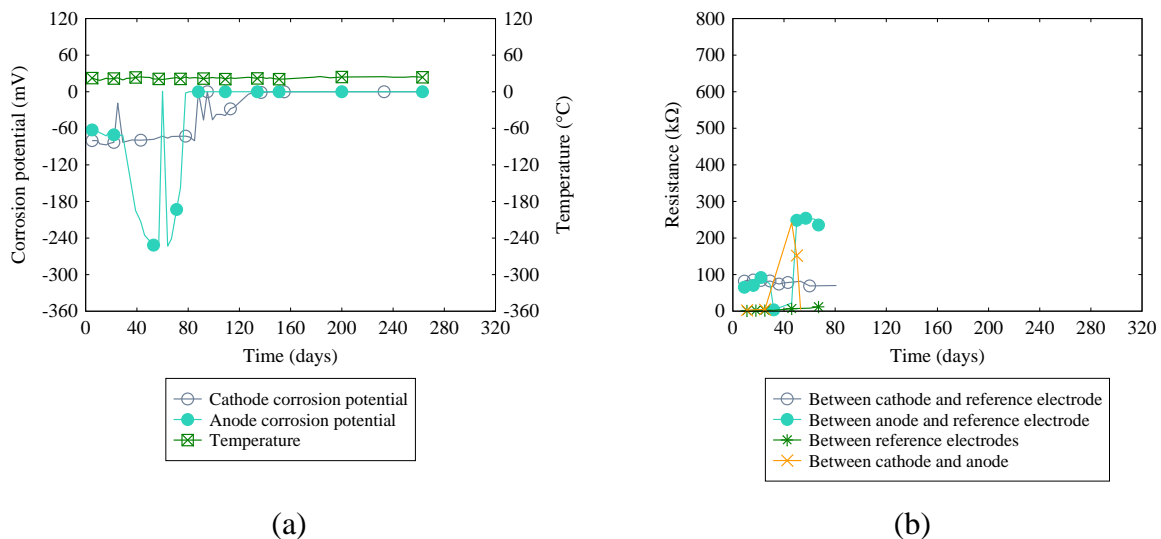


Figure 20-1. Corrosion readings for specimen 5/100D1 (a) Corrosion potential (b) Resistance

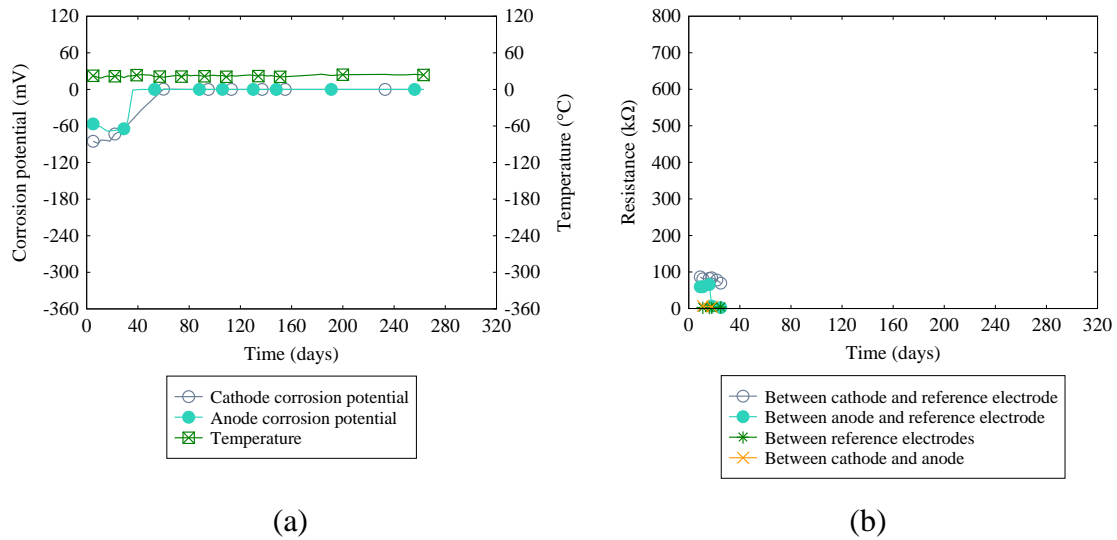


Figure 20-2. Corrosion readings for specimen 5/100D2 (a) Corrosion potential (b) Resistance

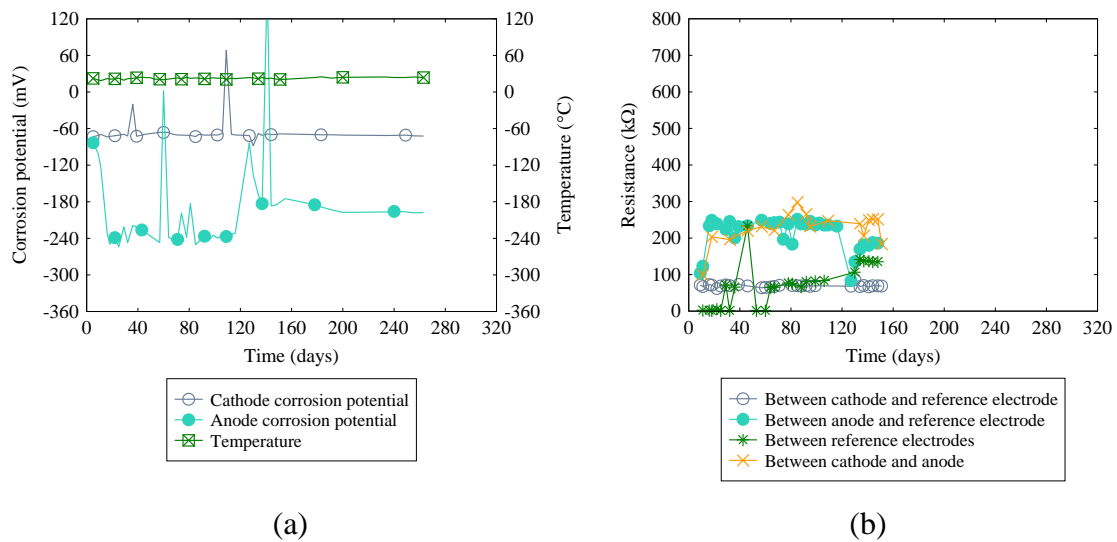


Figure 20-3. Corrosion readings for specimen 5/100C1 (a) Corrosion potential (b) Resistance

The change in drying air relative humidity (ΔRH_d) for specimens 5/100D1 and 5/100D2 is shown in Figure 20-4. If these results are compared to the CP and resistance results shown previously for the same specimens, it is apparent that the time at which the specimens are dry ($\Delta RH_d < 1\%$) agrees well with the time at which the CP approaches zero and the resistance increases to such a level as to indicate an open circuit condition. Both changes are indicative of the loss in electrolyte (free moisture) to provide the electrical continuity that sustains the corrosion process and reaction on MMO electrode surface. For 5/100D1, the time to dry was approximately 120 days and for 5/100D2 it was about 40 days (Figure 20-4). Therefore, corrosion potential and resistance readings provided a strong indirect indication of grout moisture content. Similar trends were noted in the remaining specimens (plots shown in Appendix C.2).

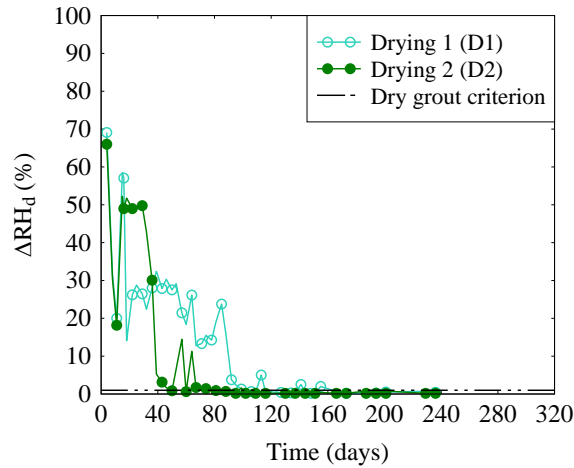


Figure 20-4. Relative humidity readings vs. time for specimen type 1 with no chlorides

Conversely, relatively negative corrosion potentials and resistance readings at a sustained level indicated elevated moisture content that was not changing. For example, 5/100D2C continued to have very negative corrosion potentials in both the anode and cathode; the corrosion potential did not converge to zero and the resistance did not increase to infinity during the entire drying period (Figure 20-5). Similarly, ΔRH_d readings did not constantly remain below the dry grout criterion (Figure 20-6). Furthermore, after dissection, the grout in this specimen was found to have about 29% moisture content in 5 PC soft grout and 23% in 100 PC normal grout.

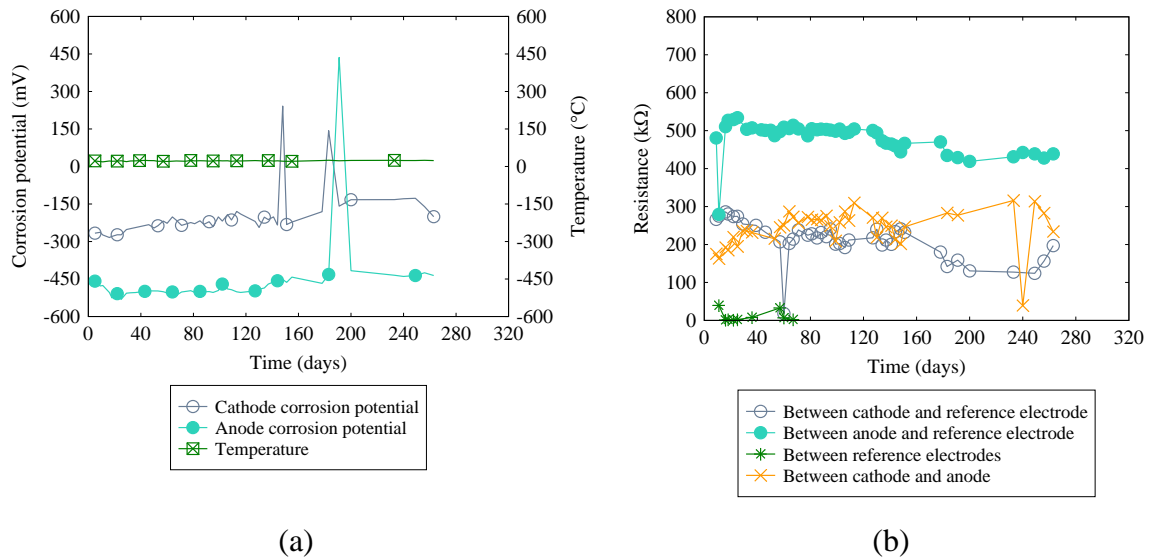


Figure 20-5. Corrosion readings for specimen 5 PC/100 PC D2C: (a) Corrosion potential; (b) Resistance

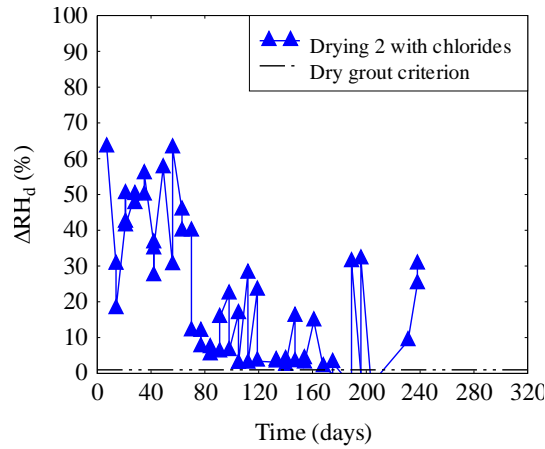


Figure 20-6. Relative humidity readings vs. time for specimen 5 PC/100 PC D2C

20.2 Post-drying

After specimens were dried, macrocell current between anode and cathode, and corrosion potential (CP) of anode and cathode with respect to their RE were measured using the automated data acquisition system (DAQ). Figure 20-7, Figure 20-8, Figure 20-11 and Figure 20-10 show typical plots of these results for dried and control specimens with and without admixed chlorides. The plots of the remaining specimens are provided in Appendix B. The plots show that the post-drying corrosion potentials for all specimens were almost constant after attaining equilibrium. In addition, macrocell current was detected mostly in control specimens admixed with chlorides. The measurements were not found to be influenced by the changes in temperature, probably because the specimen was made of non-conductive PVC with no significant size openings.

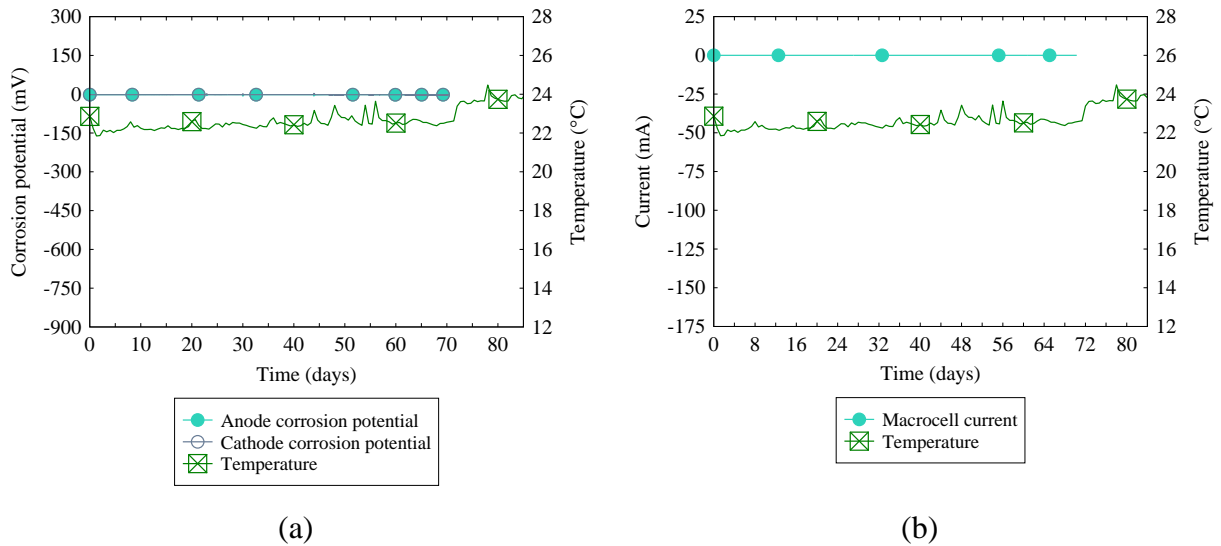
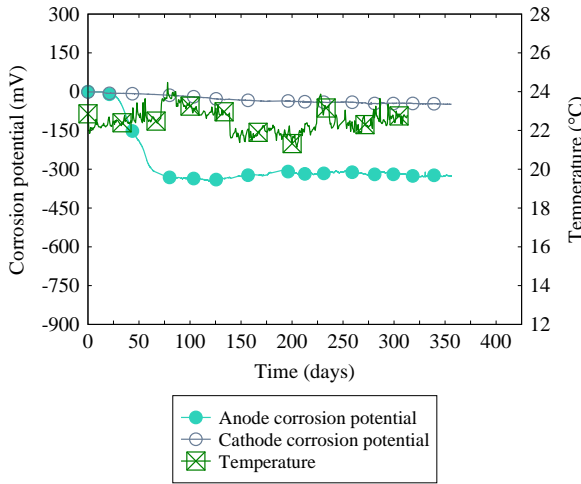
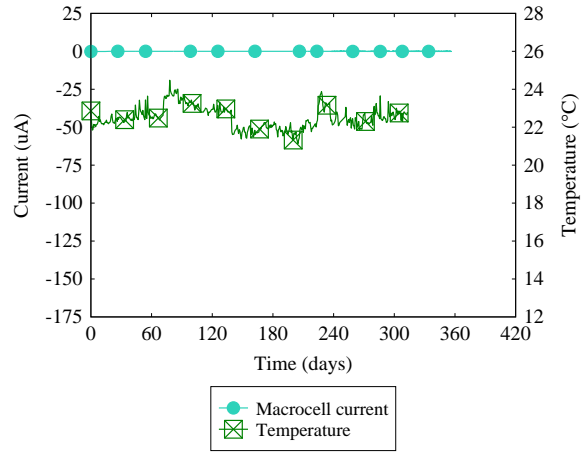


Figure 20-7. Post-drying corrosion measurements for 5/100D1: (a) Corrosion potential; (b) Macrocell current

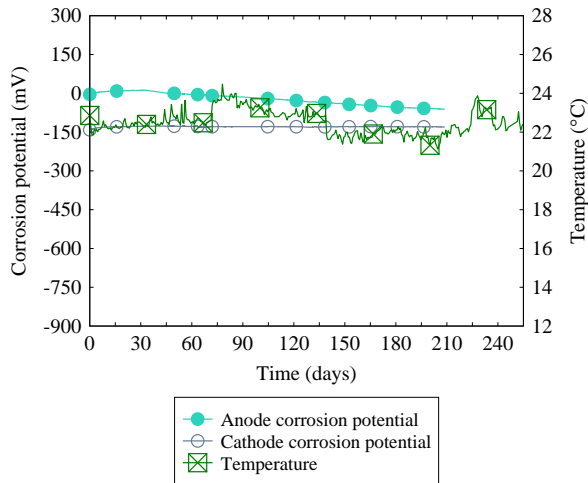


(a)

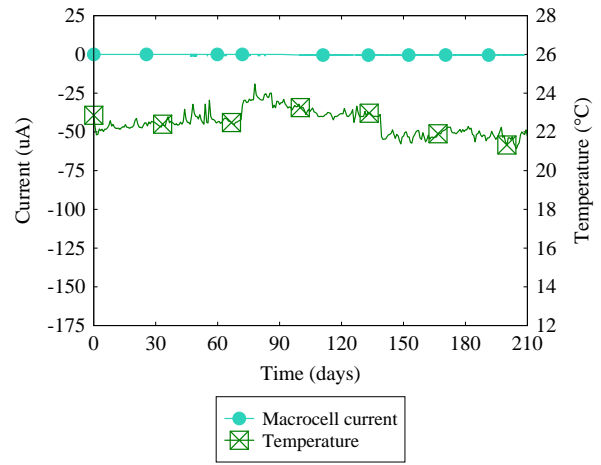


(b)

Figure 20-8. Post-drying corrosion measurements for 100/5D2C: (a) Corrosion potential; (b) Macrocell current



(a)



(b)

Figure 20-9. Post-drying corrosion measurements for 5/100C1: (a) Corrosion potential; (b) Macrocell current

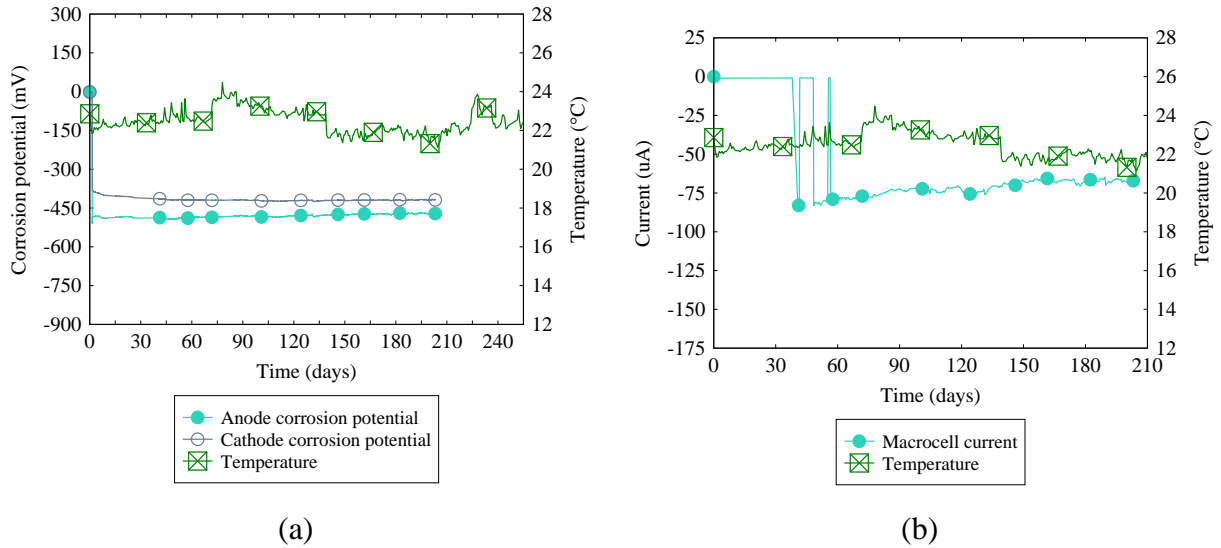


Figure 20-10. Post-drying measurements for 100/5C1C: (a) Corrosion potential; (b) Macrocell current

Based on corrosion during drying, about 40% of the dried specimens had at least one strand with CP more positive than -100 mV during drying of grout (Figure 20-11). However, this percentage of dried specimens increased to about 86% after grout was dried (Figure 20-12). On the other hand, the percentage of non-dried control specimens containing at least one strand with CP more positive than -100 mV increased from 20% during drying period to 25% during post-drying period. These results show that during the drying process there is a period of increased probability of corrosion compared to the probability of corrosion after the grout has been dried. Once the grout dried, however, corrosion potential became more positive. In general, as corrosion potential becomes more positive and approaches zero, the probability of corrosion decreases.

The drying process itself was found to cause corrosion during drying as seen in the mockup drying specimens. But it was not clear from those tests whether the corrosion continued after the grout was dried. Results from the small-scale tests reported in this chapter indicated that drying could further hinder corrosion by removing the moisture needed to support the corrosion process. This is demonstrated by the lower magnitude of corrosion potential of the strands in dried grout compared to strands in control, undried grout. In addition, the control specimens were sealed throughout the testing, which prevented recharging with oxygen. While this condition provided a consistent control specimen, it does not necessarily represent field conditions where soft grout is left in place. Over time, oxygen and moisture may penetrate corrugated post-tensioning ducts resulting in continued corrosion of the prestressing strand, which is not represented in the control specimens for these corrosion tests. This has been known to occur through the vents used during grouting that have not been filled properly.

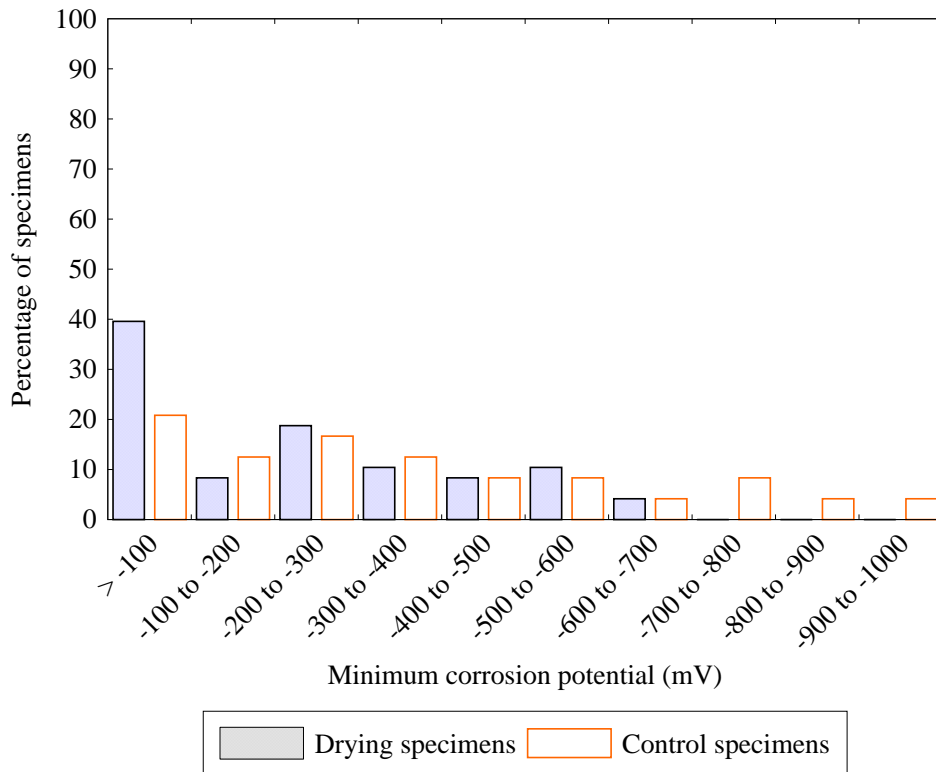


Figure 20-11. Percentage of specimens with respect to minimum corrosion potentials during drying

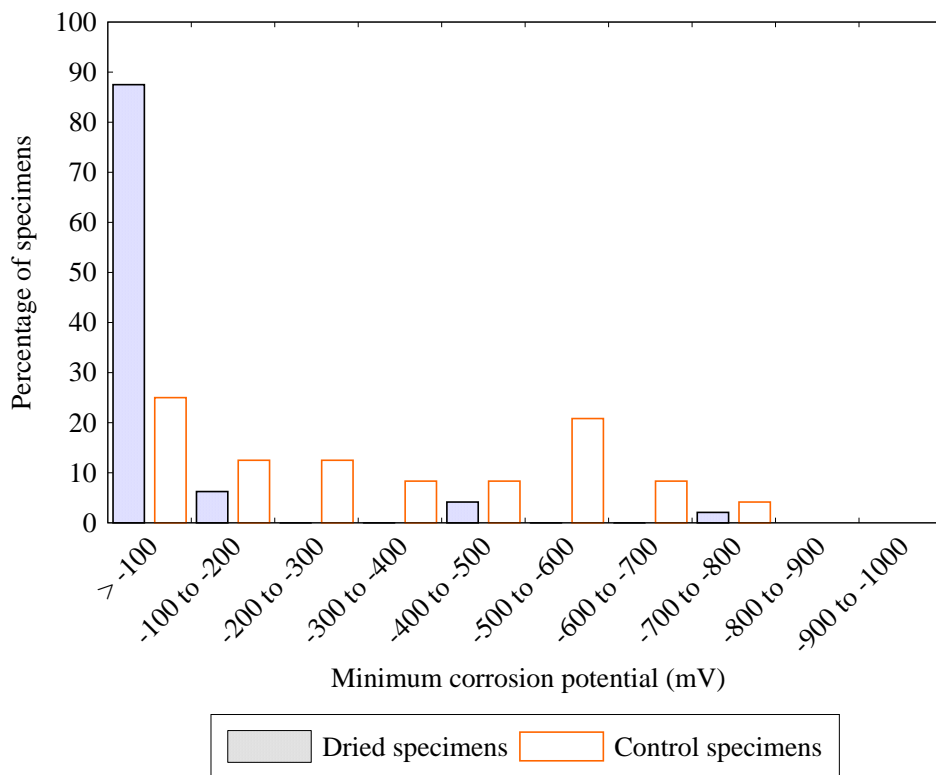


Figure 20-12. Percentage of specimens with respect to minimum corrosion potentials after drying

Macrocell current measurements provided some insight into the behavior of specimens with and without admixed chlorides. Less than 23% of the specimens in which macrocell corrosion current was measured registered any readings. This indicated that perhaps the primary mode of corrosion is not through a corrosion cell developed between two locations within the tendon, but rather a more local development of corrosion in one or other of the prestressing strands within the specimen. Of the eleven specimens that developed macrocell corrosion, nine were control specimens and one of the two dried specimens was not dried completely, providing further evidence that macrocells were not generated as a result of drying. Further, comparing results of only control specimens with and without admixed chlorides, six out of ten control specimens with macrocell current contained admixed chlorides. The dried specimens with macrocell current also contained admixed chlorides. This indicated that admixed chlorides increased the risk of macrocell corrosion in the specimens. This could also imply that corrosion, if found in specimens with no admixed chlorides, could be the result of microcell corrosion.

21 Comparison of section loss and post-drying corrosion potential measurements

In this chapter, the results of physical corrosion measurements after dissection from Chapter 19 are compared with the results of corrosion potential measurements recorded during and after drying from Chapter 20. The physical results included measurement of pitting depth and loss in section, and rating of corrosion on strands based on visual observation after dissection of specimens. Table 21-1 provides a summary of physical and corrosion potential measurements for easy cross-reference and comparison. Measurement of percentage section loss in strand wire section was more consistent than measurement of pit depths and less subjective than corrosion rating. Therefore, the percentage loss readings were expected to be more representative of the corrosion behavior. At the same time, CP was measured both during and after drying. Therefore, section loss and CP readings were used to correlate the physical corrosion results to the electrochemical corrosion results.

Readings in Table 21-1 were the minimum CP values measured over the entire drying and post-drying monitoring period. The drying period of a dried specimen was defined as the time when the grout in it was considered dried based on relative humidity readings. The drying period of control specimens was equal to time when one of its corresponding dried specimen replicates was dried. The post-drying period for the first replicate (D1) was at least 1 month, whereas for the second replicate (D2) and the control specimens (C1) it was at least four months.

ASTM C876-15 *Corrosion Potentials of Uncoated Reinforcing Steel in Concrete* provides a useful framework to view the corrosion potential results from this research. ASTM C876 provides an estimate of the probability of corrosion activity based on half-cell readings of the embedded reinforcement using a standard copper-copper sulfate reference electrode. And although the potential readings of this research are relative to the mixed-metal oxide reference electrode, it is useful to arrange the data into probabilities of corrosion based on the potential and observed corrosion severity. To that end, corrosion activity was considered to have occurred when any loss in section was detected in at least one of the strands. This delineation was used to provide a probability of corrosion occurring at that CP.

Based on comparison of loss in section and CP readings in Table 21-1, less than 10% of the dried specimens had corrosion activity when their peak CP readings were more positive than -300 mV both during and after drying. Fewer than 10% of the control specimens had corrosion activity when the CP readings were more positive than -350 mV both during and after the drying period. In Table 21-1, the CP readings for dried specimens were highlighted with green if they were more positive than -300 mV both during and after drying while the CP readings for control specimens were highlighted in yellow if they were more positive than -350 mV both during and after the drying period.

Table 21-1. Summary of results from dissection and corrosion measurements

Designation	Strand across grout interface	Presence of chlorides	Type of grout		Pitting depth class (ASTM G46)		Loss in section (%)		Corrosion rating		Age after casting at dissection	Peak (minimum) Corrosion Potential (mV)				Macrocell current (mA)	
												During drying		After drying			
			Top	Bottom	Top	Bottom	Top	Bottom	Top	Bottom		Top	Bottom	Top			
D1			5 PC	100 PC			0	0	1	1	308	-253.5	-87.2	-5.38	-2	0	
D2							0	0	1	1	448	-68.5	-88.6	-3.93	-11.95	0	
C1							0	0	1	1	448	-254	-88	-61.4	-140.87	0	
D1 C		x				C2	C1	6.36	2.98	6	4	308	-453.1	-323.4	-2.07	-3	0
D2 C		x						5.76	0.068	7	4	448	-531.4	-284	-496	-499	-50
C1 C		x						0	0	2	4	448	-460.3	-278.5	-524.9	-519	-10
D1 E	x							0	0	1	1	308	-74.8	-67	-2	-4.9	0
D2 E	x						C5	0	0	1	1	448	-73.1	-74.8	-2	-7	0
C1 E	x							12.9	0	1	1	448	-141	-79.3	-121.9	-129	0
D1 CE	x	x					C2	3.24	0	5	3	308	-417.5	-351.6	-2	-2	0
D2 CE	x	x						13.1	0	6	4	448	-527.8	-447.5	-1.8	-2.27	0
C1 CE	x	x						11.2	0	4	2	448	-544.9	-340.5	-283	-458	-45
D1			100 PC	5 PC		C3	0	3.85	1	1	308	-94.9	-135.6	-2.2	-3.9	0	
D2							0	0	1	1	448	-69.2	-91.8	-2.2	-2.7	0	
C1							0	0	1	1	448	-111.6	-237.5	-137.9	-44.5	0	
D1 C		x				C1		0.49	0	3	5	308	-283.8	-516	-6	-114	0
D2 C		x						0.87	1.80	5	5	448	-273.9	-283.8	-38	-346.9	0
C1 C		x						14	2.02	3	7	448	-293.9	-717	-424.5	-492	-75
D1 E	x							0	0	1	2	308	-65.6	-82.1	-2.3	-2	0
D2 E	x							0	0.23	1	1	448	-58.2	-92.9	-2	-2	0
C1 E	x							0	0.72	1	1	448	-128.3	-152.6	-132	-127	0
D1 CE	x	x					C1	0.2	2.81	1	7	308	-223.4	-272.3	-2	-1	0
D2 CE	x	x				0	0	3	4	448	-261	-428.9	-2	-2.88	0		

Designation	Strand across grout interface	Presence of chlorides	Type of grout		Pitting depth class (ASTM G46)		Loss in section (%)		Corrosion rating		Age after casting at dissection	Peak (minimum) Corrosion Potential (mV)				Macrocell current (mA)			
												During drying		After drying					
			Top	Bottom	Top	Bottom	Top	Bottom	Top	Bottom		Top	Bottom	Top					
C1 CE	x	x			C1	C1	16.8	1.59	3	5	448	-327.7	-557	21.8	-481.6	-50			
D1			5 PC	15 PC			0	0	1	1	308	-59.9	-609	-868	-731.7	0			
D2									0	0	1	1	448	-79.8	-105	-5.38	-2.63	0	
C1								C1	0	0	1	1	448	-865	-861	-1.38	-1.29	-124	
D1 C		x						C2	C2	3.46	3.22	7	6	308	-513	-543.1	-6.07	-11.06	0
D2 C		x							C1	16.5	3.39	5	5	448	-646.5	-457.4	-5.4	-3.2	0
C1 C		x								14.7	0	6	4	448	-913	-663	-755	-852.3	0
D1 E	x									0.42	0.17	2	1	308	-830	-122.4	-75.9	-2.06	0
D2 E	x									0	0	2	1	448	-81	-156.8	-469	-524.6	0
C1 E	x									0	0	2	1	448	-166.8	-941	-688	-720.29	0
D1 CE	x	x						C1		7.05	1.61	7	7	308	-740	-652.1	-155	-278.2	0
D2 CE	x	x								13.2	0.13	6	4	448	-574	-584.8	-6	-2.87	0
C1 CE	x	x								13.7	0	4	2	448	-708	-867	-657	-891.9	0
D1					15 PC	5 PC			0	0	1	1	308	-154.6	-681	-21.1	-1.32	0	
D2									0	0	1	1	448	-694	-147.7	-7.4	-1.51	0	
C1									0	0	1	1	448	-296.1	-758	-648	-541	0	
D1 C		x						C1	1.88	4.38	4	6	308	-659.2	-579.2	-21.5	-213.65	0	
D2 C		x						C1	18.2	13.37	6	6	448	-480.7	-670.2	-2.3	-666.1	0	
C1 C		x								0	0	2	3	448	-725	-911	-903	-496	0
D1 E	x		15 PC	5 PC			0	0	5	3	308	-154	-85.3	-3.46	-6.22	0			
D2 E	x								0	0	1	2	448	-612	-256	-2	-214.36	0	
C1 E	x								0	0	1	1	448	-87.6	-920	-191.8	-114.1	0	
D1 CE	x	x						C2	C3	1.85	9.89	6	7	308	-647.9	-682	-2.97	-4.14	0
D2 CE	x	x								17.1	3.31	6	5	448	-594.9	-651.8	-2.4	-6.1	-1
C1 CE	x	x								0	0	1	5	448	-556	-922	-552.6	-567.3	-3
D1			PT	100 PC			0	0	1	2	308	-59.3	-65.9	-2	-2	0			

Designation	Strand across grout interface	Presence of chlorides	Type of grout		Pitting depth class (ASTM G46)		Loss in section (%)		Corrosion rating		Age after casting at dissection	Peak (minimum) Corrosion Potential (mV)				Macrocell current (mA)
												During drying		After drying		
			Top	Bottom	Top	Bottom	Top	Bottom	Top	Bottom		Top	Bottom	Top		
D2							0	0	1	1	448	-282.9	-78.2	-2.2	-4	0
C1							0	0	2	1	448	-595.6	-210.9	-477	-293	-10
D1 C		x			C2	C1	1.89	1.50	6	4	308	-432.8	-296.2	-2	-2	0
D2 C		x					12.3	0	4	3	448	-382	-415	-2.5	-2.3	0
C1 C		x				C4	0	0.52	4	4	448	-454.3	-430.8	62.92	-504	0
D1			100 PC	PT			0	0	1	6	308	-120.8	-331	-3.78	-38	0
D2							0	0	1	4	448	-74.6	-369.3	-14.8	-20.6	0
C1							0	0	1	3	448	-70.5	-546.9	-269	-443.8	-15
D1 C		x			C2	C2	2.06	6.20	4	7	308	-2138	-567.9	-152.6	-342	0
D2 C		x					13.9	0	4	3	448	-302.6	-375.3	-4.1	-5.8	0
C1 C		x			11.8	0	4	6	448	-313	-577	-309	-519.96	-22		
D1			5 PC	5 PC			0	0	1		308	-50.8	-	-4.33	-	-
D2							0	0	1		448	-43.6	-	-2.1	-	-
C1							9.79	0	1		448	-907	-	-555.6	-	-
D1 C		x					0.82	0	4		308	-348.9	-	-3.2	-	-
D2 C		x	5 PC	5 PC			0	0	5		448	-436.5	-	-3	-	-
C1 C		x					12.6	0	4		448	-507.7	-	-576	-	-
D1			100 PC	100 PC			0	0	1		308	-62.4	-	-144.7	-	-
D2							14.1	0	1		448	-61.3	-	-3	-	-
C1							0	0	1		448	-61.3	-	-3	-	-
D1 C		x			C2		0	0	2		308	-249.3	-	-3.28	-	-
D2 C		x					18.1	0	4		448	-252.3	-	-46	-	-
C1 C		x					12.4	0	3		448	-458.2	-	-339.3	-	-

22 Summary and conclusions

Two techniques of soft grout rehabilitation were tested and evaluated: hydrodemolition removal of the defective grout and drying of the defective grout. Hydrodemolition involved use of a high-pressure water jet to break up and remove soft grout from inside the PT duct. The mockup specimen was constructed using 4 in. diameter electrical metal tubing (EMT) conduit to simulate a tendon in the negative bending moment regions of a bridge girder. Nineteen 0.6-in. dia. 7-wire low-relaxation strands were placed along the specimen with a prestress force of approximately one kip per strand. Grout was placed in layers with the stronger grout at lower elevation and weaker grout at higher elevation. Hydrodemolition was performed in four trials, each starting at a different section. Each trial was intended to help evaluate the level of difficulty while performing hydrodemolition in different types of grout. After performing all trials, specimens were dissected to inspect and locate any residual grout. The following conclusions are based on the observations made during hydrodemolition and after dissecting the specimens.

During hydrodemolition

- Determining the correct location to drill the inlet hole was difficult due to the distribution of the strands inside the conduit.
- Nozzles used for hydrodemolition became lodged between the strands and between strands and duct. This likely means that nozzles will be lost in the field, especially in ducts containing normal grout.
- The most effective grout removal with least obstruction was observed in section 7 when hydrodemolition was performed with a vacuum to draw water and debris from the discharge hole and the holes were drilled in close proximity to each other. This section also contained low strength grout.

Dissection of specimens

- Hydrodemolition did not completely remove grout from any one section of the mockup. In sections where grout was removed from above the strand bundle, residual grout was found trapped between the strands, and between strands and the conduit wall.
- Residual grout after hydrodemolition was visually observed to be moist.
- Hydrodemolition was not effective in soft grout with more than 15% cement content due to increased strength of grout. Furthermore, the water jet nozzle became lodged in the duct.
- For sections with grout containing 30% or higher cement content, water-blasting did not completely remove material above the strand bundle.

After evaluating hydrodemolition, drying of grout was evaluated as an alternative to rehabilitate tendons filled with soft grout. Two types of PT tendon mockup specimens were fabricated and filled with multiple layers of grout with varying quality. One specimen had alternating 5 PC and 15 PC soft grout layers and was designed to evaluate drying of tendons containing isolated soft grout (named “Isolated Soft Grout” ISG in Figure 6-4). The other configuration had alternating 5 PC and 100 PC layers and was used to study the effectiveness in drying of soft grout trapped between normal grout layers (named “Trapped Soft Grout” TSG in Figure 6-4). Normal grout has lower porosity than soft grout and was anticipated to obstruct air flow and delay moisture removal. Drying involved passing dehumidified air through the tendon to remove moisture. This technique required drilling of only two holes for inlet and outlet of air, which will minimize girder damage caused by the technique. The difference in relative humidity

measurements of drying air at the inlet and outlet (ΔRH_d) provided an indicator of the degree of dryness of the soft grout dried. After performing drying on the mockup tendon specimens, soft grout was found to have a moisture content of less than 5% and was considered to be dry. Leaks in tendons and the presence of normal grout, however, reduced the speed of drying. Consequently, the rate of drying was not predictable. Conclusions are based on the observations made from dissection; results of moisture content of samples collected during dissection; and the analysis of RH measurements collected throughout the drying process. Findings are also based on the drying experimentation process.

Grout consistency

- Moisture content measurements on dried layers of 5 PC and 15 PC grout were consistently below 1%, which indicated that drying had effectively removed moisture from the soft grout. This was also true for the dried 5 PC layers trapped between 100 PC hardened grout
- Drying resulted in grout shrinkage, which was manifested by transverse, regularly spaced cracks in the grout. Dried soft grout was friable, porous, and not well-bonded to strands.
- Drying was much less effective at removing moisture at the ends of the specimens outside of the air injection and outlet ports.
- These results in specimen TSG were similar to that of specimen ISG, indicating that the air flow through the hardened normal grout layers was sufficient to dry the trapped layer of 5 PC grout. The final “dried” moisture content of the 100 PC grout layers, however, was between 5% and 10% and was unlikely to decrease notably with further drying.

ΔRH_d Readings

- Specimen TSG had ΔRH_d readings higher than specimen ISG during the end of drying period. This was likely caused by the higher moisture content measured in the 100 PC grout, which is typical of normal grout.
- Based on the ΔRH_d readings, specimen ISG dried in approximately 110 to 120 days and specimen TSG in approximately 140 to 150 days. It is thought that the drying rate of specimen TSG was reduced by the presence of the 100 PC grout.
- Based on dryness check readings (ΔRH_{di} and ΔRH_{df}), ISG specimen was found dried on day 117 and TSG specimen was found dried on day 167.

RH_g Readings

- RH_g readings for dried soft grout (5 PC and 15 PC) ranged from 15% to 40% RH for temperatures between 15°C and 35°C. On the other hand, RH_g readings for dried normal grout (100 PC) varied over a wider range of 30% to 70% for the same temperature range.

Strand Corrosion

- Dried specimens exhibited strand corrosion in several locations, which did not occur in the control specimens.
- The porosity of dry grout combined with the constant supply of air provided the strands a direct access to a steady oxygen supply.
- Carbon dioxide in drying air was thought to carbonate the grout, which probably reduced pH below 11 and the passive layer of strands became unstable.
- Sufficient moisture from bleed water of grout, along with lower pH and oxygen, was probably responsible for corrosion.

Based on these findings, hydrodemolition was deemed unsuccessful in removing the soft grout completely from the tendon. In addition, a significant amount of water remained in the duct after hydrodemolition, either as water absorbed by the soft grout or as pockets of water that formed in grooves and spaces cleared by hydrodemolition. On the other hand, drying was found to be successful in drying the soft grout by removing nearly all free moisture. Since corrosion was found in the dried specimens, additional specimens called corrosion specimens were tested for corrosion during and after drying. Corrosion specimens were categorized into twelve types based on the combination of grout types present in them. Each type of corrosion specimen had three replicates, two that were subjected to drying (designation: D1 and D2) and one that was not dried (designation: C1). In total, four-eight drying and twenty-four control corrosion specimens were designed and fabricated. These specimens had either two grout layers or a single grout layer. Each grout layer was embedded with a pair of strand and reference electrode (RE). Each specimen type had a replicate with admixed chlorides to aggravate corrosion and the study effect of chloride presence on corrosion due to drying. Specimens were monitored for corrosion during and after drying. During drying, corrosion potential (CP) between strand and its RE, resistance between of strand and its RE, resistance between strands and resistance between REs was measured. Whereas, after drying, CP between strand and its RE, and macrocell current between the strands was measured. After drying, dried specimens D1 were monitored for at least one month, whereas dried specimens D2 and control specimens C1 were monitored for at least four months. After the post-drying monitoring, specimens were dissected to examine grout and strands for corrosion. The following findings and conclusions were made based on results from corrosion and drying process monitoring, and dissection analysis:

Grout drying process

- Specimens with at least one normal grout layer took longer to dry than specimens with no normal grout layer.
- Specimens with the soft grout layer close to outlet dried faster than specimens with normal grout layer close to outlet. Soft grout near outlet was thought to expedite moisture removal process by reducing the distance required for the moisture to travel out of the specimen.
- Specimens dried fastest if they consisted of only soft grout with continuous strand. Continuous strand was thought to provide a continuous passage for drying air to flow and remove moisture.

Grout moisture content

- Drying was successful in removing most of the free moisture in soft, defective and normal grouts.
- Average moisture content (MC) of soft grout (5 PC and 15 PC) in dried specimens was 0.7% and in control specimens was 36%.
- Average MC of expired and prehydrated defective prepackaged grout in dried specimens was 4.47% and in control specimens was 50.61%.
- Average MC of normal grout in dried specimen was 3.76% and in control specimen was 26.51%.
- The criterion of difference in relative humidity between inlet and outlet air (ΔRH_d) < 1% successfully predicted that soft grout was dried in the corrosion specimens.

Grout pH

- The pH of dried grout was lower than pH of grout in control specimens, which was attributed to carbonation of grout during the drying process due to introduction of carbon dioxide by the air injected in the dried specimens.
- The average pH of dried soft grout (5 PC and 15 PC), conditioned defective prepackaged grout (PT) and normal grout (100 PC) was 8.7, 8.7 and 9.5 respectively. The average pH of soft grout, defective PT grout and normal grout in control specimen was 11.8, 11 and 12.3 respectively.
- The pH of soft and defective PT grout was less than pH of normal grout in both dried and control specimens.
- No trend was observed in the case of change in pH of grout along direction of air flow from inlet end to outlet end.

Strand Corrosion Rating

- In general, 36 out of 72 dried and control corrosion specimens had strands rated with at least second level of corrosion rating, which indicated corrosion present on the strands.
- Out of these 36 specimens, 33 specimens contained admixture chlorides in grout mixture which indicated presence of chlorides could be one of the reasons for corrosion in strands.
- The average corrosion rating of strands in dried specimens D1 (3.3) was similar to that in dried specimens D2 (3).
- The average ratings for unacceptable strands placed in soft grout, defective PT grout and normal grout in dried specimens were 5.6, 5.4 and 4.1 respectively. The average ratings for unacceptable strands in soft grout, defective PT grout and normal grout in control specimens were 4.9, 5 and 4 respectively. Therefore, the strand corrosion rating was greater for strands in dried specimens compared to strands in control specimens.

Section loss and pit depth

- In general, 25 out of 48 dried specimens and 11 out of 24 control specimens had loss in section of strand wires, measurable using a caliper. Out of these, only 4 dried and 3 control specimens did not have admixed chlorides in their grout formulations.
- Average loss in section of strand wires in soft grout and defective PT grout of dried specimens was 5.8% and 6.8%, and in dried normal grout was 5.4%. This average included 21 out of 24 number of dried specimens with admixed chlorides and 4 out of 24 dried specimens with no admixed chlorides.
- Average loss in section of strand wires in soft, and defective PT grout of control specimens was 10 and 0% respectively, and in normal grout of control specimens was 11.1%. This average included 9 out of 12 number of control specimens with admixed chlorides and 3 out of 12 control specimens with no admixed chlorides.
- The average loss in section in dried specimens D2 (7.5%) was greater than in dried specimens D1 (2.5%), probably because specimens D1 were dissected at the age of 308 days whereas specimens D2 were dissected at the age of 448 days, providing strands in specimens D2 longer time to corrode.
- Dried specimens D1 and D2 had similar corrosion rating, which indicated that different loss in section values can correspond to similar strand ratings.
- Loss in section was less in dried specimens than in control specimens probably due to drying, which is necessary for corrosion.

- Measurable pitting corrosion was observed in 14 out of 48 dried specimens, and 2 out of 24 control specimens. Out of the total 16 specimens with pitting corrosion, only one dried and one control specimen had no admixed chloride.
- Loss in section and pitting corrosion was predominantly present in specimens with chlorides.
- Measuring pitting depth on small diameter strand wires was difficult and therefore not accurate, especially in the case of twisted outside wires.

Corrosion potential and macrocell current measurements

- The percentage of dried specimens with at least one strand with CP more positive than -100 mV increased from 40% during drying of grout to about 86% after drying. On the other hand, the percentage of non-drying control specimens containing at least one strand with CP more positive than -100 mV increased from 20% during drying period to 25% during post-drying period. This showed that drying of grout in the specimens was more effective in reducing the magnitude of corrosion potential of strands, i.e., making the corrosion potential more positive.
- Only two of the eleven specimens detected with macrocell current were dried specimens, one of which (5/100D2C) later dissection indicated that it had not completely dried. Therefore, drying appeared to reduce the risk of corrosion, especially macrocell corrosion, after the grout was completely dried.
- Six out of nine control specimens with macrocell current contained admixed chlorides. This indicated that the admixed chlorides increased the risk of macrocell corrosion in the specimens. This could also imply that corrosion, if found in specimens with no admixed chlorides, could be a result of microcell corrosion.

Comparison of section loss and corrosion potential measurements

- A corrosion activity in a specimen was indicated by any loss in section in at least one of the strands.
- Based on comparison of loss in section and corrosion potential (CP) readings in the Table 21-1, less than 10% of the dried specimens had corrosion activity, when their CP readings were more positive than -300 mV both during and after drying.
- Whereas less than 10% of the control specimens had corrosion activity when the CP readings were more positive than -350 mV both during and after the drying period.

23 Implementation and future work

Testing indicated that a significant portion of the free moisture inside PT tendons containing soft grout could be removed by drying. To determine if the grout was successfully dried, relative humidity (RH) of the inlet and outlet air was measured. Soft grout was deemed to be dry when the difference between RH readings at inlet and outlet (ΔRH_d) was less than 20%. Dissection of the specimens indicated that the moisture content of the soft grout was near zero, which confirmed that the technique was successful.

Mockup testing was conducted in laboratory-controlled conditions. In practical conditions, however, such as a PT tendon embedded in a girder, potential recharging of soft grout with moisture through joints, voids, or cracks is possible. This may further affect the relationship between soft grout moisture content and ΔRH_d . This report recommended that ΔRH_d should be no more than 5% to ensure grout was dried. However, if potential recharging of soft grout through a defect is thought to prevent ΔRH_d from reducing below 5%, additional outlet RH measurements along the length of a girder would be advisable to determine if a crack or leak is influencing the ΔRH_d readings. The additional locations for outlet RH measurements should include at least one location before and one after the location of possible defect.

Future research work should focus on refining the relationship between the relative humidity of the air used to dry the specimen and the actual moisture content of the soft grout within the duct. This work should also incorporate the possibility that the tendon could be recharged with moisture. One possible test protocol is to conduct concurrent drying of multiple replicates of PVC specimens filled with soft grout from the same batch. Periodically, ΔRH_d readings can be correlated with moisture content of grout by dissecting one of the replicate specimens at regular intervals and measuring its grout moisture content. During this same testing some of the specimens could have moisture introduced to simulate recharging.

Drying using atmospheric air was found to cause corrosion most probably due to supply of oxygen and carbonation of grout. As an alternative, use of an inert gas such as nitrogen, would help reduce the availability of oxygen to drive the corrosion process, if moisture happens to be available. Nitrogen gas has been successfully used for drying unbonded strands (Vander Velde, 2002). Soft grout was found to be friable and porous after drying and could allow oxygen and moisture to reach strands, resulting in corrosion, particularly if recharging with moisture is possible. Given the unknowns of field application of this method and the fact that corrosion occurred during drying during both mockup and small-scale testing, it is advisable to inject a corrosion inhibitor into the tendon immediately following air drying. Whitmore and Lasa (2018) reported on the use of a corrosion inhibitor intended to inhibit corrosion in tendons containing soft grout. For PT tendons with chloride-contaminated grout, it is also advisable to use an inert gas for drying followed by injection with a corrosion inhibitor effective in high-chloride environments.

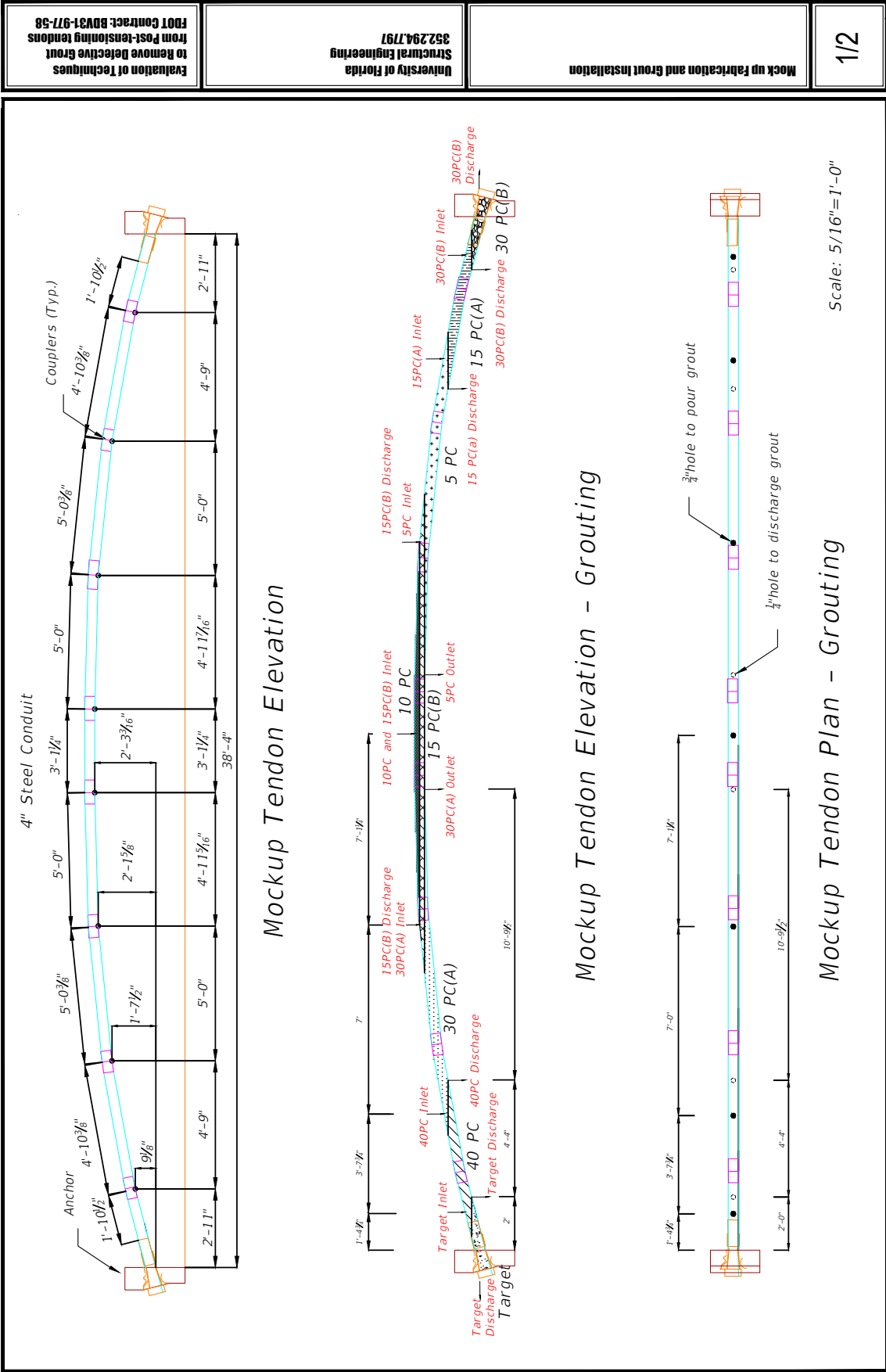
24 References

- Anania, L., Badalà, A., & D'Agata, G. (2018). Damage and collapse mode of existing post tensioned precast concrete bridge: The case of Petrulla viaduct. *Engineering Structures*, 162(November 2016), 226–244. <https://doi.org/10.1016/j.engstruct.2018.02.039>
- ASTM C566-13. (2013). Standard Test Method for Total Evaporable Moisture Content of Aggregate by Drying. <https://doi.org/10.1520/C0566-13.2>
- ASTM D2216-10. (2010). Standard Test Methods for Laboratory Determination of Water (Moisture) Content of Soil and Rock by Mass. <https://doi.org/10.1520/D2216-10.N>
- Aziznamini, A., & Gull, J. (2012). *Improved Inspection Techniques for Steel Prestressing/Post-tensioning Strand (Florida Department of Transportation Report BDK80 977-13)*. Florida International University (Vol. I). Miami, Florida.
- Corven Engineer Inc. (2001). *Final Report - Mid-bay Bridge Post-Tensioning Evaluation*. Tallahassee, FL.
- Heiyantuduwa, R., Alexander, M. G., & Mackechnie, J. R. (2006). Performance of a Penetrating Corrosion Inhibitor in Concrete Affected by Carbonation-Induced Corrosion. *Journal of Materials in Civil Engineering*, 18(6), 842–850. [https://doi.org/10.1061/\(asce\)0899-1561\(2006\)18:6\(842\)](https://doi.org/10.1061/(asce)0899-1561(2006)18:6(842))
- Lee, S.-K., & Zielske, J. (2014). An FHWA special study: post-tensioning tendon grout chloride thresholds (FHWA Technical Report DTFH61-08-C-00005). *The State University of New Jersey*, (May). Retrieved from <http://www.fhwa.dot.gov/publications/research/infrastructure/structures/bridge/14039/index.cfm>
- López, W., & González, J. A. (1993). Influence of the degree of pore saturation on the resistivity of concrete and the corrosion rate of steel reinforcement. *Cement and Concrete Research*, 23(2), 368–376. [https://doi.org/10.1016/0008-8846\(93\)90102-F](https://doi.org/10.1016/0008-8846(93)90102-F)
- Pawlick, L., Stoner, G., & Clemena, G. (1998). Development of an embeddable reference electrode for reinforced concrete structures. *University of Virginia*. Retrieved from <http://ntl.bts.gov/lib/37000/37000/37031/99-CR1.pdf>
- Rafols, J. C., Lau, K., Lasa, I., Paredes, M., & ElSafty, A. (2013). Approach to Determine Corrosion Propensity in Post-Tensioned Tendons with Deficient Grout. *Open Journal of Civil Engineering*, 3(September), 182–187.
- Randell, A., Aguirre, M., & Hamilton, H. R. (2015). Effects of Low Reactivity Fillers on the Performance of Post-tensioning Grout. *PTI Journal*, 11(August), 17–28.
- Sason, A. S. (1992). Evaluation of Degree of Rusting on Prestressed Concrete Strand. *PCI Journal*, 37(3), 25–30. <https://doi.org/10.15554/pcij.05011992.25.30>
- Sprinkel, M. M., & Balakumaran, S. S. G. (2017). Problems with Continuous Spliced Posttensioned – Prestressed Concrete Bulb-Tee Girder Center Spans at West Point , Virginia, (2642), 46–54.
- Trejo, D., Pillai, R. G., Hueste, M. B. D., Reinschmidt, K. F., & Gardoni, P. (2009). Parameters influencing corrosion and tension capacity of post-tensioning strands. *ACI Materials Journal*, 106(2), 144–153. <https://doi.org/10.14359/56461>
- Vaisala. (2007). *User's Guide Vaisala DRYCAP® Dewpoint*. Vaisala Oyj. Helsinki, Finland.
- Vander Velde, H. (2002). Corrosion, testing and rehabilitation of unbonded post-tensioned cables in “Push-through” or “Heat-sealed” sheaths. *Seminar on Parking Garages, Technical University of Nova Scotia*.

- Vigneshwaran, K., & Lau, K. (2016). *Corrosion of post tensioned tendons with deficient grout (Florida Department of Transportation Report BDV29-977-04)*. Florida International University. Miami, Florida.
- Whitmore, D., & Lasa, I. (2018). Impregnation technique provides corrosion protection to grouted post-tensioning tendons. *ICCRRR*, 05008. <https://doi.org/10.1201>
- Zhou, Y., Gencturk, B., Willam, K., & Attar, A. (2014). Carbonation-Induced and Chloride-Induced Corrosion in Reinforced Concrete Structures. *Journal of Materials in Civil Engineering*, 27(9), 04014245. [https://doi.org/10.1061/\(asce\)mt.1943-5533.0001209](https://doi.org/10.1061/(asce)mt.1943-5533.0001209)

APPENDIX A— Hydrodemolition

A.1 Detailed drawings



Evaluation of Techniques
to Remove Defective Grout
from Post-tensioning Tendons
FDOT Contract: BDV31-977-58

University of Florida
Structural Engineering
332.294.7191

Mock up Fabrication and Grout Installation

1/2

Figure A.1-1. Hydrodemolition mockup fabrication and grout installation

Mixture Proportions

ID	Weight of Cement (lbs)	Weight of Filler (lbs)	Actual % of Filler	Weight of Water (lbs)	Actual w/s	Actual w/c	Total Weight (lbs)	Total Volume (ft ³)	Design Volume (gal)	Required Volume (gal)
Target	39.39	0.00	0.00	9.07	0.23	0.23	48.46	0.40	3.00	0.78
40 PC	12.34	18.84	0.60	14.54	0.47	1.18	45.72	0.40	3.00	1.65
30 PC-A	9.36	21.82	0.70	14.54	0.47	1.55	45.72	0.40	3.00	2.43
15PC-B	6.33	35.25	0.85	19.38	0.47	3.06	60.96	0.53	4.00	3.19
10PC	4.27	37.31	0.90	19.38	0.47	4.54	60.96	0.53	4.00	2.68
5PC	1.58	29.60	0.95	14.54	0.47	9.19	45.72	0.40	3.00	2.43
15 PC-A	4.69	26.49	0.85	14.54	0.47	3.10	45.72	0.40	3.00	1.65
30PC-B	9.48	21.70	0.70	14.54	0.47	1.53	45.72	0.40	3.00	0.77

Procedure for pouring layers in the Mock up test:

The process will be done at both ends of the frame during the same day. Odd numbers assigned to the holes in the top of the conduit are used for injection of grout. Even numbers at the bottom of the conduit are used for discharge. Holes five and seven will serve for injection and discharge purposes. For each batch mix the design volume listed on the mixture proportions table, the approximate required volume for each layer is listed as required volume. Note, that for each layer grout pouring should stop once grout falls through the specified discharge hole. Dispose the remaining grout.

- 1: Drill holes in the top and bottom of the conduit as specified in the drawings. The diameter of the Holes in the top should be of 1".*
- 2: Mix Target grout according to mixture design. Pour through inlet hole until grout discharges from anchor cap. Seal the Hole in the anchor cap and continue pouring until grout discharges in the bottom hole. Perform the same process at the east side of the frame using 30PC(B).*
- 3: Mix 40PC grout according to mixture design. Pour through inlet hole until grout discharges from bottom hole. Perform the same process at the east side of the frame using 15PC(A).*
- 4: Mix 30PC(A) grout according to mixture design. Pour through inlet hole until grout discharges from bottom hole. Perform the same process at the east side of the frame using 5PC.*
- 5: Mix 15PC(B) grout according to mixture design. Pour through inlet hole until grout discharges from both discharge holes. Perform the same process at the east side of the frame using 5PC.*
- 6: Mix 10PC grout according to mixture design. Pour through inlet hole until not more grout fills in.*

Figure A.1-2. Hydromolition mockup: Mixture proportions and injection procedure

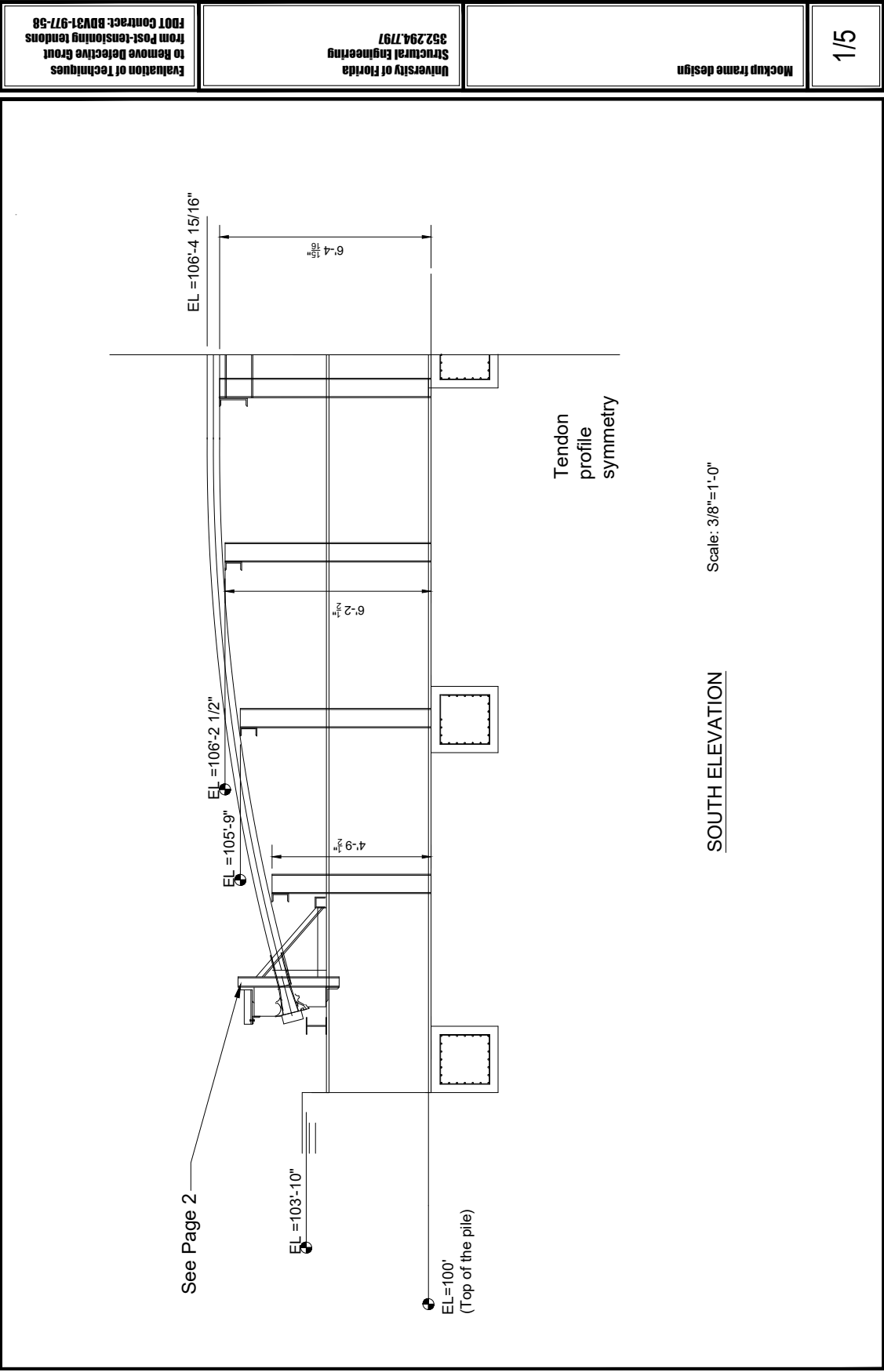


Figure A.1-3. Hydrodemolition mockup frame design (sheet 1/5)

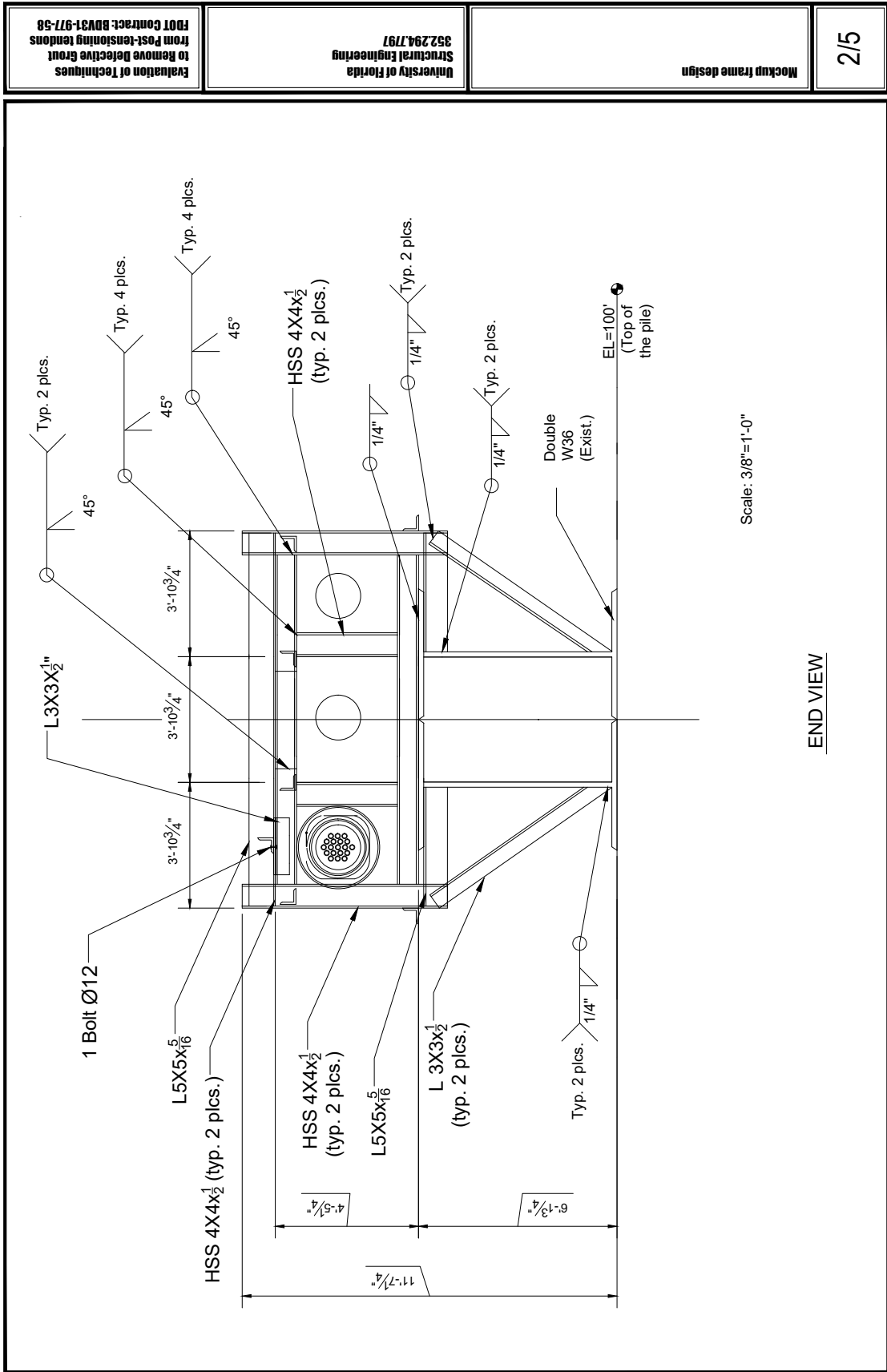


Figure A.1-4. Hydrodemolition mockup frame design (sheet 2/5)

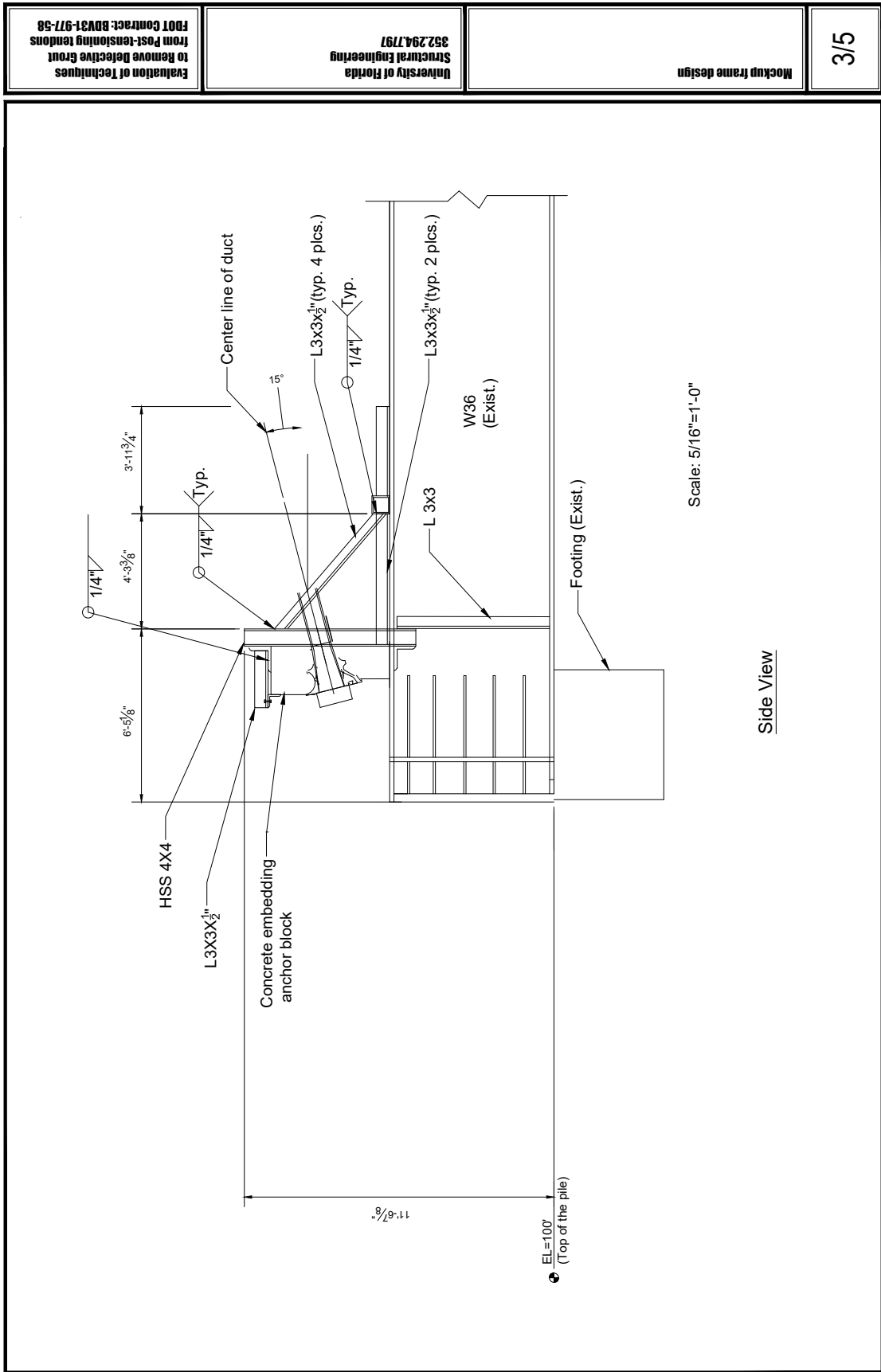


Figure A.1-5. Hydrodemolition mockup frame design (sheet 3/5)

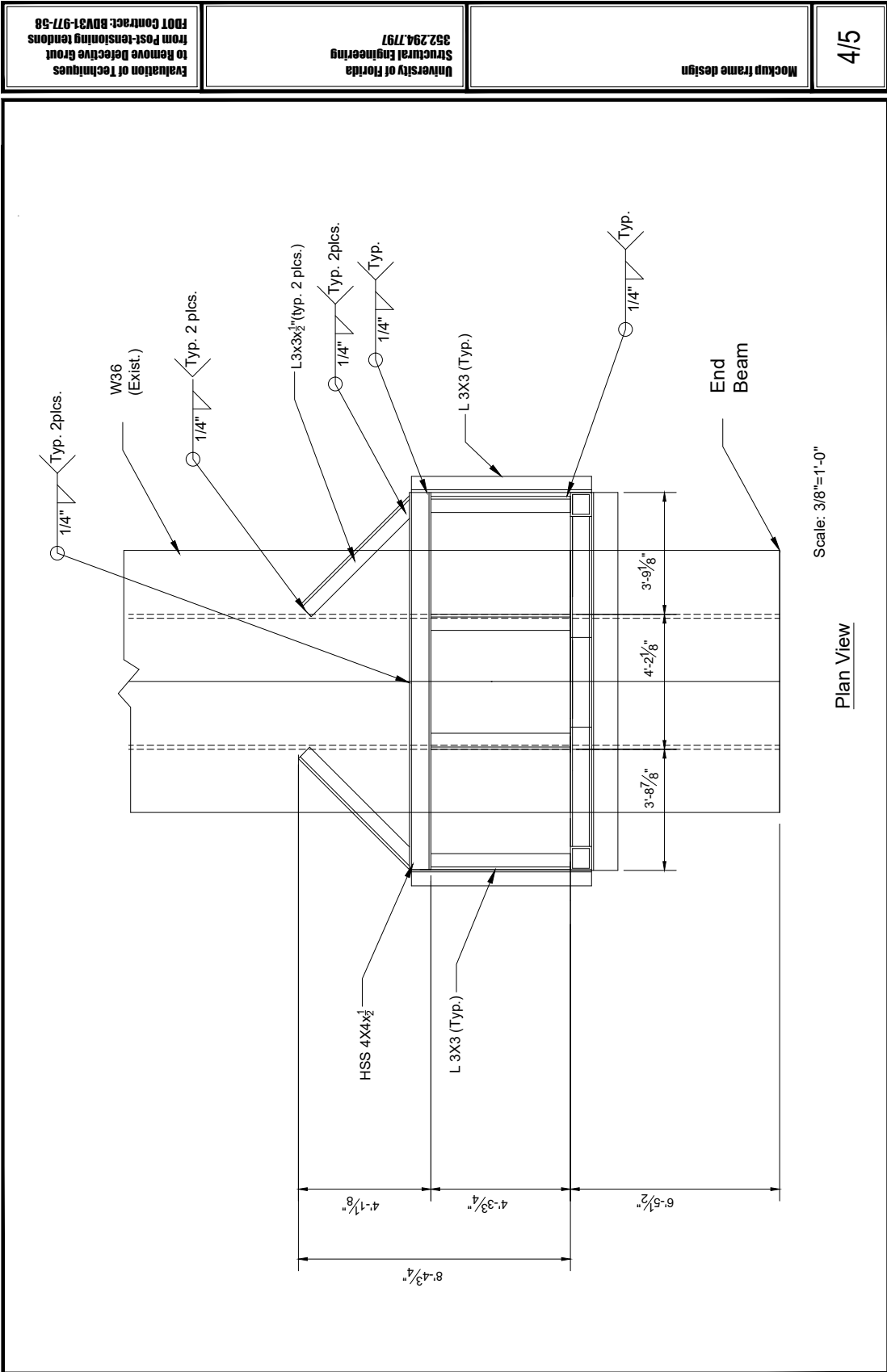


Figure A.1-6. Hydrodemolition mockup frame design (sheet 4/5)

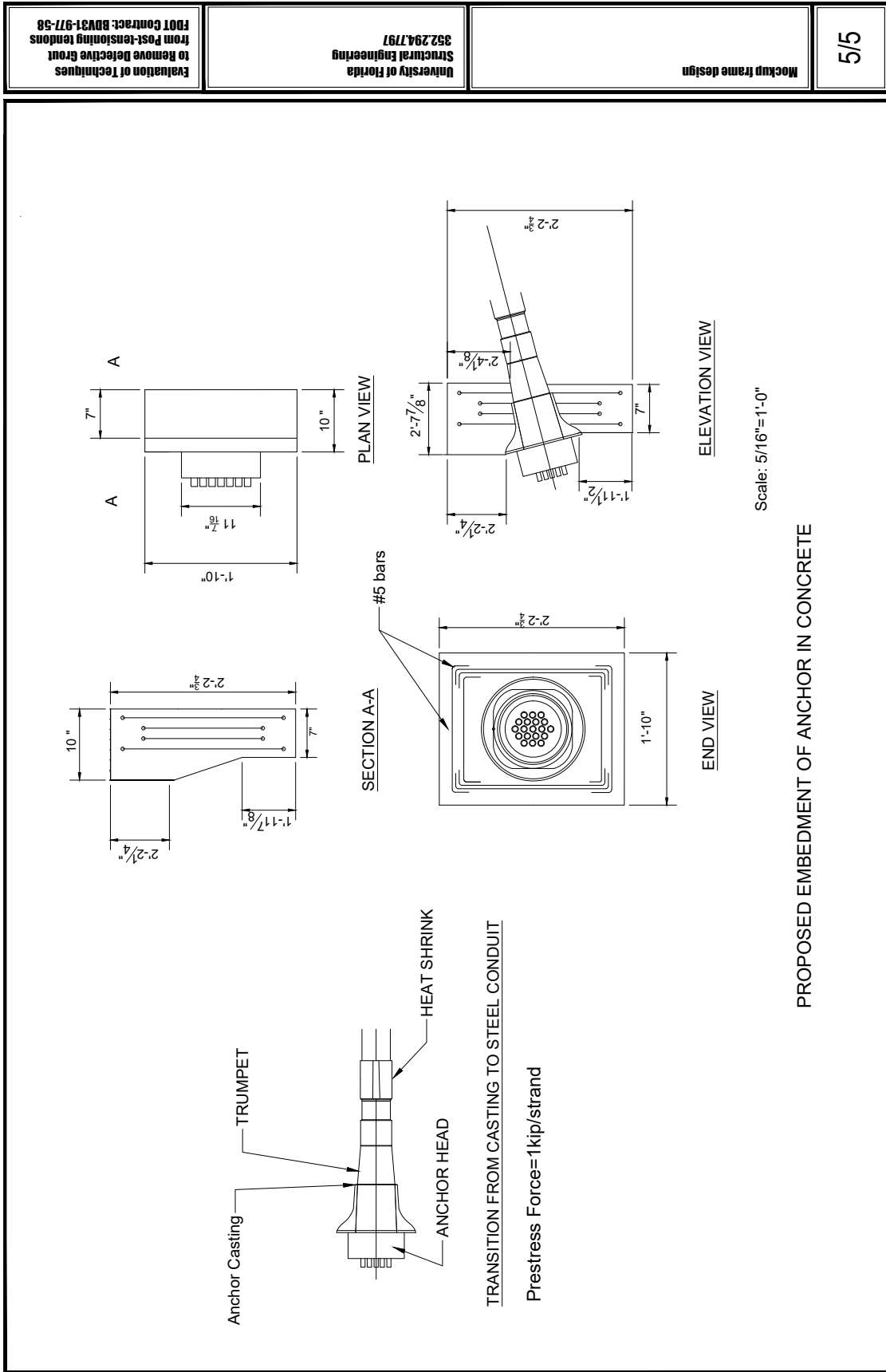


Figure A.1-7. Hydrodemolition mockup frame design (sheet 5/5)

A.2 Hydrodemolition test design

Two different specimens were designed to test the hydrodemolition process. The first specimen type was modeled after the inclined grout test and was intended to fully develop the process of mixing and placing soft grout in a consistent and repeatable manner (Figure A.2-1). In addition, some preliminary hydrodemolition trials were conducted on these specimens to gage the likelihood of success.

The second specimen design simulated a tendon in the negative moment region (over a support) of a post-tensioned continuous beam with internal tendons (Figure A.2-2 and Figure A.2-3). The specimen was constructed using electrical metal tubing (EMT), which was intended to simulate metal post-tensioning duct. The specimen was composed of nine straight segments of EMT connected with couplers and shrink-wrap to approximate the curved profile of a PT tendon (Figure A.2-4). The conduit had nominal outside diameter of 4 in. and nominal wall thickness of 0.08 in. Nineteen 0.6-in. seven-wire low-relaxation strands were bundled and placed in the EMT. Each strand was prestressed to a force of approximately one kip per strand. To simulate the thickness of the concrete surrounding the tendon in field conditions, two wood pieces of 2x8 timber were attached in the sides of the EMT (Figure A.2-5). To start hydrodemolition, holes were drilled through wood to access the EMT. The specimen was assembled on the steel frame located at the FDOT Structures Laboratory and had a total length of 38.3 ft with 8 supports between the anchors. The frame was designed to accommodate the EMT with an angle of 14° at each end of the frame (Figure A.2-3). Detailed drawings are provided in Appendix A (Figure A.1-1 through Figure A.1-7).

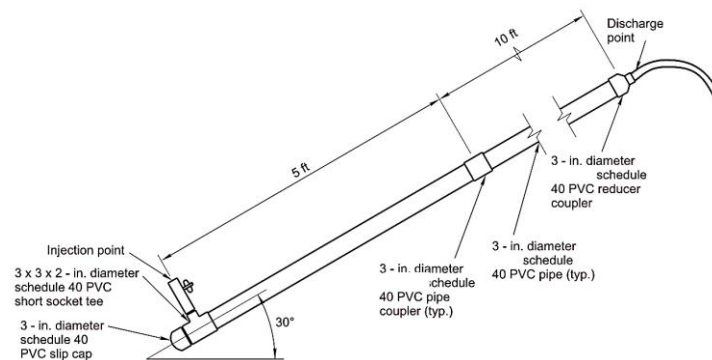


Figure A.2-1. Inclined hydrodemolition specimen design

Multiple grout layers were placed in this specimen as shown in Figure A.2-7. Denser grout layers like 30 PC and 40 PC with higher cement content were poured near the ends of the specimen, while less dense grout was poured in the elevated middle region of the specimen. The intent of such placement was to simulate grout segregation observed in bridge tendons.



Figure A.2-2. Hydrodemolition specimen: schematic figure with location of 2x8

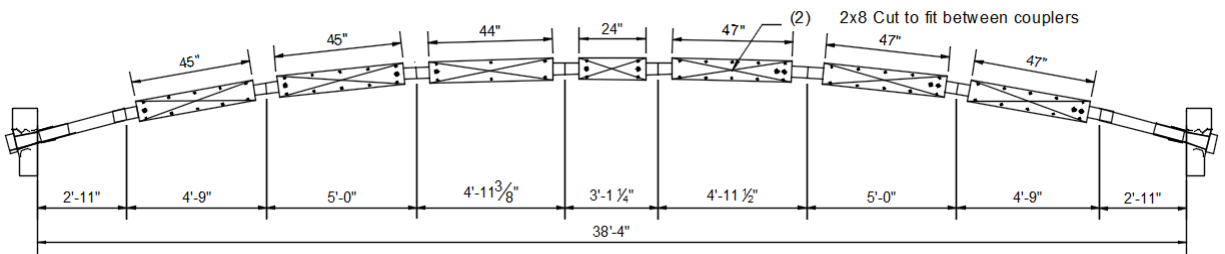


Figure A.2-3. Hydrodemolition specimen: EMT before installation of 2x8



Figure A.2-4. Shrink wrap and coupler connecting two EMT sections

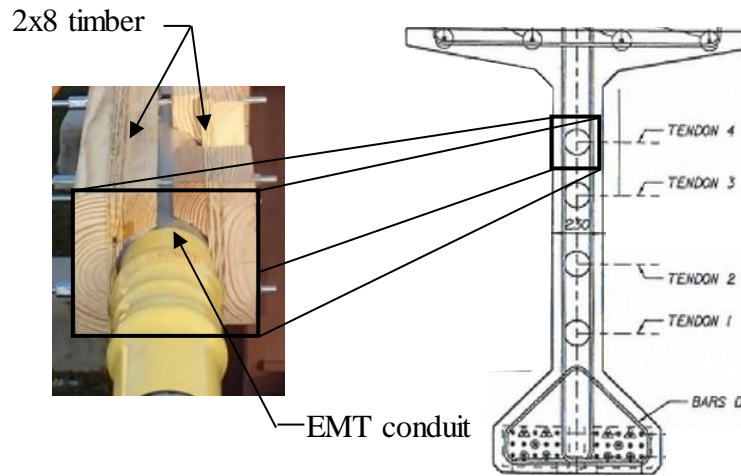


Figure A.2-5. Simulation of concrete surrounding a tendon using wood

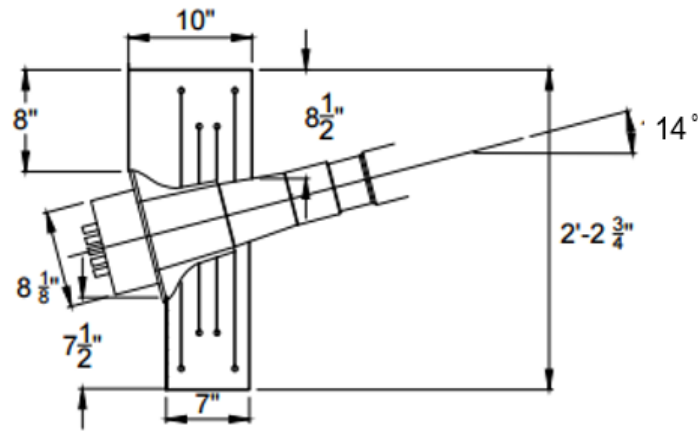


Figure A.2-6 Anchor details

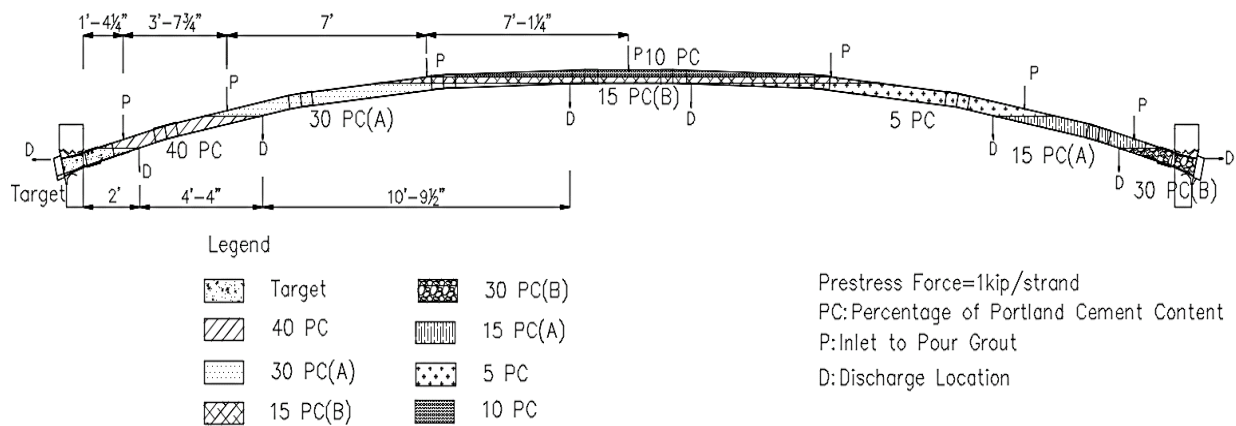


Figure A.2-7. Grout layers used in hydrodemolition specimen

A.3 Inclined hydrodemolition tests

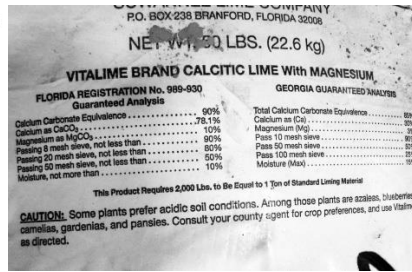
Following the development of a mixture design for the soft grout (Task 2), three PVC inclined tube specimens were constructed and injected to determine if the desired quantity of soft grout could be produced in a 15-ft-long specimen similar to that of the 3-ft-long mini-inclined specimens. Following confirmation of the soft grout mixture in the PVC specimens, three EMT (electrical metal tubing) specimens were constructed with prestressing steel and grout. Both PVC and EMT specimens were constructed and cleaned by FDOT personnel at the FDOT Structures Laboratory.

Construction:

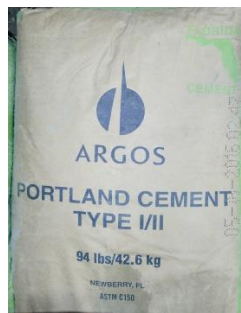
Table A.3-1 lists the mixture proportions used for the testing of PVC specimens. Two specimens were tested with 2.5% Portland cement content (2.5 PC) and one specimen with 5.0% Portland cement content (5 PC). Figure A.3-1 shows the portland cement and ground limestone used to prepare the mixtures. Figure A.3-2a shows the specimens in the inclined frame and ready for injection. Note that the PVC specimens did not contain prestressing strands.

Table A.3-1. Mixture proportion for PVC inclined testing

Grout ID	Portland Cement PC (lbs)	Ground Limestone GL (lbs)	Actual PC ratio (%) (PC/PC+GL)	Water (lbs)	w/cm	Total weight (lbs)	Total volume (ft ³)
5 PC	16.4	317	4.9	155	0.47	489	4.41
2.5 PC	8.4	325	2.5	155	0.46	489	4.41



(a)



(b)

Figure A.3-1 Grout mixture material: (a) ground limestone; (b) portland cement



(a)



(b)

Figure A.3-2. Inclined specimens using: (a) PVC pipe and; (b) electrical metal tubing

The procedure for grout injection was as follows:

1. PVC tubes were placed and secured in the frame (Figure A.3-2a).
2. Grout mixtures were prepared according to Table A.3-1. Mixing time was under 3 minutes using a CG600 Chemgrout grout plant (Figure A.3-3)
3. Pump hose was attached to the injection point of the inclined tube. The injection point was located at the bottom of the inclined tube as shown in Figure A.3-4.
4. Grout was injected until 2 gallons were collected at the discharge point of the tube. The injection process required less than two minutes to completely fill each specimen.



Figure A.3-3. Grout Plant



Figure A.3-4. Injection point

Three EMT specimens with varying grout characteristics and numbers of strand were constructed (Figure A.3-2b and Figure A.3-5). Several grout mixtures were used to construct the EMT specimens (Table A.3-2). Each specimen was constructed with two layers of grout and bundle of either 15 or 19 0.6-in diameter prestressing strands (Table A.3-3).

Grout layers were incorporated into the specimens to simulate the variation of grout consistency along a slope; harder grout was placed at the bottom of the inclined EMT tube and softer grout was placed near the top. This allowed the effectiveness of the grout removal to be tested as the strength of grout varied along the tube. The strength of the grout increases with increasing portland cement content.

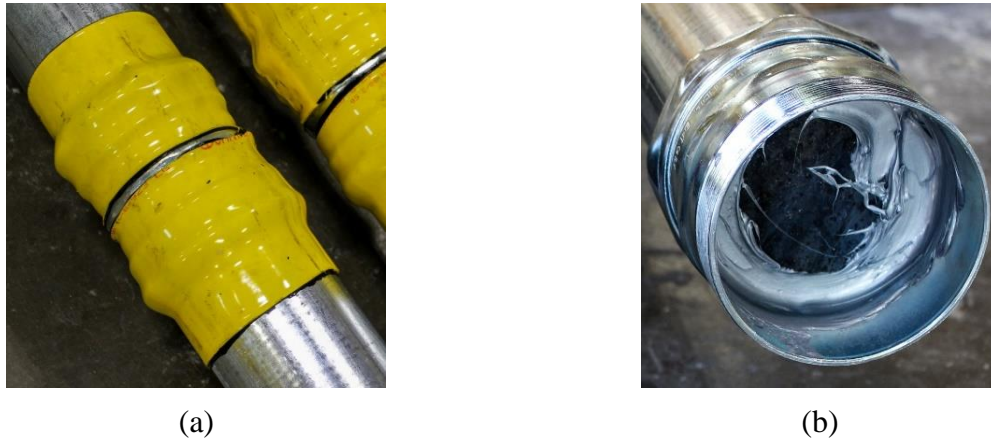


Figure A.3-5. EMT conduit: (a) coupling and; (b) shrink-wrap sleeves used to seal couplings

Table A.3-2. Mixture proportion for EMT inclined testing

Grout ID	Portland Cement PC (lbs)	Ground Limestone GL (lbs)	Actual PC ratio (%) (PC/PC+GL)	Water (lbs)	w/cm	Total weight (lbs)
10 PC	3.86	33.58	17.46	0.466	54.89	0.50
20 PC	7.36	30.08	17.46	0.466	54.89	0.50
30 PC	11.16	26.28	17.46	0.466	54.89	0.50
Prepackaged	47.63	-	12.67	0.266	60.30	0.49

Table A.3-3. EMT specimen matrix

Specimen	Number of Strands	Bottom Grout Layer	Top Grout Layer
EMT1	19	20 PC	10 PC
EMT2	15	20 PC	10 PC
EMT3	15	Target	30 PC

EMT specimen construction was similar with the exception of the injection procedure. The grout pump was not used because of mechanical issues cause by the grout mixtures. Instead, grout was mixed using five-gallon buckets and poured directly from the buckets into a tube that

was inserted in the open top of the inclined tube. The tube formed an improvised tremie to deliver the grout to the surface of the fresh grout in the specimen. The construction of the specimens occurred as follows:

1. Four EMT conduits were placed in the frame (Figure A.3-5 a). Note that four EMT conduits are shown, but three were used for hydrodemolition trials.
2. Water was weighed into the buckets according the particular mixture design (Table A.3-2).
3. Specified proportions of portland cement and ground limestone proportions were added while mixing with a paddle mixer and electric hand drill. (Figure A.3-6)
4. Grout was poured into a funnel, which was attached to a hose inserted to the base of the tube to form a tremie (Figure A.3-7).
5. As grout was poured into the funnel, the hose was slowly retracted to ensure that the discharge of the tube was in close proximity to the surface of the grout.
6. When mid-height was reached, a new mixture was prepared and used to fill the remainder of the tube.



Figure A.3-6. Grout preparation for EMT specimens with buckets, paddle mixer, and power drill

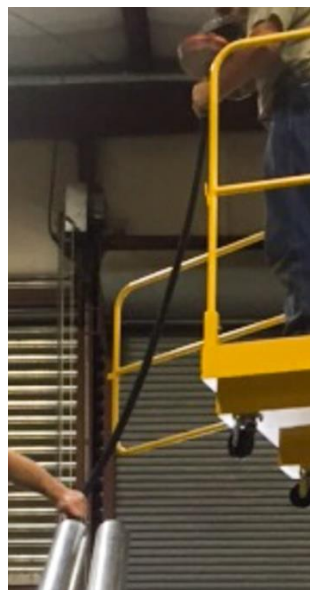


Figure A.3-7. Pouring grout into EMT specimen with funnel and tube

PVC specimen inspection:

PVC specimens were cured for one day prior to opening and inspection. Initial set (if it occurred at all) was expected to take place in 24 hours, so the specimens were allowed to cure for that time prior to verification that soft grout was present. The quantity of soft grout was measured by inserting a rod from the top opening of the tube until resistance prevented further penetration; this length was measured for each specimen. Soft grout volume was computed as the percentage of the entire volume based on the length of penetration (Table A.3-4). All three specimens had relatively consistent volumes of soft grout of approximately 90%.

Table A.3-4. Results of soft grout PVC specimens

Trial	1	2	3
Grout ID	5 PC	2.5 PC	2.5 PC
Soft Grout Length (ft)	13.7	13.2	13.5
% soft grout	91%	88%	90%
Penetrometer (psi)	700	50	60

To confirm consistency and extent of the soft grout, windows were cut into the PVC tubes to expose the grout (Figure A.3-8). The opening length was approximately 4 ft from the low end of the slope. The grout inside of the tubes varied depending on the amount of portland cement used. As the portland cement content was decreased, the consistency of the grout showed decreasing firmness to the point of mud (Figure A.3-9).

In the areas that the grout still exhibited some firmness, a penetrometer was used to measure the hardness. Penetrometer was used in several locations along the tube opening as shown in Figure A.3-8. The results obtained from the penetration tests are listed in Table A.3-4. It was observed that the specimen having 5% PC had 700 psi resistance, which is considerably higher than the 2.5% PC specimens, which had 50 psi and 60 psi resistance.



Figure A.3-8. Partial removal of PVC for inspection



Figure A.3-9. Verification of soft grout

PVC specimen trial cleaning:

A preliminary cleaning trial was conducted to determine the effectiveness of cleaning the grout using a household pressure washer with a delivery pressure of 2,700 psi. 2.5 PC and 5 PC were cleaned using this approach.

To clean and remove the soft grout inside the tubes, holes were drilled every 2 ft as shown in Figure A.3-10a. The process of grout removal started from the discharge point of the tube. Softer grout was found at the discharge point of the tube as expected. At this location, the removal of grout had success until it reached the lower part of the tube. Then, holes were drilled every 1ft as seen in Figure A.3-10c, facilitating the removal for that section.

When comparing both specimens, grout removal from 2.5% PC was easier than that of 5% PC. While the level of difficulty was higher for the specimen having 5% PC, grout was removed from both specimens satisfactorily. At the end, while most of the removed particles were small or liquid (see Figure A.3-10d), thick solid pieces of grout were also observed along the tube. For these trials, the grout was quite soft and there was no interference from prestressing strands.



(a)



(b)



(c)



(d)

Figure A.3-10. Trial clean-out conducted on PVC specimens: (a) 2-ft spacing of holes; (b) Conducting clean out; (c) 1-ft spacing of holes; (d) Debris at specimen end after clean out

EMT specimen hydrodemolition:

Hydrodemolition was performed at the FDOT Structures Laboratory by personnel from a company specializing in hydroblasting using their cleaning equipment (Figure A.3-11). Hydrodemolition consisted of injecting a high-pressure water jet through an opening in the duct and removing soft grout debris through a discharge opening. Specimens were prepared by coring an injection and discharge hole through the steel wall of the conduit to allow access to the grout for cleaning (Figure A.3-12). A water jetting nozzle was then placed into the injection opening to blast the exposed grout for removal (Figure A.3-13). The water jet pressure was increased from 7,000 psi to 10,000 psi for clearing the grout from around the opening. The space cleared near the inlet allowed a flexible tube and nozzle to be inserted inside the specimen. The nozzle was bullet shaped and was connected to a 1/16 in. diameter high-pressure flexible tube. The nozzle and tube were continuously fed into the duct through the injection hole as the water cleared grout, and the wastewater and grout debris were forced out of the discharge hole.



Figure A.3-11 Cleaning equipment



(a)

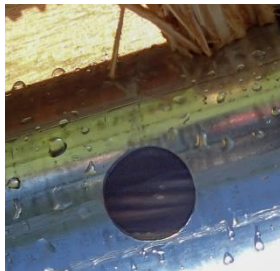


(b)

Figure A.3-12. Demonstration of preparing hydrodemolition specimen: (a) coring hole; (b) opening in duct



(a)



(b)

Figure A.3-13. Demonstration of cleaning of opening: (a) lance used to clear grout away from opening; (b) grout cleared from opening

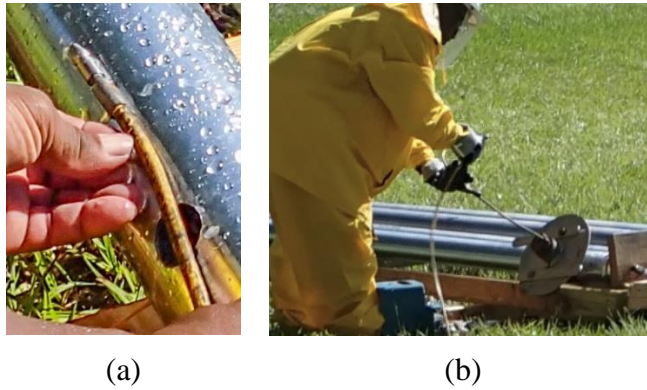


Figure A.3-14. Demonstration of performing hydrodemolition: (a) flexible tube and nozzle; (b) inserting nozzle and tube into the specimen

In EMT1 a hole was drilled approximately 13 in. from the end with the 20 PC grout. The jetting nozzle was placed into the hole to blast the exposed grout for removal. The initial water pressure was set at 7,000 psi to clear the grout from around the duct opening. The pressure was increased to 10,000 psi to further clear grout from the opening. The space cleared near the opening allowed the flexible tube and nozzle to be inserted into the duct. The process continued as the nozzle cleared grout; waste water and grout debris were forced back out of the hole in which the tube was being fed. The time required to complete a single specimen was approximately 2 hours. A similar procedure was used on the last two specimens. EMT1 and EMT2 were completed, but there was insufficient time to complete EMT3.

After completing the hydrodemolition process, specimens were dissected to inspect for removal of soft grout. Soft grout was partially removed from EMT1 and EMT2 (Figure A.3-15). EMT3 was started, but was not completed due to insufficient time (Figure A.3-16).



Figure A.3-15. EMT1 and EMT2 after hydrodemolition



Figure A.3-16. EMT3 after hydrodemolition

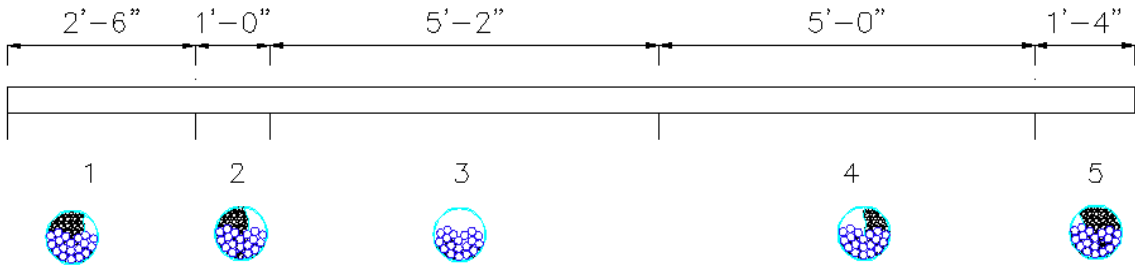
Visual inspection indicated that the pressurized water created a path through the grout, but did not clean the entire cross-section. Grout was found in the area surrounding the path and between the strands. Note that grout removal was more efficient towards the middle of the tube compared to the ends as shown in Figure A.3-17, but grout was still observed in the middle section between the strands and between the strands and the tube wall. Removal was considered better in the middle section because one hose was used at each end, meaning that both hoses met in the middle resulting in better removal. At the ends of the tube, grout was only removed along the path created by the tube.



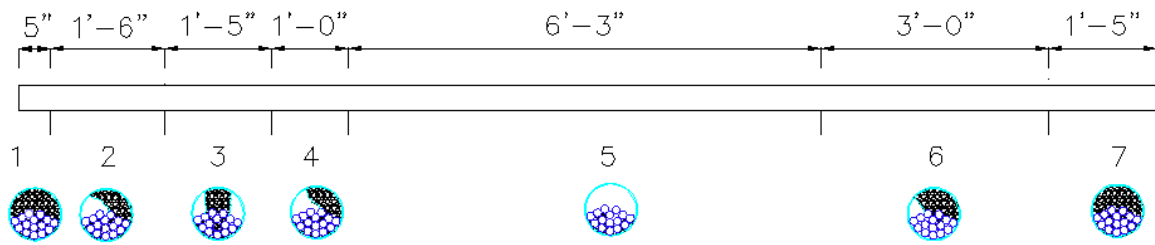
Figure A.3-17. Visual Inspection of 19S20PC-10 PC after grout removal

To estimate the effectiveness of the removal process, the tube was divided in sections to estimate visually the percentage of grout remaining in the tube (Figure A.3-18). Sections for each tube were established using the shape of the remaining grout along the tube. It was assumed that the shapes were constant for the assigned section to calculate an approximate volume of remaining grout.

Figure A.3-18a shows the five sections of EMT1 tube. Grout removal was efficient in section 3 located in the middle. Note that for both tubes minimal removal was observed at the ends of the tubes. Figure A.3-18b illustrates the seven sections of EMT2. Grout removal was more efficient in section five, which corresponded to the middle section of the tube as previously discussed. Section 2, 3, 4 and 6 show similar remaining volume of grout, but with different distribution.



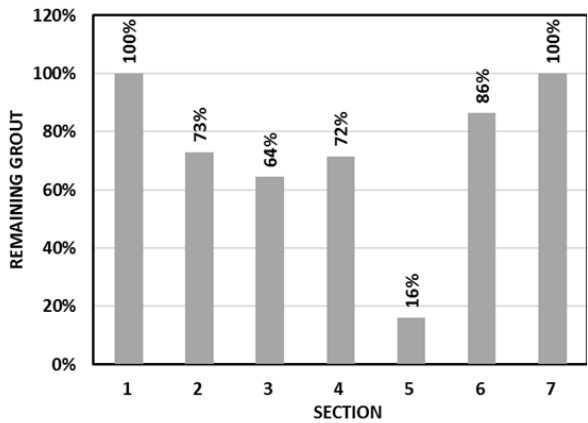
(a)



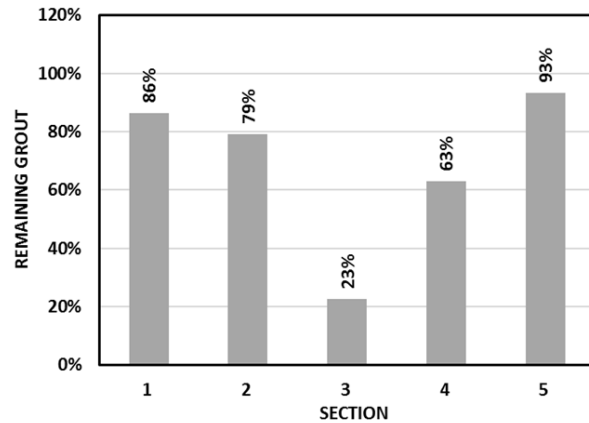
(b)

Figure A.3-18. Distribution of grout per section: (a) EMT1; (b) EMT2

Remaining grout was quantified by calculating the remaining percentage of grout using the geometry of the tube and shape of the grout along each section (Figure A.3-19). Same behavior is observed for both tubes in terms of remaining grout. It was also noted that using either 15 or 19 strands did not have a significant effect on the final results of the removal process.



(a)



(b)

Figure A.3-19. Percent of remaining grout per section: (a) EMT1; (b) EMT2

A.4 Mockup hydrodemolition tests

Hydrodemolition was conducted on the mockup specimen in four separate trials. In some cases, water blasting proceeded in one direction and in others the blasting occurred in both directions from the hole drilled. Sections 5, 6, and 7 were cleaned from both directions. Table A.4-1 and Figure A.4-2 describe the trials with the respective start points and covered sections. Each trial is discussed in further detail in the following sections.

Hydrodemolition was performed using three different procedures with varying configurations of water injection and debris discharge hole locations. The conduit length was divided into sections to isolate each method (Figure A.4-1). The first method consisted of drilling a water injection hole at one end of a section to inject the pressurized water with a discharge hole placed at the other end of the section; the holes were 40 in. apart. The second method was similar to the first method but had the water injection hole and discharge hole on opposite sides of the conduit. The third method consisted of drilling injection and discharge holes 3 in. apart, allowing debris to flow back out of a hole that was placed in close proximity to the injection hole. This was thought to provide a more practical approach in the field since both operations could occur on the same side of the girder web. Hydroblasting specialist provided a special fitting for this procedure.

Table A.4-1. Details of hydrodemolition trials

Trial	Drilled Hole Size	Nozzle Size (in)	Implemented Section	Elapsed Time (min)	Sections blasted
1	1.5"	1/16	1	25	NA
2			3	23	2, 3, 7
3			7	12	5, 6, 7
4			5	15	3,5, 6, 7

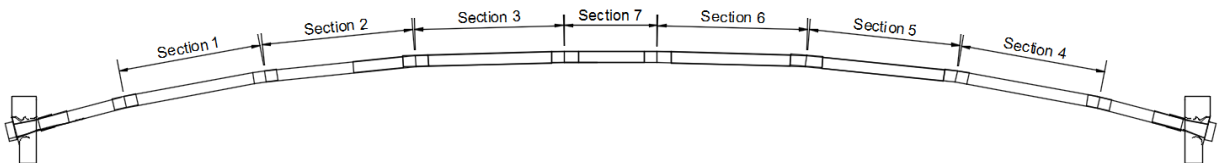
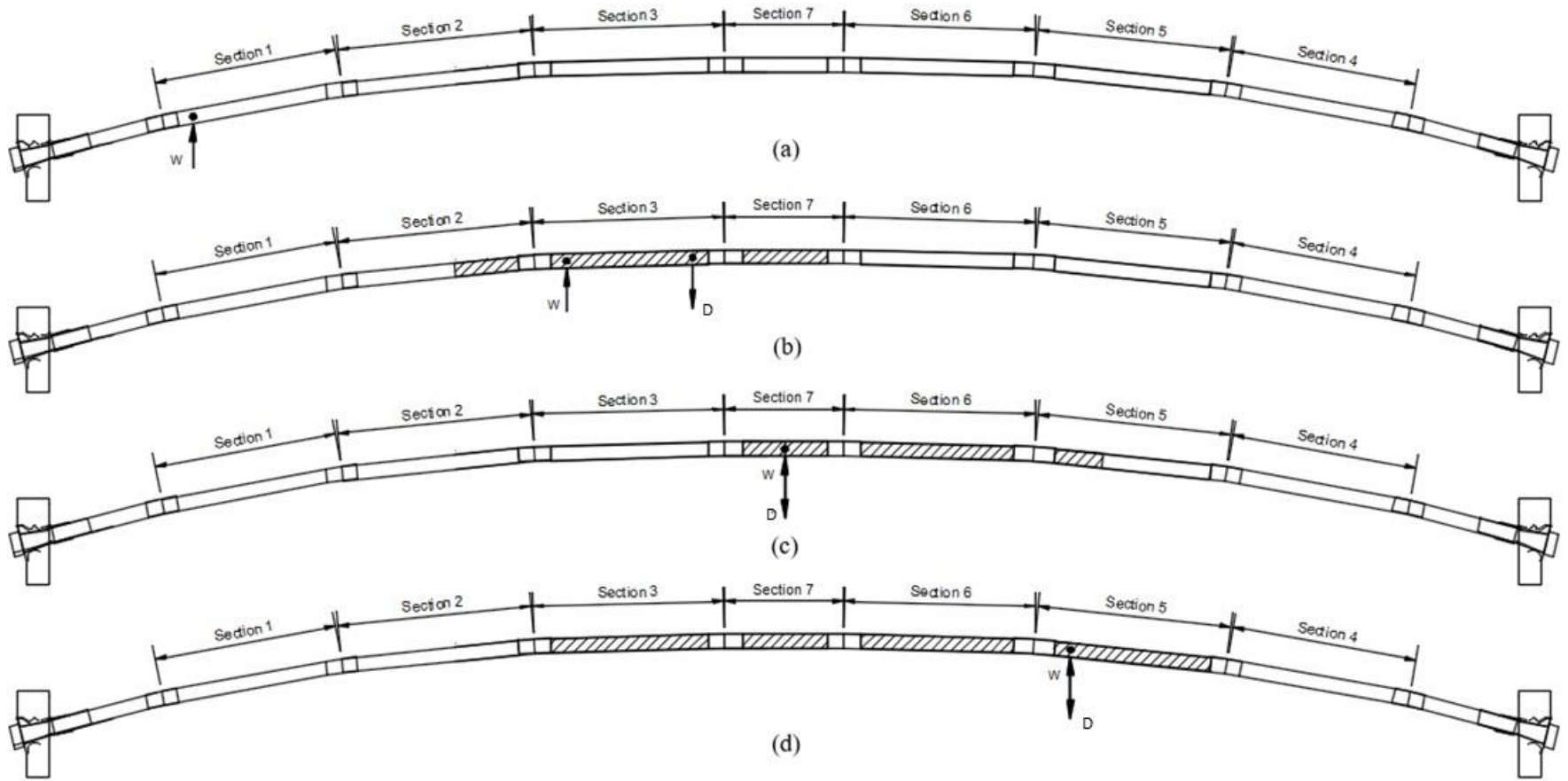


Figure A.4-1. East elevation of mockup section identification.



W: Water injection hole
 D: Discharge hole

Figure A.4-2. Sections covered by each trial to remove grout: (a) Trial 1; (b) Trial 2; (c) Trial 3; and (d) Trial 4

Construction:

Grout mixtures were prepared using portland cement, ground limestone filler, and water. These components were added to a plastic container and mixed using a paint mixture and power drill. Each grout type was poured along the specimen in their respective locations as shown in Figure A.2-7. One grout layer was poured per day, starting with higher strength layers at the ends and finishing with weaker soft grout layer in the middle region. The inlet points (P) shown on Figure A.2-7 were used to pour the grout. Pouring was terminated when grout was observed flowing out of the discharge points (D) closest to the respective inlet points.

Trial 1:

In trial 1 the injection hole was drilled in section 1. This trial was not able to progress due to the distribution of the strands inside the conduit. Grout inside the hole could be remove just enough to allow insertion of the flexible tubing (Figure A.4-3). Inspection of the opening indicated that the prestressing strand was near the top of the section, which effectively prevented insertion of the nozzle for hydrodemolition. Consequently, trial 1 was terminated.

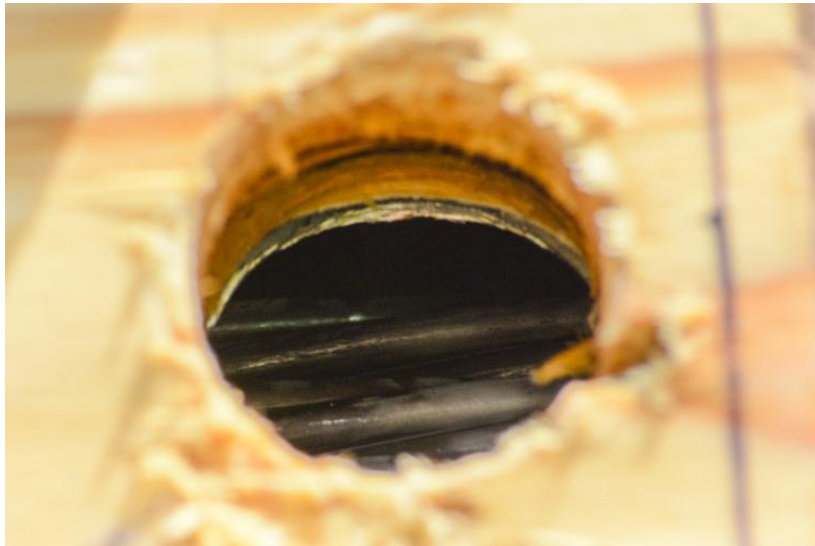


Figure A.4-3. Hole drilled for Trial 1: prestressing strand prevented insertion of blasting nozzle.

Trial 2:

Trial 2 was initiated in section 3 at the left end. Note that section 2 was not selected to avoid blockage similar to section 1 in Trial 1. In section 3, it was expected that the strands would be low enough in the duct to allow insertion of the blasting nozzle. Similar to Trial 1, however, it was difficult to drill a hole through the wood and EMT conduit. A rectangular portion of the wood blocks was removed to allow access to the upper part of the conduit for drilling (Figure A.4-4). The required time for the drilling process was of approximately 25 minutes. A discharge hole was drilled 40 in. along the duct and on the opposite side of the section to allow application of a vacuum.



Figure A.4-4. Insertion of nozzle into the hole opening prior to hydrodemolition in trial 2

When sufficient grout was removed, the nozzle was inserted in the conduit and hydrodemolition was initiated. The nozzle used in the blasting had a flow capacity of 5 gal/minute at a pressure of 15,000 psi. Initially, the nozzle was directed towards section 7. As the nozzle advanced, the debris and water was vacuumed from the conduit. The nozzle was advanced to the beginning of section 6. The nozzle was then withdrawn and redirected into section 2. Section 2 was filled with 30 PC grout, which resulted in slow progress as the nozzle was advanced. About halfway into section 2, the nozzle became lodged between the grout and the conduit and could not be withdrawn. Water-blasting was terminated, and the flexible conduit was cut leaving the nozzle and excess tubing inside the duct for later recovery.

Trial 3:

Trial 3 was initiated at the middle part of section 7. The set up at this section consisted of using the same hole for water injection and vacuuming of residues with the special fitting provided by hydroblasting company (Figure A.4-5). This trial was intended to remove grout from sections 4, 5 and 6. Drilling the hole at this section was easier compared to the previous two trials because the strands were gathered at the bottom of the conduit as a result of the prestress force. After inserting the nozzle into the conduit, grout was removed up to the beginning of section 5. In this trial, the nozzle was not moving forward, and instead was getting tangled with the strands.



Figure A.4-5. Fitting for hydrodemolition used in trial 3

Trial 4:

Trial 4 was initiated at the left end of section 5 (Figure A.4-6). The same method used in trial 3 was used for trial 4, by using the special fitting for water-blasting and vacuuming of debris. Grout removing process started to the right towards section 4. Grout was removed from section 5, but the nozzle could not advance to section 4. Later, the nozzle was directed towards the left side for a final attempt to remove grout in sections 2, 3, 7 and 6, which was unsuccessful.



Figure A.4-6. Execution of trial 4

Mockup dissection:

Dissection of the specimen took place on the day following hydrodemolition. Two longitudinal cuts were made along the top of the conduit so that the top portion could be removed for visual inspection. Only sections where hydrodemolition was successfully initiated were evaluated (hatched region of duct in Figure A.4-7a, sections 2, 3, 7, 6 and 5). The results for each of these sections of the conduit are summarized in Figure A.4-7b. In general, most of the grout above the strands was removed on every section dissected, except for section 2. Section 2 was mostly filled by 30 PC grout, meaning that hydrodemolition effectiveness substantially decreased with an increase in grout strength. On the other hand, residual grout was observed between strands and conduit wall, and between the strands in all the dissected sections. The following subchapters provide detailed discussion regarding observation in each section which was dissected.

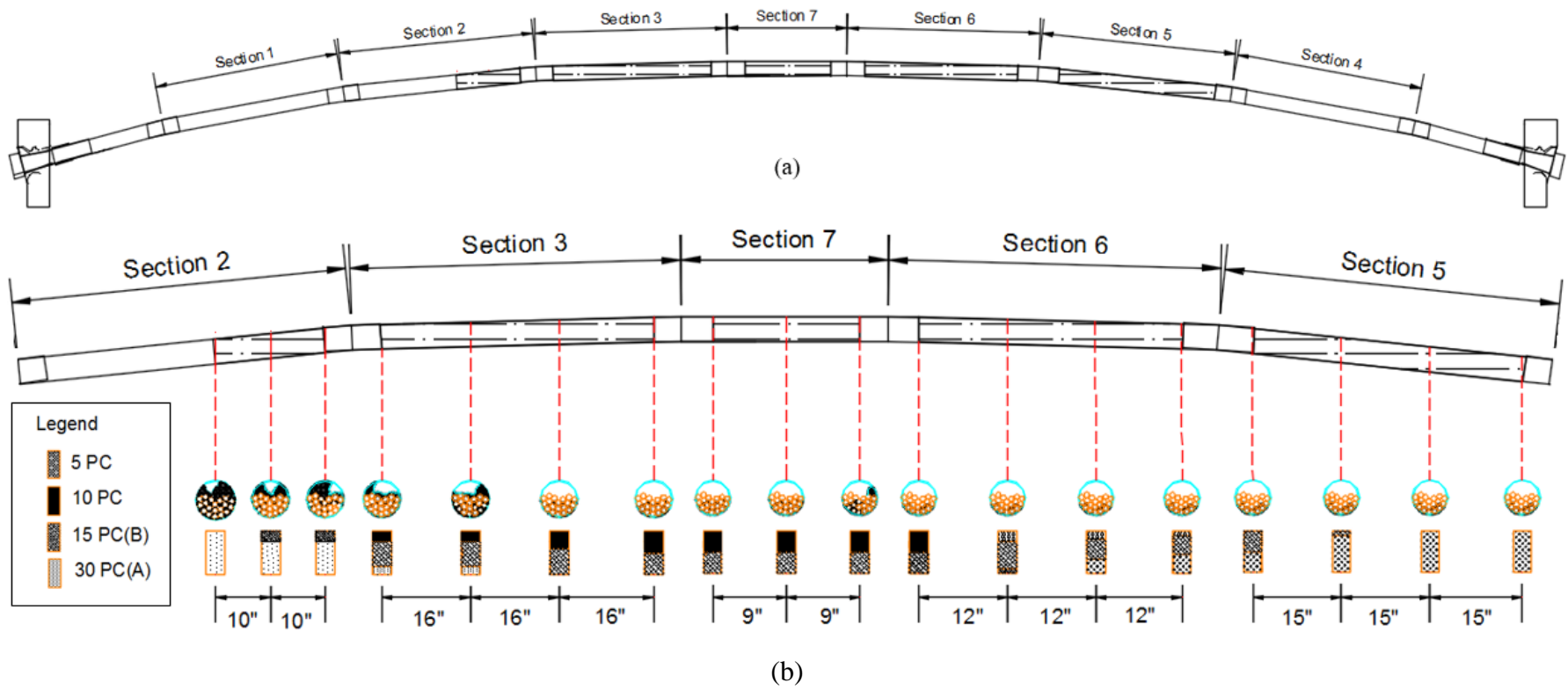


Figure A.4-7. Summary of residual grout after hydrodemolition

As previously described, section 2 was filled with stronger grout (15 PC and 30 PC) compared to the rest of the soft grout sections, resulting in more difficulty removing grout from this section. The residual grout in the section had a solid appearance and hard consistency (Figure A.4-8). Rather than removing grout, the water jet nozzle opened a narrow channel in the grout while it was advanced into the tendon. Recall from trial 2, that the nozzle was stuck in this section between the EMT conduit and the grout.



Figure A.4-8. Visual inspection of section 2 after water-blasting

Section 3 was filled with 3 layers of grout (10 PC, 15 PC and 30 PC). Removal in this section was better than in section 2, especially in areas near 10 PC grout. Large solid grout particles remained in the tendon (Figure A.4-9). In general, grout removal was effective in the section above the strands, but grout remained buried between and under the strands.



Figure A.4-9. Visual inspection of section 3 after water-blasting

Section 7 of the conduit was filled with 10 PC and 15 PC grout. Grout removal was effective in the section above the strands, but grout was present under and between strands. Fewer large particles remained in the tendon compared to section 3 (Figure A.4-10). Recall that at this section, injection and vacuuming was done using the special fitting.



Figure A.4-10. Visual inspection of section 7 after water-blasting

Section 6 had similar results as section 3 and 7. This section consisted of 10 PC and 15 PC grout, and a small part of 5 PC grout was present on the right side. Most of the grout above the strands was removed but still leaving behind large solid particles (Figure A.4-11). Note that this section consisted of weakest grout mixtures, so effective removal was expected.



Figure A.4-11. Visual inspection of section 6 after water-blasting

Section 5 had the weakest grout (5 PC) among all grout layers. Grout was removed from above the surface of the strands and between strands with the exception of some accumulations next to the conduit wall (Figure A.4-12). The consistency of the remaining grout was similar to wet sand due to the low percentage of portland cement. The EMT conduit was completely removed to observe the residual grout around the strand bundle. Soft grout was observed in the bottom section of the conduit. This soft grout was very moist and may have contributed to strand corrosion if left in place (Figure A.4-13).



Figure A.4-12. Visual inspection of section 7 after water-blasting



Figure A.4-13. Consistency of remaining grout below strands

APPENDIX B— Grout drying

B.1 Detailed drawings

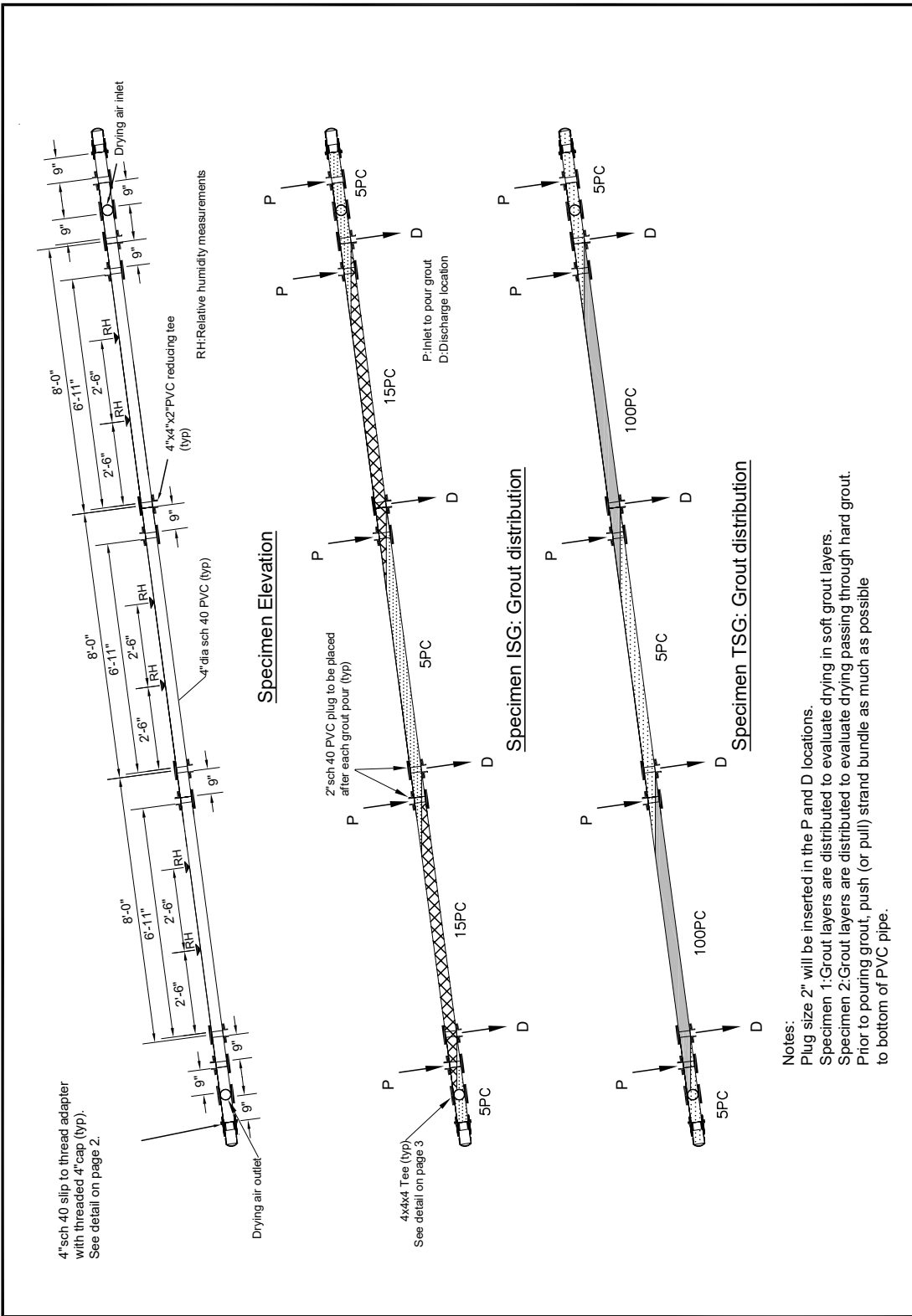


Figure B.1-1. Drying of PVC specimens: grout layer distribution

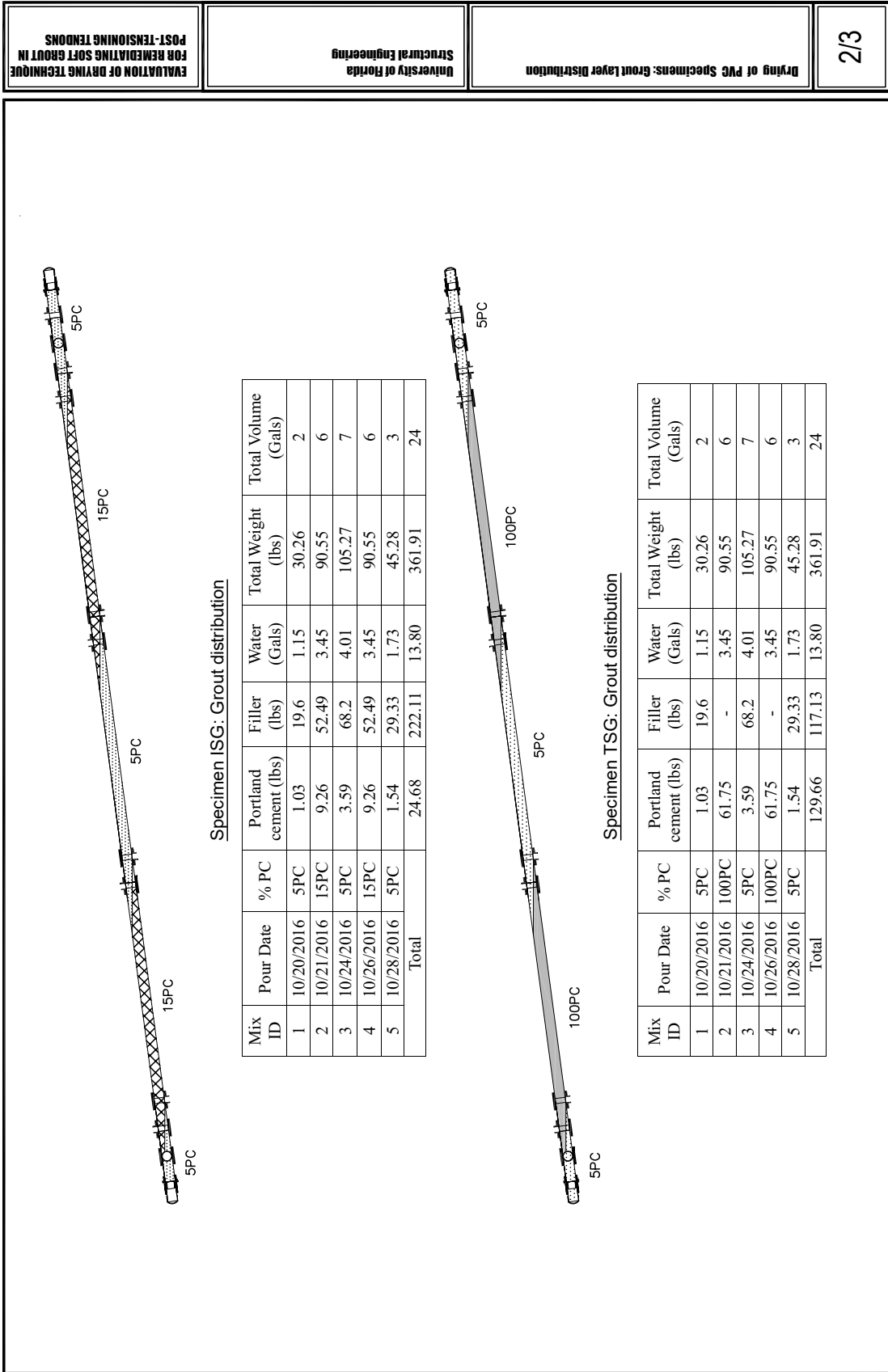


Figure B.1-2. Drying of PVC specimens: grout mixture design

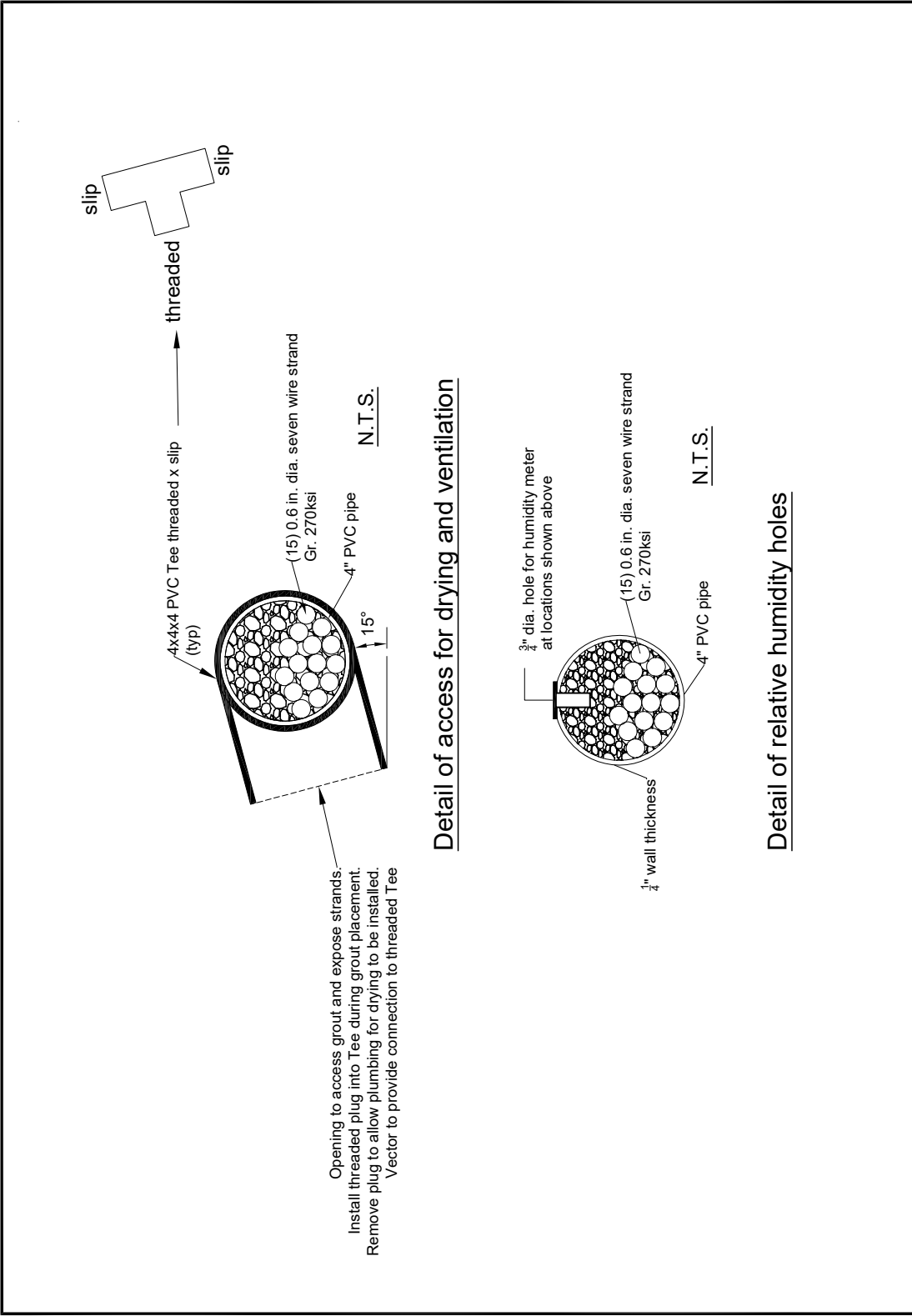


Figure B.1-3. Drying of PVC specimens: details of key cross-section

B.2 Procedure for RH measurements

The procedure for ΔRH_d measurement was as follows:

1. Connect the HDPE tube at inlet/outlet of specimen to the inlet of dewpoint meter while the dry air system is operating (see 1 in Figure 7-4).
2. Record the RH reading, once stabilized, from the MI70 indicator (see 2 in Figure 7-4).

Detailed procedure to operate the dewpoint meter can be obtained from user's guide for DM70 (Vaisala, 2007).

The procedure for measuring RH_g was adapted from ASTM F2170 Standard Test Method for Determining Relative Humidity in Concrete Floor Slabs Using in situ Probes. Table B.2-1 provides description of procedures adapted or modified from ASTM F2170-16b for determining relative humidity using in situ probes.

Table B.2-1. Comparison of ASTM F2170 procedures and adapted procedures

Variable	ASTM F2170-16b	Adapted method
Forming holes in grout	ASTM provides two procedures for forming holes for RHP measurement. Procedure A of drilling holes involves dry coring of grout using a drill, whereas procedure B involves placing liner tubes before placing concrete. See § 10.3 for more details.	Procedure A from ASTM F2170-16b was used for drilling holes in grout.
Depth of hole	ASTM requires depth of hole drilled in slabs to be determined based on drying conditions and depth of slab. For example, drill hole of depth 20% of thickness of slab, if slab is drying from top and bottom surfaces.	Hole was drilled up to mid-depth of the tendon.
Number of test locations	Perform three tests for the first 1000 ft ² and at least one additional for each additional 1000 ft ² .	At least one test for each type of grout layer in the specimen.
Test locations	Areas of potential high moisture content is recommended for test locations.	Test location was away from interface of two different grout layers if any to ensure RH_g readings are corresponding to a particular grout type.
Probe equilibrium	Probes are considered to be in equilibrium when placed inside the hole if RHP reading has less than 1% drift over 5 minutes. Equilibrium may take from several hours to several days, and probe should be placed in the hole during this time.	Based on testing conducted early in the research, probes were typically assumed to achieve equilibrium after 10 minutes of placing them inside a hole.

In general, the following procedure were developed to measure grout RH (RH_g) readings:

1. Stop the drying system (To avoid water ejecting from the port when air blows through the specimens).
2. Place a probe in each port (A probe was used in same probe hole each time to ensure consistency in readings).

3. Leave the probe inside the port for at least 15 minutes if $RH > 50\%$ or until equilibrium is attained if $RH < 50\%$.
4. Connect moisture meter to each probe.
5. Take measurement of relative humidity (RH), Dry bulb temperature (T) and Dewpoint temperature (Td) for each probe. Look at the screen for at least 10s to ensure there is no variation. If values of temperature and relative humidity remain the same, record: RH, T, and Td.

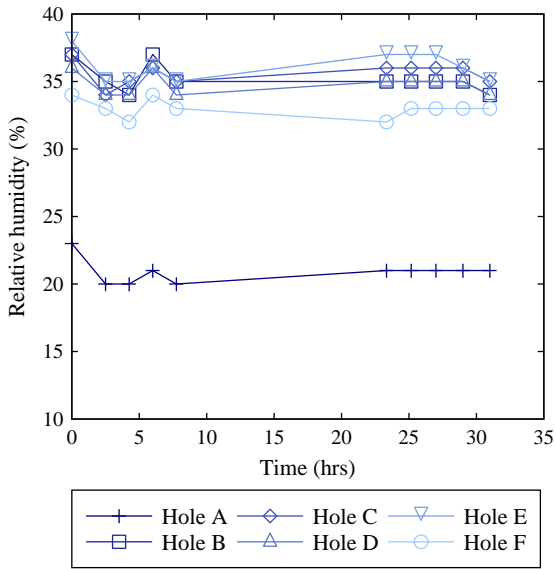
B.3 Probe response time

To determine the variation in measured RH_g with time, four tests were conducted in which the probes were allowed to remain in the specimen for multiple readings. These tests were conducted late in the drying test when the RH readings were well below 50%. The drying system was turned off at least one day before inserting probes in specimens. Probes were then placed in specimens until the last day of the test. For each test period, RH_g readings were recorded three times per day at approximately two-hour intervals. At the start of each test, the probes required more than 30 minutes (probe manufacturer recommended time) to equilibrate with grout RH and stabilize readings. The procedure is explained in Appendix C. The dates of different tests performed are mentioned in Table B.3-1.

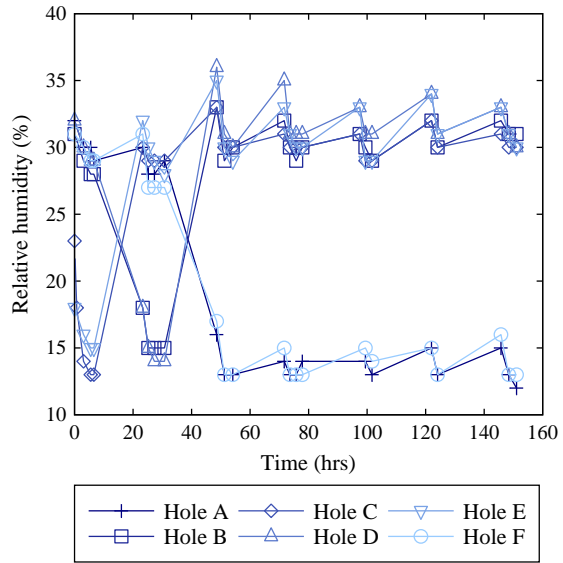
Table B.3-1. Tests to determine variation in RH with time

Test no.	Specimen no.	Start date	End date
1	ISG	04/25/2017	04/26/2017
2	ISG	05/08/2017	05/16/2017
3	TSG	04/25/2017	04/26/2017
4	TSG	05/08/2017	05/12/2017

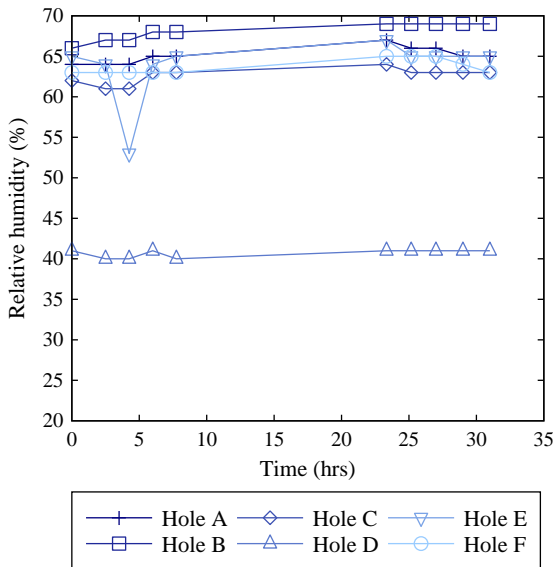
During test 1 and 3, RH_g for specimen ISG and TSG varied in a range of $\pm 4\%$ RH after 2 hours of placing the probes (Figure B.3-1). Similarly, during test 2 and 4, RH_g readings did not stabilize to a constant value, but had lower RH values than in test 1 and 3, probably due to drying of grout between the two tests. Test 2 and 4 readings also varied in a range of $\pm 4\%$ but after 100 hours of placing the probes. The variation in test 2 and 4 readings during first 60 hours was because of not placing probes in their designated holes. But after 60 hours, the probes were placed in their designated holes which reduced variation in readings.



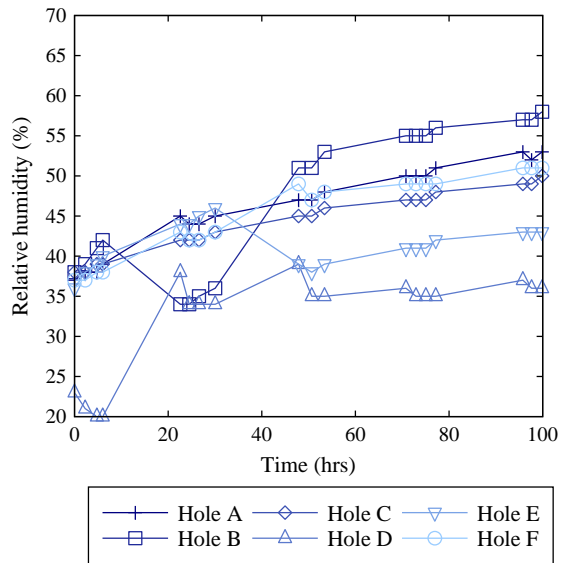
(a)



(b)



(c)



(d)

Figure B.3-1. Test results for probe response time for each of the four tests: (a) Test 1 (Specimen ISG); (b) Test 2 (Specimen ISG); (c) Test 3 (Specimen TSG); (d) Test 4 (Specimen TSG)

In conclusion, probes did not stabilize even after placing them in holes for longer than 30 minutes. The instability of probe readings can be attributed to thin layer of grout in the holes, shrinkage cracks in grout and leaks in specimens.

B.4 Effect of probe port depth on RH_g readings

Effect of probe port depth on RH_g reading was studied using the plots of RH_g in ports E and F vs. time for both specimens (Figure 8-33 and Figure 8-34). Port depth was 1 in. for port E and 1.5 in. (or up to the strands) for port F. Therefore, port E measured RH of top section of grout whereas port F measured RH of bottom section of grout. The difference in moisture content between top and bottom grout sections was found to be not greater than 7% in the case of undried and dried grout near ports E and F in both ISG and TSG. However, even with about 7% difference in moisture content, neither of the ports had constantly higher or lower RH reading with respect to each other throughout the drying period. For example, in the case of specimen ISG (Figure 8-33), RH_g in the port F was higher than port E during days 40 to 60; whereas RH_g in port E was higher than port F during the days 80 to 100 and during 100 to 110 days. Thus, it was found that port depth did not affect RH readings.

B.5 Dryness evaluation using corrosion potential charts

The contractor providing the drying services for this project typically utilizes the plot shown in Figure B.5-1 to identify if unbonded cables are exposed to corrosive environment (Vander Velde, 2002). This corrosion potential evaluation (CPE) chart includes three lines, where each line is intended to represent unique air moisture content inside the duct. The green line, red line and blue line in CPE chart correspond to moisture contents of 0.3%, 0.7% and 1% by mass of air respectively (Table B.3-1). The area between each line represents the corrosion potential of cable subjected to CPE testing. CPE testing, developed by Vanco Structural Services, involved passing of dry nitrogen gas through greased and sheathed unbonded, single-strand tendons and measuring RH and temperature of gas at outlet of cable. This measured RH and temperature was then plotted on CPE chart to predict corrosion potential of the tested cable. Calibration of CPE charts for different structures was performed by visual and instrument inspection of randomly selected cables after completion of CPE testing. Such a calibration was done for parking garages by Post-Tech along with National Research Council of Canada in Calgary, Canada (Vander Velde, 2002) (Figure B.5-2). Based on this calibration, CPE charts were found conservative and effective non-destructive tool to characterize corrosion potential of cables and help plan required protective measures.

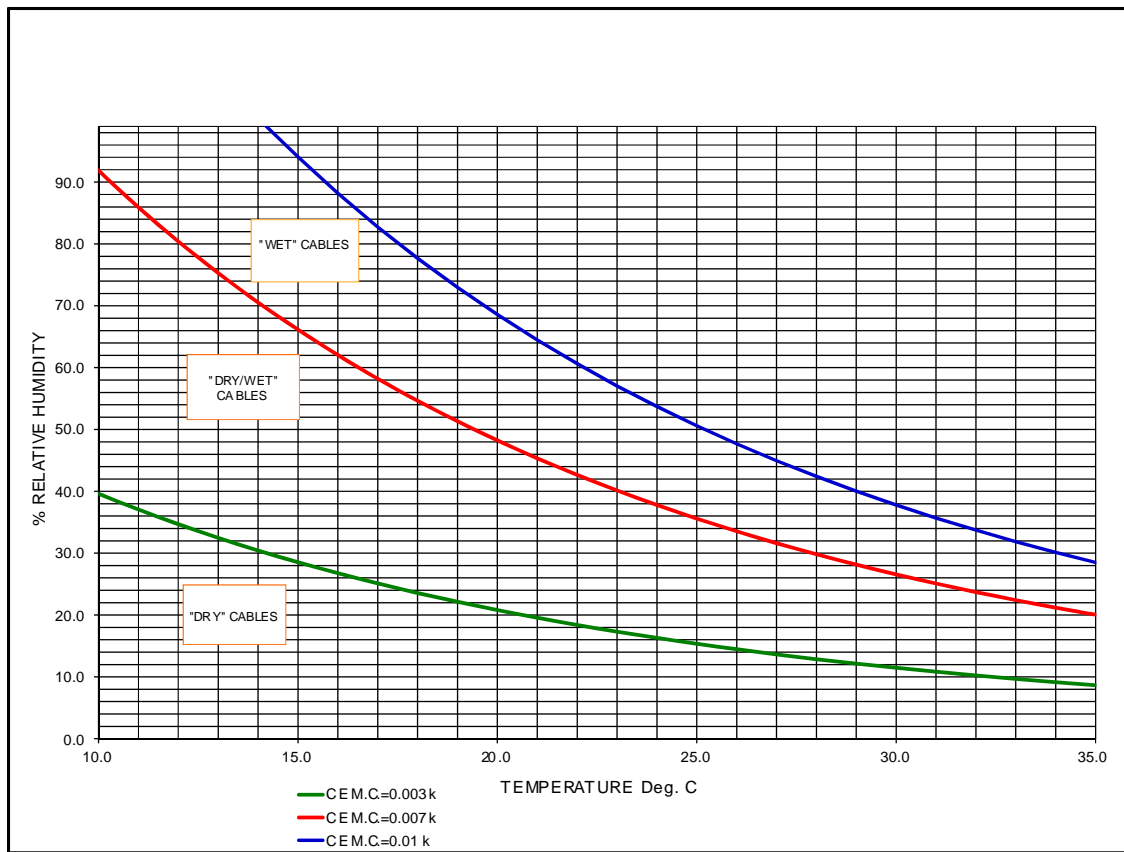


Figure B.5-1. Corrosion potential evaluation (CPE) chart

Although not developed for grouted multistrand tendons, this CPE chart developed by Post-Tech, was applied to the current investigation in order to determine its applicability in terms of evaluating dryness of cables. The chart was applied by plotting ΔRH_d readings vs. temperature and a specimen was considered dried when a reading dropped below the green line in CPE chart. This criterion was also used to judge RH_g readings measured in probe ports and ΔRH_d readings measured at inlet and outlet of specimens.

Table B.5-1. Corrosion Potential Evaluation Grading System

CE Grade	Exposure Conditions and Potential for Corrosion		
	Moisture Content (%)	Description	Corrosion Potential
0	N/A	No Test	N/A
1	MC = < 0.3	Dry	Low
2	0.3 < MC < 0.7	Moist	Moderate
3	0.7 = < MC	Wet	High

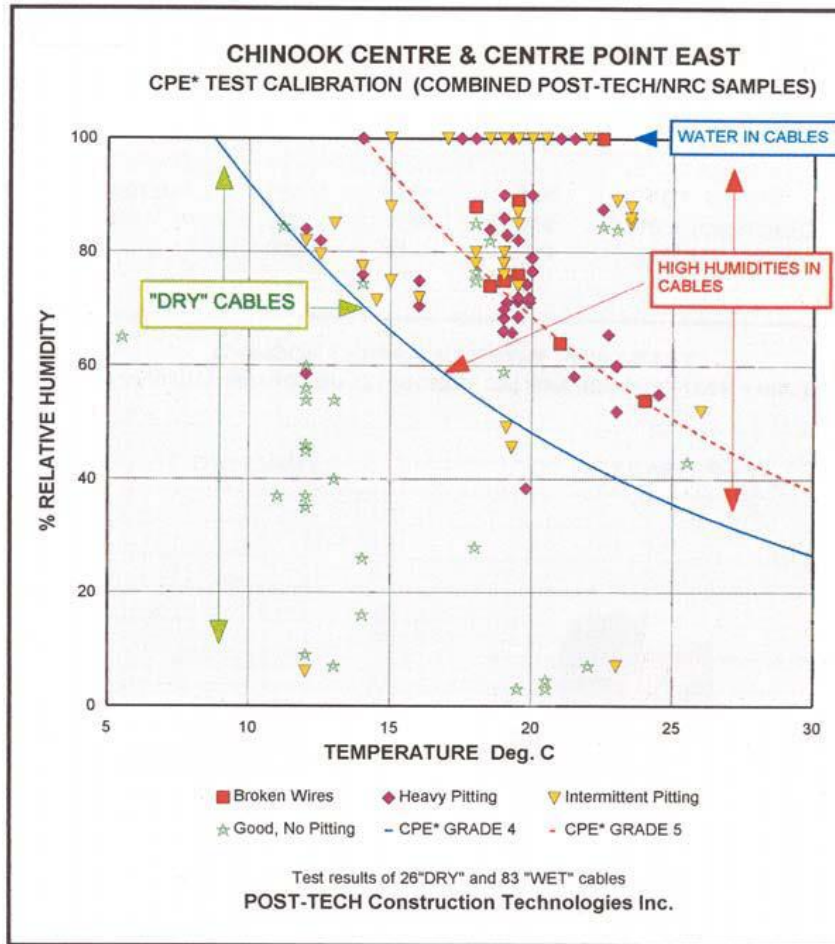


Figure B.5-2. Calibration of CPE by Post-Tech (Vander Velde, 2002) dry air rating

ΔRH_d evaluation:

ΔRH_d readings were taken at air outlets and plotted on the CPE chart (Figure B.5-3). Lighter color symbols represent latest readings. ΔRH_d readings were generally taken along with RH_g readings which caused external air to leak in the specimen when ports drilled in grout were opened. To avoid this air leakage, RH_g readings were not taken along with ΔRH_d readings towards the end of drying period (readings shown with Δ).

Within the last three weeks (days 157 to 180) ΔRH_d readings for specimen ISG and TSG were below green line, and the soft grout in specimens was found dry when dissected. The CPE grading system, hence, was applicable to predict if soft grout was dry using ΔRH_d readings.

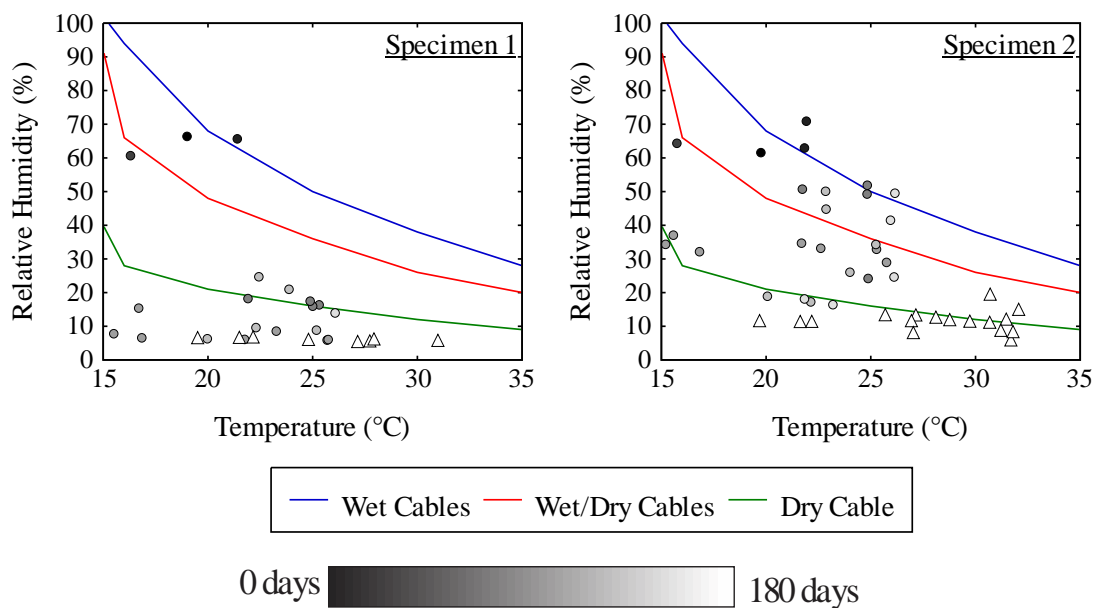
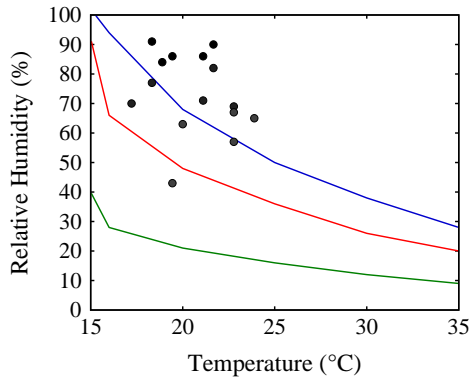


Figure B.5-3. Drying air relative humidity readings over drying period

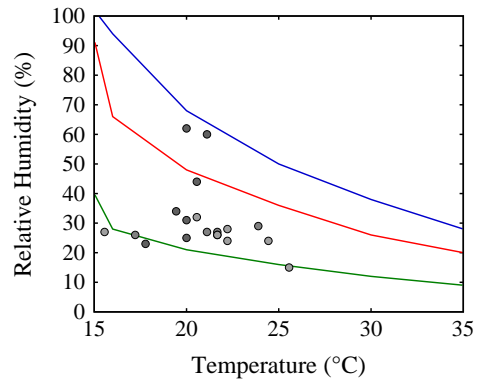
Specimen ISG RH_g dryness evaluation:

RH_g readings overlaid on the CPE chart for specimen ISG are shown in Figure B.5-4 through Figure B.5-9. Recall that specimen ISG consisted of two different types of soft grout. For each dried specimen, readings are split into two months span from drying initiation and plotted in three different plots. RH_g readings in first two months were above the blue line in the rating chart, indicating wet conditions. As drying continued, RH_g readings decreased steadily in the dried specimen. In the control specimen, however, RH_g readings varied little and typically remained above 80% during the entire drying time, which indicated wet conditions in control specimen. This comparison of readings between the control and dried specimens provided confirmation moisture was removed by the process.

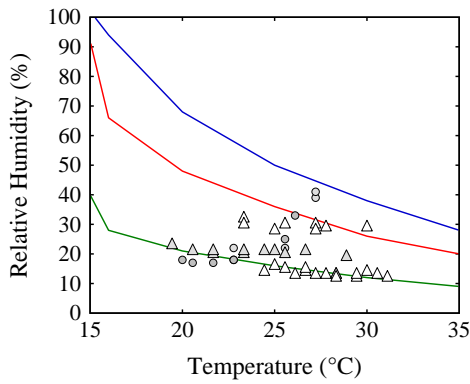
RH_g readings during fifth and sixth month of drying indicated air in ports drilled in grout had moisture content below 0.7% (red line) (Figure B.5-4 through Figure B.5-9). These readings predominantly remained between 15% and 40% RH even though temperature varied between 15°C to 35°C. After dissecting, it was found that soft grout had negligible moisture content after six months of drying. Therefore, CPE chart indicated soft grout in specimen ISG was dry when RH_g dropped below red line, i.e., moisture content of air in drilled ports was below 0.7%.



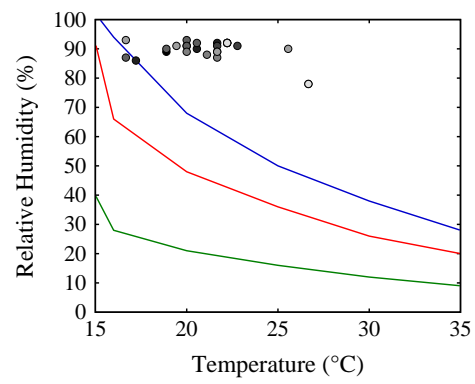
(a) Dried specimen (Months 1 – 2)



(b) Dried specimen (Months 3 – 4)



(c) Dried specimen (Months 5 – 6)



(d) Control specimen

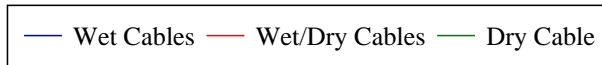
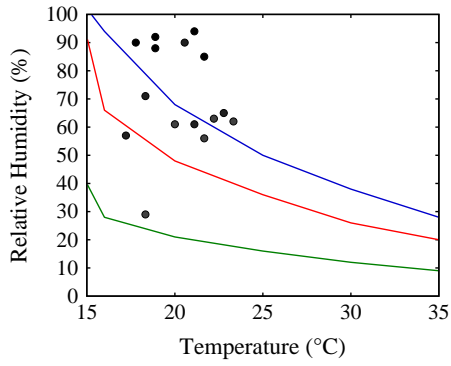
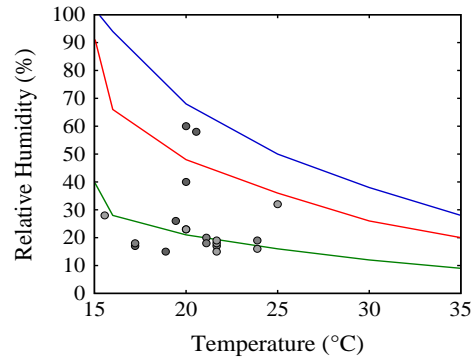


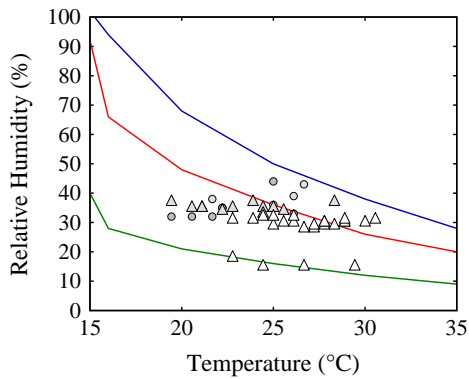
Figure B.5-4. RH probe readings at port A (15 PC grout layer)



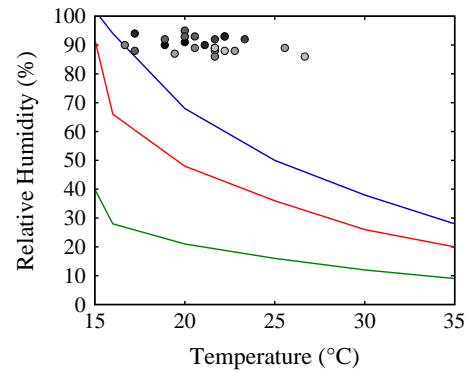
(a) Dried specimen (Months 1 – 2)



(b) Dried specimen (Months 3 – 4)



(c) Dried specimen (Months 5 – 6)



(d) Control specimen

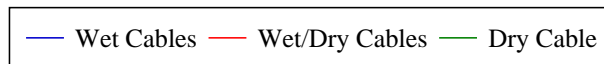
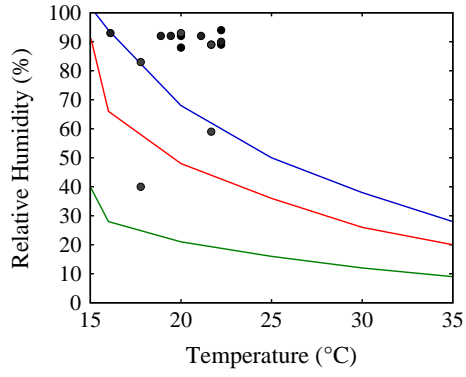
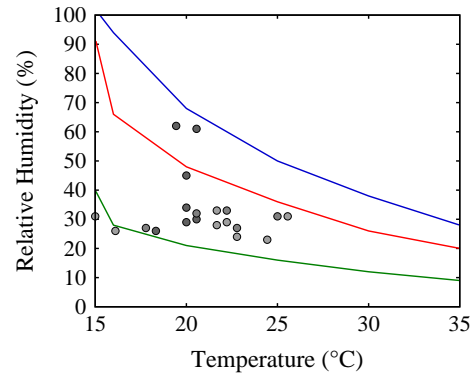


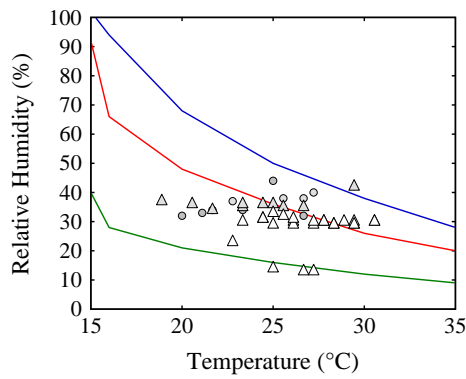
Figure B.5-5. RH probe readings at port B (15 PC grout layer)



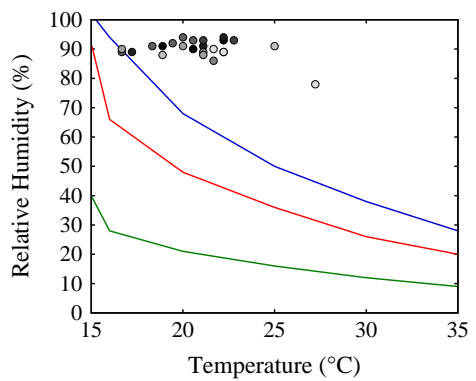
(a) Dried specimen (Months 1 – 2)



(b) Dried specimen (Months 3 – 4)



(c) Dried specimen (Months 5 – 6)



(d) Control specimen

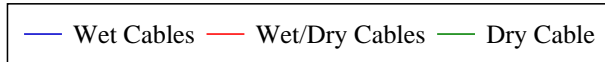
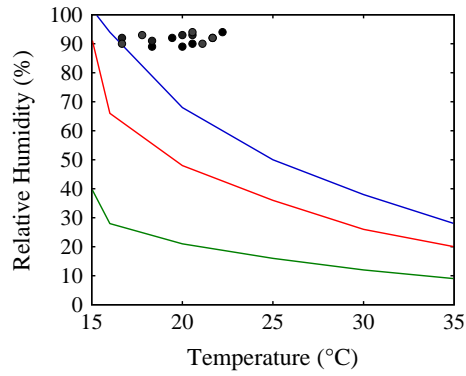
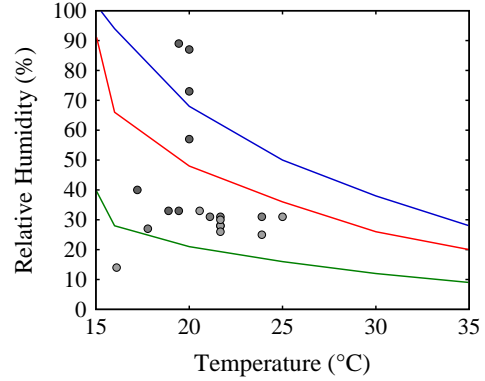


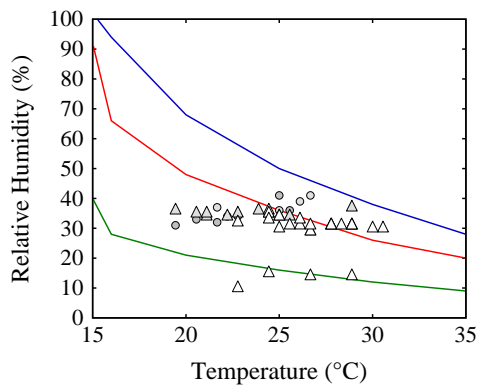
Figure B.5-6. RH probe readings at port C (5 PC grout layer)



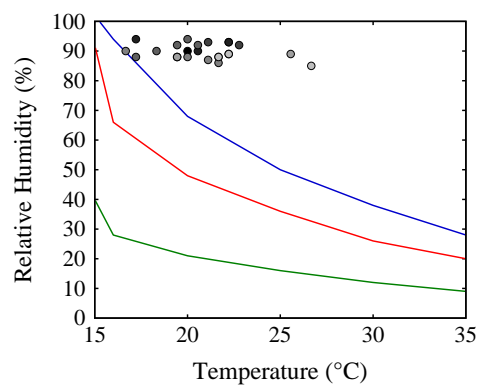
(a) Dried specimen (Months 1 – 2)



(b) Dried specimen (Months 3 – 4)



(c) Dried specimen (Months 5 – 6)



(d) Control specimen

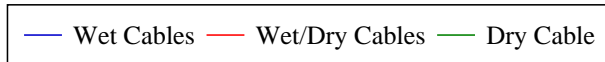
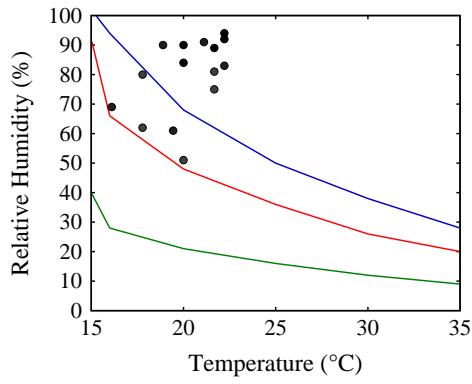
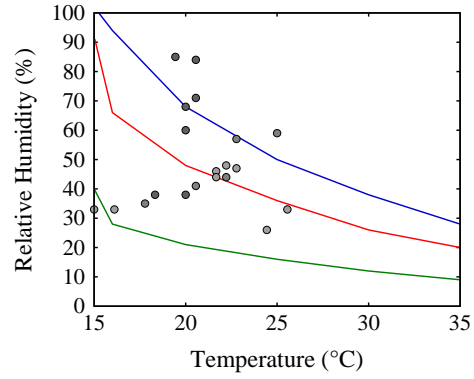


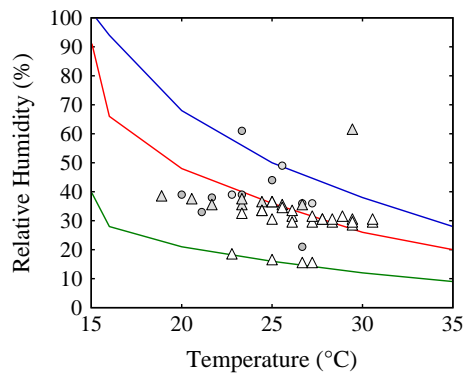
Figure B.5-7. RH probe readings at port D (5 PC grout layer)



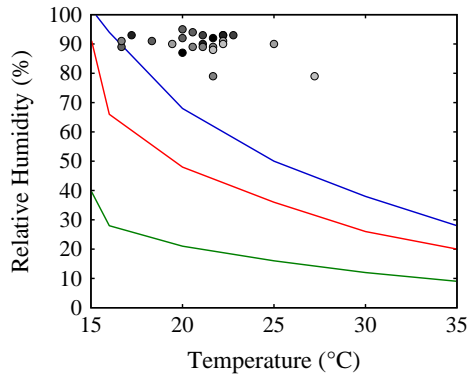
(a) Dried specimen (Months 1 – 2)



(b) Dried specimen (Months 3 – 4)



(c) Dried specimen (Months 5 – 6)



(d) Control specimen

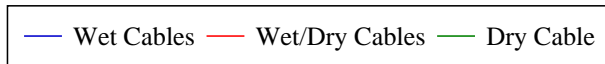


Figure B.5-8. RH probe readings at port E (15 PC grout layer)

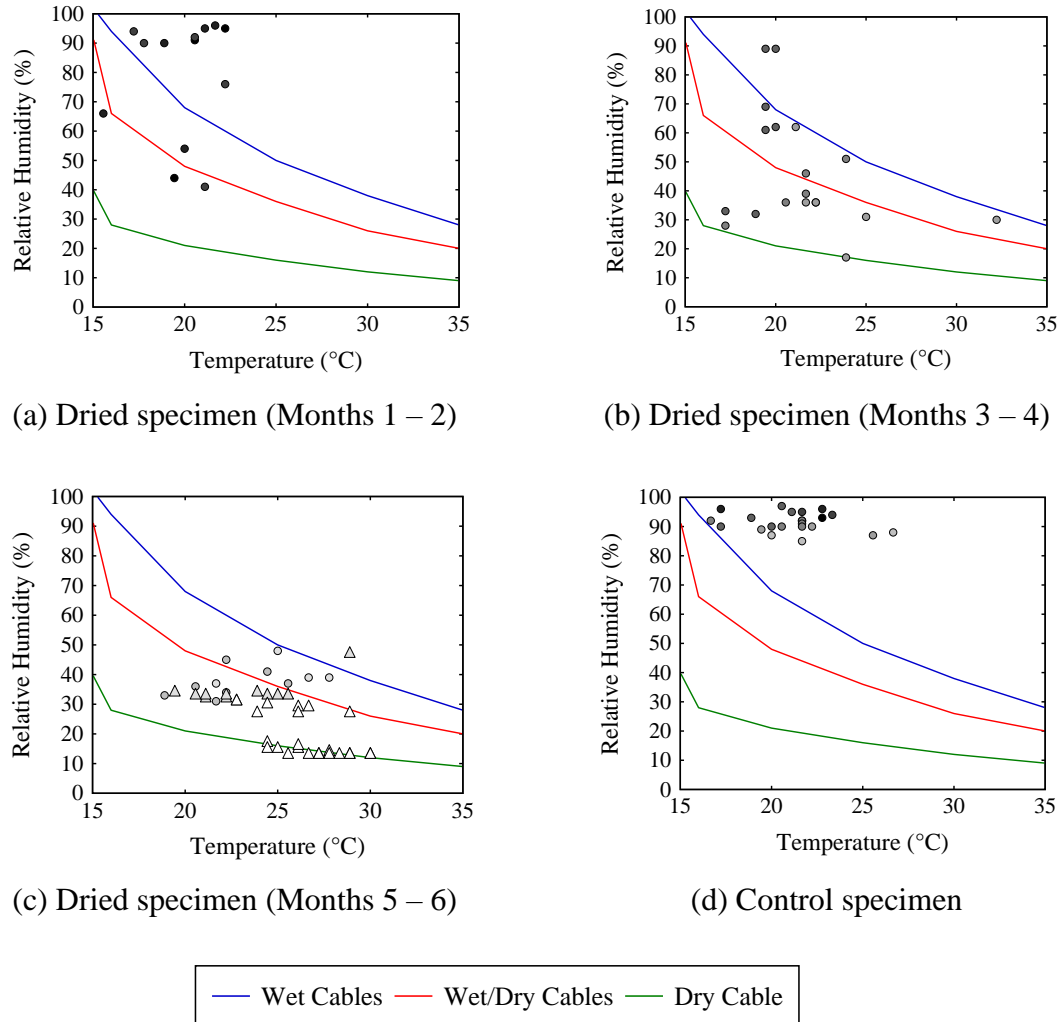


Figure B.5-9. RH probe readings at port F (15 PC grout layer)

Specimen TSG RH_g dryness evaluation:

Specimen TSG consisted of a soft grout layer trapped between two normal grout layers as explained in Chapter 6. Figure B.5-10 through Figure B.5-15 show RH_g readings for specimen TSG plotted on the CPE chart. RH_g readings for first two months were over the blue line in the rating chart, indicating wet conditions. During fifth and sixth drying month, RH_g readings decreased and were clustered around the wet (blue) line for ports A, B, E and F with normal grout and port C with layer of overlapped normal grout and soft grout. RH_g readings for port D with only soft grout were, however, predominantly present below red line.

On dissection after six months of drying, soft grout in dried specimen TSG had negligible moisture content. Therefore, CPE chart indicated that layer consisting of only soft grout in specimen TSG was dry when RH_g dropped below red line, i.e., moisture content of air in drilled ports was below 0.7%. Similar to dried specimen ISG, RH_g readings during fifth and sixth month of drying in port D of specimen TSG with only soft grout varied predominantly in between 15% to 40% RH. In the control specimen, on the other hand, RH_g readings in port D varied little

during the six months and typically were over blue line, which classified them wet. On the other hand, these readings for normal grout varied in a wider range of 30% to 70%.

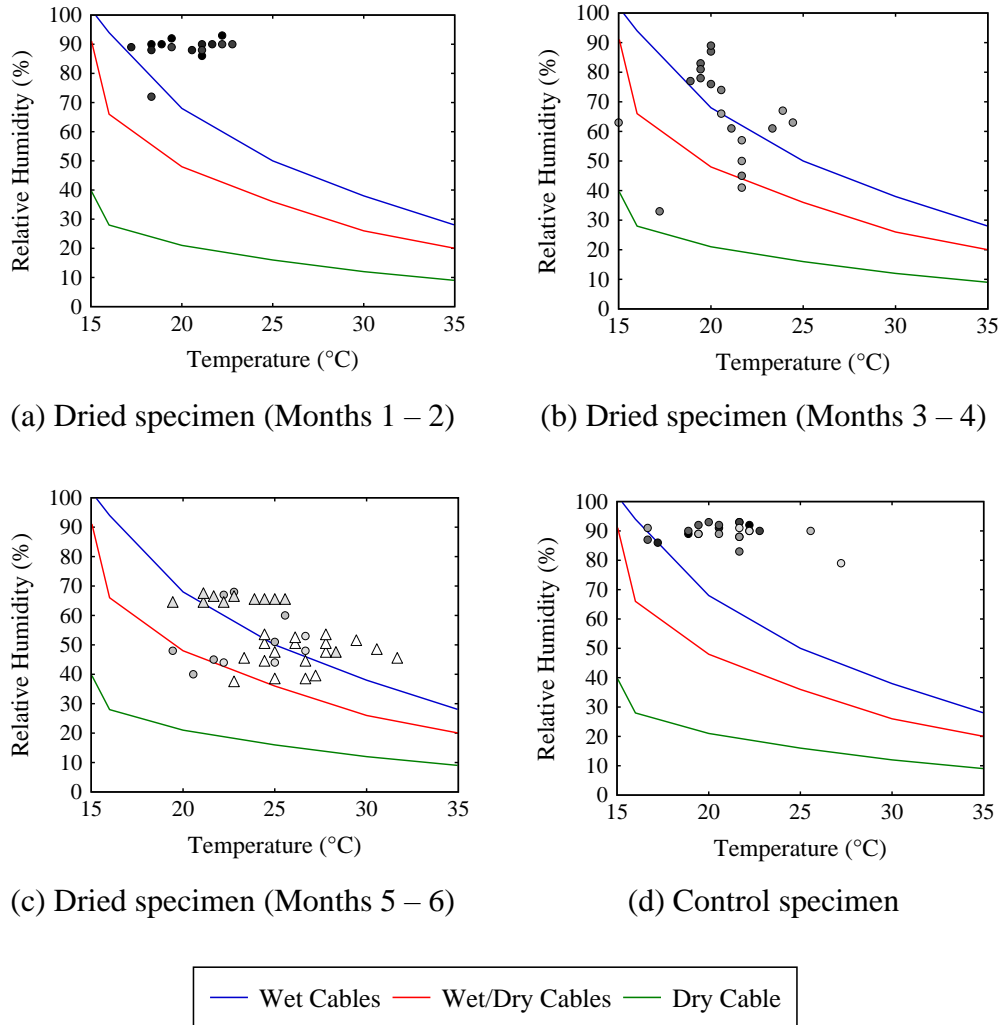
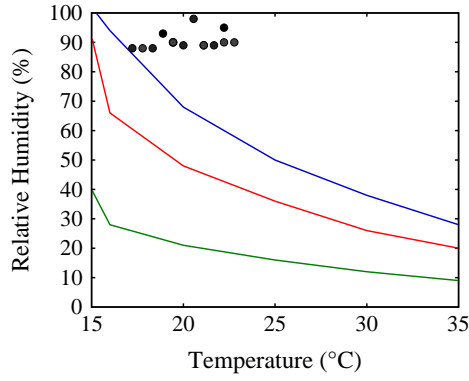
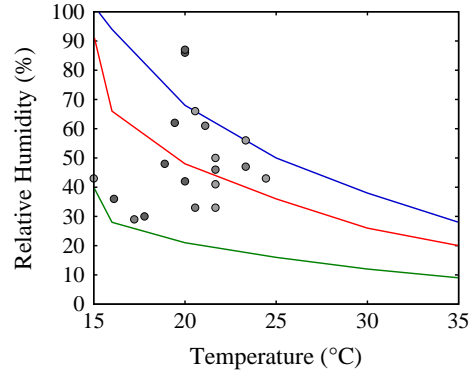


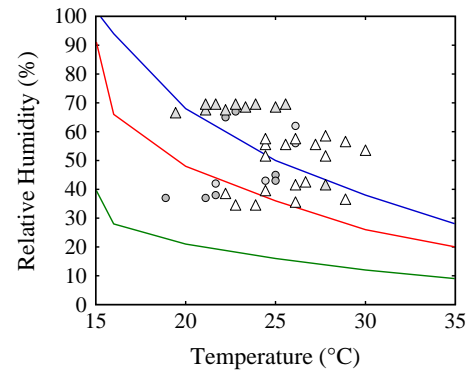
Figure B.5-10. RH probe readings at port A (100 PC grout layer)



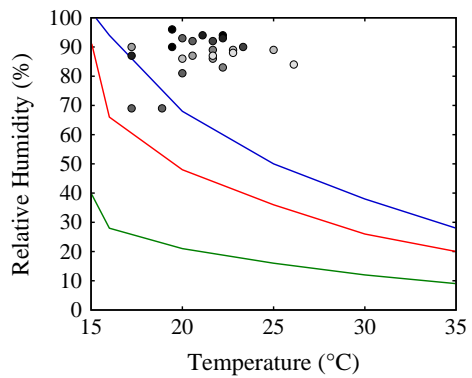
(a) Dried specimen (Months 1 – 2)



(b) Dried specimen (Months 3 – 4)



(c) Dried specimen (Months 5 – 6)



(d) Control specimen

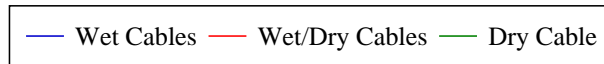
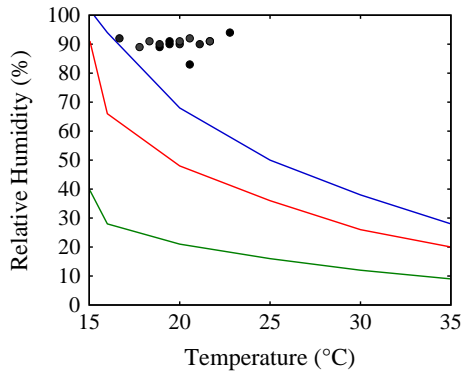
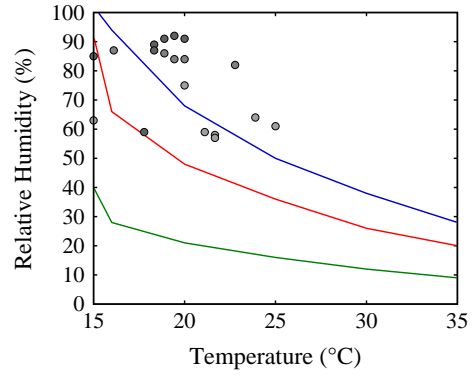


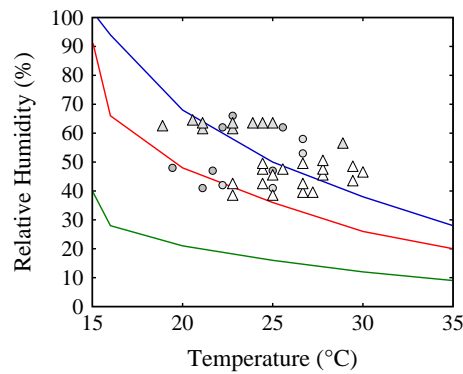
Figure B.5-11. RH probe readings at port B (100 PC grout layer)



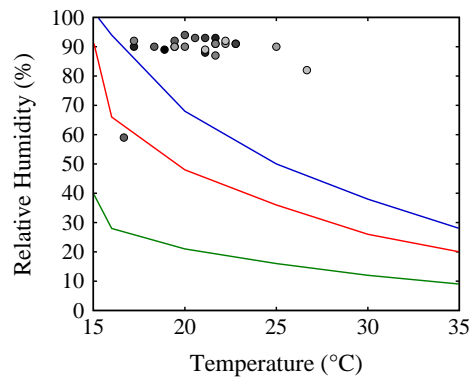
(a) Dried specimen (Months 1 – 2)



(b) Dried specimen (Months 3 – 4)



(c) Dried specimen (Months 5 – 6)



(d) Control specimen

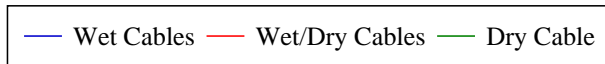
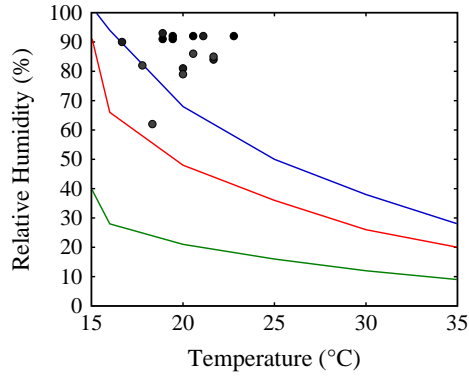
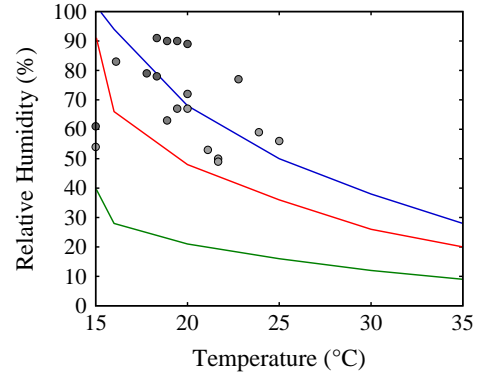


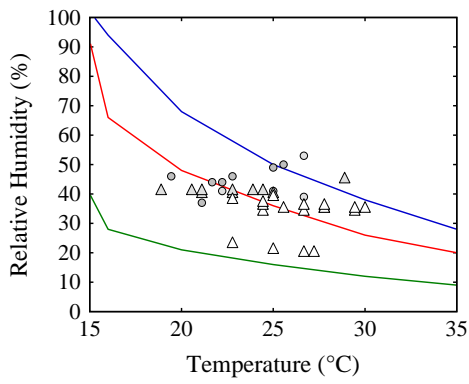
Figure B.5-12. RH probe readings at port C (5 PC and 100 PC overlap grout layer)



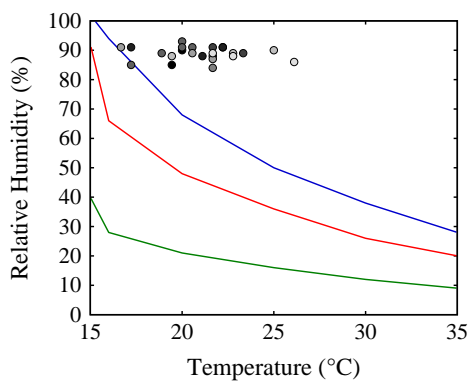
(a) Dried specimen (Months 1 – 2)



(b) Dried specimen (Months 3 – 4)



(c) Dried specimen (Months 5 – 6)



(d) Control specimen

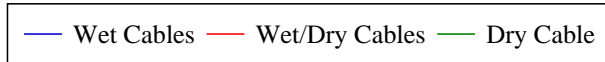
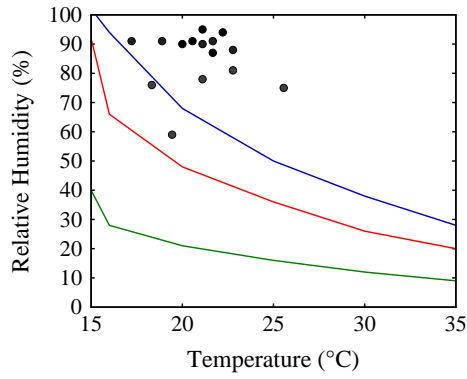
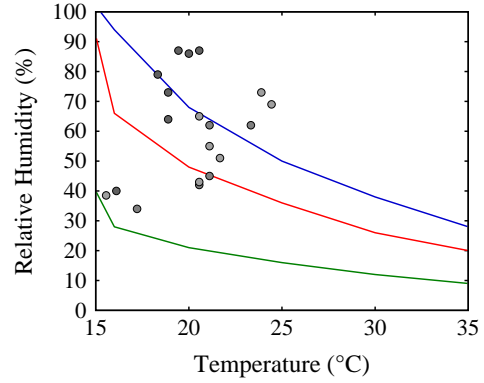


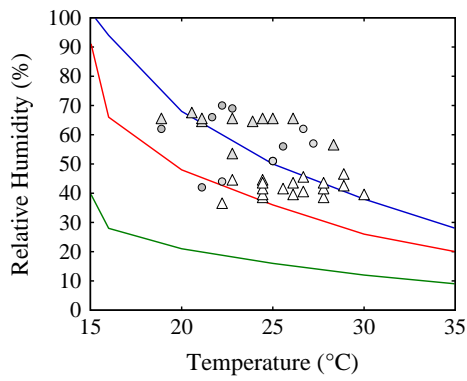
Figure B.5-13. RH probe readings at port D (5 PC grout layer)



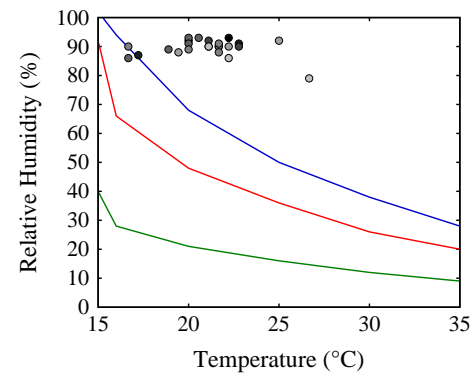
(a) Dried specimen (Months 1 – 2)



(b) Dried specimen (Months 3 – 4)



(c) Dried specimen (Months 5 – 6)



(d) Control specimen

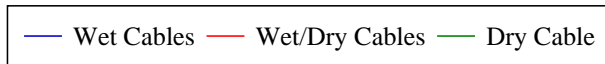


Figure B.5-14. RH probe readings at port E (100 PC grout layer)

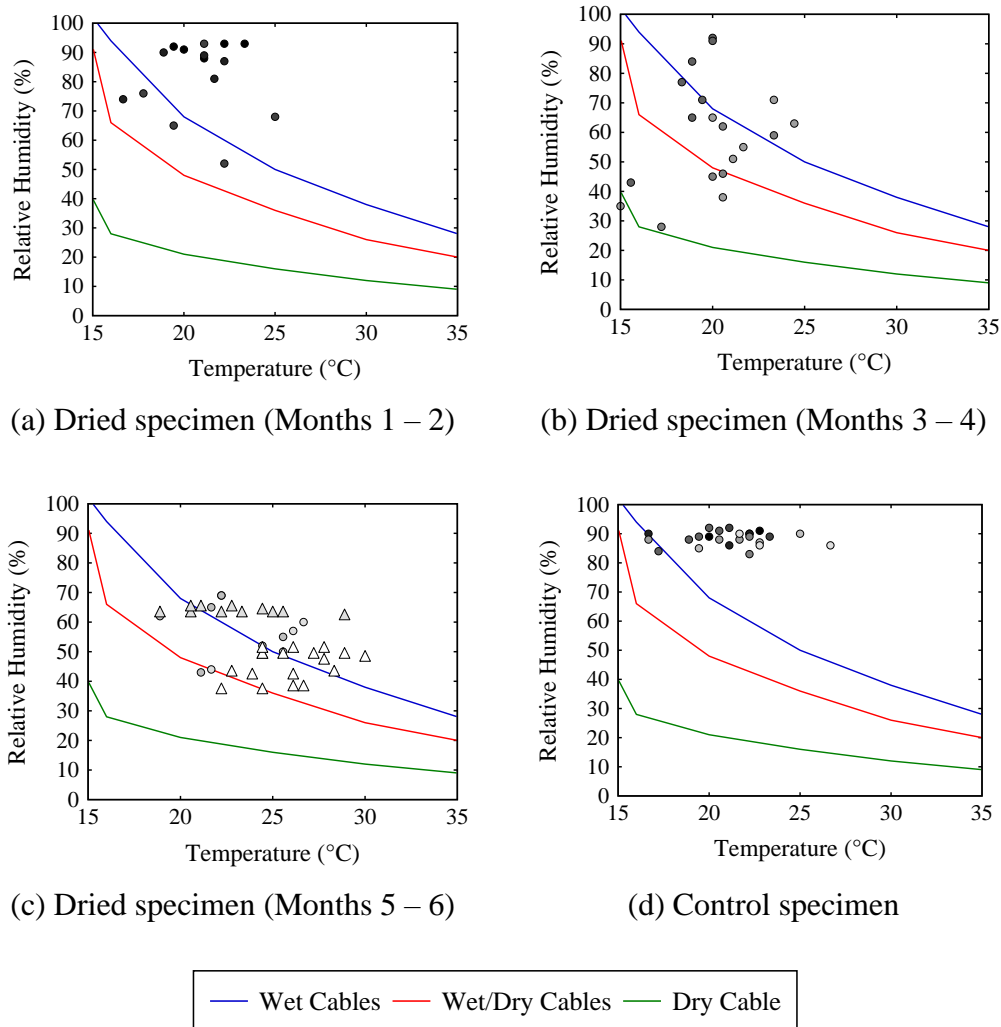


Figure B.5-15. RH probe readings at port F (100 PC grout layer)

B.6 Delta T analysis

Difference between dry bulb temperature and dew point temperature, ΔT , was analyzed. ΔT vs. time was plotted except for days when system was turned off, inlet RH was high and refrigerant dryer was not working. In ΔT analysis, ΔT increases when grout dries. Accordingly, for specimen ISG, Figure B.6-1 shows that 15 PC layers started drying before 5 PC layer (Holes C and D). ΔT started increasing after 20 days for 15 PC layers, and after 40 days for 5 PC layer. For time period between 70 and 110 days, ΔT was almost constant for holes A, C and D; after 110 days, ΔT for all layers had almost similar value. The variation of ΔT between 70 and 110 days was attributed to use of damaged probes. As soft grout was found dry on dissection after drying period, soft grout (5 and 15 PC) can be considered dry if ΔT is between 25°F and 30°F when inlet air RH is 5% (± 2). Rate of drying was found by dividing ΔT to days required to reach target ΔT (25°F to 30°F). Rate of increase in ΔT for different probe holes in specimen ISG was similar and is shown as follows:

- Hole A – 28.7°F / 69 days = 0.42°F/day
- Hole B – 32.5°F / 55 days = 0.59°F/day

- Hole C – 28.1°F / 69 days = 0.41°F/day
- Hole D – 30.19°F / 76 days = 0.4°F/day.
- Hole E – 26.4°F / 73 days = 0.36°F/day.
- Hole F – 28.5°F / 73 days = 0.39°F/day.

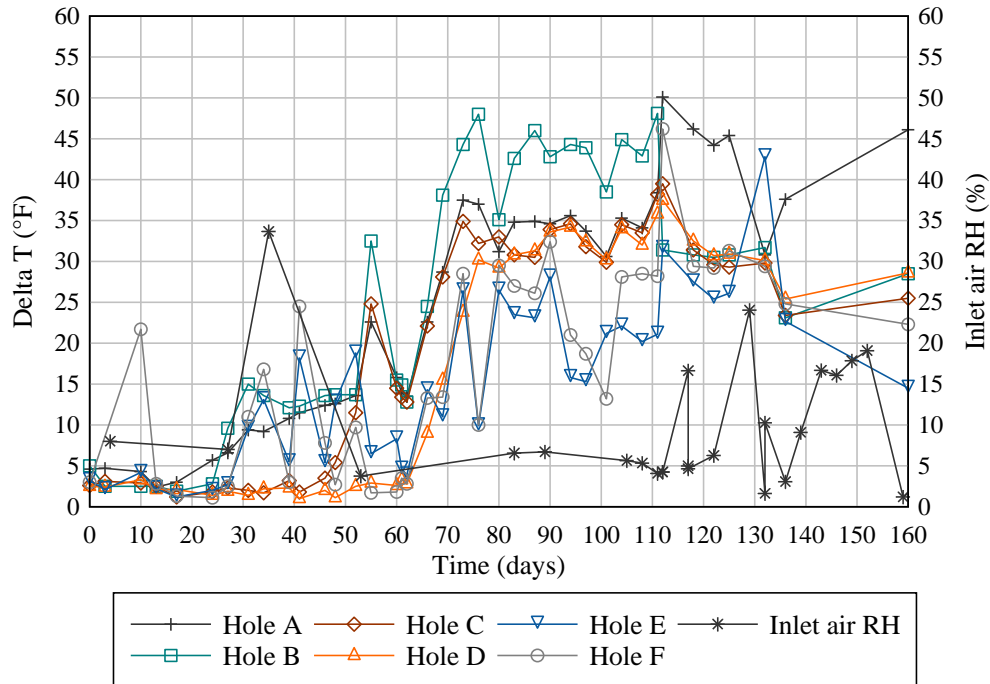


Figure B.6-1. Delta t vs. time for dried specimen ISG

In the case of dried specimen TSG, 5 PC and 100 PC layers started drying gradually after 40 days (Figure B.6-2). Similar to specimen ISG, variation of ΔT between 70 and 110 days was attributed to use of damaged probes. As soft grout was found dry on dissection after drying period, soft grout in specimen TSG can be considered dry if ΔT is between 15°F to 25°F when inlet RH is 5% (± 2). This range of ΔT for specimen TSG was less than range for specimen ISG due to presence of 100 PC near 5 PC, and 100 PC not completely losing moisture. Similar to specimen ISG, rate of increase in ΔT was calculated for specimen TSG. This rate for soft grout in specimen TSG was found lower than that for specimen ISG due to presence of 100 PC in specimen TSG. These rates are as follows:

- Hole A – 15.2°F / 118 days = 0.13°F/day
- Hole B – 25°F / 111 days = 0.22°F/day
- Hole C – 20.1°F / 122 days = 0.16°F/day
- Hole D – 17.1°F / 112 days = 0.15°F/day
- Hole E – 16.3°F / 111 days = 0.14°F/day
- Hole F – 26.1°F / 118 days = 0.22°F/day

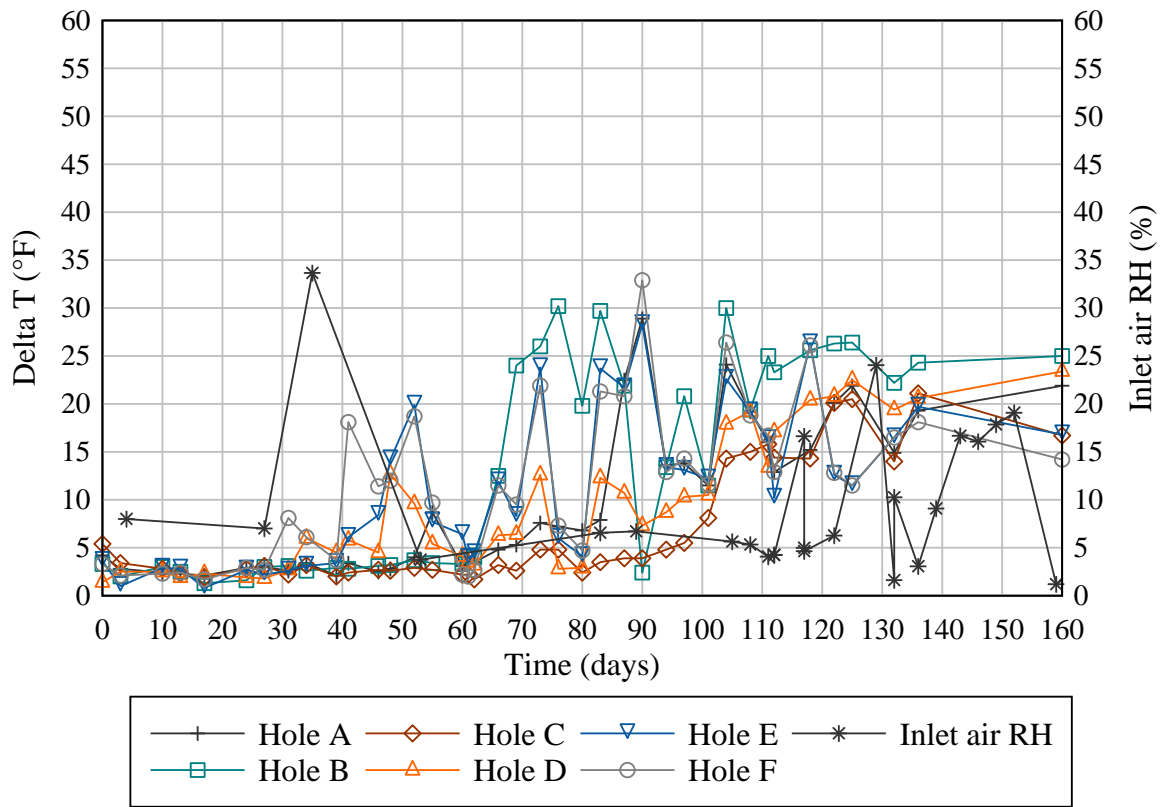


Figure B.6-2. Delta t vs. time for dried specimen TSG

APPENDIX C— Corrosion specimens

C.1 Schematic drawings of corrosion specimens

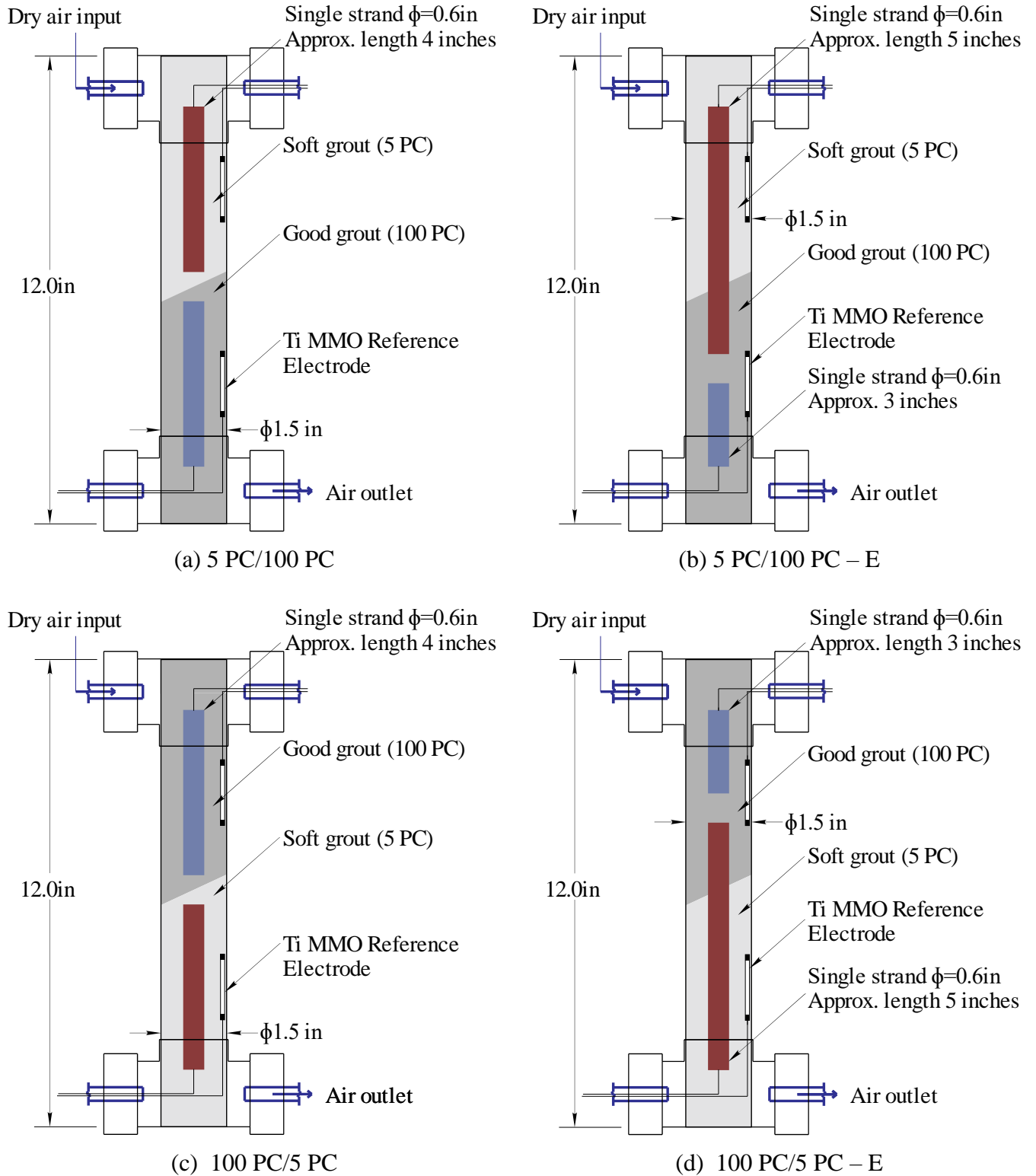
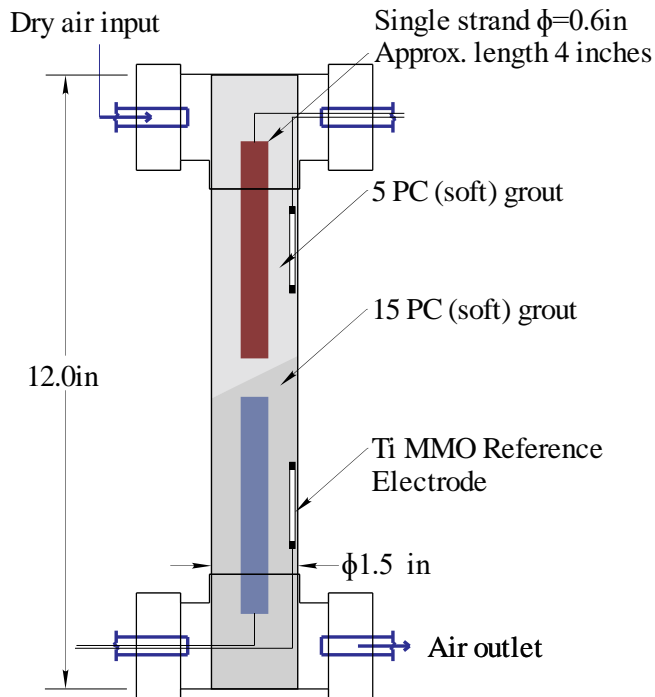
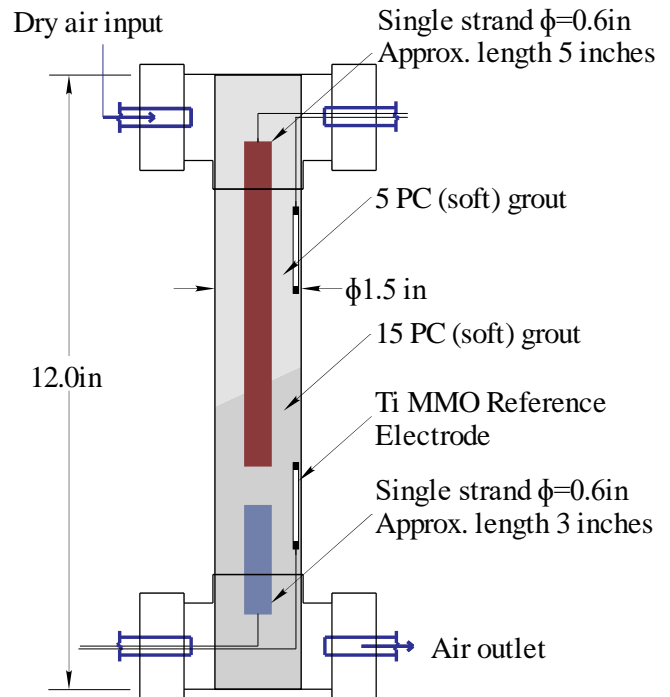


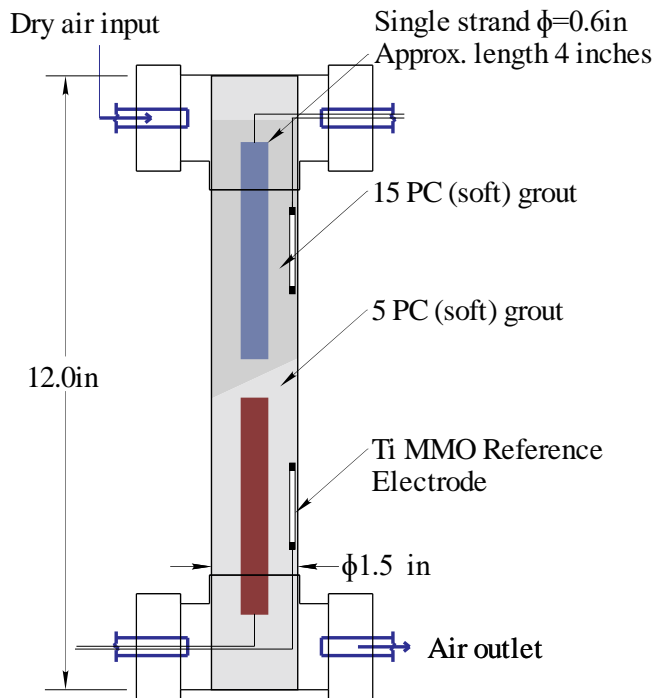
Figure C.1-1. Schematic drawings of corrosion specimens



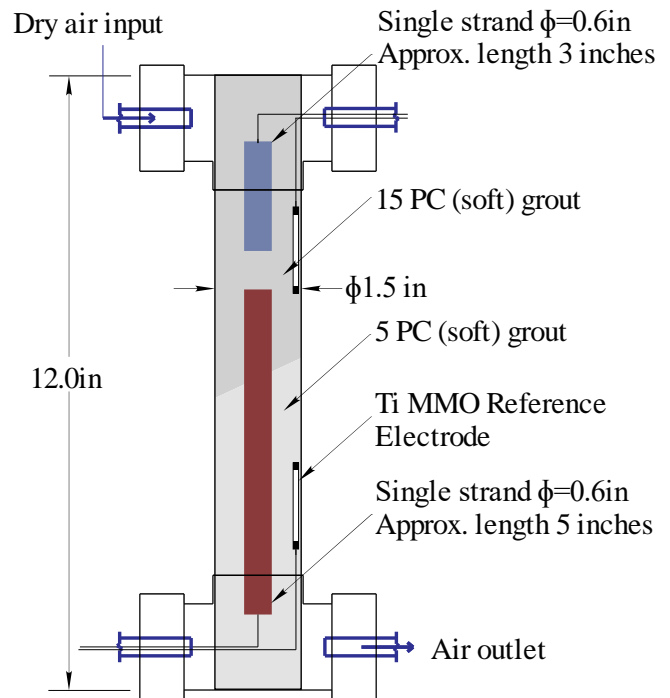
(e) 5 PC/15 PC



(f) 5 PC/15 PC – E



(g) 15 PC/5 PC



(h) 15 PC/5 PC – E

Figure C.1-1. Schematic drawings of corrosion specimens

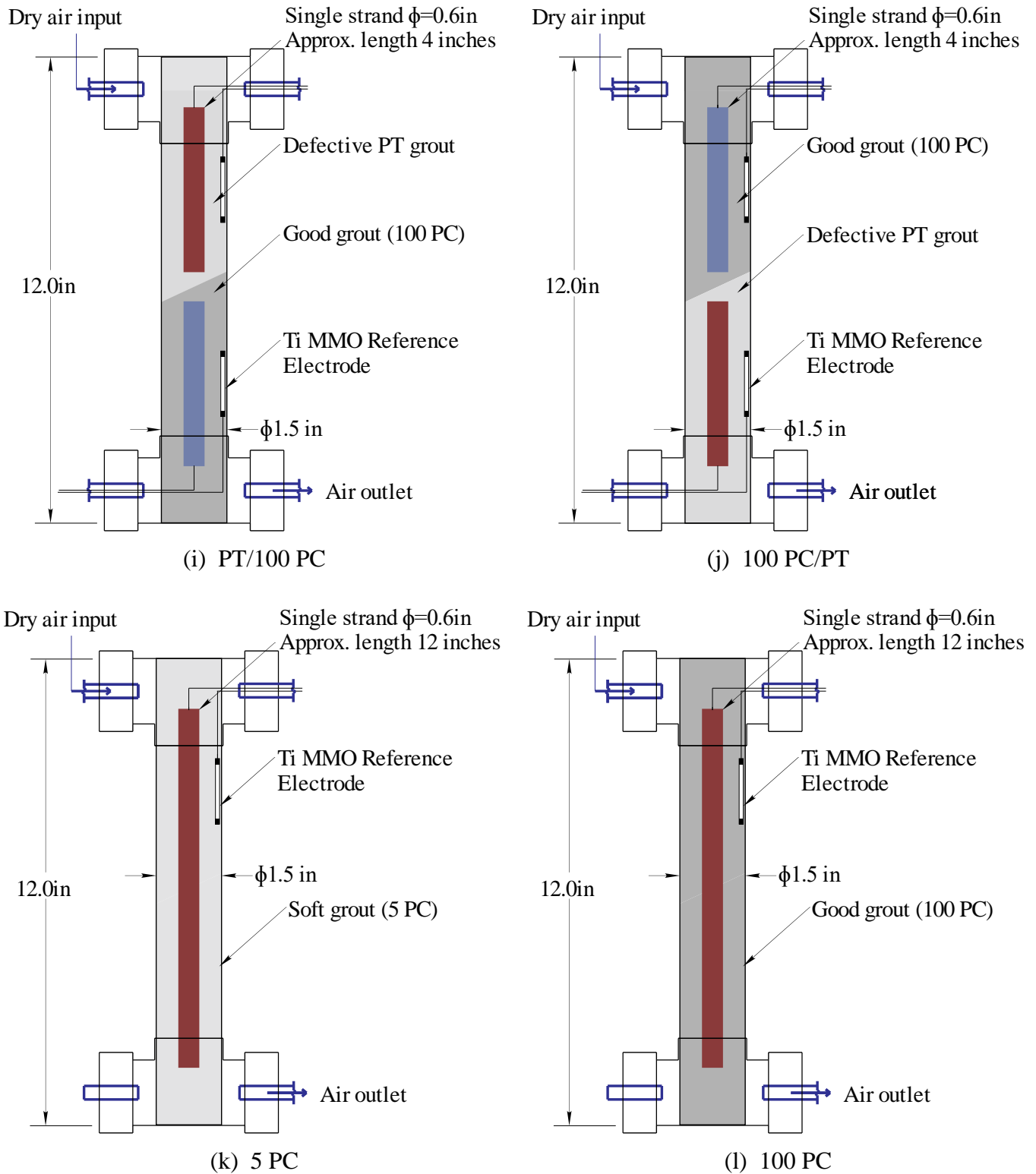


Figure C.1-1. Schematic drawings of corrosion specimens

C.2 Corrosion readings during drying

#	Specimen label	Corrosion potential readings	Resistance readings
1	5/100D1		
2	5/100D2		
3	5/100C1		

#	Specimen label	Corrosion potential readings	Resistance readings
4	5/100D1C		
5	5/100D2C		
6	5/100C1C		

#	Specimen label	Corrosion potential readings	Resistance readings
7	5/100D1E	<p>Corrosion potential (mV) vs Time (days) and Temperature (°C). Legend: Cathode corrosion potential (open circles), Anode corrosion potential (filled circles), Temperature (green squares).</p>	<p>Resistance (kΩ) vs Time (days). Legend: Between cathode and reference electrode (open circles), Between anode and reference electrode (filled circles), Between reference electrodes (green asterisks), Between cathode and anode (orange crosses).</p>
8	5/100D2E	<p>Corrosion potential (mV) vs Time (days) and Temperature (°C). Legend: Cathode corrosion potential (open circles), Anode corrosion potential (filled circles), Temperature (green squares).</p>	<p>Resistance (kΩ) vs Time (days). Legend: Between cathode and reference electrode (open circles), Between anode and reference electrode (filled circles), Between reference electrodes (green asterisks), Between cathode and anode (orange crosses).</p>
9	5/100C1E	<p>Corrosion potential (mV) vs Time (days) and Temperature (°C). Legend: Cathode corrosion potential (open circles), Anode corrosion potential (filled circles), Temperature (green squares).</p>	<p>Resistance (kΩ) vs Time (days). Legend: Between cathode and reference electrode (open circles), Between anode and reference electrode (filled circles), Between reference electrodes (green asterisks), Between cathode and anode (orange crosses).</p>

#	Specimen label	Corrosion potential readings	Resistance readings
10	5/100D1C E		
11	5/100D2C E		
12	5/100C1C E		

#	Specimen label	Corrosion potential readings	Resistance readings
13	100/5D1	<p>Corrosion potential (mV) vs Time (days) and Temperature (°C). Legend: Cathode corrosion potential (open circles), Anode corrosion potential (filled circles), Temperature (crosses).</p>	<p>Resistance (kΩ) vs Time (days). Legend: Between cathode and reference electrode (open circles), Between anode and reference electrode (filled circles), Between reference electrodes (crosses), Between cathode and anode (asterisks).</p>
14	100/5D2	<p>Corrosion potential (mV) vs Time (days) and Temperature (°C). Legend: Cathode corrosion potential (open circles), Anode corrosion potential (filled circles), Temperature (crosses).</p>	<p>Resistance (kΩ) vs Time (days). Legend: Between cathode and reference electrode (open circles), Between anode and reference electrode (filled circles), Between reference electrodes (crosses), Between cathode and anode (asterisks).</p>
15	100/5C1	<p>Corrosion potential (mV) vs Time (days) and Temperature (°C). Legend: Cathode corrosion potential (open circles), Anode corrosion potential (filled circles), Temperature (crosses).</p>	<p>Resistance (kΩ) vs Time (days). Legend: Between cathode and reference electrode (open circles), Between anode and reference electrode (filled circles), Between reference electrodes (crosses), Between cathode and anode (asterisks).</p>

#	Specimen label	Corrosion potential readings	Resistance readings
16	100/5D1C		
17	100/5D2C		
18	100/5C1C		

#	Specimen label	Corrosion potential readings	Resistance readings
19	100/5D1E		
20	100/5D2E		
21	100/5C1E		

#	Specimen label	Corrosion potential readings	Resistance readings
22	100/5D1C E		
23	100/5D2C E		
24	100/5C1C E		

#	Specimen label	Corrosion potential readings	Resistance readings
25	5/15D1		
26	5/15D2		
27	5/15C1		

#	Specimen label	Corrosion potential readings	Resistance readings
28	5/15D1C		
29	5/15D2C		
30	5/15C1C		

#	Specimen label	Corrosion potential readings	Resistance readings
31	5/15D1E		
32	5/15D2E		
33	5/15C1E		

#	Specimen label	Corrosion potential readings	Resistance readings
34	5/15D1CE		
35	5/15D2CE		
36	5/15C1CE		

#	Specimen label	Corrosion potential readings	Resistance readings
37	15/5D1		
38	15/5D2		
39	15/5C1		

#	Specimen label	Corrosion potential readings	Resistance readings
40	15/5D1C		
41	15/5D2C		
42	15/5C1C		

#	Specimen label	Corrosion potential readings	Resistance readings
43	15/5D1E	<p>Corrosion potential (mV) vs Time (days) and Temperature (°C). Legend: Cathode corrosion potential (open circles), Anode corrosion potential (filled circles), Temperature (filled squares).</p>	<p>Resistance (kΩ) vs Time (days). Legend: Between cathode and reference electrode (open circles), Between anode and reference electrode (filled circles), Between reference electrodes (asterisks), Between cathode and anode (crosses).</p>
44	15/5D2E	<p>Corrosion potential (mV) vs Time (days) and Temperature (°C). Legend: Cathode corrosion potential (open circles), Anode corrosion potential (filled circles), Temperature (filled squares).</p>	<p>Resistance (kΩ) vs Time (days). Legend: Between cathode and reference electrode (open circles), Between anode and reference electrode (filled circles), Between reference electrodes (asterisks), Between cathode and anode (crosses).</p>
45	15/5C1E	<p>Corrosion potential (mV) vs Time (days) and Temperature (°C). Legend: Cathode corrosion potential (open circles), Anode corrosion potential (filled circles), Temperature (filled squares).</p>	<p>Resistance (kΩ) vs Time (days). Legend: Between cathode and reference electrode (open circles), Between anode and reference electrode (filled circles), Between reference electrodes (asterisks), Between cathode and anode (crosses).</p>

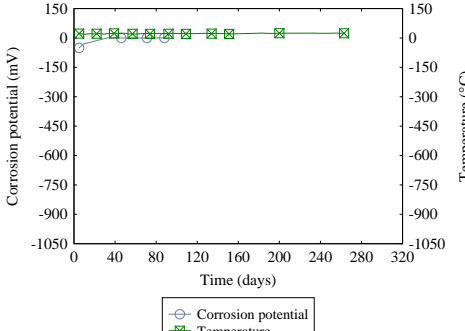
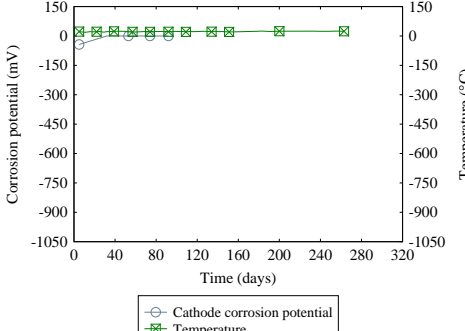
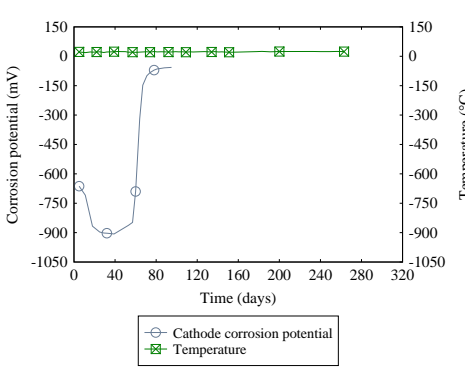
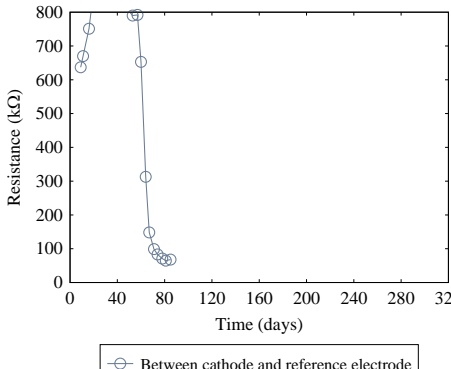
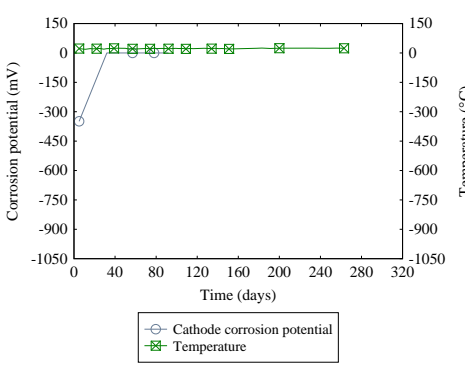
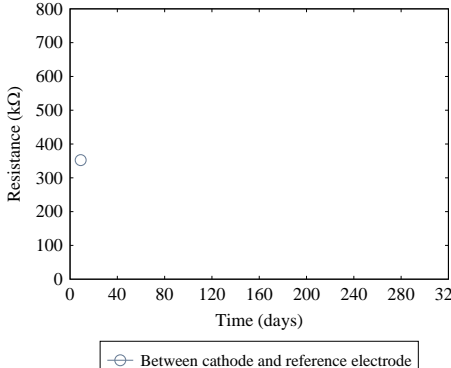
#	Specimen label	Corrosion potential readings	Resistance readings
46	15/5D1CE		
47	15/5D2CE		
48	15/5C1CE		

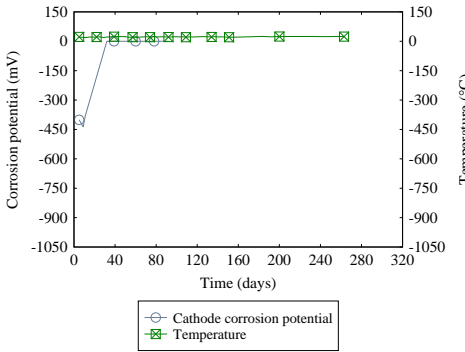
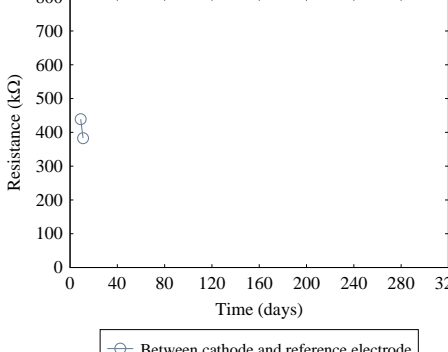
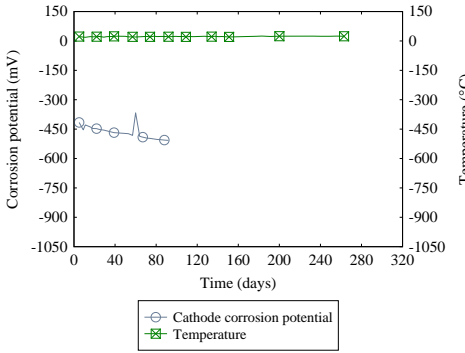
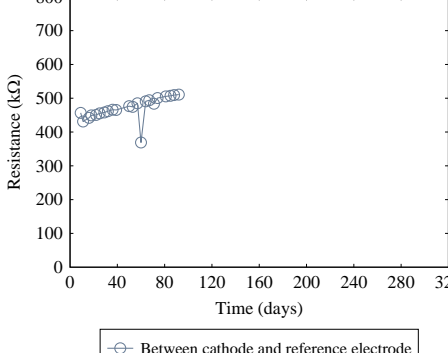
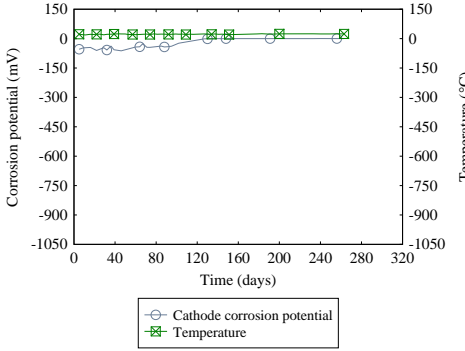
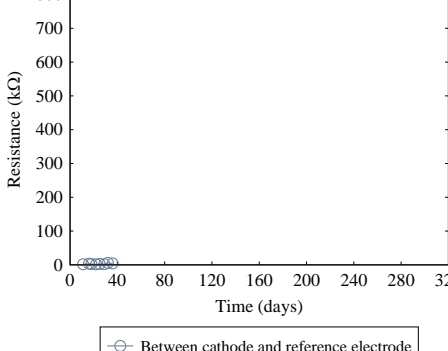
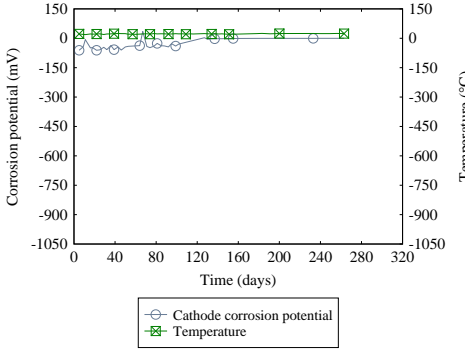
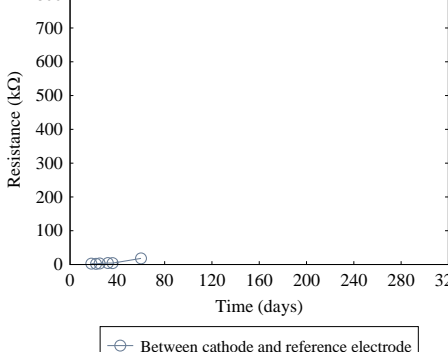
#	Specimen label	Corrosion potential readings	Resistance readings
49	PT/100D1		
50	PT/100D2		
51	PT/100C1		

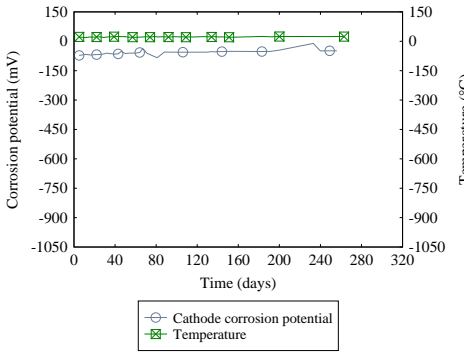
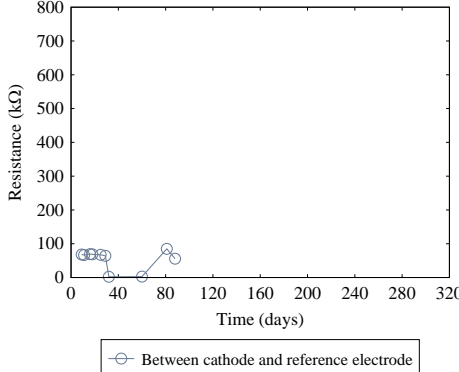
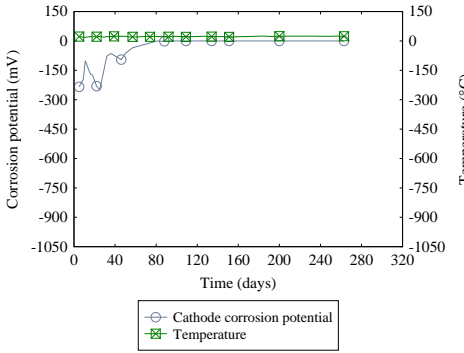
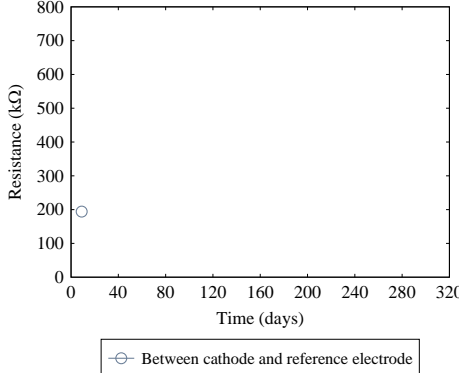
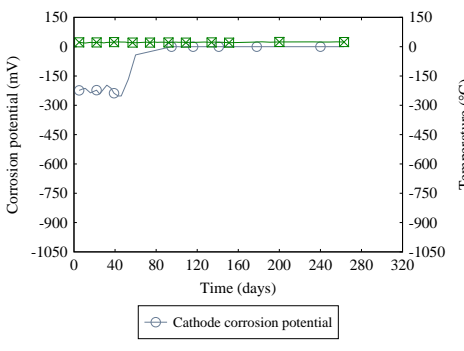
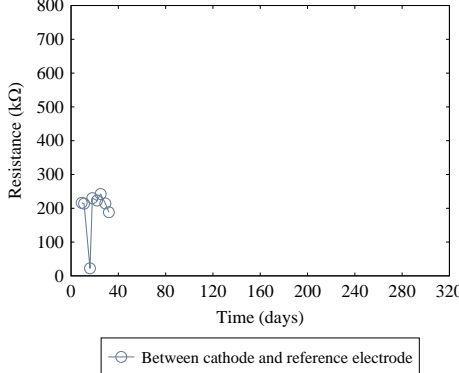
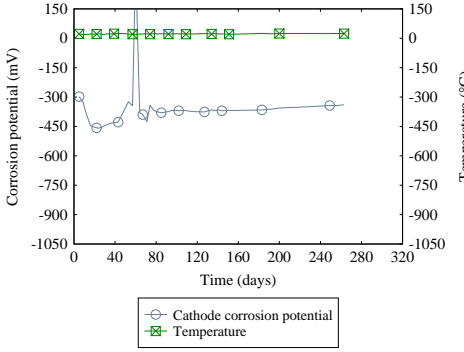
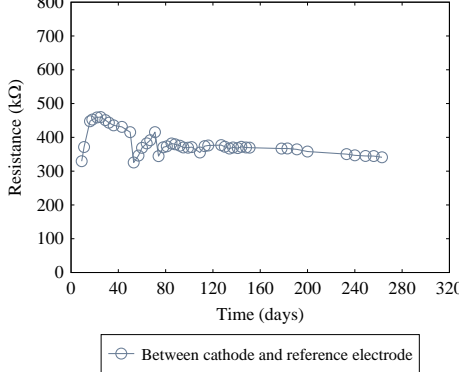
#	Specimen label	Corrosion potential readings	Resistance readings
52	PT/100D1 C		
53	PT/100D2 C		
54	PT/100C1 C		

#	Specimen label	Corrosion potential readings	Resistance readings
55	100/PTD1		
56	100/PTD2		
57	100/PTC1		

#	Specimen label	Corrosion potential readings	Resistance readings
58	100/PTD1 C		
59	100/PTD2 C		
60	100/PTC1 C		

#	Specimen label	Corrosion potential readings	Resistance readings
61	5D1	 <p>Corrosion potential (mV) vs Time (days) and Temperature (°C). The corrosion potential (blue circles) remains relatively constant around -100 mV. The temperature (green squares) remains constant at approximately 0°C.</p>	
62	5D2	 <p>Cathode corrosion potential (mV) vs Time (days) and Temperature (°C). The cathode corrosion potential (blue circles) remains relatively constant around -100 mV. The temperature (green squares) remains constant at approximately 0°C.</p>	
63	5C1	 <p>Cathode corrosion potential (mV) vs Time (days) and Temperature (°C). The cathode corrosion potential (blue circles) shows significant fluctuations, starting around -600 mV, dipping to -900 mV at 40 days, and then rising to -100 mV by 80 days. The temperature (green squares) remains constant at approximately 0°C.</p>	 <p>Resistance (kΩ) vs Time (days). The resistance (blue circles) starts at approximately 750 kΩ and drops sharply to about 50 kΩ by 80 days.</p>
64	5D1C	 <p>Cathode corrosion potential (mV) vs Time (days) and Temperature (°C). The cathode corrosion potential (blue circles) starts at approximately -400 mV and rises to 0 mV by 40 days, remaining stable thereafter. The temperature (green squares) remains constant at approximately 0°C.</p>	 <p>Resistance (kΩ) vs Time (days). The resistance (blue circles) starts at approximately 350 kΩ and remains stable.</p>

#	Specimen label	Corrosion potential readings	Resistance readings
65	5D2C	 <p>Corrosion potential (mV) vs Time (days) and Temperature (°C). The graph shows Cathode corrosion potential (blue circles) starting at -450 mV at day 0 and stabilizing at 0 mV by day 40. Temperature (green squares) remains constant at 0°C.</p>	 <p>Resistance (kΩ) vs Time (days). The graph shows resistance (blue circles) starting at 400 kΩ at day 0 and remaining constant at 400 kΩ throughout the 320-day period.</p>
66	5C1C	 <p>Corrosion potential (mV) vs Time (days) and Temperature (°C). The graph shows Cathode corrosion potential (blue circles) starting at -450 mV at day 0 and stabilizing at -500 mV by day 80. Temperature (green squares) remains constant at 0°C.</p>	 <p>Resistance (kΩ) vs Time (days). The graph shows resistance (blue circles) starting at 450 kΩ at day 0 and stabilizing at 500 kΩ by day 80.</p>
67	100D1	 <p>Corrosion potential (mV) vs Time (days) and Temperature (°C). The graph shows Cathode corrosion potential (blue circles) starting at -100 mV at day 0 and stabilizing at 0 mV by day 40. Temperature (green squares) remains constant at 0°C.</p>	 <p>Resistance (kΩ) vs Time (days). The graph shows resistance (blue circles) starting at 0 kΩ at day 0 and remaining constant at 0 kΩ throughout the 320-day period.</p>
68	100D2	 <p>Corrosion potential (mV) vs Time (days) and Temperature (°C). The graph shows Cathode corrosion potential (blue circles) starting at -100 mV at day 0 and stabilizing at 0 mV by day 40. Temperature (green squares) remains constant at 0°C.</p>	 <p>Resistance (kΩ) vs Time (days). The graph shows resistance (blue circles) starting at 0 kΩ at day 0 and remaining constant at 0 kΩ throughout the 320-day period.</p>

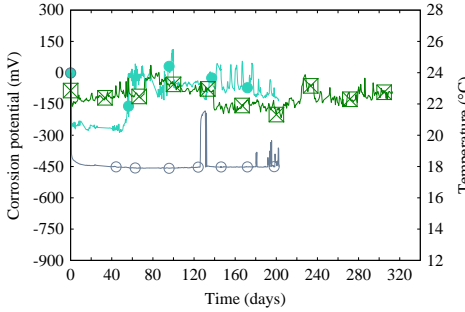
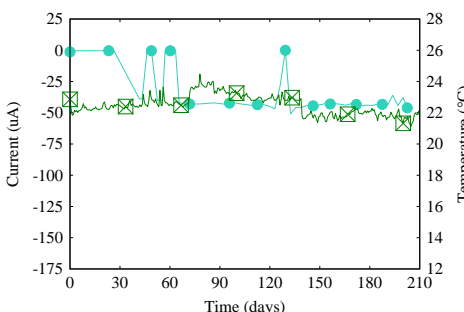
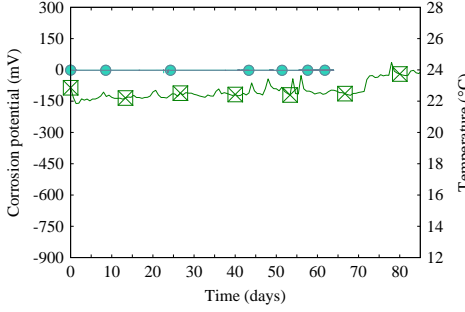
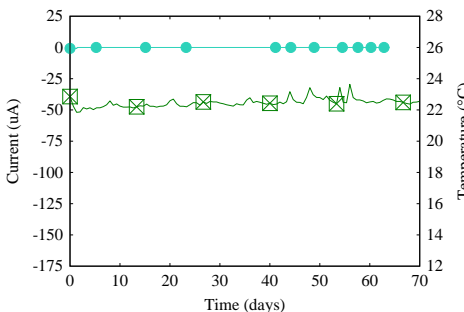
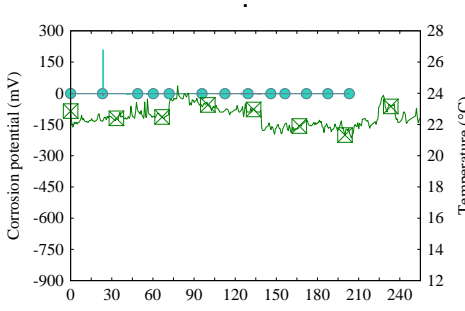
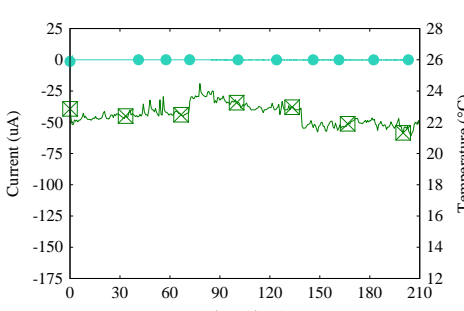
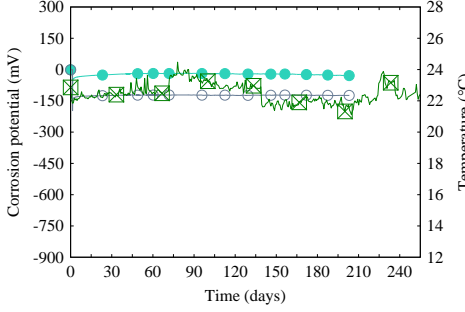
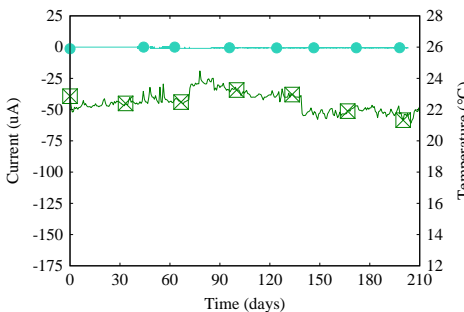
#	Specimen label	Corrosion potential readings	Resistance readings
69	100C1	 <p>Corrosion potential (mV) vs Time (days) and Temperature (°C). The graph shows Cathode corrosion potential (blue circles) and Temperature (green squares) over 320 days. Cathode corrosion potential remains relatively stable around -100 mV, while temperature stays near 0°C.</p>	 <p>Resistance (kΩ) vs Time (days). The graph shows resistance between the cathode and reference electrode (blue circles) over 320 days. Resistance values are low, fluctuating between approximately 50 and 100 kΩ.</p>
70	100D1C	 <p>Corrosion potential (mV) vs Time (days) and Temperature (°C). The graph shows Cathode corrosion potential (blue circles) and Temperature (green squares) over 320 days. Cathode corrosion potential starts at -150 mV and stabilizes at 0 mV after 40 days. Temperature remains near 0°C.</p>	 <p>Resistance (kΩ) vs Time (days). The graph shows resistance between the cathode and reference electrode (blue circles) over 320 days. Resistance is very low, around 200 kΩ.</p>
71	100D2C	 <p>Corrosion potential (mV) vs Time (days). The graph shows Cathode corrosion potential (blue circles) over 320 days. Cathode corrosion potential starts at -200 mV and stabilizes at 0 mV after 40 days.</p>	 <p>Resistance (kΩ) vs Time (days). The graph shows resistance between the cathode and reference electrode (blue circles) over 320 days. Resistance is low, around 200 kΩ.</p>
72	100C1C	 <p>Corrosion potential (mV) vs Time (days) and Temperature (°C). The graph shows Cathode corrosion potential (blue circles) and Temperature (green squares) over 320 days. Cathode corrosion potential starts at -300 mV and stabilizes at -450 mV after 40 days. Temperature remains near 0°C.</p>	 <p>Resistance (kΩ) vs Time (days). The graph shows resistance between the cathode and reference electrode (blue circles) over 320 days. Resistance is high, around 400-500 kΩ.</p>

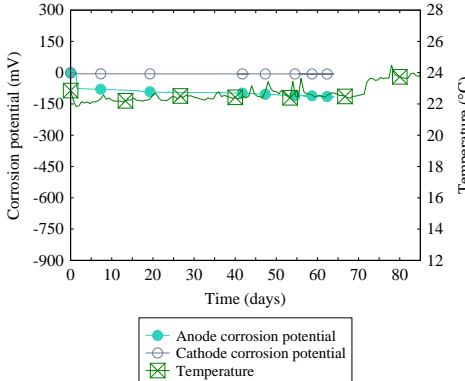
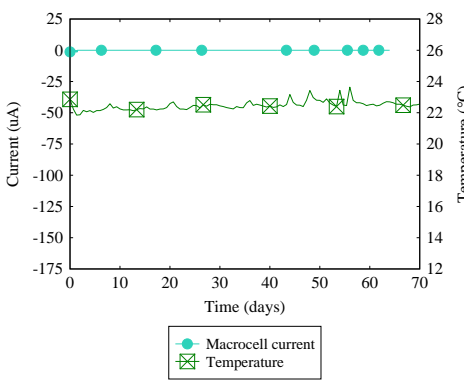
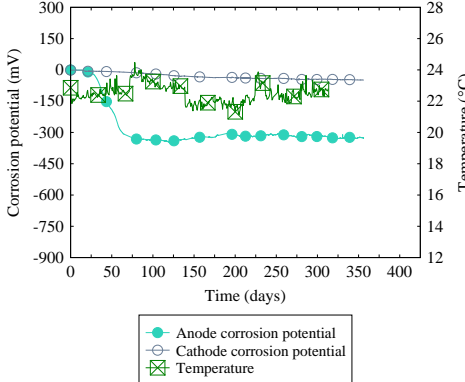
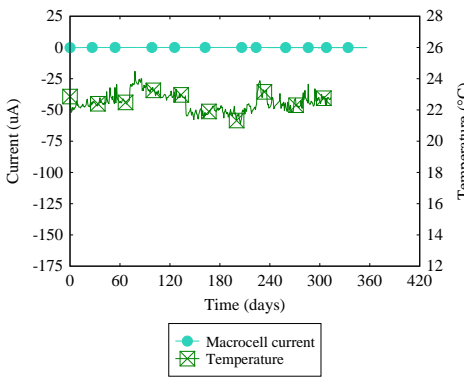
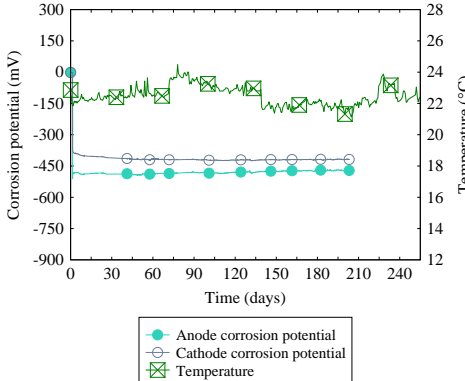
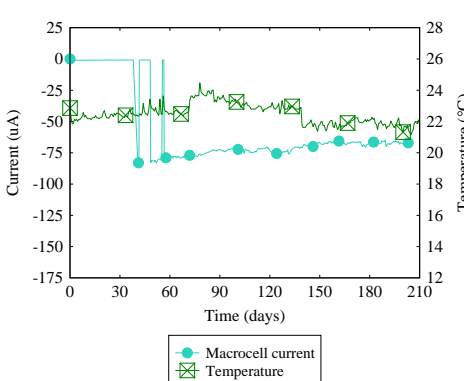
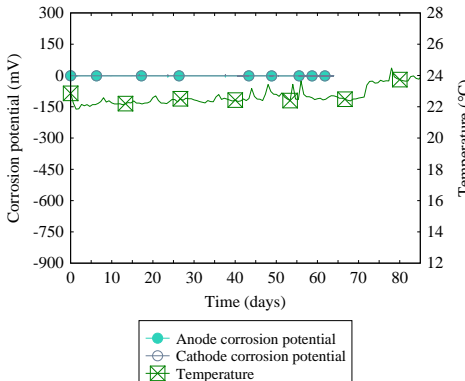
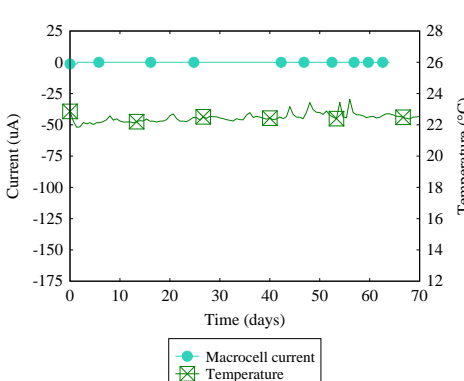
C.3 Corrosion readings after drying

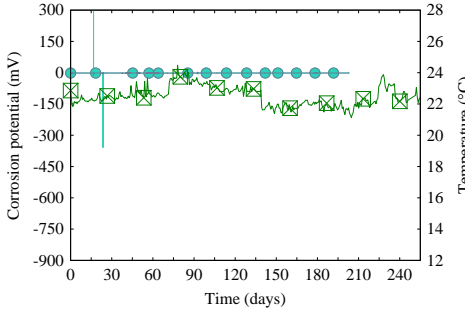
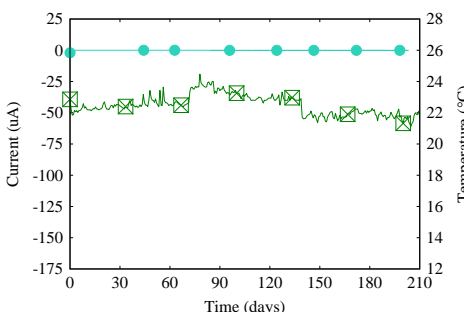
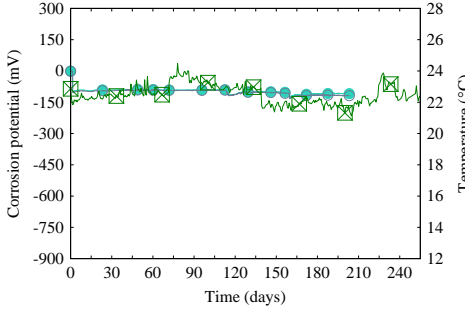
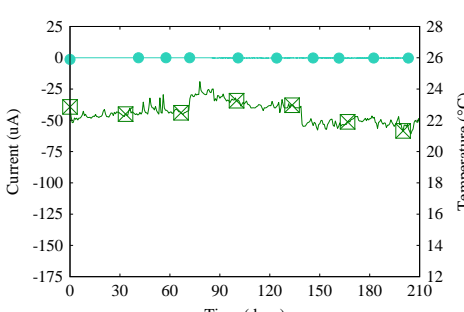
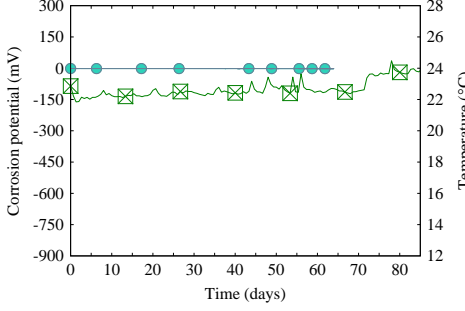
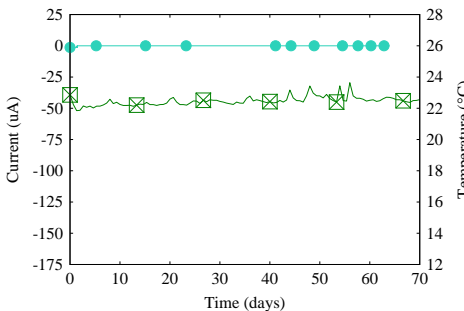
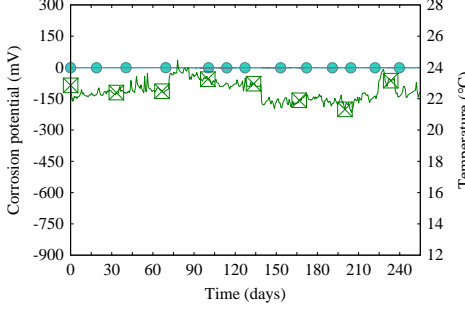
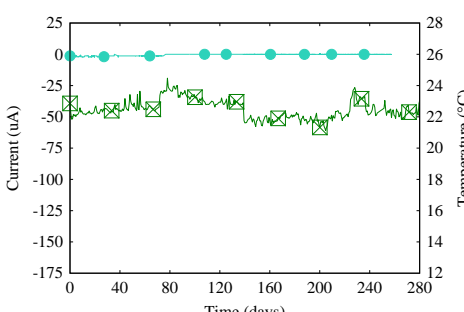
#	Specimen name	Corrosion potential readings	Macrocell current readings
1	5/100D1		
2	5/100D2		
3	5/100C1		

#	Specimen name	Corrosion potential readings	Macrocell current readings
4	5/100D1C		
5	5/100D2C		
6	5/100C1C		
7	5/100D1E		

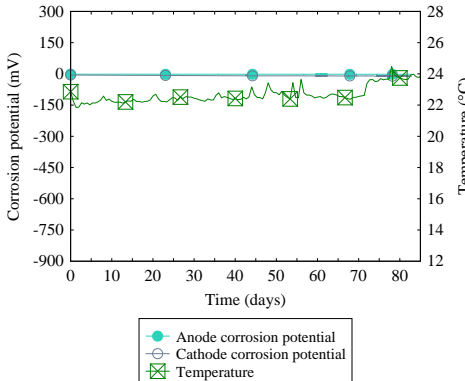
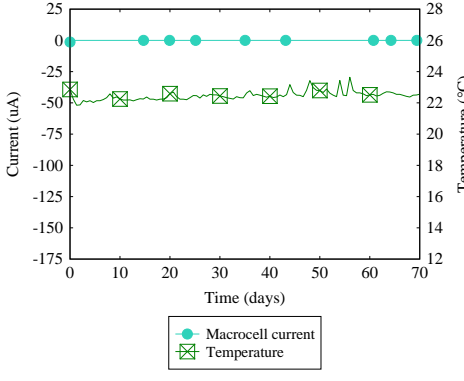
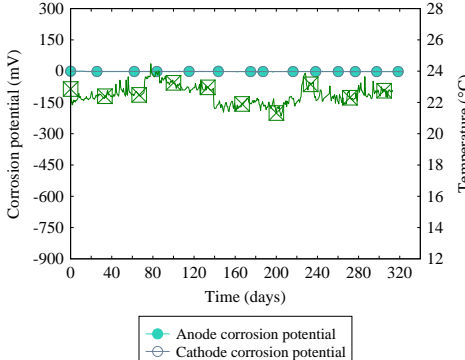
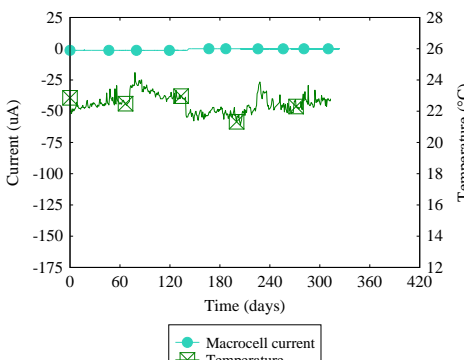
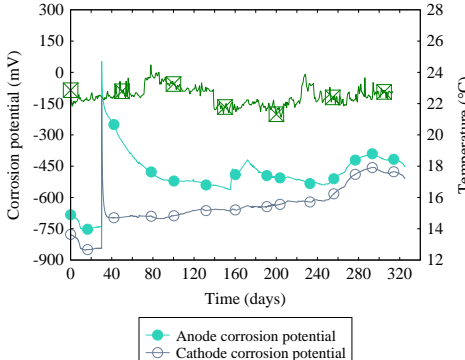
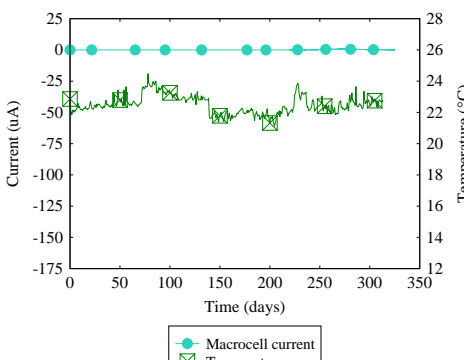
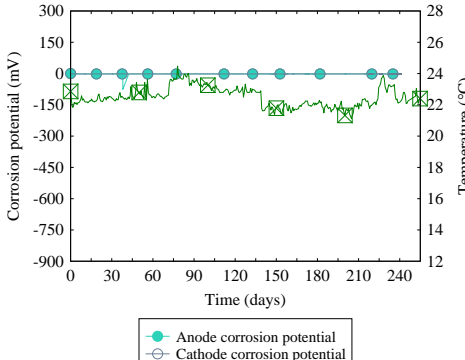
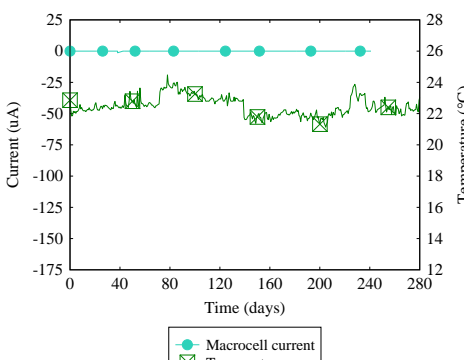
#	Specimen name	Corrosion potential readings	Macrocell current readings
8	5/100D2E	<p>Corrosion potential (mV) vs Time (days) and Temperature (°C). Legend: Anode corrosion potential (red circles), Cathode corrosion potential (blue squares), Temperature (green crosses).</p>	<p>Current (uA) vs Time (days) and Temperature (°C). Legend: Macrocell current (red circles), Temperature (green crosses).</p>
9	5/100C1E	<p>Corrosion potential (mV) vs Time (days) and Temperature (°C). Legend: Anode corrosion potential (red circles), Cathode corrosion potential (blue squares), Temperature (green crosses).</p>	<p>Current (uA) vs Time (days) and Temperature (°C). Legend: Macrocell current (red circles), Temperature (green crosses).</p>
10	5/100D1C E	<p>Corrosion potential (mV) vs Time (days) and Temperature (°C). Legend: Anode corrosion potential (red circles), Cathode corrosion potential (blue squares), Temperature (green crosses).</p>	<p>Current (uA) vs Time (days) and Temperature (°C). Legend: Macrocell current (red circles), Temperature (green crosses).</p>
11	5/100D2C E	<p>Corrosion potential (mV) vs Time (days) and Temperature (°C). Legend: Anode corrosion potential (red circles), Cathode corrosion potential (blue squares), Temperature (green crosses).</p>	<p>Current (uA) vs Time (days) and Temperature (°C). Legend: Macrocell current (red circles), Temperature (green crosses).</p>

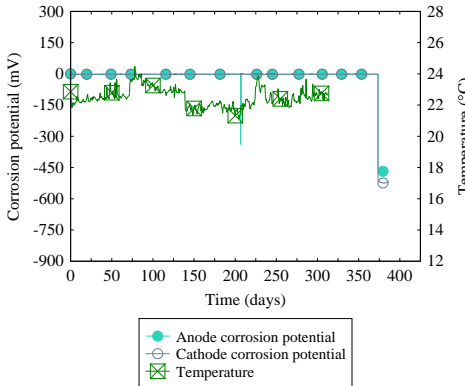
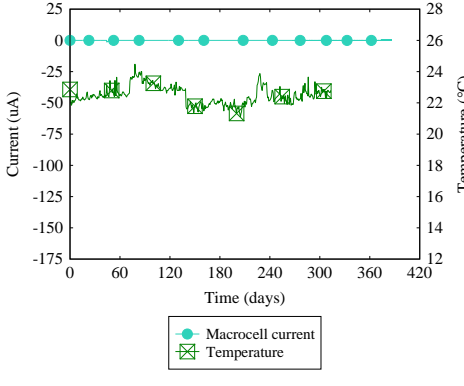
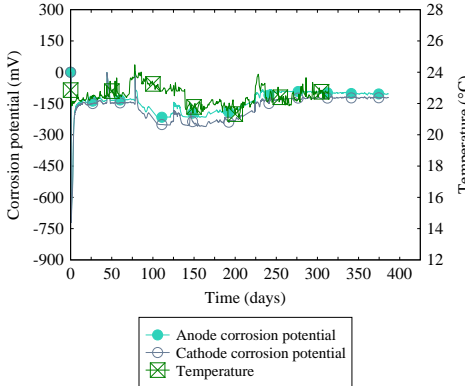
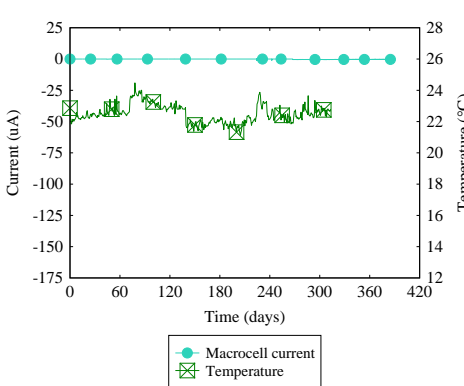
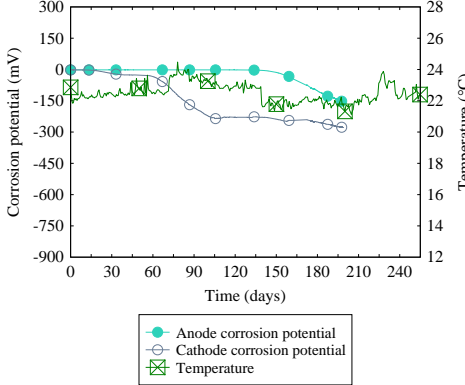
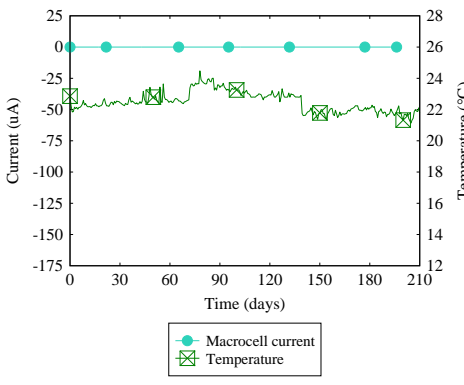
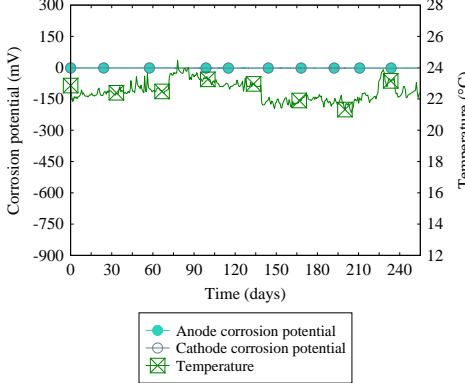
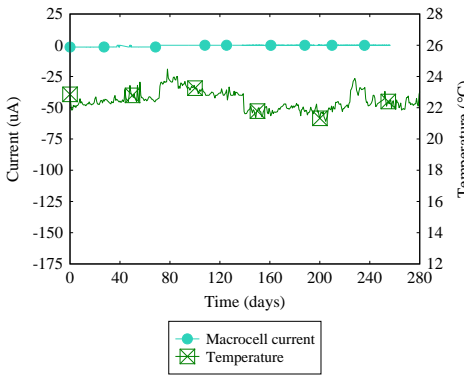
#	Specimen name	Corrosion potential readings	Macrocell current readings
12	5/100C1C E	 <p>Corrosion potential (mV) vs Time (days) and Temperature (°C). Legend: Anode corrosion potential (red circles), Cathode corrosion potential (blue circles), Temperature (green crosses).</p>	 <p>Current (uA) vs Time (days) and Temperature (°C). Legend: Macrocell current (red circles), Temperature (green crosses).</p>
13	100/5D1	 <p>Corrosion potential (mV) vs Time (days) and Temperature (°C). Legend: Anode corrosion potential (red circles), Cathode corrosion potential (blue circles), Temperature (green crosses).</p>	 <p>Current (uA) vs Time (days) and Temperature (°C). Legend: Macrocell current (red circles), Temperature (green crosses).</p>
14	100/5D2	 <p>Corrosion potential (mV) vs Time (days) and Temperature (°C). Legend: Anode corrosion potential (red circles), Cathode corrosion potential (blue circles), Temperature (green crosses).</p>	 <p>Current (uA) vs Time (days) and Temperature (°C). Legend: Macrocell current (red circles), Temperature (green crosses).</p>
15	100/5C1	 <p>Corrosion potential (mV) vs Time (days) and Temperature (°C). Legend: Anode corrosion potential (red circles), Cathode corrosion potential (blue circles), Temperature (green crosses).</p>	 <p>Current (uA) vs Time (days) and Temperature (°C). Legend: Macrocell current (red circles), Temperature (green crosses).</p>

#	Specimen name	Corrosion potential readings	Macrocell current readings
16	100/5D1C	 <p>Corrosion potential (mV) vs Time (days) and Temperature (°C). Legend: Anode corrosion potential (red circles), Cathode corrosion potential (blue circles), Temperature (green crosses).</p>	 <p>Current (uA) vs Time (days) and Temperature (°C). Legend: Macrocell current (red circles), Temperature (green crosses).</p>
17	100/5D2C	 <p>Corrosion potential (mV) vs Time (days) and Temperature (°C). Legend: Anode corrosion potential (red circles), Cathode corrosion potential (blue circles), Temperature (green crosses).</p>	 <p>Current (uA) vs Time (days) and Temperature (°C). Legend: Macrocell current (red circles), Temperature (green crosses).</p>
18	100/5C1C	 <p>Corrosion potential (mV) vs Time (days) and Temperature (°C). Legend: Anode corrosion potential (red circles), Cathode corrosion potential (blue circles), Temperature (green crosses).</p>	 <p>Current (uA) vs Time (days) and Temperature (°C). Legend: Macrocell current (red circles), Temperature (green crosses).</p>
19	100/5D1E	 <p>Corrosion potential (mV) vs Time (days) and Temperature (°C). Legend: Anode corrosion potential (red circles), Cathode corrosion potential (blue circles), Temperature (green crosses).</p>	 <p>Current (uA) vs Time (days) and Temperature (°C). Legend: Macrocell current (red circles), Temperature (green crosses).</p>

#	Specimen name	Corrosion potential readings	Macrocell current readings
20	100/5D2E	 <p>Corrosion potential (mV) vs Time (days) and Temperature (°C). Legend: Anode corrosion potential (red circles), Cathode corrosion potential (blue circles), Temperature (green crosses).</p>	 <p>Current (uA) vs Time (days) and Temperature (°C). Legend: Macrocell current (red circles), Temperature (green crosses).</p>
21	100/5C1E	 <p>Corrosion potential (mV) vs Time (days) and Temperature (°C). Legend: Anode corrosion potential (red circles), Cathode corrosion potential (blue circles), Temperature (green crosses).</p>	 <p>Current (uA) vs Time (days) and Temperature (°C). Legend: Macrocell current (red circles), Temperature (green crosses).</p>
22	100/5D1C E	 <p>Corrosion potential (mV) vs Time (days) and Temperature (°C). Legend: Anode corrosion potential (red circles), Cathode corrosion potential (blue circles), Temperature (green crosses).</p>	 <p>Current (uA) vs Time (days) and Temperature (°C). Legend: Macrocell current (red circles), Temperature (green crosses).</p>
23	100/5D2C E	 <p>Corrosion potential (mV) vs Time (days) and Temperature (°C). Legend: Anode corrosion potential (red circles), Cathode corrosion potential (blue circles), Temperature (green crosses).</p>	 <p>Current (uA) vs Time (days) and Temperature (°C). Legend: Macrocell current (red circles), Temperature (green crosses).</p>

#	Specimen name	Corrosion potential readings	Macrocell current readings
24	100/5C1C E		
25	5/15D1		
26	5/15D2		
27	5/15C1		

#	Specimen name	Corrosion potential readings	Macrocell current readings
28	5/15D1C	 <p>Corrosion potential (mV) vs Time (days) and Temperature (°C). Legend: Anode corrosion potential (red circles), Cathode corrosion potential (blue circles), Temperature (green crosses).</p>	 <p>Current (uA) vs Time (days) and Temperature (°C). Legend: Macrocell current (red circles), Temperature (green crosses).</p>
29	5/15D2C	 <p>Corrosion potential (mV) vs Time (days) and Temperature (°C). Legend: Anode corrosion potential (red circles), Cathode corrosion potential (blue circles), Temperature (green crosses).</p>	 <p>Current (uA) vs Time (days) and Temperature (°C). Legend: Macrocell current (red circles), Temperature (green crosses).</p>
30	5/15C1C	 <p>Corrosion potential (mV) vs Time (days) and Temperature (°C). Legend: Anode corrosion potential (red circles), Cathode corrosion potential (blue circles), Temperature (green crosses).</p>	 <p>Current (uA) vs Time (days) and Temperature (°C). Legend: Macrocell current (red circles), Temperature (green crosses).</p>
31	5/15D1E	 <p>Corrosion potential (mV) vs Time (days) and Temperature (°C). Legend: Anode corrosion potential (red circles), Cathode corrosion potential (blue circles), Temperature (green crosses).</p>	 <p>Current (uA) vs Time (days) and Temperature (°C). Legend: Macrocell current (red circles), Temperature (green crosses).</p>

#	Specimen name	Corrosion potential readings	Macrocell current readings
32	5/15D2E	 <p>Corrosion potential (mV) vs Time (days) and Temperature (°C). Legend: Anode corrosion potential (red circles), Cathode corrosion potential (blue circles), Temperature (green crosses).</p>	 <p>Current (uA) vs Time (days) and Temperature (°C). Legend: Macrocell current (red circles), Temperature (green crosses).</p>
33	5/15C1E	 <p>Corrosion potential (mV) vs Time (days) and Temperature (°C). Legend: Anode corrosion potential (red circles), Cathode corrosion potential (blue circles), Temperature (green crosses).</p>	 <p>Current (uA) vs Time (days) and Temperature (°C). Legend: Macrocell current (red circles), Temperature (green crosses).</p>
34	5/15D1CE	 <p>Corrosion potential (mV) vs Time (days) and Temperature (°C). Legend: Anode corrosion potential (red circles), Cathode corrosion potential (blue circles), Temperature (green crosses).</p>	 <p>Current (uA) vs Time (days) and Temperature (°C). Legend: Macrocell current (red circles), Temperature (green crosses).</p>
35	5/15D2CE	 <p>Corrosion potential (mV) vs Time (days) and Temperature (°C). Legend: Anode corrosion potential (red circles), Cathode corrosion potential (blue circles), Temperature (green crosses).</p>	 <p>Current (uA) vs Time (days) and Temperature (°C). Legend: Macrocell current (red circles), Temperature (green crosses).</p>

#	Specimen name	Corrosion potential readings	Macrocell current readings
36	5/15C1CE		
37	15/5D1		
38	15/5D2		
39	15/5C1		

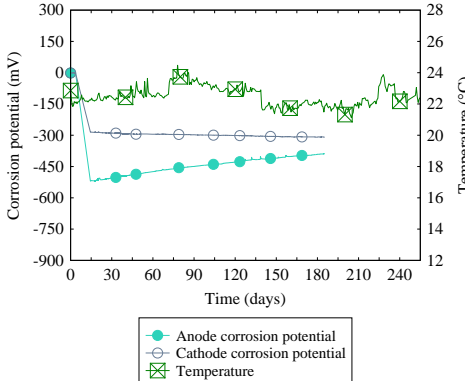
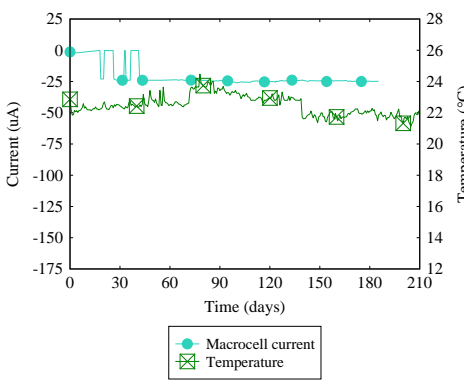
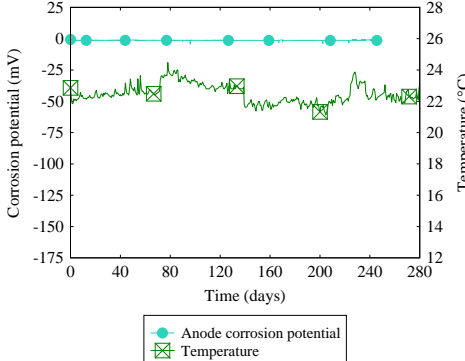
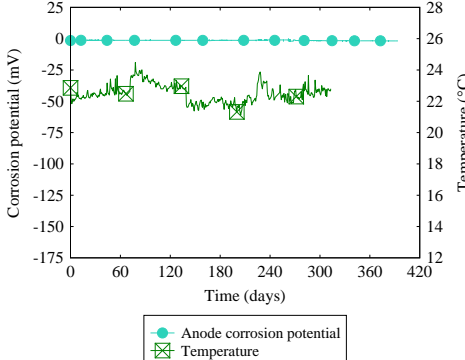
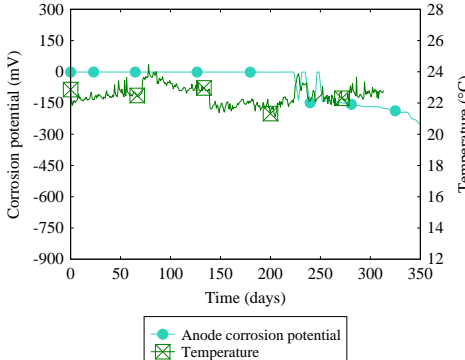
#	Specimen name	Corrosion potential readings	Macrocell current readings
40	15/5D1C		
41	15/5D2C		
42	15/5C1C		
43	15/5D1E		

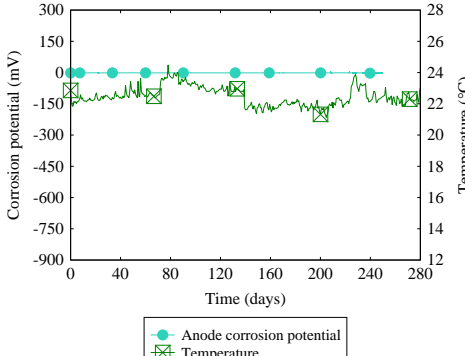
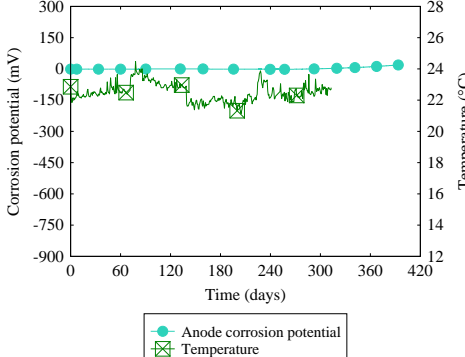
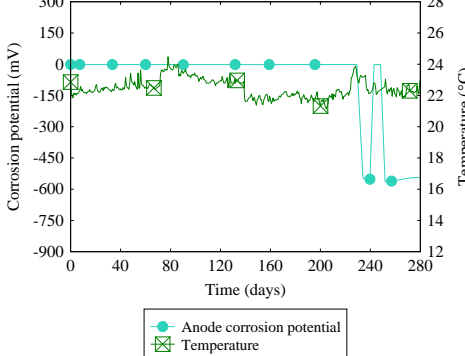
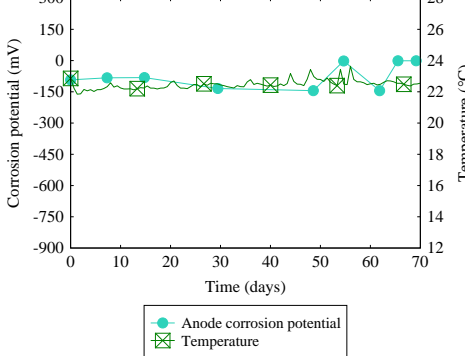
#	Specimen name	Corrosion potential readings	Macrocell current readings
44	15/5D2E		
45	15/5C1E		
46	15/5D1CE		
47	15/5D2CE		

#	Specimen name	Corrosion potential readings	Macrocell current readings
48	15/5C1CE		
49	PT/100D1		
50	PT/100D2		
51	PT/100C1		

#	Specimen name	Corrosion potential readings	Macrocell current readings
52	PT/100D1 C	<p>Corrosion potential (mV) vs Time (days) and Temperature (°C). The anode corrosion potential (red circles) remains constant at 0 mV. The cathode corrosion potential (blue circles) remains constant at -450 mV. The temperature (green crosses) fluctuates between approximately 22°C and 23°C.</p>	<p>Current (uA) vs Time (days) and Temperature (°C). The macrocell current (red circles) remains constant at 0 uA. The temperature (green crosses) fluctuates between approximately 22°C and 23°C.</p>
53	PT/100D2 C	<p>Corrosion potential (mV) vs Time (days) and Temperature (°C). The anode corrosion potential (red circles) remains constant at 0 mV. The cathode corrosion potential (blue circles) remains constant at -450 mV. The temperature (green crosses) fluctuates between approximately 22°C and 23°C.</p>	<p>Current (uA) vs Time (days) and Temperature (°C). The macrocell current (red circles) remains constant at 0 uA. The temperature (green crosses) fluctuates between approximately 22°C and 23°C.</p>
54	PT/100C1 C	<p>Corrosion potential (mV) vs Time (days) and Temperature (°C). The anode corrosion potential (red circles) remains constant at 0 mV. The cathode corrosion potential (blue circles) remains constant at -450 mV. The temperature (green crosses) fluctuates between approximately 22°C and 23°C.</p>	<p>Current (uA) vs Time (days) and Temperature (°C). The macrocell current (red circles) remains constant at 0 uA. The temperature (green crosses) fluctuates between approximately 22°C and 23°C.</p>
55	100/PTD1	<p>Corrosion potential (mV) vs Time (days) and Temperature (°C). The anode corrosion potential (red circles) remains constant at 0 mV. The cathode corrosion potential (blue circles) remains constant at -450 mV. The temperature (green crosses) fluctuates between approximately 22°C and 23°C.</p>	<p>Current (uA) vs Time (days) and Temperature (°C). The macrocell current (red circles) remains constant at 0 uA. The temperature (green crosses) fluctuates between approximately 22°C and 23°C.</p>

#	Specimen name	Corrosion potential readings	Macrocell current readings
56	100/PTD2		
57	100/PTC1		
58	100/PTD1 C		
59	100/PTD2 C		

#	Specimen name	Corrosion potential readings	Macrocell current readings
60	100/PTC1 C	 <p>Corrosion potential (mV) vs Time (days) and Temperature (°C). Legend: Anode corrosion potential (red circles), Cathode corrosion potential (blue circles), Temperature (green crosses).</p>	 <p>Current (uA) vs Time (days) and Temperature (°C). Legend: Macrocell current (red circles), Temperature (green crosses).</p>
61	5D1	 <p>Corrosion potential (mV) vs Time (days) and Temperature (°C). Legend: Anode corrosion potential (red circles), Temperature (green crosses).</p>	
62	5D2	 <p>Corrosion potential (mV) vs Time (days) and Temperature (°C). Legend: Anode corrosion potential (red circles), Temperature (green crosses).</p>	
63	5C1	 <p>Corrosion potential (mV) vs Time (days) and Temperature (°C). Legend: Anode corrosion potential (red circles), Temperature (green crosses).</p>	

#	Specimen name	Corrosion potential readings	Macrocell current readings
64	5D1C	 <p>Graph showing Corrosion potential (mV) and Temperature (°C) versus Time (days) for specimen 5D1C. The x-axis ranges from 0 to 280 days. The left y-axis ranges from -900 to 300 mV, and the right y-axis ranges from 12 to 28 °C. The Anode corrosion potential (red circles) remains near 0 mV. The Temperature (blue squares) fluctuates between approximately 22°C and 24°C.</p>	
65	5D2C	 <p>Graph showing Corrosion potential (mV) and Temperature (°C) versus Time (days) for specimen 5D2C. The x-axis ranges from 0 to 420 days. The left y-axis ranges from -900 to 300 mV, and the right y-axis ranges from 12 to 28 °C. The Anode corrosion potential (red circles) remains near 0 mV. The Temperature (blue squares) fluctuates between approximately 22°C and 24°C.</p>	
66	5C1C	 <p>Graph showing Corrosion potential (mV) and Temperature (°C) versus Time (days) for specimen 5C1C. The x-axis ranges from 0 to 280 days. The left y-axis ranges from -900 to 300 mV, and the right y-axis ranges from 12 to 28 °C. The Anode corrosion potential (red circles) is near 0 mV until day 240, where it drops sharply to approximately -600 mV. The Temperature (blue squares) fluctuates between approximately 22°C and 24°C.</p>	
67	100D1	 <p>Graph showing Corrosion potential (mV) and Temperature (°C) versus Time (days) for specimen 100D1. The x-axis ranges from 0 to 70 days. The left y-axis ranges from -900 to 300 mV, and the right y-axis ranges from 12 to 28 °C. The Anode corrosion potential (red circles) fluctuates around -150 mV. The Temperature (blue squares) fluctuates between approximately 22°C and 24°C.</p>	

#	Specimen name	Corrosion potential readings	Macrocell current readings
68	100D2	<p>Graph showing Corrosion potential (mV) and Temperature (°C) versus Time (days) for specimen 100D2. The x-axis ranges from 0 to 280 days, and the y-axis ranges from -900 to 300 mV. The temperature (green line with 'x' markers) fluctuates between approximately 22°C and 24°C. The anode corrosion potential (blue line with circle markers) remains stable near 0 mV throughout the 280-day period.</p>	
69	100C1	<p>Graph showing Corrosion potential (mV) and Temperature (°C) versus Time (days) for specimen 100C1. The x-axis ranges from 0 to 210 days, and the y-axis ranges from -900 to 300 mV. The temperature (green line with 'x' markers) fluctuates between approximately 22°C and 24°C. The anode corrosion potential (blue line with circle markers) remains stable near 0 mV throughout the 210-day period.</p>	
70	100D1C	<p>Graph showing Corrosion potential (mV) and Temperature (°C) versus Time (days) for specimen 100D1C. The x-axis ranges from 0 to 70 days, and the y-axis ranges from -900 to 300 mV. The temperature (green line with 'x' markers) fluctuates between approximately 22°C and 24°C. The anode corrosion potential (blue line with circle markers) remains stable near 0 mV throughout the 70-day period.</p>	
71	100D2C	<p>Graph showing Corrosion potential (mV) and Temperature (°C) versus Time (days) for specimen 100D2C. The x-axis ranges from 0 to 280 days, and the y-axis ranges from -900 to 300 mV. The temperature (green line with 'x' markers) fluctuates between approximately 22°C and 24°C. The anode corrosion potential (blue line with circle markers) remains stable near 0 mV throughout the 280-day period.</p>	

#	Specimen name	Corrosion potential readings	Macrocell current readings																																																
72	100C1C	<p>The graph displays two data series over a 420-day period. The Anode corrosion potential (red circles) starts at 0 mV at day 0, drops to -150 mV at day 30, and then stabilizes around -300 mV from day 60 to 240. The Temperature (green squares) fluctuates between approximately 20°C and 24°C throughout the period.</p> <table border="1"> <caption>Approximate data points from the graph</caption> <thead> <tr> <th>Time (days)</th> <th>Anode corrosion potential (mV)</th> <th>Temperature (°C)</th> </tr> </thead> <tbody> <tr><td>0</td><td>0</td><td>22</td></tr> <tr><td>30</td><td>-150</td><td>22</td></tr> <tr><td>60</td><td>-300</td><td>22</td></tr> <tr><td>90</td><td>-300</td><td>22</td></tr> <tr><td>120</td><td>-300</td><td>22</td></tr> <tr><td>150</td><td>-300</td><td>22</td></tr> <tr><td>180</td><td>-300</td><td>22</td></tr> <tr><td>210</td><td>-300</td><td>22</td></tr> <tr><td>240</td><td>-300</td><td>22</td></tr> <tr><td>270</td><td>-300</td><td>22</td></tr> <tr><td>300</td><td>-300</td><td>22</td></tr> <tr><td>330</td><td>-300</td><td>22</td></tr> <tr><td>360</td><td>-300</td><td>22</td></tr> <tr><td>390</td><td>-300</td><td>22</td></tr> <tr><td>420</td><td>-300</td><td>22</td></tr> </tbody> </table>	Time (days)	Anode corrosion potential (mV)	Temperature (°C)	0	0	22	30	-150	22	60	-300	22	90	-300	22	120	-300	22	150	-300	22	180	-300	22	210	-300	22	240	-300	22	270	-300	22	300	-300	22	330	-300	22	360	-300	22	390	-300	22	420	-300	22	
Time (days)	Anode corrosion potential (mV)	Temperature (°C)																																																	
0	0	22																																																	
30	-150	22																																																	
60	-300	22																																																	
90	-300	22																																																	
120	-300	22																																																	
150	-300	22																																																	
180	-300	22																																																	
210	-300	22																																																	
240	-300	22																																																	
270	-300	22																																																	
300	-300	22																																																	
330	-300	22																																																	
360	-300	22																																																	
390	-300	22																																																	
420	-300	22																																																	